TARGETING *RHT-A1* FOR THE GENERATION OF NOVEL SEMI-DWARFING ALLELES IN WHEAT

Thesis submitted to The University of Nottingham for the degree of Doctor of Philosophy

SEPTEMBER 2019

Abstract

The dramatic wheat yield increases of the Green Revolution are partially attributed to the development of high yielding, lodging resistant, semi-dwarf varieties through the introduction of the alleles *Rht-B1b* and *Rht-D1b* into elite wheat cultivars. These alleles contain gain-of-function mutations in the *RHT-1* genes, encoding DELLA proteins that repress gibberellin (GA) signalling. GAs promote the targeted degradation of DELLAs, relieving their repression and allowing for GA-responsive growth. *Rht-1* dwarfing alleles encode abnormal DELLA proteins that are not believed to be recognized for degradation, causing constitutive repression of GA responses and pleiotropic effects such as: reduced fertility during heat stress and impaired seedling emergence and establishment. Currently, this limits the ability of *Rht-1* alleles for further improving wheat grain yields.

The hexaploid bread wheat genome contains three homoeologous *Rht-1* genes; *Rht-A1/B1/D1,* although presently dwarfing alleles have only been identified in *Rht-B1* and *D1*. This thesis describes the characterization of the novel allele *Rht-A1b* through phenotyping, GA-dose response assays, hormononics and transcriptomics analyses. Studies confirmed that *Rht-A1b* is the first reported *Rht-A1* allele that causes GA-insensitive dwarfism and represents a potential tool for wheat breeders.

To extend the collection of *Rht-A1* dwarfing alleles available to wheat breeders suppressor screens was conducted on M_2 ethyl methanesulfonate mutagenised *Rht-A1b* populations. Intragenic *Rht-A1b* mutants were identified in the field and the BC_2F_3 generation characterized in the field and glasshouse. All intragenic alleles were found to rescue plant height in comparison to *Rht-A1b* with six alleles demonstrating a potentially beneficial intermediate phenotype. Testing following an introduction into elite germplasm could establish their potential as superior dwarfing alleles and provided insights into DELLA structure-function in wheat.

In addition, a reverse genetics-based approach, TILLING, was used to generate *Rht-1* knock out lines, which were subsequently stacked. The triple mutant produced the first identified GA overdose phenotype in wheat, suggesting that DELLA is the negative regulator of GA in wheat. Limited phenotypic differences between combinatorial mutants suggests that there is limited homoeologue specificity in the *Rht-1* genes.

Acknowledgements

Firstly, the biggest thank you must go to my Rothamsted supervisors: Steve Thomas, Peter Hedden and Andy Phillips for their patience and support throughout the PhD. You have been excellent to work with and your knowledge and advice has guided me through the PhD process. Thanks also go to my University of Nottingham supervisor Zoe Wilson for her advice and suggestions during the project.

I would like to thank the past and present members of the lab group for their help and advice and for making the lab such a pleasant place to work. I'd particularly like to thank Matt D., Pat, Matt C. and Manpartik for their friendship, great company and help harvesting my final field trial. Thank you to Jill, Jack and Tom for your help growing all the wheat plants in the glasshouse and to Steve, Suzanne and Dan for helping with the stats and bioinformatics for this project. This work was completed with support from the BBSRC Doctoral Training Partnership between Rothamsted Research and The University of Nottingham.

A huge thank you goes to all the Rothamsted students, who have made the last 4 years so enjoyable. The coffee breaks and nights at the Pav were exactly what I needed.

Finally, I want to thank my family, who fostered my love of science when I was small and have been my biggest cheerleaders ever since. Mum, who sent fantastic care packages and was always available to talk. My Dad, who had the extended family send notes of encouragement to help push me through the final weeks of writing up. My sister, Lizzy, who kept me grounded with trips to London and evenings drinking cocktails. Also, my gorgeous dog Coast, who kept me company in the field during the suppressor screens.

Contents Table

List of Figures

List of Tables

List of Abbreviations

AGF1	GA feedback 1
AM	Anther primordia
BRZ1	BRASSINAZOLE-RESISTANT1
cDNA	Complementary deoxyribonucleic acid
cm	Centimetre
CPS	*ent*-copalyl diphosphate synthase
D8	*Dwarf-8*
DE	Differentially expressed
DIP	DELLA interacting protein
DNA	Deoxyribonucleic acid
EMS	Ethylmethanesulphonate
ER	Endoplasic reticulum
ET	Ethylene
FM	Floret meristem
GA	Gibberellin
GA20ox	Gibberellin-20 oxidase
GA2ox	Gibberellin-2 oxidase
GA3ox	Gibberellin-3 oxidase
GAF1	GAI-ASSOCIATED FACTOR1
GAI	Gibberellin insensitive
GC MS	Gas chromatography mass spectrometry
GFP	Green fluorescent protein
GGPP	Geranylgeranyl diphosphate
GID1	GIBBERLLIN INSENSITIVE DWARF1
GP	Glume primordia
HFN	Hagburg falling number
ID1	INDETERMINATE1
IDD	ID1 domain protein
IM	Inflorescence meristem
IWGSC	International Wheat Genome Sequencing Consortium
JAZ	Jasmonic acid
KAO	*ent*-kaurenoic acid oxidase
KO	*ent*-kaurene oxidase
KS	*ent*-kaurene synthase
LM	Lemma primordia
mm	Millimetre
mM	Millimolar
MOC1	MONOCULM 1
NMR	Nuclear magnetic resonance
PCD	Programmed cell death
PCM	Pollen mother cellls
PCR	Polymerase chain reaction
PFD5	PREFOLDIN 5

PIF	PHYTOCHROME INTERACTING FACTORS
PKL	Pickle
PP	Pistil primordia
RGA	Repressor of *ga1-3*
RGL	Repressor of *ga1-3* like
RHT	Reduced height
RNA	Ribonucleic acid
RNA-seq	RNA sequencing
SA	Salicyclic acid
SAM	Shoot apical meristem
SCL-3	SCARECROW-LIKE 3
SCR	Scarecrow
SLN1	Slender 1
SLR1	Slender 1
SNP	Single Nucleotide Polymorphism
STP	Stamen primordia
TF	Transcription factor
TILLInG	Targeted Induced Legions in Genome
TPR	TOPLESS-RELATED
µg	Microgram
µl	Microlitre
µm	Micrometre
µM	Micromolar
2-ODDs	2-oxoglutarate-dependent dioxygenases

Chapter 1: Introduction

1.1 Wheat *(Triticum aestivum L.)*

Modern bread wheat (*Triticum aestivum L.)* is the world's most widely cultivated crops, a staple food source for a third of global population, with over 600 million tonnes harvested annually (Mayer et al. 2014; Shewry 2009). Modern bread wheat is a disomic allo-hexaploid, consisting of three diploid genomes: A, B and D, the result of two hybridisation events over the last 500,000 years (Figure 1.1.)

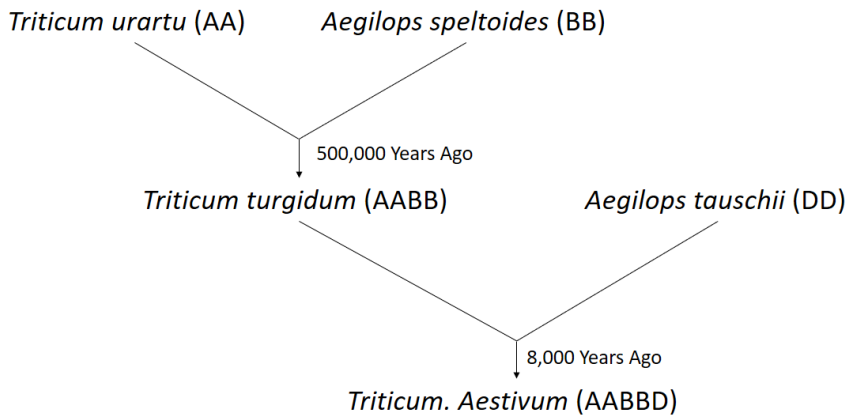

Figure 1.1: The evolution of hexaploid wheat. Two distinct diploid progenitors: *Triticum urartu* and *Aegilops speltoides*, hybridised to form the tetraploid *Triticum turgidum* approximately 500,000 years ago. *T. turgidum* then hybridised with another wild progenitor, *Aegilops tauschii,* to give rise to the modern hexaploid species *Triticum aestivum L.*, approximately 9,000 years ago (adapted from Kimber and Sears, 1987).

The first hybridisation event occurred approximately 500,000 years ago in south-eastern Turkey, where diploid *Triticum Urartu* (AA) and *Aegilops speltoides* (BB), hybridised to form the tetraploid *Triticum turgidum* (AABB) (Heun et al. 1997; Dubcovsky and Dvorak 2007). Cultivation of *T. turgidum* spread to the Near East, where the second hybridisation with *Aegilops tauschii* (DD) occurred in the Fertile Crescent approximately 9,000 years ago, resulting in hexaploid (AABBDD) *Triticum aestivum L.* (Feldman, Bonjean, and Angus 2001; McFadden and Sears 1946). Today, *T. aestivum L.* is grown throughout the world. This is partially due to its polyploid genome, the increased genetic diversity allowed for the domestication of wheat varieties adapted to a range of climates and cultivation practices (Koornneef et al. 1985; Salamini et al. 2002; Marcussen et al. 2014).

As the wheat genome is hexaploid and contains a high proportion of repetitive DNA, it is one of the largest ever studied, being approximately 17,000 MB in size (Bennett and Leitch 1995). Additionally the A, B and D genomes carry approximately the same homoeologous genes in the same positions, increasing the number of functional copies of each gene (Appleford et al. 2006). This makes wheat an extremely genetically complex species, more difficult to work with than simple model organisms such as *Arabidopsis thaliana (Dubcovsky and Dvorak 2007)*. Recently, the first fully annotated reference sequence has been released for the variety Chinese Spring, called IWGSC RefSeq v1.0 (Appels et al. 2018). The completeness of IWGSC v1.0, with 107,891 high-confidence gene models, will enable insights into global genome composition, the impact of homoeologues on developmental processes and the determination of complex gene co-expression networks.

1.2 The Green Revolution

In the ~9,000 years since *T. aestivum L.* first arose, humans have worked to increase yields by domesticating region-specific varieties and improving cultivation practices and technologies (McFadden and Sears 1946: Salamini et al. 2002: Marcussen et al. 2014). By the 1960s these improvements produced record yields of approximately 1.1 tonnes/Ha of wheat (OECD/FAO 2012). However, this coincided with the post Second World War (WW2) baby boom where population growth threatened to outstrip food production, resulting in increasing concerns about the global food-population balance (Ehrlich 1968).

At the time, the majority of agronomically important wheat varieties were tall and prone to yield losses through lodging, where the crop would buckle under its own weight, or due to wind and rain. To prevent plants from growing too tall and unstable, farmers limited their fertiliser usage, which was also a major limiting factor on yield improvement (Law, Snape, and Worland 1978; Griffiths et al. 2012). Attempts to commercially grow dwarf wheat varieties, that were less prone to lodging, were unsuccessful as the crops produced lower yields (Law, Snape, and Worland 1978). As a result, plant breeders began to focus on developing shorter, high yielding wheat varieties.

High yielding, short wheat varieties have existed for centuries in Asia, having been first identified in Korea in the 3rd or 4th Century (Cho, Kyu, and Lee 1993) and reaching Japan in the 16th Century (Borojevic 2005). During the 1910s and 1920s, a Japanese breeder Mr Gonjiro Inazuka, crossed the native Japanese dwarf wheat variety, Daruma, with two American wheat varieties, Fultz and Turkey Red, to create the high-yielding semi-dwarf wheat variety, Norin-10 (Figure 1.3) (Reitz and Salmon 1968). Following the end of WW2, Norin-10 was identified as a highly desirable wheat variety by the broader agricultural community. Its shorter, thicker stems were more resistant to lodging than conventional varieties. Norin-10 also produced more grain per plant, as improved assimilate partitioning to the developing ear increased floret survival (Flintham et al. 1997). As a result, seed was taken from Japan to the Washington Agricultural Experimental Station in the USA, where Dr Orvill Vogel created two crosses: Norin 10-Brevor and Norin 10-Baart (Law, Snape, and Worland 1978). In 1952, seed from both these crosses were transferred to Dr Norman Borlaug at the Centro Internacional de Mejoramiento de Maiz y Trigo (CIMMYT) in Mexico. At the time Dr Borlaug was working on producing wheat varieties with increased resistance to lodging and stem and leaf rust (Borlaug 1981). He crossed Norin 10-Brevor to various Mexican wheat varieties and used an innovative shuttle breeding programme, so that two generations per year could be grown across two locations in Mexico. By 1962, two high-yielding semi-dwarf wheat varieties, Pitic 62 and Penjamo 62, were made available commercially (Borlaug 1981). Additional varieties were then also developed (Figure 1.2).

This large number of semi-dwarf varieties was adapted to a range of climates, enabling their uptake around the globe (Borlaug 1968). Their prevalence, in combination with developing agricultural practices, such as: increased mechanization, fertilizer, pesticide and herbicide usage, meant that crop yields increased three fold between the 1960s to 2000s. (Khush 2001; Hedden 2003). This time is referred to as the Green Revolution, during which increases in annual world agricultural output (2.2-2.5%) outstripped population growth (2-1.3%) (Hedden 2003; Population Council 2013). For his work, Dr Borlaug the ‘Father of the Green

Revolution' was awarded the 1970 Nobel Peace Prize (Hedden 2003; Wilhelm, Boulton, et al. 2013; Dalrymple 1986). Today, approximately 70% of modern wheat varieties contain at least one of the two Green Revolutions semi-dwarfing alleles derived from Norin-10 (Hedden 2003).

1.3 The Green Revolution Alleles

The desirable semi-dwarf phenotype of Norin-10 and the varieties bred by Dr Norman Borlaug is caused by two alleles: *Rht1* and *Rht2*. Genetic studies revealed that *Rht1* and *Rht2* are located near the centromeres on the short arms of 4B and 4D respectively (Gale, Law, and Worland 1975; Gale and Marshall 1976; McVitte et al. 1978). Additional *Rht-1* alleles were also identified at these loci: *Rht3* (Gale et al. 1975)*, Rht1S* and *RhtKrasnodari l* on 4B (Worland 1986), *Rht10* and *RhtAi-bian 1a* on 4D (Börner and Mettin 1988). The nomenclature of these alleles was confusing and did not follow the recommended gene naming rule in wheat. This requires that in homoeologous sets of genes, the basic symbol (*Rht*) is followed by a hyphen then locus designation (the genome symbol: A, B or D), then a homoeologous set number (1, 2, 3...). After the locus designation, alleles are then designated by a lower case letter (a, b, c…)(Börner et al. 1996). A unified nomenclature was first proposed by Dr

Table 1.1: Original and adopted nomenclature of the GA insensitive *Rht-1* alleles in wheat

	Original Nomenclature	**Proposed Nomenclature**	**Associated Height Reduction**
Chromosome 4B	*Rht* (tall allele)	*Rht-B1a*	NA
	Rht1	*Rht-B1b*	12-15% (Flintham et al. 1997)
	Rht3	*Rht-B1c*	50% (Gale and Marshall 1975)
	Rht1S	*Rht-B1d*	11% (Worland and Petrovic 1988)
	RhtKrasnodari 1	*Rht-B1e*	20% (Worland 1986)
	Rht17	*Rht-B1p*	33% (Bazhenov et al. 2015)
Chromosome 4D	*Rht* (tall allele)	*Rht-D1a*	NA
	Rht2	*Rht-D1b*	16-20% (Flintham et al. 1997)
	Rht10	*Rht-D1c*	50% (Börner and Mettin 1988)
	RhtA1-bain 1a	*Rht-D1d*	25% (Börner et al. 1991)

Adapted from (Börner et al. 1996).

M.D. Gale and Dr R.A. McIntosh (Worland and Petrovic 1988), however the accepted nomenclature (Table 1.1) was proposed by Börner et al (1996).

As a result, *Rht1* and *Rht2* are now referred to as *Rht-B1b* and *Rht-D1b*, respectively, whilst the wild type allele of each homoeologue is referred to as *Rht-B1a* or *Rht-D1a* (Boerner et al. 1993).

The presence of *Rht-1* alleles results in shorter stature plants because the alleles are gain-of-function mutations of the *REDUCED HEIGHT-1* (*Rht-1)* gene. This causes constitutive gibberellin insensitivity through repression of gibberellin signalling, which limits plant stem elongation (Gale and Marshall 1973).

1.4 Gibberellins Act as Phytohormones

All higher plants produce gibberellins (GAs), tetracyclic carboxylic acids involved in plant growth and development. Gibberellins were initially identified in the 1920s, from the fungal pathogen *Gibberella fujikuroi*, which causes 'bakanae' or 'foolish seedling' disease in rice. Affected plants over-elongate as seedlings and produce lower grain yields as adults (Kurosawa 1926). However, the importance of GAs as plant growth regulators wasn't widely recognised until the mid-1950s, following studies examining the response to exogenous GA in wild type, dwarf or rosette mutants in different plant species: e.g. pea (*Pisum sativum*) (Brian and Hemming 1955; Brian 1957), maize (Phinney 1956). Such studies identified recessive mutants that were responsive to exogenous GA and dominant mutants that were not. Analysis of GA responsive dwarf mutants would later be used to dissect the GA biosynthetic pathways (Section 1.6), whilst non-responsive mutants were used to examine the role of GA signalling in plant development. Bioactive GAs are vital in modulating growth and development throughout the plant lifecycle (Figure 1.3).

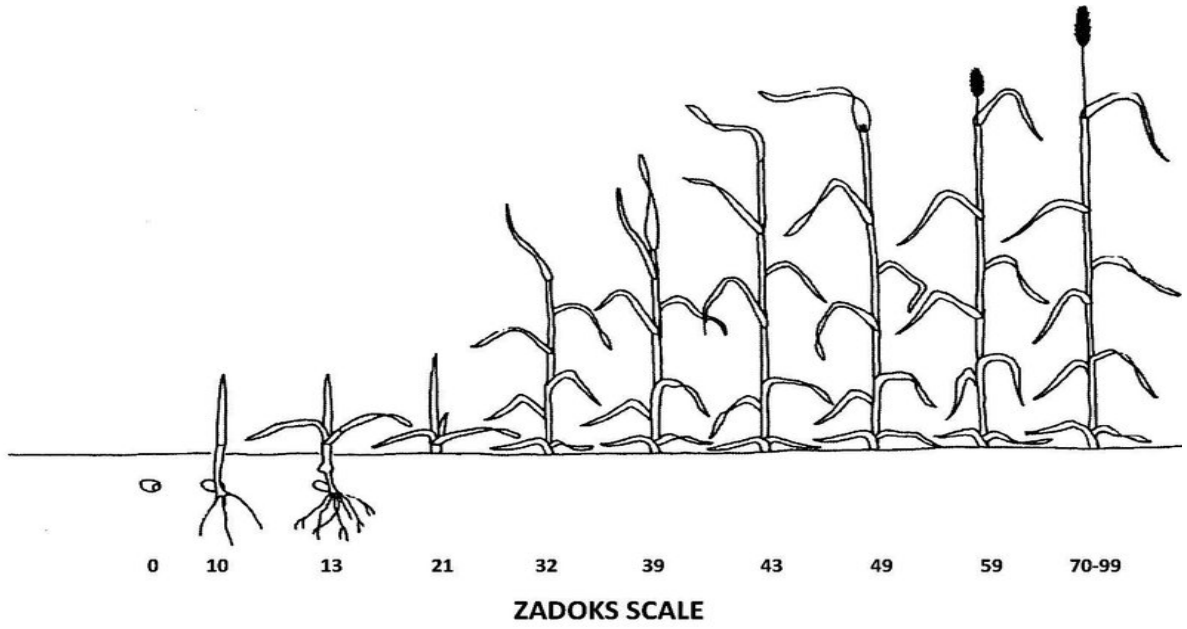

Figure 1.3: Wheat Lifecycle, shown on Zadoks Scale. 0= dry seed, 10= first leaf through coleoptile, 13= 3 leaves unfolded, 21= beginning of shooting (first shoot detectable), 32= node 2 at least 2cm above node 1, 39= flag leaf stage (flag leaf fully unrolled, ligule just visible), 43= mid-boot stage (flag leaf sheath just visibly swollen), 49= first awns visible, 59= end of heading (inflorescence fully emerged) 70-99= development of fruit, ripening and senescence. Figure from (Fowler 2018)

As a result, their concentrations vary *in planta* depending on the tissue, the developmental stage and influence of environmental factors. The role of GAs in controlling different developmental processes is described in the following sections.

1.4.1 GAs promote Germination and Seedling Emergence

Germination is the first crucial step in post-embryonic plant development, defined by testa and endosperm rupture resulting in the visible protrusion of the radical (Karssen et al. 1989). Bioactive GAs play a key role in this process (Hashimoto 1959), as they are required to break seed dormancy. GA deficient seeds are unable to germinate in the absence of exogenous GA (Groot and Karssen 1987), whilst application of exogenous GAs has also been shown to remove seed requirements for environmental cues for germination (Bewley and Black, 1982). In dicots, the biosynthesis of bioactive GAs in embryo tissues promotes radical and hypocotyl

growth elongation (Karssen et al. 1989) by inducing the expression of genes involved in cell elongation (Finkelstein et al. 2008). Additionally, GAs relieve mechanical constraint on the embryo by inducing the expression of hydrolysing enzymes, endo-β-glucanases, that induce the breakdown of the micropylar endosperm (CAP) (Groot and Karssen 1987). In monocots GAs mainly promote germination through perception by the aleurone layer (Figure 1.4).

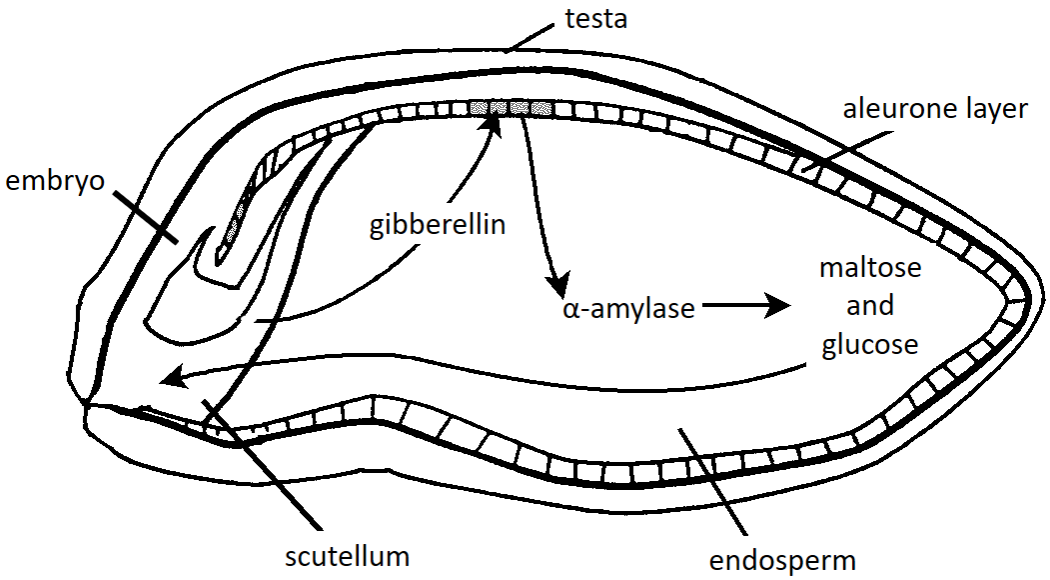

Figure 1.4: The Role of the Aleurone Response to GA in Cereal Seed Germination. Bioactive GAs from the scutellum epithelium of the embryo are perceived by the seed aleurone layer. This induces the de novo synthesis of α-amylase, which is secreted into the endosperm, where it hydrolyses starch into glucose and maltose. These sugars are then used as nutrients by the seed embryo. Adapted from http://plantphys.info/plant_physiology/gibberellin.shtml

However, gibberellins are not essential for germination in cereals, since knocking out the GA receptor GID1 (Gibberellin Insensitive Dwarf 1) in rice does not inhibit germination (Ueguchi-Tanaka et al. 2005), suggesting that GA is not essential for germination.

In monocots, bioactive GAs are produced in the scutellum epithelium of the embryo and transported to the seed aleurone layer (Kaneko et al. 2003). GA is perceived by

the aleurone layer and induces the *de novo* synthesis of α-amylase (Gubler et al. 1995), which is secreted into the endosperm. The α-amylase hydrolyses starch in the endosperm, producing glucose and maltose which act as nutrients for the seed embryo, sustaining heterotrophic growth of the germinating seedlings until they are capable of auxotrophic growth (Fath et al. 2000; Jacobsen, Gubler, and Chandler 1995). By contrast, dicots lack a seed aleurone layer and most of their seed starch stores are in the embryo (Koning 1994). Therefore, bioactive GAs induces the production of α-amylase in the embryo where the enzyme degrades the starch stores, releasing glucose and maltose directly in the embryo tissue (Koning 1994).

1.4.2 Seedling Development and Leaf Expansion

Post-germination, GAs promote seedling development and maturation in dicots through hypocotyl elongation and leaf and root growth (Brian and Hemming 1955; Hooley 1994). Light stimulation represses GA biosynthesis (Alabadi et al. 2008). The absence of light under the soil triggers the upregulation of GA, which promotes the targeted degradation of DELLA proteins that repress GA signalling (Hirano et al. 2010). Once this repression is relieved, GAs stimulate seedling growth in response to darkness (skotomorphogenesis), enabling rapid hypocotyl elongation and seedling emergence through the soil layer (Alabadi et al. 2008). Hypocotyl elongation ceases following light exposure and the process of de-etiolation occurs (Davies 1995). This allows the cotyledons to expand through GA-mediated cell elongation (Koornneef and Vanderveen 1980). Light exposure also stimulates the differentiation of etioplasts into chloroplasts, enabling seedlings to begin photosynthesis (Kami et al. 2010). The GA content of cotyledons is a signalling source for the growth of unfolded primary leaves, with their premature removal resulting in diminished young leaf expansion (Humphries and Wheeler 1963).

1.4.3 Stem Elongation

Stem elongation, which is crucial for light interception and shade avoidance (Page et al. 2010), is closely regulated by GA signalling, which is reflected in the dwarf phenotypes of GA-deficient and insensitive mutants (Koornneef and Vanderveen 1980; Youssefian, Kirby, and Gale 1992a). Cereal stems consist of a series of

phytomers: a unit comprising of a leaf, axillary bud and node and internode tissues (Galinat 1959) (Figure 1.5A).

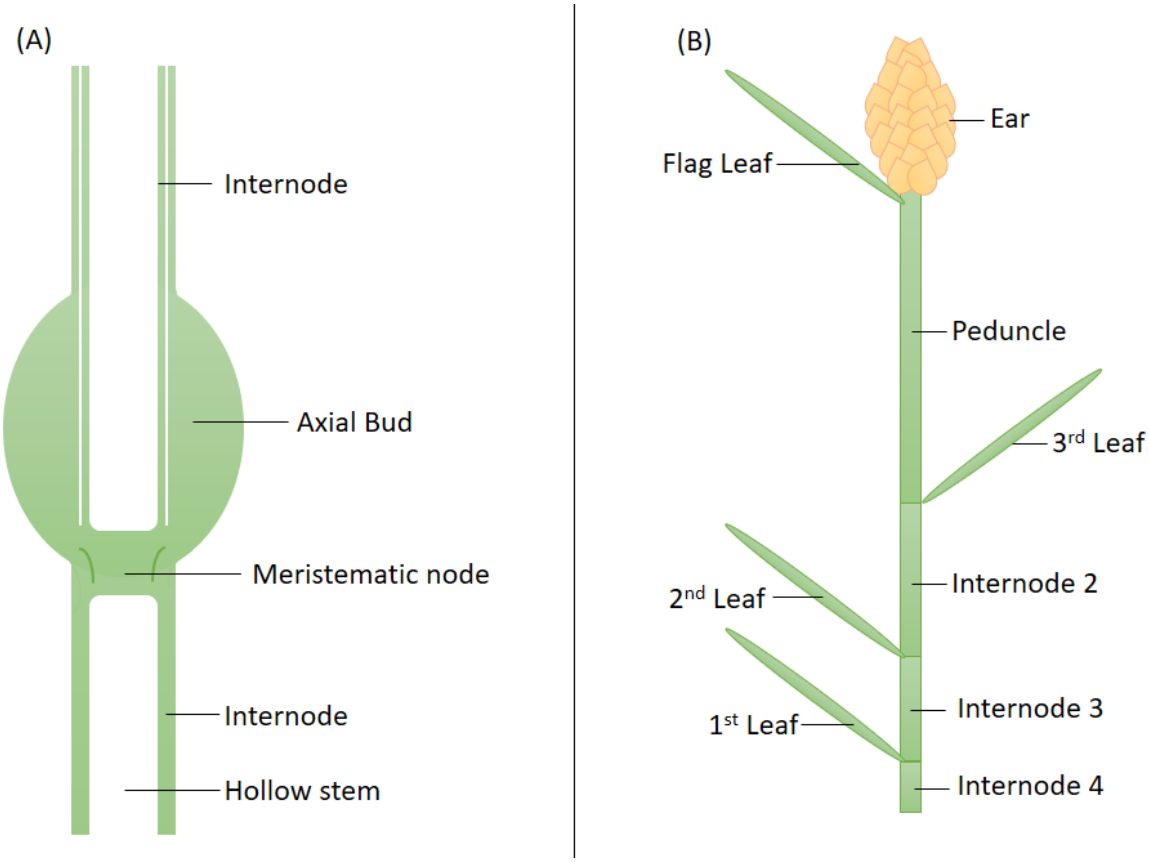

Figure 1.5: Physiology of Wheat Stems and Internodes (A) Tissues of Developing Wheat Stem. (B) Mature Wheat Stem Physiology. Adapted from www.wheatbp.net.

During stem elongation, new cells form in the internode just above the meristematic node (Figure 1.5A). The process of cell division is regulated by GA, which promotes increased cell number by increasing cell proliferation (Lee et al. 2012{Sachs, 1965 #256)}. The new cells then begin to elongate and migrate away from the meristematic node, pushed forward by new cells forming behind them. Cell elongation is also mediated by GA, which promotes elongation by increasing cell wall extensibility (Hoogendoorn, Rickson, and Gale 1990). Maximal stem extension occurs at or close to the meristematic node, where GA biosynthesis occurs and concentrations are highest (Hoogendoorn, Rickson, and Gale 1990). Subsequently, cell extension slows as the cells migrate away from the node due to decreasing GA concentrations until they reach their full size (Hoogendoorn, Rickson,

and Gale 1990). Once internode elongation is half complete, the elongation process begins for the internode above. The lowest internode in a wheat stem elongates the least, with the internodes further up the stem elongating longer than the one below (Kirby and Appleyard 1981). The final, uppermost internode, the peduncle, extends the most (Figure 1.4.2B). Stem elongation is considered complete by the time of anthesis (Kirby and Appleyard 1981).

1.4.4 Shooting

Shooting is an agronomically important trait that partially determines crop yield in wheat (Power and Alessi 1978), with reduced shooting deemed desirable as this limits inter-seed competition for nutrients, resulting in greater seed weights (Kebrom et al. 2012). Shoots grow from auxiliary buds between unexpanded basal internodes, which is inhibited by internode elongation (Kirby, Appleyard, and Fellowes 1985). As a result, shoot buds neighbouring elongating internodes do not display the outgrowth and maturation response (Foster 1977). This is potentially because shooting is negatively regulated by GA signalling, with GA deficient rice plants showing increased shooting and the growth of shoot buds suppressed by the application of exogenous GA (Ito, Yamagami, and Asami 2018; Lo et al. 2008). This is because in rice, the shoot outgrowth promoter MONOCULM 1 (MOC1) has been shown to bind to the rice DELLA, SLR1, which inhibits degradation of MOC1. GAs mediate the degradation of SLR1 and therefore MOC1, leading to increased stem elongation and reduced shoot number (Liao et al. 2019).

1.4.5 Booting

A vital stage in wheat growth is the booting stage, which begins when the developing head of wheat becomes visible inside the sheath of the stem and finishes the top of the head, the awns, becomes visible (Alghabari et al. 2014). This stage is closely linked to final grain yield, as assimilate partitioning in the developing ear determines floret survival and therefore grain yield potential. (Miralles, Richards, and Slafer 2000). Reduced competition between stem elongation and floret development, as seen in the *Rht* semi-dwarves, is associated with improved grain yields, whilst environmental stress (for example: heat, drought or water

logging) during this time is associated with reduced grain yields (Alghabari et al. 2014; Khakwani et al. 2012).

1.4.6 Floral Induction and Development

The transition from vegetative to reproductive growth involves the reprogramming of vegetative shoot apical meristem (SAM) that produces leaf primordia to an inflorescence meristem (IM) that produces spiklets (Gol, Tome, and von Korff 2017). In cereal crops, the timing of this process influences reproductive success and therefore crop yield. Winter wheat requires vernalisation (a prolonged period of cold) to prevent floral organs developing too early and being damaged by the cold as well as exposure to long days (increased photoperiod during the growing season) (Tamaki et al. 2007). Gibberellin appears to play a role in the vernalisation and photoperiod responses. Winter wheat varieties that have undergone vernalisation flower faster following the application of bioactive GA (Razumov, Lmarj, and Ke-Wei 1960). While the application of bioactive GA to photoperiod sensitive wheat plants grown under short days also accelerated spike development (Pearce, Vanzetti, and Dubcovsky 2013). Furthermore, treatments with the GA biosynthesis inhibitor paclobutrazol (PAC), delayed spike development in plants transferred from short to long days (Pearce, Vanzetti, and Dubcovsky 2013).

Prior to the transition to reproductive growth, the shoot apex is conical with single ridges of leaf primordia. During the transition, the apex becomes more cylindrical and a second ridge forms, consisting of spikelet primordia, which differentiate into spikelets until the final, terminal spikelet forms (Gardner, Hess, and Trione 1985). The spikelet structures then begin to elongate. The empty glumes are the first spikelet structures to differentiate, followed by the lemmas and finally the stamen and pistil (Gardner, Hess, and Trione 1985) (Figure 1.6).

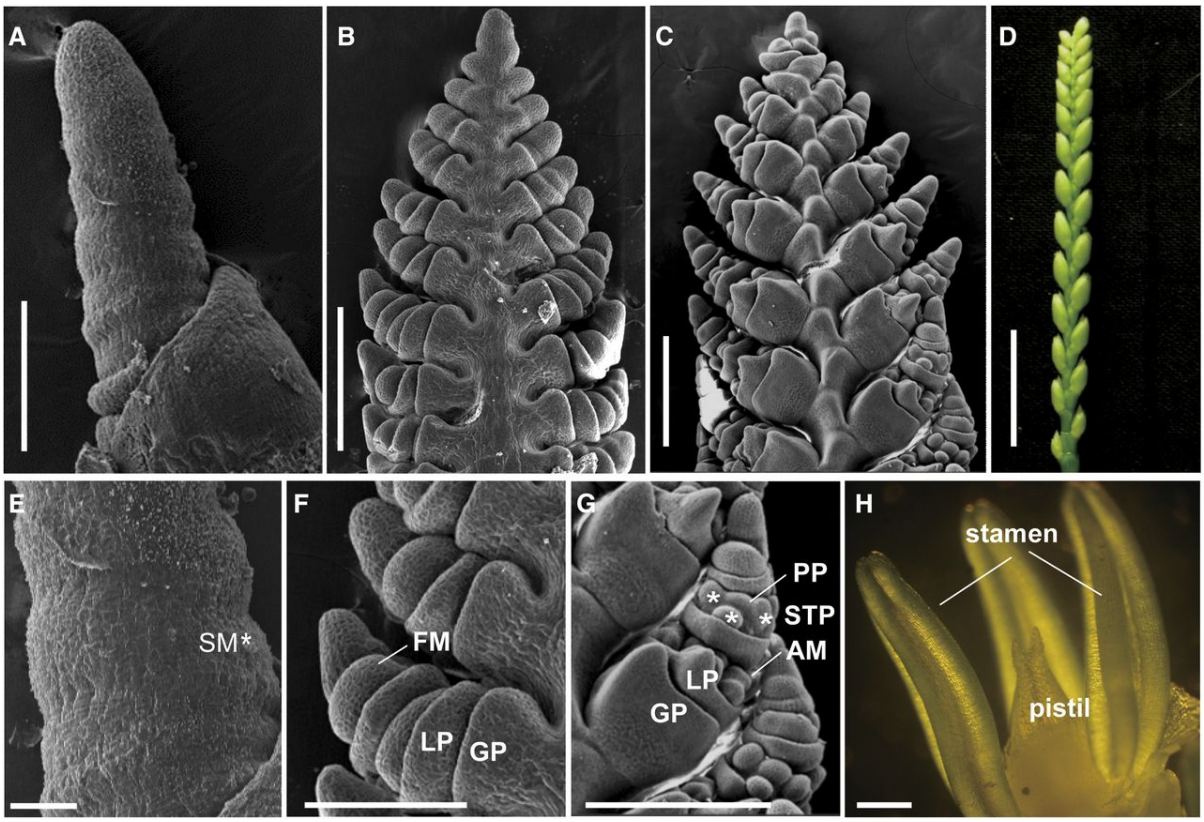

Figure 1.6: Key developmental stages of early wheat inflorescences. (A) and (E): Double ridge stage with initiating spikelet meristems (SM, indicated by *). (B) and (F): Floret meristem (FM) stage with the glume primordia (GP) followed by lemma primordia (LP) and floret meristems. (C) and (G): Anther primordia stage with stamen (STP, indicated by *), pistil primordia (PP) and anther primordia (AM). (D) and (H): Tetrads stage with elongating styles. (E) to (H): are magnifications of A to D. A to C and E to G are SEM images. D and H were taken under a stereomicroscope. Bars: A to C, 0.5 mm; D, 1 cm; E, 0.05 mm; F, 0.25 mm; G and H, 0.5 mm. Figure from (Feng et al. 2017)

By the time the peduncle begins to elongate for ear emergence, the glumes have enclosed and protect the newly formed stamens and pistil (Gardner, Hess, and Trione 1985).

1.4.7 Pollen Development

Although they are not involved in the differentiation of floral organs (Griffiths et al. 2006), the availability of GA is a deciding factor in successful pollen development. This is defined as the production of haploid reproductive gametes with nutrient reserves and a protective coating to enable fertilisation (Vergne, Delvallee, and Dumas 1987) (Figure 1.7).

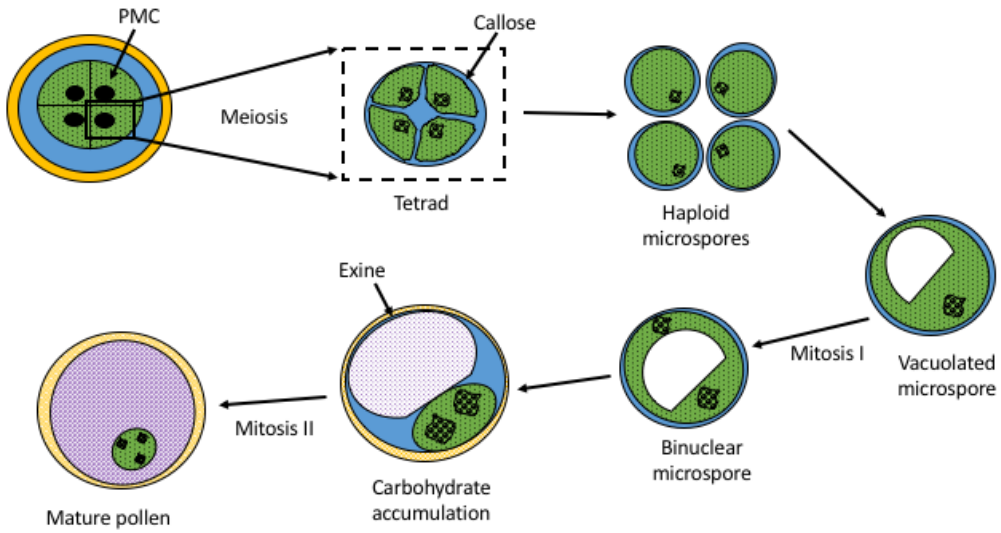

Figure 1.7: Typical Pollen Development in Angiosperms. Meiosis of the pollen mother cell (PMC) results in the formation of a tetrad of microspore cells. These are released into the anther locule following degradation of the callose wall. Free microspores then undergo two rounds of mitosis, accumulate carbohydrates and develop a pollen coat to form mature pollen (adapted from McCormick, 1993).

During the formation of the anther, a primary sporogenous and a primary parietal layer form. The cells in these layers differentiate into pollen mother cells (PMCs) and the three layers of the anther wall: endothecium, middle layer and tapetum (Wilson and Zhang 2009; Zhang and Yang 2014). Meiosis of the PMCs forms tetrads of microspore cells with a callose wall. The callose wall is degraded by enzymes from the tapetum layer of the anther locule (Plackett et al. 2011), which releases the haploid microspores into the anther locule (McCormick 1993). The microspores then undergo two rounds of mitosis, which produces the vegetative cell that maintains pollen function and the two sperm cells required for fertilisation of the ovary and endosperm (McCormick 1993). During mitosis, a vacuole develops in the pollen cells and carbohydrate accumulation begins, resulting in the cells developing a spherical shape (McCormick 1993). The pollen cell walls also begin to form, comprising an inner intine layer and an outer extine layer, which participates in cell-cell recognition during fertilisation (McCormick 1993). During mitosis and the

formation of the exine wall, the tapetum layer undergoes programmed cell death (PCD), releasing components required for pollen development (Plackett et al. 2011; Parish and Li 2010). The completion of the pollen cell wall and cell swelling through carbohydrate accumulation coincides with the degradation of anther wall tissues, enabling the anther theca to split and release pollen into the environment (Matsui, Omasa, and Horie 1999).

Cell-type-specific transcriptome analysis in developing anthers suggests that GA signalling occurs throughout the process of pollen development, with GA-biosynthesis genes most strongly expressed in post-meiotic pollen at the bicellular and tricellular stages (Tang et al. 2010). In rice, severe GA biosynthesis and signalling mutants display male sterility due to the arrest of pollen development (Aya et al. 2009). In the signalling mutant *gid1-4* PMC meiosis fails to complete, whilst in the biosynthesis mutant, *oscps1-1,* pollen development does not proceed beyond the microspore release from the tetrads (Aya et al. 2009). GA signalling also appears to play a crucial role in the activation of PCD of the tapetum layer. Transcriptome analysis has identified an upregulation in GA biosynthesis in the tapetum prior to PCD (Hirano et al. 2010), with the activation of PCD blocked in GA biosynthesis and signalling mutants (Aya et al. 2009). Failure to produce competent pollen is highly detrimental to cereal crops, with reduced fertility negatively impacting crop yield.

1.4.8 Grain Development

Seed development involves two fertilisation events, the initial fertilisation of the egg cell in the female gametophyte and the second fertilisation of the central cell. These result in the formation of the embryonic sporophyte and the endosperm, respectively (West and Harada 1993). GA signalling plays a role in endosperm development, with increased GA content resulting in larger heavier wheat grains in comparison to seeds treated with the GA biosynthesis inhibitor paclobutrazol (Kondhare et al. 2014). While GA stimulation of α-amylase formation occurs during germination (Section 1.4.1) premature α-amylase production and starch degradation (for example due to grains imbibing during wet weather) result in lower quality grain with a low Hagberg Falling Number (HFN), a measure of α-

amylase content in the grain (Lunn et al. 2001). This can result in financial losses as the grain is less desirable and cannot be sold for bread-making (Mares and Mrva 2008).

1.5 *Rht-1* Alleles Disrupt GA-signalling and Plant Development

In contrast to dicot species, which have multiple DELLA paralogues with overlapping functions ((e.g. *RGA, GAI, RGL1, RGL2 and RGL3* in *Arabidopsis* (Dill, Jung, and Sun 2001), monocot species such as wheat, rice and barley contain a single DELLA gene (*RHT, SLR1* and *SLN1*, respectively) that acts to repress all aspects of GA responsive growth (Ikeda et al. 2001; Chandler et al. 2002; Daviere and Achard 2013). Therefore, disruption of these cereal DELLA genes results in plant-wide disruption to GA-signalling (Gallego-Bartolome et al. 2010; Tyler et al. 2004). In wheat, the three *Rht-1* homoeologues*: Rht-A1, Rht-B1* and *Rht-D1*, are expressed at similar levels throughout the plant (Pearce et al. 2011). Therefore, dominant gain-of-function mutations in one homoeoallele (e.g. *Rht-B1b* or *Rht-D1b*) impact all plant developmental processes and cause multiple phenotypic characteristics, known as pleiotropic effects. These can be beneficial, such as reducing stem length but may also negatively impact the plant. Examples of the pleiotropic effects of *Rht-1* mutants are discussed in the following sections.

1.5.1 Plant Organ Expansion

The primary effect of the dwarfing *Rht-1* alleles is a reduction in plant height, with there being a strong correlation between the degree of dwarfism and the reduced responsiveness to GAs (Lenton, Hedden, and Gale 1987; Lenton and Appleford 1991; Pinthus et al. 1989). In a study comparing the effect of *Rht-1* mutants on height in multiple wheat varieties (Bearded April, Bersée, Maris Widegeon and Maris Huntsman) the *Rht-B1b, -D1b* and *-B1c* mutations were found to cause a percentage reduction in height relative to the relevant tall control of 17%, 14% and 50%, respectively. Where mutations were stacked, as in *Rht-B1b+D1b* and *Rht-D1b+B1c,* a cumulative dwarfing effect was observed, with height reductions of 42% and 59%, respectively. The same proportional height reduction was found across the different varieties, regardless of the standard variety height (Flintham et al. 1997). The *Rht-1* alleles do not appear to affect the duration of leaf, stem or ear

development (Fischer and Stockman 1986; Youssefian, Kirby, and Gale 1992b), although one study suggests *Rht-B1c* shows delayed flowering (Wu et al. 2011) Instead, the *Rht-1* alleles produce dwarf and semi-dwarf phenotypes through reduced cell elongation (Keyes 1987; Keyes, Paolillo, and Sorrells 1989) through a reduced cell wall extensibility (Tonkinson et al. 1995; Keyes, Paolillo, and Sorrells 1989).

Reduced cell elongation negatively impacts seedling emergence in drought conditions, where deep-sowing practices may are deployed (Rebetzke et al. 1999). Severe GA insensitive alleles, such as *Rht-B1c*, produce shorter coleoptiles that are less able to emerge and establish, with increased yield losses compared to tall lines (Sojka, Stolzy, and Fischer 1981; Nizam Uddin and Marshall 1989; Amram et al. 2015). Additionally, *Rht-1* genotypes have an increased sensitivity to sowing time, with delayed sowing time negatively impacting grain yield (Balyan and Singh 1994; Kertesz, Flintham, and Gale 1991).

Whilst the leaves of *Rht-1* semi-dwarfs and dwarfs may have a reduced size due to reduced cell elongation (Tonkinson et al. 1995), this is compensated for by upregulation of chlorophyll biosynthesis genes and improved photosynthetic rates (Lecain, Morgan, and Zerbi 1989; Park et al. 2013), that ensure plants are as energetically productive as tall *Rht-1* lines.

1.5.2 Yield and Grain Quality

Improvements to grain yield and quality in the *Rht-1* semi-dwarf lines are a secondary effect of reduced GA signalling. Spikelet number is not increased in *Rht-1* dwarfs and semi-dwarfs (Flintham and Gale 1982; Miralles et al. 1998). Instead, assimilate 'savings' from reduced stem growth are partitioned to the developing ear, which reduces pre-anthetic abortion of distal florets, increasing the total number of viable florets at anthesis (Youssefian, Kirby, and Gale 1992a, 1992b). This more than compensates for reduced plant fertility, as *Rht-D1b* and *Rht-B1b* lines have reduced anther extrusion due to repressed filament elongation (He et al. 2016). Increased infertility is also seen in *Rht-B1c*, through poor anther extrusion and male sterility in the female parent (Boeven et al. 2016), although *Rht-B1c* has

been shown to improve grain yield in April Bearded, Bersée and Maris Widgeon compared to *Rht-1* controls (Flintham et al. 1997).

Increased grain number in *Rht-1* lines is associated with a decrease in grain size and weight, as there is greater inter-floret competition for assimilates (Gooding, Addisu, et al. 2012; Flintham et al. 1997). This was demonstrated in *Rht-B1c* and tall isolines, which produce grains of the same size when shoot number and grains per ear are surgically controlled, minimizing competition between florets (Flintham and Gale 1983).

The grain yield effect of *Rht-1* dwarfing genes is dependent on height of the variety in which they are introduced. Shorter varieties require weaker dwarfing alleles than tall varieties to produce shoot lengths that enable maximal grain yield (70-100 cm) (Flintham et al. 1997; Miralles, Richards, and Slafer 2000) (Figure 1.8).

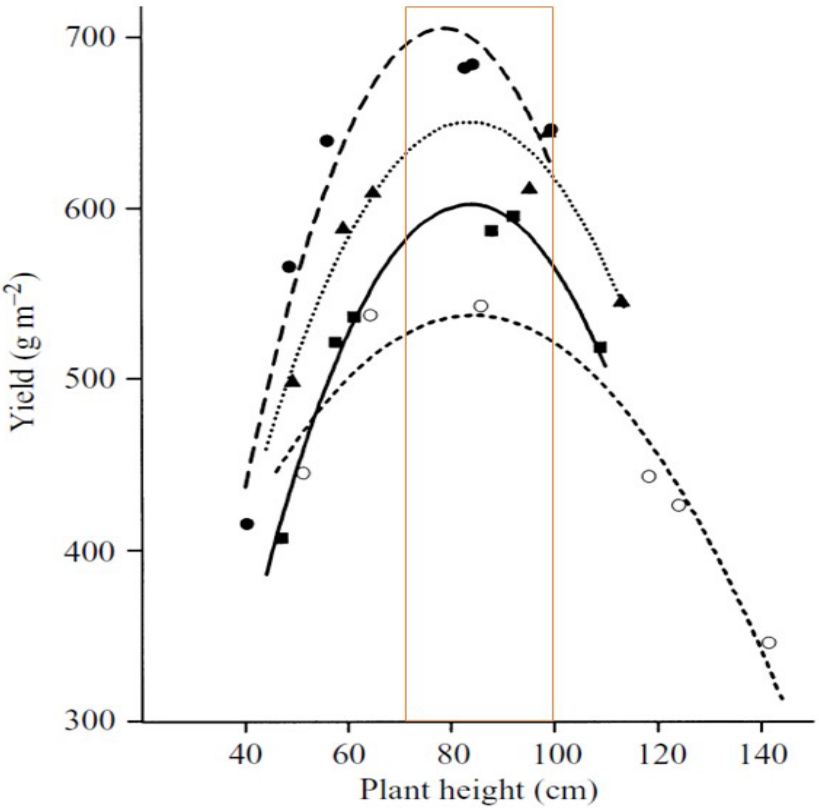

Figure 1.8: Grain yields of different varieties with varying *Rht-1* allele combinations. Points are variety/ *Rht* genotype means over six trials X six replicates, fitted curves are shown as follows: Maris Huntsman (--•--) Grain yield = 28.34(Ht)-0.180(Ht^2)-408, Maris Widgeon (-■-) Grain yield = 22.99(Ht)-0.137(Ht^2)-359, Bersée (..▲..) Grain yield = 20.35(Ht)-0.122(Ht^2)-201, Bearded April (-○-) Grain yield = 10.52(Ht)-0.063(Ht^2)+94. *Rht* genotypes are not labelled. The optimum height to yield ratio is highlighted within an orange box. Figure adapted from (Flintham et al. 1997)

This is reflected in the Flintham (1997) study, the tallest wheat variety Bearded April had the maximum grain yield with the most severe alleles: *Rht-B1c* and *-B1b+D1b,* Bersée and Maris Widegeon saw improved yields compared to the tall controls with the addition of *Rht-B1b, -D1b,* and *-B1c,* whilst the yield of the shortest variety Maris Huntsman was only improved with *Rht-B1b* and *-D1b*.

Across these varieties, increased grain number was associated with reduced grain weight (Flintham et al. 1997), a characteristic that has also been identified in a study if *Rht-1* alleles in isogenic of Maringa spring wheat (Miralles and Slafer 1995).

An additional study of *Rht* dwarfing alleles (*Rht-B1b+Rht-D1b, Rht-B1b, Rht-D1b* and *Rht-1*) in isogenic Maringa lines also determined that a semi-dwarf (*Rht-B1b* or *Rht-D1b*) lines produced the highest grain set (Miralles and Slafer 1997). This was attributed to their radiation use efficiency (RUE), the crop biomass produced per unit of total solar radiation intercepted by the canopy. Pre-anthesis, the reduced height lines had lower RUE, most likely due to poorer canopy architecture through shorter leaf sheath and internode lengths and potentially through reduced canopy CO_2 exchange. However, post-anthesis RUE was inversely correlated to height due to improved sink capacity in the shorter lines and also positively correlated to number of grains set per unit biomass at anthesis (Miralles and Slafer 1997).

GA directly promotes α-amylase production in wheat seeds (Gubler et al. 1995); high quantities of α-amylase in mature grain negatively affects the breadmaking quality of wheat flour (Chamberlain, Collins, and McDermott 1982). During baking, α-amylase degrades the starch in flour, impeding the doughs rising ability and resulting in discoloured and misshapen loaves (Edwards et al. 1989). Hagberg falling number (HFN), the time taken for an object to fall through a hot water/flour mixture can be used to indirectly assess α-amylase amount and activity. If α-amylase activity is high, starch is hydrolysed, which thins out the mixture causing a shorter falling time and low HFN. If α-amylase activity is low, the mixture remains viscous resulting in longer falling time and high HFN (Perten 1964), indicating that the flour is suitable for breadmaking (Mares and Mrva 2008). As the presence of dwarfing *Rht-1* alleles increases GA insensitivity, α-amylase production is reduced in mature seeds (Mares and Mrva 2008), resulting in higher HFNs (Lunn et al. 2001). This is reflected in improved HFNs in the wheat varieties Maris Huntsman (Gold and Duffus 1993), Spica and Lerma 52 (Mrva and Mares 1996) containing *Rht-B1b, -D1b* or *-B1c*, and in the variety Maringá containing *Rht-B1c* derived alleles, which have additional intragenic mutations in the proteins functional C-terminal GRAS domain (Van de Velde, Ruelens, et al. 2017).

Despite affecting HFN, GA insensitivity in *Rht-1* dwarf and semi-dwarf lines has only a limited effect on seed dormancy (Gooding, Uppal, et al. 2012). *Rht-B1b, -D1b* and *-D1c* germinate as readily as *Rht-1* in isogenic lines of Mercia, Maris Widgeon and

Maris Huntsman (Gooding, Uppal, et al. 2012). To date, only *Rht-B1c* has been shown to also increase seed dormancy (Gooding, Uppal, et al. 2012). Unlike *Rht-B1b* and *Rht-D1b, Rht-B1c* seed aleurone activity remains inhibited following exposure to exogenous GA, which may contribute to dormancy (Flintham and Gale 1982). This increased dormancy compared to *Rht-1* is also seen in Maringá varieties containing *Rht-B1c* and *Rht-B1c* derived alleles (Van de Velde, Ruelens, et al. 2017).

1.5.3 Stress Responses

The *Rht-1* alleles have also been demonstrated to alter the responses to abiotic and biotic stresses. Drought conditions during the growing period act to reduce both grain number and weight in *Rht-1* dwarfs and semi-dwarfs compared to tall controls (Fischer and Wood 1978; Dev et al. 1980; Duwayri 1984), due to reduced water efficiency in the *Rht-1* phenotypes (Nizam Uddin & Marshall 1989: Richards 1992b). During heat stress, the shorter *Rht-1* phenotypes produce smaller shoots and leaves, as well as having reduced grain set (Bush and Evans 1988). The timing of the heat stress causes a reduction in yield through different mechanisms. If heat stress occurs at ear initiation, the resulting ears have fewer competent florets. Heat stress during meiosis results in a decline in pollen viability, whilst post-anthesis exposure reduces grain-filling (Hoogendoorn and Gale 1988). As observed in the study by Flintham and colleagues (1997), the impact of the pleiotropic effects varies according to the combination of wheat variety and *Rht-1* allele, with *Rht-B1b+D1b* in Maringa (var.) and *Rht-B1c* in Nainari 60 (var.) being particularly vulnerable to heat stress (Hoogendoorn and Gale 1988). Where plants containing *Rht-B1b, Rht-D1b* or both are stressed with both high temperatures and drought post-anthesis, the yield improvements they usually confer are almost completely eroded (Hoogendoorn and Gale 1988). For this reason these alleles are often not present in commercial varieties grown in regions with hot, dry summers (Kertesz, Flintham, and Gale 1991) . Under these environments, less potent dwarfing alleles such as *Rht-B1d* or Rht8 are used instead (Worland 1986; Börner et al. 1991).

The *Rht-1* dwarf mutants also display altered responses to biotic stresses. During infection, interactions between the phytohormones salicylic acid (SA), ethylene (ET) and jasmonic acid (JA) activate different defence pathways depending on the

whether the pathogen is a biotroph (obtains nutrients from living cells) or a necrotroph (kills cells to obtain nutrients) (Lewis 1973; Saville et al. 2012). The SA and JA/ET defence pathways are antagonistic, with the former associated with improved resistance to biotrophs and later associated with resistance to necrotrophs (Navarro et al. 2008). DELLAs potentiate JA signalling, with gain-of-function mutants such as the *Rht-1* dwarfs further potentiating JA signalling (Navarro et al. 2008). This results in improved resistance to necrotrophs such as *Fusarium graminearum* and *Oculimacula acuformis* in *Rht-1* dwarfs, whilst there is reduced resistance to biotrophic pathogens (e.g. *Botryis graminis*) (Saville et al. 2012).

1.6 Gibberellin Biosynthesis

To date, 136 different gibberellins have been identified and their structures confirmed through a combination of gas chromatography/mass spectrometry (GC/MS) and nuclear magnetic resonance (NMR) studies (MacMillan 1997). Most GAs are inactive intermediates, which are created and catabolised during the biosynthesis of bioactive GAs (e.g. GA_1, GA_3 and GA_4 in wheat) (Hedden and Phillips 2000; Webb et al. 1998). The biosynthetic pathways for bioactive GAs are complex and were initially elucidated in the original source of GAs, the fungus *G. fujikuroi* and were then elucidated in higher plants (MacMillan 1997).

The GA biosynthetic pathway in higher plants occurs in three parts (Figure 1.9), defined by the subcellular compartment and the class of enzymes involved (Hedden and Kamiya 1997).

1) In the plastid, the conversion of geranylgeranyl diphosphate (GGPP) to *ent*-kaurene by diterpene cyclases.
2) In the endoplasmic reticulum (ER) membranes, the conversion of *ent*-kaurene to GA_{12} and GA_{53} by cytochrome P450 mono-oxygenases.
3) In the cytoplasm, the conversion of GA_{12} and GA_{53} to bioactive GA_4 and GA_1, respectively, via 2-oxoglutarate-dependent dioxygenases (2-ODDs) in the non-13-hydroxylation pathway and 13-hydroxylation pathway, respectively.

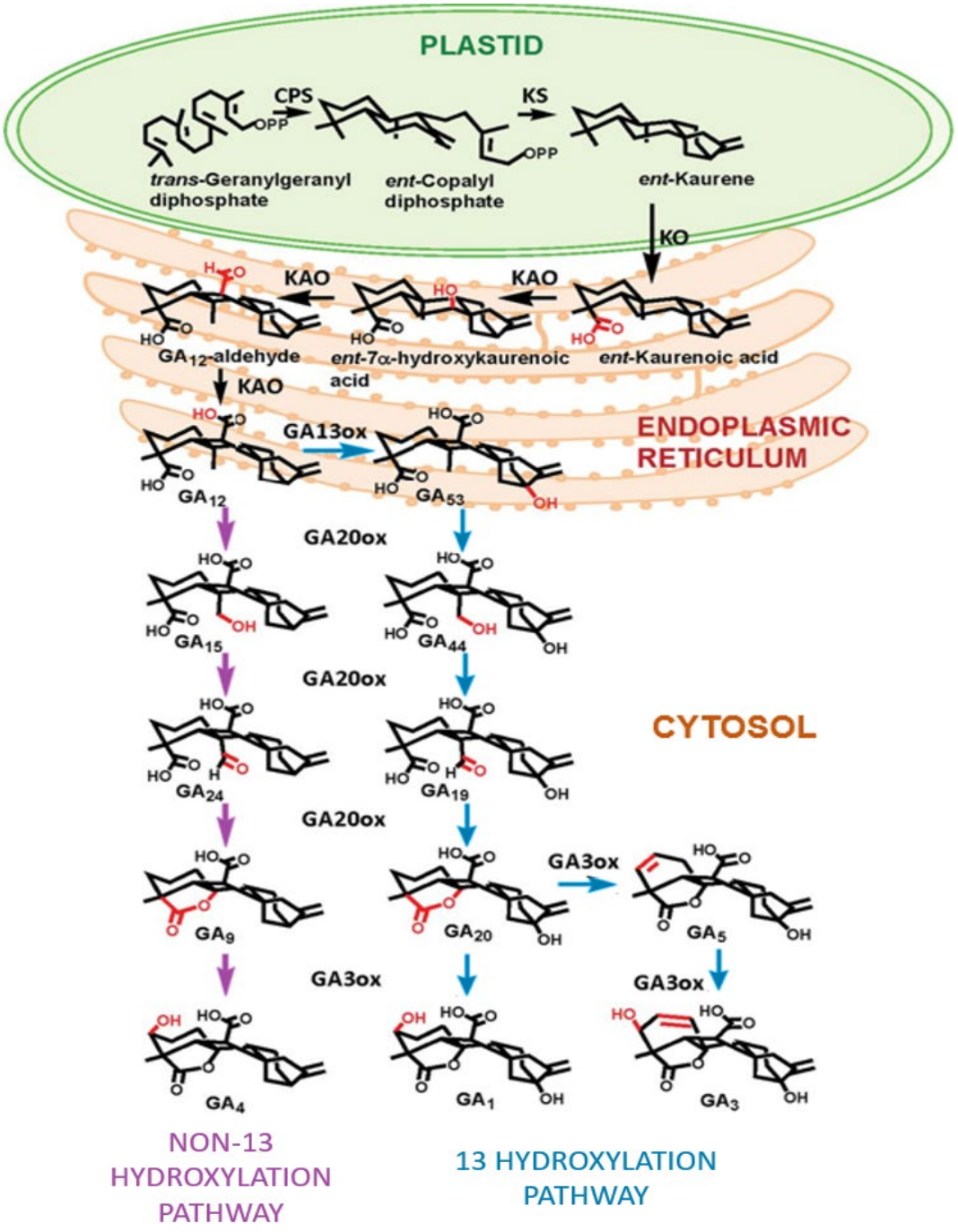

Figure 1.9: The Non-13 Hydroxylation and 13-Hydroxylation Gibberellin Biosynthesis Pathways. Both pathways share common biosynthesis steps (black arrows) in the plastid and endoplasmic reticulum, before diverging into separate pathways in the endoplasmic reticulum and cytosol: purple arrows = non-13 hydroxylation pathway, blue arrows = 13 hydroxylation pathway. The names of the enzymes which catalyse each step are shown. The names and chemical structures of bioactive GAs and their non-bioactive precursors are also shown. Adapted from Hedden and Thomas 2012.

1.6.1 GGPP to *ent*-kaurene

The first part of GA biosynthesis pathway, the conversion of GGPP to *ent*-kaurene, is a two-step process that occurs in the plastids (Aach et al. 1997). The first step is catalysed by the diterpene synthase enzyme, *ent*-copalyl diphosphate synthase (CPS), which converts GGPP into *ent*-copalyl diphosphate (Hedden and Kamiya 1997). The gene encoding this enzyme in *Arabidopsis*, *GA1*, was first identified from the *Arabidopsis* GA-biosynthetic mutant *ga1-3,* using genomic subtraction cloning (Sun, Goodman, and Ausubel 1992). The wheat orthologue *TaCPS* was initially mapped to the long arm of chromosome 7 in wheat (Spielmeyer et al. 2004) and three *TaCPS* genes: *TaCPS1, TaCPS2* and *TaCPS3* cloned *in vitro* using rapid amplification of cDNA ends (RACE) following a BLASTn search of the wheat var. Nourin-61-gou with the nucleotide sequences of rice diterpene cyclase genes (*OsCPS1, OsCPS2/OsCyc2,* and *OsCPS4/OsCyc1*) (Toyomasu et al. 2009; Sakamoto et al. 2004). Two additional *TaCPS* genes *(TaCPS4* and *TaCPS5*) were later cloned using RACE (Wu et al. 2012). To date *TaCPS1-4* have been shown to produce *ent*-CPS (Toyomasu et al. 2009; Wu et al. 2012), while *TaCPS5* is believed to be non-functional (Wu et al. 2012).

A second terpene synthase, *ent*-kaurene synthase (KS), then converts *ent*-copalyl diphosphate into *ent*-kaurene (Hedden and Kamiya 1997). *KS* was initially cloned from a pumpkin cDNA library screen (Yamaguchi et al. 1996) and then from *Arabidopsis* by homology (Yamaguchi et al. 1998). The wheat orthologue, *TaKS,* was identified through blasting the wheat EST database with the nucleotide sequence of the barley *KS* (*HvKS*) and the three homoeologues cloned using PCR-based cloning from Chinese Spring wheat (Huang et al. 2012). *TaKS* has been mapped to the long arm of chromosome 2 in wheat (Spielmeyer et al. 2004; Huang et al. 2012).

1.6.2 *ent*-kaurene to GA_{12}

In the endoplasmic reticulum and chloroplast envelope (Helliwell, Sullivan, et al. 2001), *ent*-kaurene is oxidised to *ent*-kaurenoic acid by the P450 mono-oxygenase, *ent*-kaurene oxidase (KO*).* This is followed by the oxidation of *ent*-kaurenoic acid to GA_{12} via GA_{12}-aldehyde by another P450 mono-oxygenase, *ent*-kaurenoic acid oxidase (KAO). *KO* was originally identified and cloned from an *Arabidopsis* mutant

lacking *ent*-kaurene oxidase activity (Helliwell et al. 1998) and the rice gene was isolated by homology (Itoh et al. 2004). Meanwhile, *KAO* was identified from a GA-deficient barley mutant which lacked *ent*-kaurenoic acid activity and then isolated from *Arabidopsis* (Helliwell, Chandler, et al. 2001). In wheat there are three *TaKO* and *TaKAO* homoeologous genes. These were cloned from Chinese Spring wheat after their sequences were isolated by blast searching *HvKO* and *HvKAO* nucleotide sequences (Huang et al. 2012). The genes have been mapped to chromosomes 7A/B/D and 4A/B/D respectively (Huang et al. 2012).

1.6.3 GA_{12} to GA_4 or GA_1 and GA_3

Following the biosynthesis of GA_{12} the pathway diverges into two parallel pathways, the non-13 hydroxylation pathway and the 13-hydroxylation pathway, which both compete in the cytosol and produce the bioactive GAs, GA_4 and GA_1, respectively (Hedden and Kamiya 1997) (Figure 1.9). The separation of the two pathways is catalysed by GA 13-hydroxylase (GA13ox), which converts GA_{12} to GA_{53} by adding a 13-OH group. This addition is the first step in the 13-hydroxylation pathway, which dominates In wheat (Hedden and Kamiya 1997). GA 13-oxidases were first identified in rice and their function demonstrated through overexpression in transgenic *Arabidopsis* lines (Magome et al. 2013). To identify GA 13-oxidases in wheat, the rice peptide sequences were blasted to identify orthologous genes in *Brachypodium*. The nucleotide sequences of these *Brachypodium* genes were then blasted against the genomic survey sequence from the International Wheat Genome Sequencing Consortium (IWGSC), resulting in the identification of *TaGA13ox1* and *TaGA13ox2* (Pearce et al. 2015).

GA_{53} is then converted into bioactive GA_1 and GA_3 through the creation and conversion of a series of intermediate GAs by 2-oxoglutarate-dependent dioxygenases; GA 20-oxidases (GA20ox) and GA 3-oxidases (GA3ox). These enzymes also act to convert GA_{12} into GA_4 through the same mechanism (Hedden and Kamiya 1997). *GA20ox* genes were first cloned from pumpkin by screening for GA dioxygenase activities expressed as T7 gene 10 fusion proteins in recombinant Escherichia coli (Lange 1997). Meanwhile *GA3ox* genes were initially identified in *Arabidopsis* by screening a cDNA library with a probe isolated from a line containing

an insertion at the *GA4* locus (Chiang, Hwang, and Goodman 1995). The wheat orthologues of these genes (*TaGA20ox1* and TaGA3ox*2*) were cloned by homology from a cDNA library from the wheat variety Maris Huntsman containing the *Rht-B1c* (*Rht3*) allele (Appleford et al. 2006). Four *TaGA20ox* (*TaGA20ox1-4)* and one *TaGA3ox* (*TaGA3ox3), TaGA3ox2* has been renamed *TaGA1ox-B1* as it was found to encode a GA 1-oxidase, genes have been identified in wheat (Pearce et al. 2015).

1.6.4 Gibberellin 2-oxidase

The GA inactivation gene, *GA2ox*, encodes a 2-oxoglutarate-dependent dioxygenase that catalyses the conversion of bioactive GAs and their precursors to inactive products through 2β-hydroxylation (Thomas, Phillips, and Hedden 1999). There are two classes of GA2oxs, C_{19}-GA2oxs and C_{20}-GA2oxs, which are separated based on their substrates (Schomburg et al. 2003). C_{19}-GA2oxs catabolise C_{19}-GAs, the bioactive GA_1 and GA_4 as well as their precursors GA_9 and GA_{20} (Lester et al. 1999). Meanwhile, C_{20}-GA2oxs catabolise C_{20}-GAs, GA_{12} and GA_{53} to GA_{10} and GA_{97}, respectively (Schomburg et al. 2003; Sakamoto et al. 2004). The conversion to products that are inactive and cannot be converted to active products prevents accumulation of bioactive GAs, enabling their levels to be tuned appropriately for plant tissues or developmental stage (Thomas, Phillips, and Hedden 1999).

Ten *GA2ox* genes, consisting of both C_{19}-GA2oxs and C_{20}-GA2oxs, have been identified in rice (Sukai et al. 2002; Nakamura et al. 2007). These genes have been shown to be differentially expressed during rice development. For example RT-PCR has demonstrated that *GA2ox2* and *GA2ox6* have low expression levels during vegetative growth and high expression during the reproductive development stages (Lo et al. 2008). The remaining eight genes have been shown to be most highly expressed during vegetative growth (Lo et al. 2008). Overexpression of both C_{19}-GA2oxs and C_{20}-GA2oxs in transgenic rice results in crop height reductions, without appearing to affect male fertility or crop yield (Sakamoto et al. 2003; Huang et al. 2010). In wheat, there appear to be fourteen *Ga2ox* genes (Braun et al. 2019). The semi-dwarf phenotype of the wheat mutant *Rht18* is due to the overexpression of *GA2oxA9*, a C_{20}-GA2ox which reduces the availability of GA_1, presenting an alternative means to reduce crop height without affecting DELLA function (Vikhe et

al. 2017; Ford et al. 2018). Additionally, *GA2ox12* (formerly *GA2ox14*) appears to be upregulated in the semi-dwarf wheat mutant *Rht12* although the nature of the interaction between the two genes remains unclear (Sun et al. 2019).

1.6.5 GA Biosynthesis is Feedback Regulated

Gibberellins are key regulators of most plant developmental processes; therefore, their endogenous levels must be fine-tuned. Although the molecular mechanisms are still to be fully described, GA homeostasis appears to be depend on GA signalling components (Sun 2011) to feedback control different steps in the GA biosynthesis pathway (Martin, Proebsting, and Hedden 1999).

The idea that GAs regulate their biosynthesis came from the discovery that wheat lines containing the DELLA mutations *Rht-D1b* and *Rht-B1b* are insensitive to the application of exogenous GA but have elevated GA levels (Radley 1970), and the subsequent discovery that *Rht-B1b* and *Rht-B1c* lines accumulate C_{19} GAs but not C_{20} GAs in comparison to WT *Rht-B1a* lines (Appleford and Lenton 1991). These results were duplicated in studies of *dwarf-8* in maize (Fujioka et al. 1988) and *gai* in *Arabidopsis* (Talon, Koornneef, and Zeevaart 1990), suggesting that GA20ox activity was upregulated in gain-of-function DELLA mutants. This concept was later backed up by biochemical studies on the *dwarf-8* mutant in maize, which lacks GA3ox activity (Spray et al. 1996). These identified that levels of GA_{53} and GA_{19} were significantly lower in *dwarf-8* plants than wild-type plants. As GA_{53} and GA_{19} are substrates of GA20ox, this suggested that expression of *GA20ox* was higher in the mutant lines. The application of exogenous GA reversed this effect, increasing levels of GA_{53} and GA_{19}, which suggested that GA20ox was subject to feedback regulation (Hedden and Croker 1992).

It has since been shown that most members of the *GA20ox* and *GA3ox* gene families are targets of a feedback-mediated regulatory mechanism (Hedden and Phillips 2000), with substantial evidence suggesting that DELLAs directly mediate this process (Hedden and Thomas 2012). Transcriptional studies in pea and *Arabidopsis* have demonstrated low transcript levels of *GA20ox* and *GA3ox* in null DELLA mutants and high transcript levels in gain-of-function mutants (Weston et al. 2008;

Dill, Jung, and Sun 2001; Silverstone et al. 2001; Dill and Sun 2001). Similarly, *Arabidopsis* mutants lacking essential signalling components (GID1 and GID2/SLY1) for GA mediated degradation of DELLA show high transcript levels of *GA20ox* and *GA3ox* (Griffiths et al. 2006; Sasaki et al. 2003; McGinnis et al. 2003).

Observations in different plant species suggest that there may be multiple feedback mechanisms for *GA20ox* and *GA3ox,* which mostly have not been described fully. For example, in *Arabidopsis,* the overexpression of AT-hook protein of GA feedback 1 (AGF1) results in upregulated transcript levels of *At3ox1*. AGF1 contains a DNA binding motif and has been shown to localize in the nucleus using AGF1-GFP fusion proteins in transgenic *Arabidopsis* lines, suggesting it functions as a transcriptional regulator of *At3ox1* (Matsushita et al. 2007). Similarly, the nuclear localization of b-ZIP transcription factor REPRESSION OF SHOOT GROWTH (RSG) in tobacco has been found to be inhibited by the presence of GA, preventing *NtGA20ox1* expression (Fukazawa et al. 2010), while GA enhanced the expression of the C_2C_2 zinc finger protein OsYABBY1 in rice that suppresses *OsGA3ox* expression (Dai et al. 2007). However, the mechanism of action and potential link to DELLA has not yet been established.

A more elucidated mechanism involves the GAI-ASSOCIATED FACTOR1 (GAF1). GAF1 is transcription factor with zinc finger motifs similar to INDETERMINATE1 (ID1) in maize and 16 ID1 domain (IDD) proteins in Arabidopsis (Fukazawa et al. 2014), which bind to the consensus sequence TTTTGTCG (Kozaki and Colasanti 2005). In the absence of DELLA, GAF1 interacts with TOPLESS-RELATED (TPR) which represses *AtGA20ox2* and *AtGA3ox1* expression (Fukazawa et al. 2014). Transactivation assays in *Arabidopsis* leaves has shown that the *Arabidopsis* DELLA GAI and GAF1 form a GAI-GAF1 complex, which activates the promoter of *AtGA20ox2* (Fukazawa et al. 2017). These data in combination with ChIP analysis suggest that a decrease in GA promotes the accumulation of DELLAs, which form a complex with GAF1 at the *AtGA20ox2* promoter, resulting in increased expression of this gene and the accumulation of bioactive GA. This results in the increased degradation of DELLA, which reduces the amount of GAF1-DELLA complex to bind to the *AtGA20ox* promoter (Fukazawa et al. 2017).

Not all GA homeostasis mechanisms may involve transcriptional feedback regulation. During a study on photoperiodic regulation of *GA20ox,* western blots from spinach petioles and shoot tips treated with GA biosynthesis inhibitors identified the SoGA20ox1 protein. A subsequent investigation for transcriptional feedback regulation of *SoGA20ox1* in these treated tissues returned no evidence of a change in *SoGA20ox1* transcript levels, suggesting the action of a post-transcriptional regulatory mechanism (Lee and Zeevaart 2007).

1.7 DELLAs Proteins Repress GA Signalling

Over 50 years ago, a slender garden pea (*Pisum sativum* L.) mutant, *la cry,* that produced an overgrowth phenotype independent of plant GA levels was identified (Brian 1957; Weston et al. 2008). This led to the proposal that GAs act as 'inhibitors of inhibitors', promoting growth by overcoming inhibition by *CRY* and *LA* gene products (Brian 1957). Over the following years, additional height mutants that acted independently of endogenous and exogenous GA were identified, which enhanced the idea that GA had a common mechanism to control plant growth (Talon, Koornneef, and Zeevaart 1990). Some of these mutants displayed a similar elongated phenotype to *la cry* e.g. *slr1-1* in rice (Ikeda et al. 2001) and *sln1* in barley (Foster 1977), whilst others produced a dwarf phenotype: *gai-1* in *Arabidopsis* (Koornneef et al. 1985), *Rht-B1b, Rht-D1b* and *Rht-B1c* in wheat (Gale and Marshall 1973; Radley 1970) and *d8* in maize (Phinney 1956). Studies on the dwarf mutant *gai-1* demonstrated elevated levels of GA *in planta,* from which researchers inferred that WT *GAI* encoded a GA signal transduction component (Talon, Koornneef, and Zeevaart 1990). Subsequent cloning of WT *GAI* and *gai-1*, revealed a 17 amino acid in frame deletion in the N-terminal region of *gai-1,* suggesting that GAI is a negative regulator of GA signalling and *gai-1* is a semi-dominant, gain-of-function mutant (Peng et al. 1997).

The sequencing of *GAI* revealed a substantial similarity to the *Arabidopsis* gene RGA, which was identified in a screen to identify suppressor mutations that rescued the dwarf phenotype *ga1-3* (Silverstone, Ciampaglio, and Sun 1998). Both *GAI* and *RGA* also shared substantial similarity to the C-terminal region of *SCARECROW (SCR)*, which encodes a transcription factor implicated in cell-layering in *Arabidopsis* roots

(Peng et al. 1997). These proteins were the first identified members of the GRAS family (named after GAI, RGA and SCR), whose members are defined by a highly-conserved C-terminal GRAS functional domain. GRAS proteins involved in GA signalling (e.g. GAI and RGA) also contain a highly conserved N-terminal region that has DELLA and TVHYNP motifs. This sub-group of the GRAS family has subsequently been named DELLA (Wen and Chang 2002), as the DELLA motif was part of the 17 amino acids that are lacking in the *gai* mutant (Peng et al. 1997) (Figure 1.10).

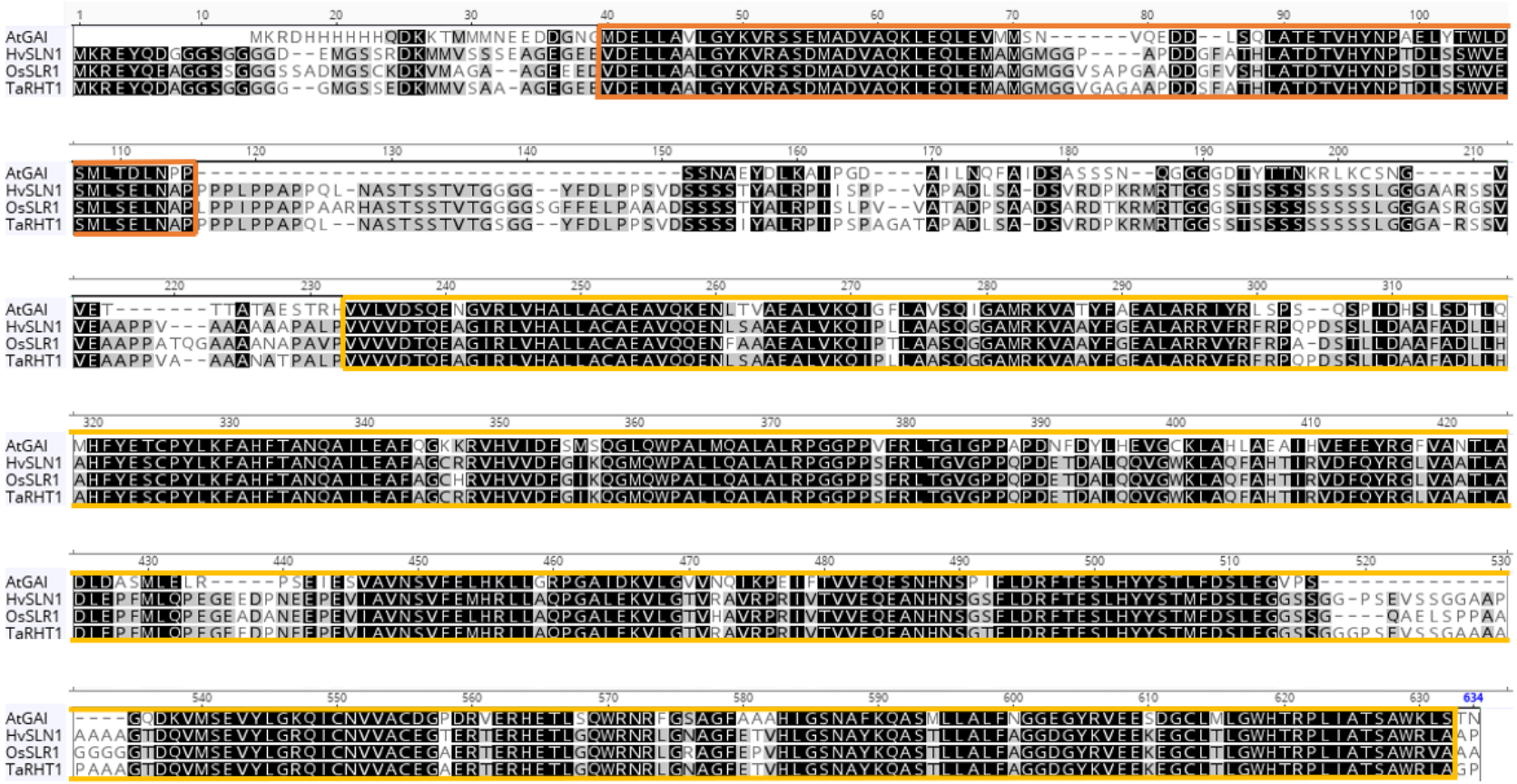

Figure 1.10: Alignment of DELLA Amino Acid Sequences. *Arabidopsis thaliana* GAI (AtGAI), *Hordeum vulgare* SLN1 (HvSLN1), *Oryza sativa* SLR1 (OsSLR1) and *Triticum aestivum L.* RHT (TaRHTA1). The conserved N-terminal domain is boxed in orange, the conserved C-terminal domain is boxed in yellow.

Following the identification of *GAI* and *RGA* as DELLA genes, many DELLA orthologues in other plant species have been identified: *RHT-1* in wheat (Peng et al. 1999), *SLENDER1 (SLR1)* in rice (Ikeda et al. 2001) and *SLENDER1* (*SLN1*) in barley (Chandler et al. 2002), the *DWARF 8* (*D8*) and *DWARF 9* (*D9*) paralogues in maize (Peng et al. 1999), *BrRGA1* in oil seed rape (Muangprom et al. 2005), *PROCERA* (*PRO*) in tomato (Jasinski et al. 2008) and *LA* and *CRY* in garden pea (Weston et al. 2008). The number of DELLA genes varies according to whether the plant is a monocot or dicot species, with dicots having multiple DELLA paralogues (Dill, Jung, and Sun 2001), whilst monocots, with the exception of maize, have a single DELLA

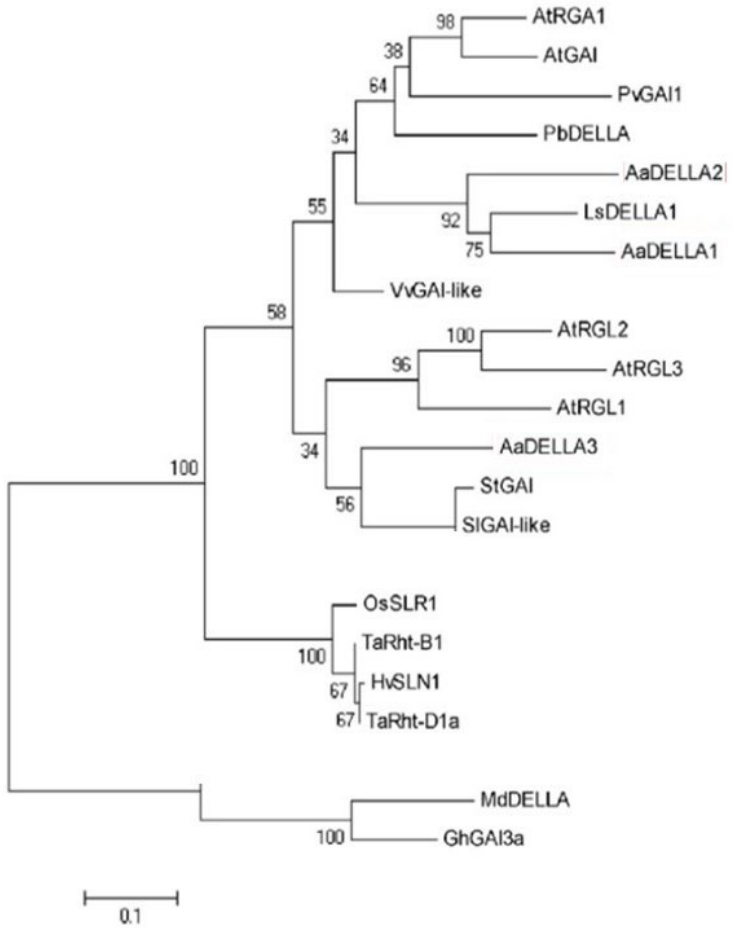

Figure 1.11: Maximum phylogenetic tree of plant DELLA proteins. Numbers of branches represent bootstrap support for 1000 replicates. DELLAs included: *Arabidopsis thaliana* RGA1 (AtRGA1), *Arabidopsis thaliana* GAI (AtGAI), *Phaseolus vulgaris* GAI1 (PvGAI1), *Pyrus bretschneideri* DELLA (PbDELLA), *Artemisia annua* DELLA2 (AaDELLA2), *Lactuca sativa* DELLA1 (LSDELLA1), *Artemisia annua* DELLA1 (AaDELLA1), *Vitis vinifera* GAI-like (VVGAI-like), *A. thaliana* RGL2 (AaRGL2), *A. thaliana* RGL3 (AtRGL3), *A. thaliana* RGL1 (AtRGL1), *A. annua* DELLA3 (AaDELLA3), *Solanum tuberosum* GAI (StGAI), *Solanum lycopersicum* GAI-like (SlGAI-like), *Oryza sativa* SLR1 (OsSLR1), *Triticum aestivum L.* Rht-B1 (TaRht-B1), *Hordeum vulgare* SLN1 (HvSLN1), *T. aestivum L.* Rht-D1a (TaRht-D1a), *Malus domestica* DELLA (MsDELLA), *Gossypium hirsutum* GAI3a (GhGAI3a). From (Shen et al. 2015)

gene, with wheat having three homoeologous *Rht* genes (Ikeda et al. 2001; Chandler et al. 2002; Daviere and Achard 2013) (Figure 1.11) .

1.7.1 Gibberellins Regulate DELLAs Through Targeted Degradation

An important breakthrough in proving the 'inhibitors of inhibitors' hypothesis (Brian 1957), that GAs inhibit DELLAs which themselves inhibit GA responses, came through the use of GFP-RGA fusion proteins in transgenic *Arabidopsis* lines. This study demonstrated that *in planta* DELLAs rapidly degrade following the application of bioactive GAs (Silverstone et al. 2001). The endogenous DELLAs of barley (Chandler et al. 2002) and rice (Itoh et al. 2002) were found to respond in the same fashion, suggesting a common mechanism where GAs relieve DELLA mediated repression by initiating the targeted degradation of DELLAs (Dill et al. 2004). Tall, slender DELLA mutants were found to be the result of loss-of-function mutations that inhibited DELLA repression of GA, resulting in GA over-dose phenotypes (Ikeda et al. 2001; Chandler et al. 2002). By contrast, dwarf DELLA mutants found to be the result of gain-of-function mutations that block GA-mediated DELLA degradation resulting in GA-insensitivity through constitutively repressed GA responses. These mutations were found in the conserved N-terminal motifs 'DELLA' and 'TVHYNP', demonstrating their importance in DELLA regulation (Figure 1.7.2) (Dill, Jung, and Sun 2001; Peng et al. 1997).

The recognition of DELLAs for degradation occurs through GA-stimulated interaction with the GA-receptor, GID1, which was first identified and cloned from the severe rice dwarf *gid1*, which is insensitive to GAs (Ueguchi-Tanaka et al. 2005). The suggested mechanism of DELLA degradation through the formation of the GA-GID1-DELLA complex is shown in Figure 1.12.

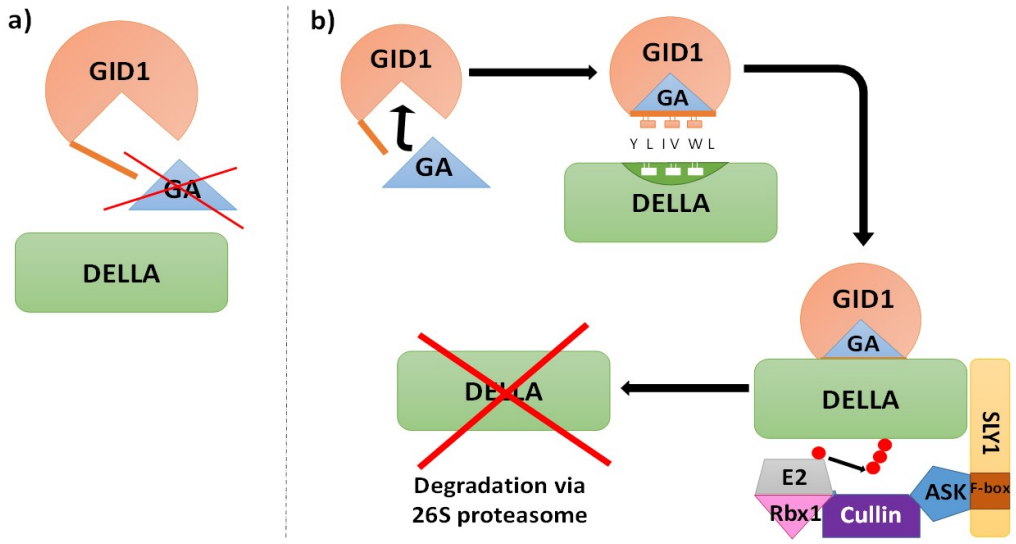

Figure 1.12: GID1 and GA mediated degradation of DELLAs. A) In the absence of GA, DELLAs are stable and act to repress GA-mediated responses. **B)** In the presence of GA, GA binds to the GA INSENSITIVE DWARF1 (GID1) receptor. The GID1 lid closes, exposing the hydrophobic residues: L, W, V, I, L and Y, which bind to the conserved N-terminal DELLA/TVHYNP motif on the DELLA protein. The SLY1/GID2 F-box component of SCF SLY1 E3 ubiquitin ligase recognises the DELLA-GID1-GA complex and binds to DELLA before catalysing the transfer of ubiquitin (red circles) from E2 to DELLA. SCFSLY1 E3 ubiquitin ligase also consists of the Skp1 homologue ASK1, Cullin and RBX1. The polyubquitination of DELLA targets DELLA for 26S proteasome-mediated degradation. Figure adapted from Nelson and Steber (2016).

In the absence of GA, (Figure 1.12A) DELLA proteins are stable and able to repress GA-regulated processes such as elongation growth (Sun 2010; Ikeda et al. 2001). When GA is present in tissues, (Figure 1.12.b) it acts as an allosteric inducer of the GIBBERLLIN INSENSITIVE DWARF1 (GID1) receptor, enabling the GID1 lid to close and expose the hydrophobic residues (L, W, V, I, L and Y), which bind to the conserved N-terminal DELLA/TVHYNP motifs on the DELLA protein. In rice, this binding is stabilized by the C-terminal GRAS domain, as the dwarf mutant *Slr1-d4* (with a G576V substitution) has diminished binding to GID1 (Hirano et al. 2010).

The DELLA-GID1-GA complex is recognised and bound to the SLY1/GID2 F-box component of an SCF ubiquitin E3 ligase. The recognition of the DELLA-GID1-GA complex by the GID2 F-box component is also dependent on the GRAS domain in rice, as the Slr1-d4-GID1-GA complex has extremely limited binding to GID2 (Hirano et al. 2010). The SCF ubiquitin E3 ligase catalyses the transfer of ubiquitin from E2

to DELLA. The polyubiquitination of DELLA then targets it for 26S proteasome-mediated degradation (Sasaki et al. 2003).

1.7.2 DELLA Function

Early DELLA studies identified that GA-insensitive dwarfing mutations in *Arabidopsis* and wheat led to the disruption to the N-terminal 'DELLA' motifs (Peng et al. 1997; Peng et al. 1999; Dill, Jung, and Sun 2001) that prevented GA-mediated degradation of DELLA proteins, resulting in constitutive repression of GA signalling (Silverstone et al. 1997; Dill, Jung, and Sun 2001). Transactivation assays in spinach leaves using truncated variations of the rice DELLA SLR1 (formerly OsGAI) then identified that amino acids 69-276 were required for activation of the reporter gene (Ogawa et al. 2000). This suggested that SLR1 functioned as a transcriptional regulator, potentially a transcriptional activator or co-activator that controlled the expression of transcriptional repressors of GA signalling (Ogawa et al. 2000).

That DELLAs function as transcriptional regulators was confirmed with a chromatin immuno-precipitation (ChIP) experiment. This determined that the *Arabidopsis* DELLA, RGA, can bind to the promotors of 14 early GA response genes, either directly or as part of a complex (Zentella et al., 2007). The genes for two GA biosynthetic enzymes (*GA20ox2* and *GA3ox1*) and two GA receptors (*GID1a* and *GID1b*) were upregulated by RGA suggesting that DELLAs may help establish GA homeostasis by promoting expression of genes associated with the targeted degradation of DELLA (Chapter 1.7.1). Additionally, RGA was found to increase the expression of downstream components: *bHLH137*, *bHLH154*, and the MYB factor *GL1,* that act as repressors of GA signalling (Qi et al. 2014)

In the absence of GA, DELLAs remain stable and repress all GA-dependent growth and development by physically interacting with a range of DELLA-interacting proteins (DIPs). DELLA-DIP interactions repress growth and development through multiple mechanisms (Van de Velde, Ruelens, et al. 2017): the activation of genes that repress plant growth and development, the sequestration of proteins that promote growth and development and the sequestration of proteins that inhibit growth repressor expression. These mechanisms enable DELLAs to mediate plant

development and adaptation to environmental conditions (Lim et al. 2013; de Lucas et al. 2008).

1.7.2.1 DELLAs Sequester Proteins to Alter Gene Expression

The first identified mechanism of DELLA-mediated regulation of transcription, involves the sequestration of PHYTOCHROME INTERACTING FACTORS (PIFs), PIF3 (Feng et al. 2008) and PIF4 (de Lucas et al. 2008) from the bHLH transcription factor (TF) family (Toledo-Ortiz, Huq, and Quail 2003). Using ChIP and transcriptional assays, PIF3 and PIF4 were shown to be inhibited by interactions with DELLA, preventing them from binding to the promoters of their target genes (Feng et al. 2008; de Lucas et al. 2008). Biochemical assays demonstrated that DELLAs bind to the conserved bHLH DNA-binding domains of PIF3 and PIF4, effectively sequestering the TFs (Feng et al. 2008; de Lucas et al. 2008). Both PIF3 (Kim et al. 2003) and PIF4 (Huq and Quail 2002) have been identified as growth-promoting, negative regulators of phytochrome-regulated responses. Thus, they provide a means to coordinate hypocotyl growth to light and gibberellin signalling. Light increases the accumulation of DELLAs (Achard et al. 2008), which sequester PIF3 and PIF4 (Feng et al. 2008; de Lucas et al. 2008). Additionally, light induces the phosphorylation and degradation of PIF3 and PIF4 by the 26S proteasome following PIF interactions with photoactivated phytochromes (de Lucas et al. 2008). The net result of these processes is the inhibition of daytime hypocotyl elongation (Feng et al. 2008). DELLAs have also been demonstrated to interact with PIF5, which alongside PIF3 and PIF4 is required for skotomorphogenesis following germination (Leivar et al. 2008). Again, DELLAs act to inhibit the activity of PIF5 through physical interaction (Gallego-Bartolome, Alabadi, and Blazquez 2011), ensuring that hypocotyl elongation and cotyledon opening occur in the correct sequence (Alabadi et al. 2008).

Additionally, DELLAs have been demonstrated to sequester the chromatin remodelling enzyme PICKLE (PKL) through direct binding (Zhang et al. 2014). Initially, PKL was shown to activate genes such as *IAA19* and *PRE1* that are involved in hypocotyl elongation by binding directly to the transcription factors PIF3 and BRASSINAZOLE-RESISTANT1 (BZR1) (Bai et al. 2012; Zhang et al. 2014), suggesting

that DELLA and PKL have an antagonist role in regulating hypocotyl elongation (Zhang et al. 2014). However, a recent RNA-sequencing (RNA-seq) study with *ga1-13* and *ga1-13 pkl* lines has allowed for the identification of genes that are either regulated by GA, PKL or both. This determined that 80% of GA responsive genes are PKL-dependent, suggesting that PKL and DELLA may have antagonist roles in regulating a range of developmental processes, from cell division and elongation to phase transitions and vegetative growth (Park et al. 2017).

1.7.2.2 DELLA-TF Interactions that Promote Gene Expression

DELLA-TF interactions do not solely involve the sequestration of TFs, DELLAs have also been shown to target gene promoters. The DELLA-GAF1 complex which activates the promoter of the GA biosynthesis gene *AtGA20ox*, promoting GA homeostasis, has already been discussed in Section 1.6.4. Additional DELLA transactivation complexes with other IDD proteins have also been shown to provide homeostatic control of the GA signalling pathways. Yeast 2-hybrid screens have demonstrated that IDD3, 4, 5, 9 and 10 bind to the *Arabidopsis* DELLA RGA and to SCARECROW-LIKE 3 (SCL3) (Yoshida et al. 2014), a GA-positive regulator that promotes GA responses by inhibiting DELLA function through direct protein-protein interaction (Zhang et al. 2011). *SCL3* is a transcriptional target for both the DELLA-IDD and SCL3-IDD complexes, with increases in SCL3 abundance associated with decreased formation of the DELLA-IDD complex and suppression of *SCL3* expression. This feedback loop enables homeostatic regulation of GA signalling by regulating the protein levels of downstream signalling components (Zhang et al. 2011).

1.7.2.3 DELLAs induce Accumulation of Prefoldin

Initially, DELLA function was believed to be limited to transcriptional control (Ogawa et al. 2000). However, in recent years transgenic *Arabidopsis* lines have been used to demonstrate that DELLA interacts with the α-subunit of the prefoldin complex, PREFOLDIN 5 (PFD5) in the absence of GA, resulting in accumulation of PFD5 in the nucleus (Locascio, Blazquez, and Alabadi 2013). This compromises α/β-tubulin heterodimer availability for microtubule organization, inhibiting microtubule growth (Locascio, Blazquez, and Alabadi 2013). As DELLA stability varies by the circadian clock, with higher stability during the day (Arana et al. 2011), this causes

microtubule orientation to oscillate diurnally with maximal growth hypocotyl growth occurring at night (Locascio, Blazquez, and Alabadi 2013).

1.8 DELLA Protein Structure-Function

DELLA proteins are a sub-group of the GRAS family of transcriptional regulators, identified initially through their highly conserved C-terminal domains: LHR1, VHIID, LHR2, PYYRE and SAW (Sun, Jones, and Rikkerink 2012). The DELLA sub-group also contains a unique combination of conserved N-terminal domains: DELLA, LExLE and TVHYNP (Murase et al. 2008) (Figure 1.13).

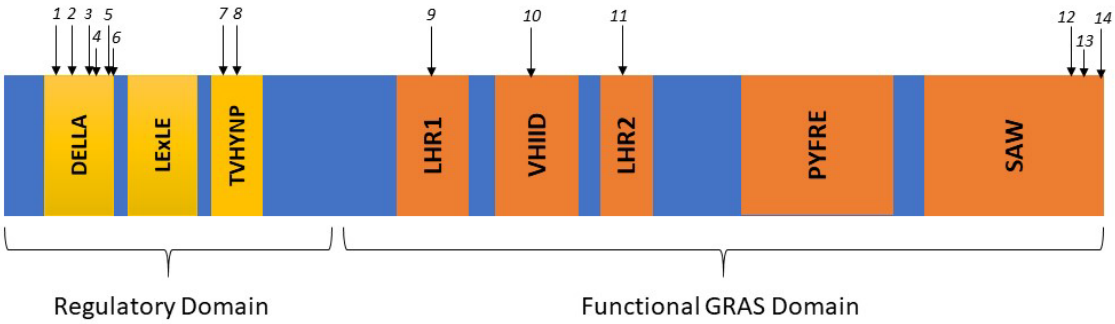

Figure 1.13: Schematic Diagram of the Conserved Motifs in DELLA Proteins. Conserved motifs in the regulatory N-terminal domain are shown in yellow. Conserved motifs in the functional C-terminal GRAS domain are shown in orange. Gain-of-function mutations: 1 = *Gai-1* (17 amino acid deletion – D^{27}-A^{43}), 2 = *Sln1-d* (G46E), 3= *Rht-B1c* (30 amino acid insertion between K^{48}-V^{49}), 4 = *Slr1-d2* (V49M), 5= *Rht-B1b* (Q65*), 6 = *Rht-D1b* (E62*), 7 = *Slr1-d3* (L99F) and 8 = *Slr1-d1* (M106K). Loss-of-function mutations: 9 = *slr1-6* (V281D), 10 = DLE420AAA, 11 = PYL321AAA, 12 = *rga* (D504N), 13 = *slr1-3* (W609*), 14 = *slr1-7* (T617P) and 15 = *slr1-4* (W620*).

The relationship between DELLA structure-function is still being uncovered; however it has been established that the conserved N-terminal motifs, DELLA, LExLE and TVHYNP, are involved in DELLA protein binding to the GA-GID1 complex (Section 1.7.1) , the first step in the targeted degradation pathway (Dill, Jung, and Sun 2001; Murase et al. 2008). Gain-of-function DELLA mutants arise from disruption to these motifs (Figure 1.12). Mutations can be in the form of amino acid deletions, *gai-1* (17 amino acid deletion D^{27}-A^{43}) in *Arabidopsis* (Peng et al. 1997); insertions, *Rht-B1c* (30 amino acid insertions between K48 and V49) or substitutions, *Sln1-d* (G46E) in barley (Chandler et al. 2002), *Slr1-d2* (V49M) and *Slr1-d3* (L99F) in rice (Asano et al. 2009) and *Rht-B1b (Q65*)* and *Rht-D1b* (E62*) in

wheat (Peng et al. 1999). The mutations inhibit the formation of the GA-DELLA-GID1 complex, preventing DELLA degradation and resulting in constitutive GA-insensitivity (Peng et al. 1997; Chandler et al. 2002; Asano et al. 2009).

The N-terminal domain does not appear to be exclusively involved in regulating GID1-mediated degradation. Yeast one-hybrid screens of the rice DELLA, SLR1, identified that the motifs DELLA and TVHYNP are important for transactivation, as deletions in either motif resulted in a decline in transactivation activity (Hirano et al. 2012). Additionally, it has been suggested that the first 70 amino acids in RHT are involved in regulating seed dormancy (Van de Velde, Chandler, et al. 2017). The *Rht-1* mutants *Rht-B1b, Rht-D1b* and *Rht-D1c* are hypothesized to produce N-terminally truncated proteins (Peng et al. 1999) that lack the first 66-70 amino acids. These truncated proteins limit stem elongation (Flintham et al. 1997; Pearce et al. 2011), but have no effect on seed dormancy, suggesting that those early amino acids are involved in the regulation of stem elongation and not seed dormancy (Van de Velde, Chandler, et al. 2017).

The C-terminal GRAS domain enables DELLA repression of GA-mediated growth and development (Peng et al. 1997). Disruption to these domains results in slender plant phenotypes, demonstrating their requirement for the repression of GA signalling (Hirano et al. 2012). In rice, the introduction of amino acid substitutions in various GRAS domains, have been shown to produce slender phenotypes in transgenic lines (Figure 1.12). However, the severity of SLR1 repression varied according to the mutation location: *slr1-6* (V281D) in LHR1, RGA in PYFRE and *slr1-3* (W609*), *slr1-7* (T617P) and *slr1-4* (W620*) produced the most severe phenotype. Meanwhile mutations in VHIID (DLE420AAA) and LHRII (PYL321AAA) had minimal effect (Hirano et al. 2012). Yeast-one hybrids also demonstrated that these regions are not involved in the transactivation activity of SLR1 and may instead be involved in interacting with the promoter region of target genes (Hirano et al. 2012).

Theoretically, DELLA GRAS domains may also be involved in DELLA-DIP interactions. *In vitro* interaction studies in yeast have demonstrated that the deletion of LHR1, PYFRE and SAW domains inhibits interactions with several DIPs: BZR1, MYC2, JAZ1 and EIN3, (Hou et al. 2010; An et al. 2012; Gallego-Bartolome et al. 2012; Hong et al.

2012). In addition, the SAW domain has been shown to interact with JAZ9 (Yang et al. 2012) and INDETERMINATE DOMAIN 2/GAI-ASSOCIATED FACTOR 1 (IDD2/GAF1) (Fukazawa et al. 2014). No DIPs that interact specifically with LHR2 and PFYRE have been identified. Additionally, results from deletion of the C-terminal domains VHIID, PYFRE and SAW, has been implicated them in a secondary interaction with GID1 and SLY1/GID2 as part of the GA-mediated DELLA degradation pathway in rice (Hirano et al. 2010; Bai et al. 2012).

1.9 RHT-1

Hexaploid bread wheat has three homoeologous DELLA genes, *Rht-A1, Rht-B1* and *Rht-D1* on chromosomes 4A, 4BS and 4DS, respectively (Peng et al. 1999; Wilhelm, Howells, et al. 2013). The three genes are very similar to one another, with 97.9% pairwise identity in the amino acid sequences, and they also display similar expression profiles (Pearce et al. 2011) (Figure 1.14). Given their similarities, it is surprising that to date, no semi-dwarf or dwarf alleles have been identified in *Rht-A1* (Pearce et al. 2011).

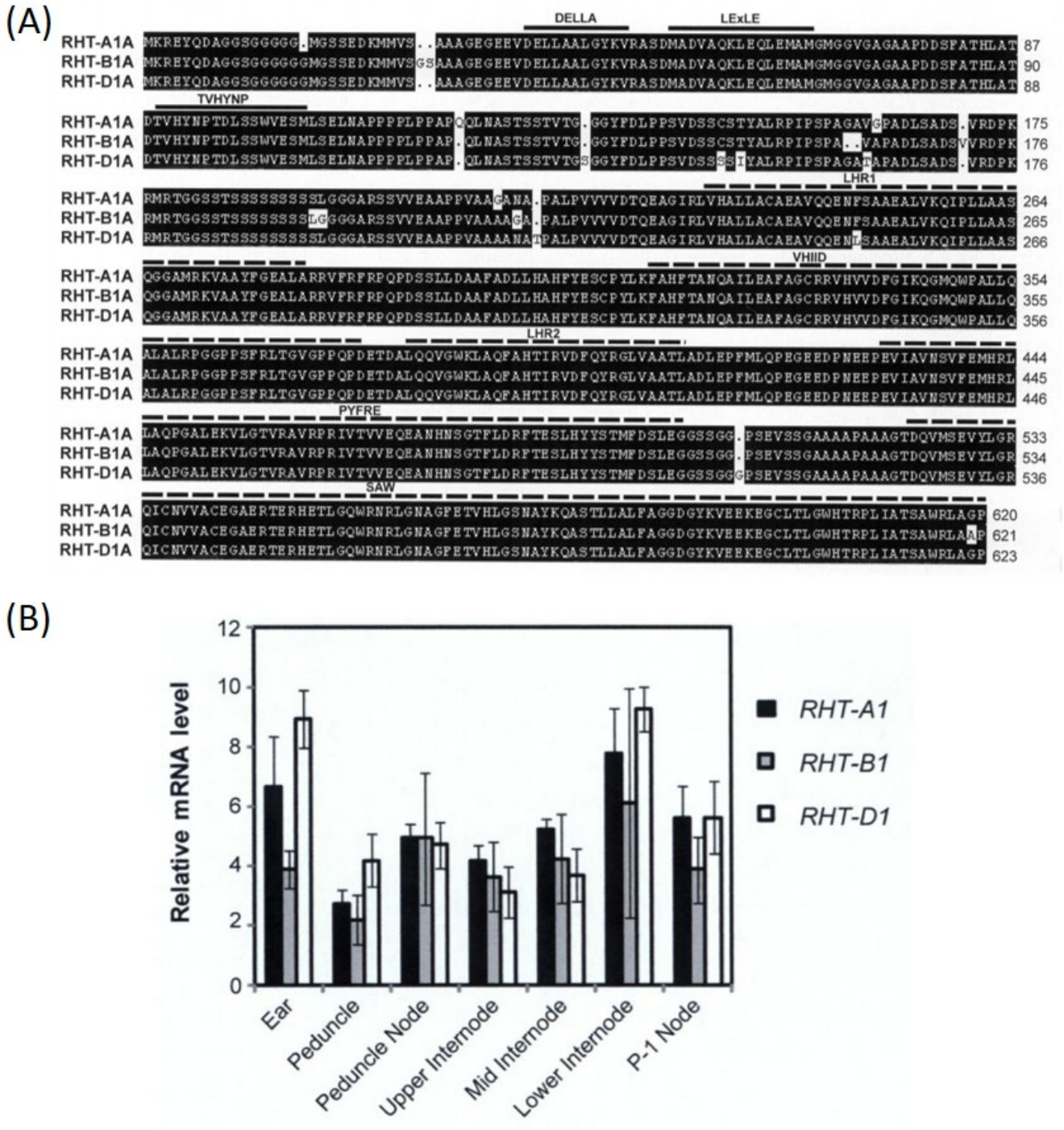

Figure 1.14: Amino acid sequence alignment of RHT-A1 A, RHT-B1 A, and RHT-D1 A proteins and their expression profiles. (A) Alignment of sequences predicted from nucleotide sequences amplified from var. Cadenza. Gaps introduced to improve the sequence alignment are indicated by dots. Conserved N-terminal regulatory motifs (DELLA, LExLE, and TVHYNP) are indicated by thick solid lines above the sequences. The C-terminal (LHR1, VHIID, LHR2, PFYRE, and SAW) functional domains are indicated by thick dashed lines above the sequence. **(B)** Expression analysis of the three Rht-1 homeologs in the upper expanding tissues of the developing wheat stem. Relative expression levels of Rht-A, Rht-B1, and Rht-D1 in different regions of the extending wheat stem at 7 weeks post-germination.
Adapted from Pearce et al (2011).

1.9.1 Rht-1 alleles

The dramatic wheat yield increases during the Green Revolution are attributed to two semi-dwarf alleles: *Rht-B1b* and *Rht-D1b* (Gale and Marshall 1973). Since their initial discovery, additional *Rht-1* alleles in *Rht-B1* and *Rht-D1* have been identified, some of which are shown in Figure 1.15

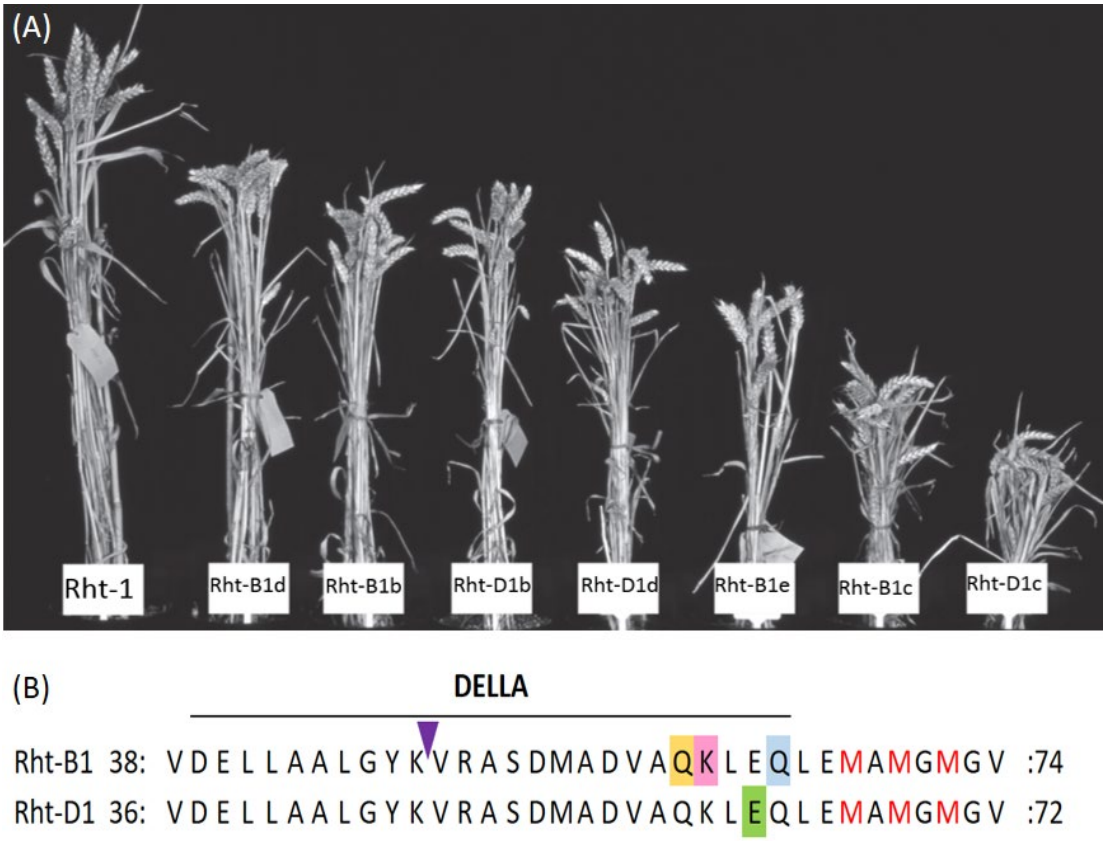

Figure 1.15: The Mutations and Phenotypes of *Rht-1* Dwarf and Semi-dwarf Mutants. (A) Near-isogenic lines of wheat containing homozygous alleles of *Rht-B1* and *Rht-D1* in cv. Mercia background. From left to right: Rht-1 (tall), Rht-B1d, Rht-B1b, Rht-D1b, Rht-D1d, Rht-B1e, Rht-B1c and Rht-D1c. Photograph from Phillips (2016) **(B) Locations of mutations in the 'DELLA' motif of *Rht-B1* and *Rht-D1* that produce dwarf and semi-dwarf wheat phenotypes.** Coloured squares denote the sites of introduced stop codons in different alleles: yellow = *Rht-B1p*, pink = *Rht-B1e,* green = *Rht-D1b, Rht-D1c* and *Rht-D1d* and blue = *Rht-B1b* and *Rht-B1d.* The purple triangle marks the position of the 30-amino acid insertion in *Rht-B1c*. Red 'M' mark the methionines hypothesized for translational reinitiation in *Rht-B1b*, *Rht-D1b* and Rht-*B1e*. Residue numbers are displayed at the start and end of each sequence fragment.

The height reduction associated with *Rht-1* alleles is the result of increased GA insensitivity (Radley 1970). Despite an accumulation of GA in *Rht-1* mutant tissues (Radley 1970), the GA insensitivity results in an overall smaller plant through reduced stem, coleoptile, leaf and culm elongation (Lenton, Hedden, and Gale 1987; Gale and Youssefian 1985), as a result of reduce cell elongation, not cell division (Keyes 1987; Keyes, Paolillo, and Sorrells 1989). These alleles do not appear to affect the rate of plant development or final ear shape (Youssefian, Kirby, and Gale 1992a; Stern and Kirby 1979) and the severity of the phenotypic change appears to be linked to the height of the cultivar. Tall cultivars (e.g. April Bearded) containing the alleles have a more pronounced percentage height reduction compared to shorter cultivars (e.g. Mercia) (Flintham et al. 1997; Gooding, Addisu, et al. 2012).

Rht-B1b and *Rht-D1b*

The most agronomically important *Rht-1* alleles: *Rht-B1b* and *Rht-D1b,* produce semi-dwarf phenotypes with a crop height reduction of 12-15% and 16-20%, respectively (Flintham et al. 1997) (Figure 1.15A). Both alleles are the result of premature stop codon mutations in the 'DELLA' motif of their respective *Rht-1*

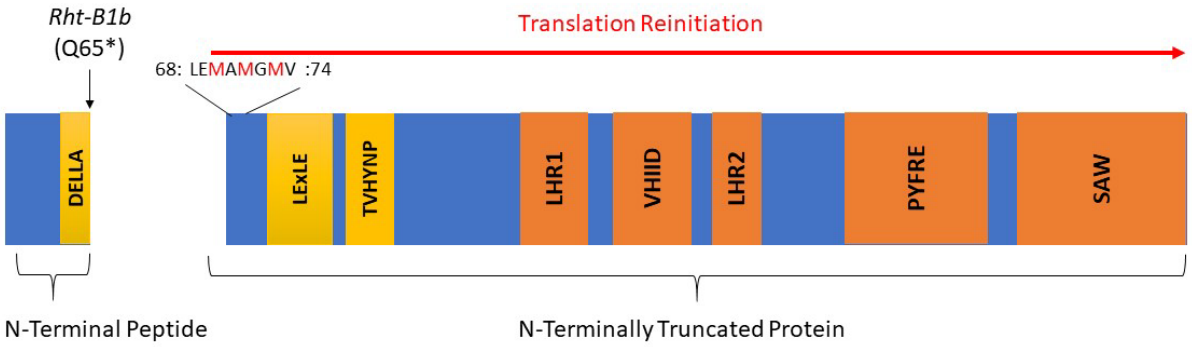

Figure 1.16: Hypothetical N-terminal Peptide and N-terminally Truncated Protein Resulting from the Premature Stop Codon Mutation *Rht-B1b.* Shown as a schematic diagram of RHT-B1 protein, including conserved domains. Yellow boxes represent conserved regulatory domains. Orange boxes represent conserved functional GRAS domains. The site of the *Rht-B1b* is shown, as well as the methionines (red Ms) hypothesized to induce translation reinitiation.

genes*:* Q65* in *Rht-B1* and E62* in *Rht-D1* (Figure 1.15B) (Hedden 2003; Peng et al. 1999). The premature stop codon mutations are followed by multiple methionine (AUG) codons (Figure 1.15B), which are predicted to induce translation reinitiation and the production of an N-terminal peptide and N-terminally truncated protein (Figure 1.16) (Futterer and Hohn 1996; Peng et al. 1999), although this has yet to be demonstrated *in planta* (Phillips 2016).

Using yeast-two hybrid experiments, Pearce and colleagues (2011) observed that while *Rht-1* and GID1 interact, neither the predicted N-terminally truncated protein or prematurely aborted N-terminal peptide interact with GID1, regardless of the presence of GA. This implies that the predicted products would not be recognised for the targeted degradation (Section 1.7.1) and could accumulate in plant tissues (Pearce et al. 2011). There is no evidence to suggest that the predicted N-terminal peptide would be capable of constitutively repressing GA mediated responses (Peng et al. 1999; Pearce et al. 2011). The current hypothesis is that the predicted N-terminally truncated protein (Figure 1.16), which contains the conserved GRAS domains that are crucial for DELLA protein function (Section 1.7.2), is capable of repressing GA mediated responses (Peng et al. 1999; Pearce et al. 2011). This is backed up by the recent identification of an intragenic amino acid substitution (E529K) in the C-terminal 'PYFRE' motif of *Rht-B1b* (Mo, Pearce, and Dubcovsky 2018). The intragenic mutant *Rht-B1b*$_{E529K}$ is taller with longer coleoptiles than *Rht-B1b* suggesting that the C-terminal domain is crucial for induction of GA insensitivity in *Rht-B1b* (Mo, Pearce, and Dubcovsky 2018).

Rht-B1d

Rht-B1d was identified from the Japanese wheat variety Saitama 27 (Worland and Petrovic 1988) and produces a semi-dwarf phenotype (Figure 1.15A), approximately 11% shorter than *Rht-1* (Worland and Petrovic 1988). Both *Rht-B1d* and *Rht-B1b* have identical coding sequences (Figure 1.15A), with a Q65* terminal mutation in the 'DELLA' motif. The exact cause of the reduced severity of *Rht-B1d* compared to *Rht*-B1b is unknown, although it has been suggested that additional mutations outside of *Rht-B1* may be responsible for affecting plant height (Pearce et al. 2011). Due to its limited ability to reduce plant height, the allele has not been used

extensively in wheat breeding (Flintham et al. 1997). *Rht-B1d* is predominantly used in cultivars grown in southern Europe, as it is more tolerant of the warmer climate than *Rht-B1b* and *Rht-D1b* (Worland 1986).

Rht-D1c and *Rht-D1d*

Both the severe dwarf allele *Rht-D1c* (50% height reduction) and semi-dwarf allele *Rht-D1d* (25% height reduction) (Figure 1.15A) are derived from the Chinese wheat variety Ai-bian 1 (Börner et al. 1991; Börner and Mettin 1988). Both alleles contain the *Rht-D1b* mutation (Figure 1.15B) (Pearce et al. 2011). The increased severity of *Rht-D1c* is due to a four-fold increase in the gene copy number, which results in increased allele expression and more efficient suppression of GA mediated growth (Börner, Roder, and Korzun 1997; Pearce et al. 2011; Li, Xiao, et al. 2012). By contrast, *Rht-D1d* is a mutant that spontaneously arose from a *Rht-D1c* population (Börner et al. 1991). Its taller phenotype, similar to *Rht-D1b,* is due to it having a single copy number (Chandler et al. 2002: Pearce et al. 2011). Neither allele is presently used in commerical breeding programmes (Pearce et al. 2011; Phillips 2016).

Rht-B1e and *Rht-B1p*

The semi-dwarf alleles, *Rht-B1e* (from Russian var. Bezostaya) (Worland 1986) and *Rht-B1p* (from 'Chris Mutant' line) (Bazhenov et al. 2015) produce greater GA insensitivity in wheat varieties than *Rht-B1b* or *Rht-D1b,* which is reflected in reduced leaf elongation, coleoptile length and plant height (20% reduction with *Rht-B1e* and 33% reduction with *Rht-B1p)* (Figure 1.15A)(Ellis et al. 2004; Bazhenov et al. 2015; Worland 1986). The alleles are the result of novel premature stop codons in the *Rht-B1* 'DELLA' motif, K61* and Q60*, respectively (Figure 1.15B) (Worland and Sayers 1995; Pearce et al. 2011; Bazhenov et al. 2015). These stop codons occur earlier in the amino acid sequence than *Rht-B1b* (Q65*), so it is possible that the shorter height phenotypes are the result of more efficient translation re-initiation and suppression of GA signalling (Pearce et al. 2011; Li, Yang, et al. 2012). To date, only *Rht-B1e* is used in breeding programmes for winter wheat varieties grown in southern Russia (Divashuk et al. 2013).

Rht-B1c

Rht-B1c produced a severe dwarf phenotype (Figure 1.15A) due to a 2-kbp retrotransposon insertion in the 'DELLA' motif (Figure 1.15B). This transposon is partially removed during splicing, resulting in an in-frame 90-bp insertion, producing a 30-amino acid insertion that inhibits DELLA interaction with the GID1 receptor (Pearce et al. 2011). Thus the mutant DELLA is not targeted for GA mediated degradation, and accumulates in plant tissues (Pearce et al. 2011; Wen et al. 2013). The severity of this dwarfing phenotype is likely due to translation of this protein being more efficient than translation re-initiation, which potentially occurs in other Rht-1 alleles such as *Rht-B1b* (Pearce et al. 2011; Phillips 2016).

Rht-B1c is not suitable for commercial breeding due to its severe phenotype. However, a recent study in Australia has demonstrated that sodium azide induced mutagenesis can be used to successfully generate *Rht-B1c* derivative lines with a tall or semi-dwarf phenotype (Chandler and Harding 2013; Derkx et al. 2017). Nineteen novel *Rht-B1c* derivative lines were identified, four stop codon and fifteen missense mutants in the C-terminal domain, which resulted in an 123-230% height increase in comparison to *Rht-B1c (Derkx et al. 2017).* Crossing and segregation analysis has demonstrated that the overgrowth phenotypes and mutated *Rht-B1c* are 100% linked, introducing the potential that mutagenesis of severe *Rht-1* mutants could be used to generate novel semi-dwarf alleles (Chandler and Harding 2013).

1.9.2 A Novel *Rht-1* allele: *Rht-A1b*

GA-insensitive *Rht-1* mutants have only been identified in *Rht-B1* and *Rht-D1*, despite *Rht-A1/B1/D1* having similar expression profiles in the elongating stem (Pearce et al. 2011). Prior to the start of this PhD, a TILLING based screen of ethyl methanesulfonate (EMS)-mutagenized wheat populations identified 17 missense mutations in *Rht-A1*. One of these mutations produced a stop codon in the same position as in *Rht-B1p,* close to the stop codon positions in *Rht-B1b* and *Rht-D1b* (Figure 1.15). This mutation was subsequently named *Rht-A1b* and similar to *Rht-B1p* it produces a more severe height phenotype than *Rht-B1b* and *Rht-D1b* (Bazhenov et al. 2015). The *Rht-A1b* allele will be the focus of my thesis project, as it

provides the opportunity to establish why there are no agronomically important *Rht-A1* alleles and produce novel and potentially agronomically important, dwarfing alleles.

1.10 Project Aims and Objectives

This project aims to add to our understanding of *Rht-A1* and determine whether *Rht-A1* alleles have the potential to be used as superior, novel semi-dwarfing alleles in wheat breeding programmes. To achieve this, this thesis will address the following questions and objectives:

Characterise the novel Rht-1 mutant Rht-A1b.

The novel mutant *Rht-A1b* will be characterised and compared to the Green Revolution semi-dwarf allele *Rht-D1b,* the severe dwarf *Rht-B1c* and WT Cadenza (*Rht-1)* to assess the effect of the mutation on plant growth and development.

- To determine the degree of GA-insensitivity due to *Rht-A1b*, GA-dose response assays will be conducted with seedlings.
- Hormone analysis will establish the effect of the mutation on endogenous GA levels and the results assessed against RNA-seq data looking into the transcription of GA biosynthesis and signalling genes.
- Additionally, a phenotypic characterisation of adult plants grown in the glasshouse will assess the effect of *Rht-A1b* on plant growth and development.

Identify and characterise Rht-A1b suppressor mutants.

Intragenic *Rht-A1b* suppressor mutations will be identified from EMS-mutagenised *Rht-A1b* populations. To establish whether any of these mutants could be used as novel semi-dwarfing alleles, backcrossed lines will be extensively phenotyped in the glasshouse and the field to determine whether they are suitable as improved *Rht-1* dwarfing alleles for wheat breeding.

Is there homoeologue specificity in Rht-1?

To determine whether there is homoeologue specificity in *Rht-1,* single, double and triple knockout lines will be phenotyped and compared to assess whether there are any phenotypic characteristics associated with each homoeologue.

Chapter 2: Materials and Methods

2.1 Plant Material and Growing Conditions

The spring wheat variety *Triticum aestivum L.* cv. Cadenza was used for all experiments. Prior to sowing, seeds were imbibed in petri dishes containing moist filter paper and kept at 4^{o}C in darkness for 4 days. Where adult plants were required, plants were grown in 13 cm diameter plastic pots containing Rothamsted prescription mix compost (75% peat, 12% sterilised loam, 3% vermiculite, 10% grit). For wheat seedling assays, seeds were sterilised using 10% (v/v) bleach solution and imbibed as described above. Plants were then grown in trays containing Vermiculite at a range of GA_3 concentrations. Controlled environment (CE) growth conditions were a 16-hour photoperiod with 21^{o}C/16^{o}C day/night temperatures. Photoperiod provided by tungsten fluorescent lamps providing 500 µmol$m^{-2}s^{-1}$ PAR unless otherwise specified. Standard glasshouse conditions were a 16-hour photoperiod using natural light supplemented with 400-1000 500 µmolm-2s-1 PAR from SON-T sodium lamps. For field experiments, plants were grown on silty clay loams with flints.

The *Rht-A1b* glasshouse characterisation (Chapter 3) was planted out in the glasshouse in June 2018 and the characterisation carried out December/January 2019.

Both the *Rht-A1b* suppressor characterisation (Chapter 5) and the *Rht-A1b* knock out characterisation (Chapter 6) were planted out in late December 2018 and characterised in between May-July 2019.

2.1.1 Suppressor Screen One

Grain was mutagenised as described in Section 2.4. Seed was bulked from 1500 M_1 plants grown in the field and 3000 M_1 plants grown in pools of 300-400 individuals in the glasshouse (section 2.1). The M_2 pools were therefore generated from 4500 M_1 plants (Figure 2.1)

Figure: 2.1: Schematic of the 2016 *Rht-A1b* suppressor screen. Twelve pools; six field grown (F1-F6) and six glasshouse grown (GH3-GH8) were planted out in randomly distributed replicates of three (labelled a-c). Four control plots containing Cadenza (WT) were included amongst the M_2 plots. Seed was planted out at approximately 100 seed/m^2.

Plants were separated into two blocks containing field grown M_2 seed and glasshouse grown M_2 seed. In 1.8m by 9m plots, six field grown pools (F1-F6) and six glasshouse grown pools (GH3-GH8) were planted out in randomly distributed replicates of three (denoted a-c). Per block, two control plots of Cadenza controls were also planted. Seed were sown at approximately 100seed/m^2 density, resulting in around 1680 M_2 grains per plot.

Seeds for this experiment were sown in late February 2016 and the suppressor screen carried out July-September 2016.

2.1.2 Suppressor Screen Two

25,000 M_1 individuals were mutagenised (Section 2.4) and divided into 13 pools of approximately 2000 individuals and planted in two 9m x 1.8m plots at an approximate density of 100 seeds/m^2. Approximately 50% of the grains germinated, therefore grains were harvested from ~1000 individuals per pool, or 13,000 M_1 individuals in total.

M_2 grain was planted in the field 6x60m plots that represented a single M_1 pool, which were numbered 8-20 (Figure 2.2). Per plot, ~36,000 M_2 seeds were planted out. Across all plots this equates to ~468,000 M_2 plants from the 13,000 M_1 individuals.

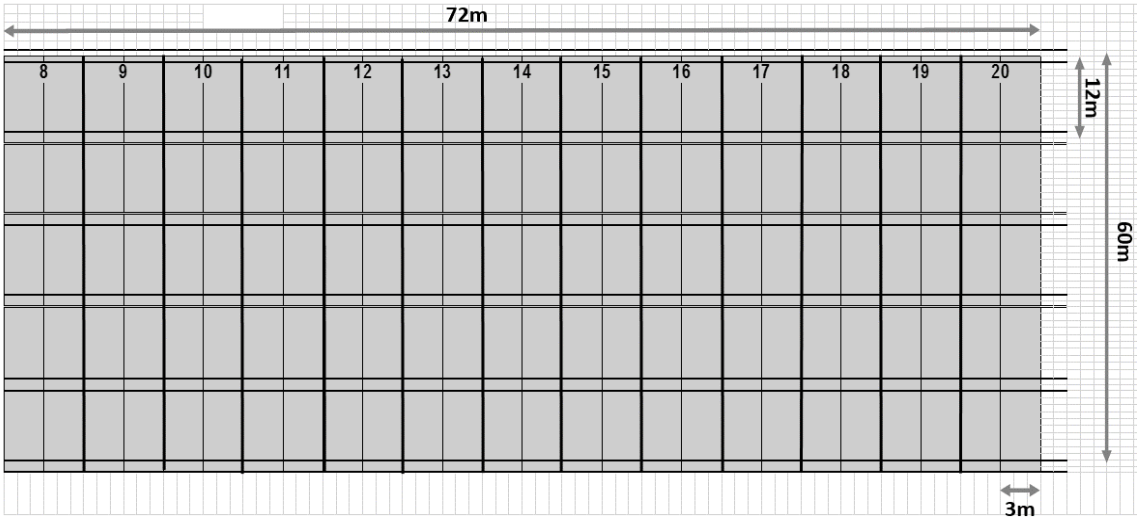

Figure: 2.2: Schematic of the 2017 *Rht-A1b* suppressor screen. Each plot is separated by a bold black line. Thin black lines that run vertical and horizontal to the thick black represent machinery tram lines. Seed was planted out at approximately 100seed/m^2.

Seeds for this experiment were planted out in late February 2017 and the suppressor screen carried out June-September 2017.

2.1.3 Field Characterisation of *Rht-A1b* Suppressor Mutants

100 BC_2F_3 seed from each of the intragenic mutants identified in suppressor screen 1 and 2 were sown into a randomised block design, with 3 blocks (0.6x0.5m plots) per genotype. (Figure 2.3). Controls for this characterisation included: *Rht-A1b* (BC_6F_4), *Rht-D1b* (BC_6F_4), *Rht-B1c* (BC_6F_4) and *Rht-1* (WT Cadenza). The null segregates for each mutant line were also sown into the field. All mutations were in a Cadenza (var.) background.

Seeds for this experiment were planted out in early March 2019 and the field characterisation performed June-September 2019.

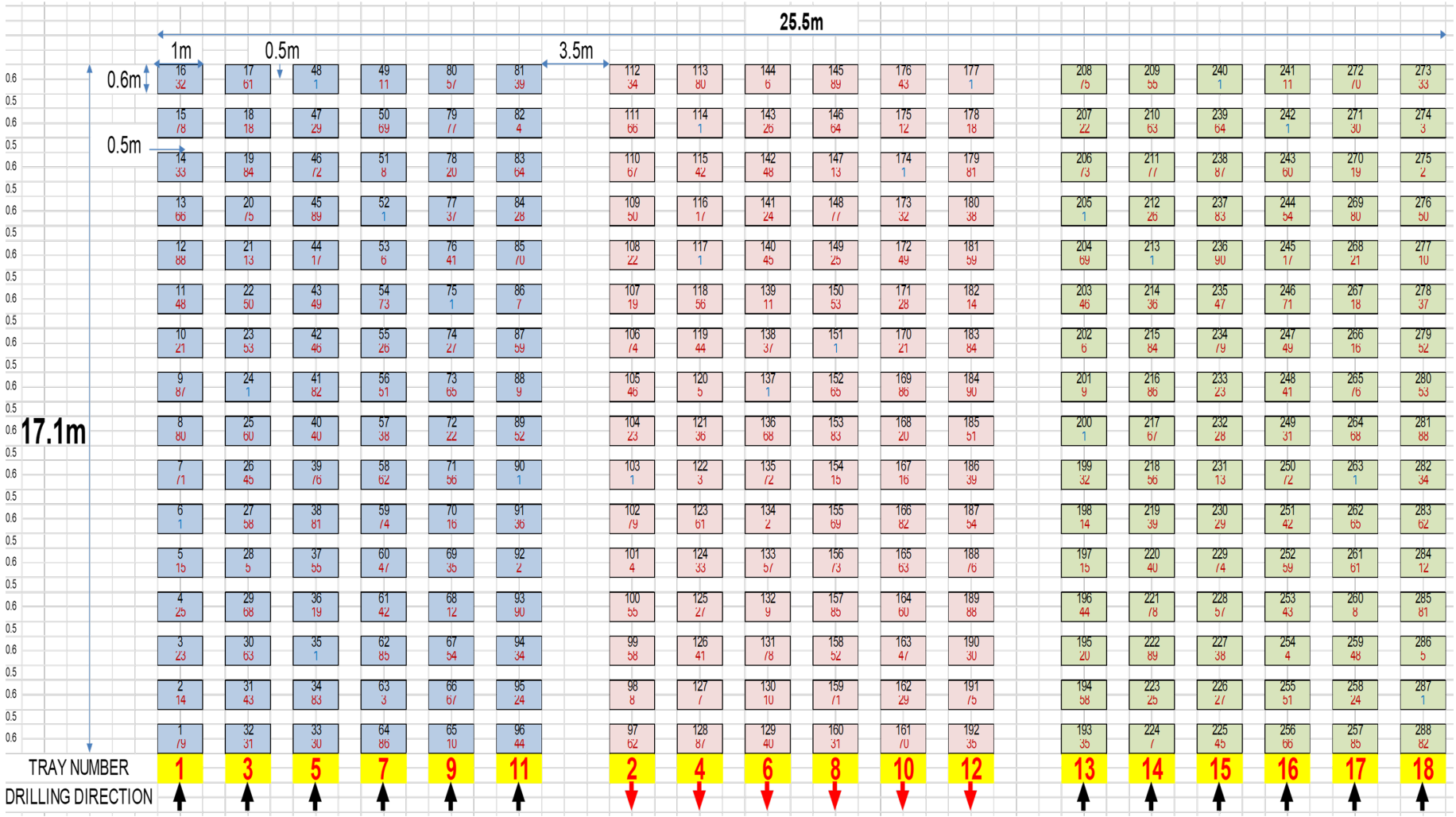

Figure: 2.3: Schematic of the 2019 Characterisation of BC_2F_3 Intragenic *Rht-A1b* Mutants. Each plot is shown as a coloured box. The blue, pink and green colour scheme represent the three replicates sown for each line.

2.2 Plant Breeding

The first 3 and last 2 spikelets and the 2 innermost florets on all the remaining spikelets were removed prior to the emasculation of selected female parents. The immature anthers (pale green/yellow in colour), were then excised from the remaining florets 1-2 days prior to anthesis and the tip of the lamella cut off (Figure 2.4A and B). Emasculated spikes were then secured in transparent crossing bags with paper clips. Once spikes of the male pollen donor entered anthesis (Figure 2.4C), they were excised and placed upside down inside the crossing bag with the emasculated spike. The pollen shedding spike was then agitated to spread the pollen around the floret positions before being secured in a tessellating position against the female parent. Grain from successful crosses (Figure 2.4D) was then harvested.

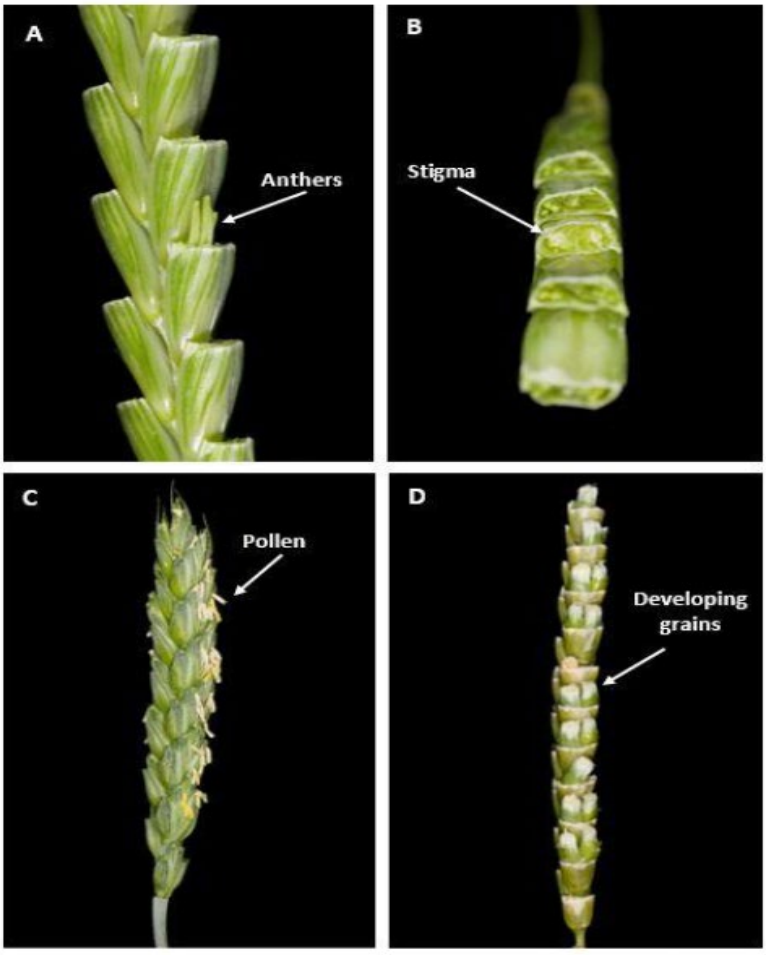

Figure 2.4: Crossing in Wheat. (A) Three anthers exposed in a wheat floret after the lamella has been cut off. (B) An emasculated floret (anthers removed), leaving the stigma exposed. (C) A wheat ear post-anthesis. (D) Grain developing post-crossing. Photographs from Dr Beth Wallis.

2.3 Plant Phenotyping

Plants were phenotyped to assess the effect of different *Rht-1* mutations on plant phenotype. Unless otherwise stated, all measurements collected were assessed using GenStat (v18, VSNI, Hemel Hempstead, U.K.).

2.3.1 Shoot Measurements

Once plants were fully mature and dried down the total number of shoots that produced grain were counted per plant (glasshouse grown plants) and shoot measurements taken for the three tallest shoots per plant (glasshouse grown plants) or for 10 shoots per plot (field grown plants). The following shoot measurements (mm) were taken: ear length, peduncle length, internode 2 (I2) length, internode 3 (I3) length, internode 4 (I4) length and total stem length (the sum of the previous measurements) (Figure 2.5).

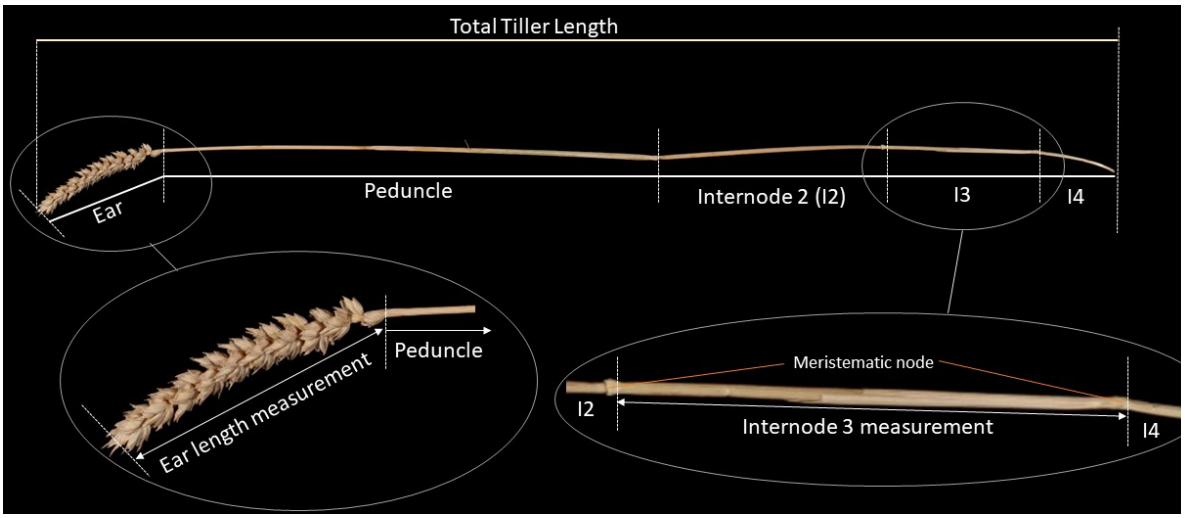

Figure 2.5: Shoot Measurements. Total shoot length was calculated as the sum of the ear, peduncle, internode 2 (I2), internode 3 (I3) length and internode 4 (I4) lengths. Ear length was measured from just from the first floret to just below the start of the ourns on the final floret at the tip of the ear. Peduncle and internode measurements went from the meristematic node (MN) that segment elongated from to the bottom of the next MN.

Ear length was measured from just from the base of the first spikelet to just below the base of the awns on the terminal spikelet. Peduncle and internode measurements went from the meristematic node (MN) that segment elongated from to the bottom of the next meristematic node.

2.3.2 Spikelet Measurements

In addition to ear lengths, the number of viable spikelets (capable of containing grain) on the ear was measured (Figure 2.6).

Figure 2.6: Spikelet Number Measurements. A side-on and front-on view of viable spikelets. Non-viable (not completely developed) spikelets are also shown,

2.3.3 Grain Measurements

Per plant, all of the ears were threshed and the total grain number counting using an Elmor C1 grain counter (Elmore, Germany). This number was then divided by the total number of shoots for that plant to provide an estimate of grain number per ear. An ANOVA was used to test whether grain number per ear was significantly different between different genotypes.

From the threshed grain, ~200 seeds per plant were measured using a Marvin grain analyser (INDOSAW, India). This provided the seed area (mm^2), seed length (mm) and seed width (mm) of each grain. Measurements were taken across the largest width and length in the 2D area. An unbalanced ANOVA was used to test whether seed measurements were significantly different between genotypes.

2.3.4 Flag Leaf Area

In the glasshouse three flag leaves per plant were measured approximately one week after heading. In the field, 10 flag leaves per plot were measured once 80% of the ears per plot had emerged. Flag leaf width and length were measured at the widest and longest point. The approximate leaf area was calculated (mm^2) using the formula: length X width X 0.835 (Miralles et al. 1998).

2.3.5 Measuring Average Plot Height in the Field

An average plot height was generated by placing a meter ruler in the centre of the plot. A polystyrene disc was then threaded through the ruler and placed to sit atop the wheat ears. Where the underside of this disc sat against the meter ruler was classed at the average plot height (mm).

2.3.6 Selecting Shoots in the Field

Shoots were selected by ignoring the ten tallest shoots in the plot and then harvesting the 10 next tallest shoots. This was to prevent any segregating individuals from being selected. The 10 harvested shoots where then measured using the methods described in sections 2.3.1 and 2.3.3.

2.4 Molecular Biology

2.4.1 Genomic DNA Extraction

Approximately 0.1g of leaf sample was harvested into 2ml tubes and freeze dried. The samples were ground using a GenoGrinder (SPEX SamplePrep, Metuchen, New Jersey, U.S.A.) until they were a fine powder. The samples were then incubated at 65^{o}C with 1ml PVP-extraction buffer. 333µl 5M potassium acetate was mixed into to each sample, which were centrifuged at 13,000 rpm for 4 minutes. 1ml of clear supernatant was transferred to fresh 2ml tubes containing 550µl chilled isopropanol. The samples were repeatedly inverted and left at room temperature for 10 minutes and spun at 13,000 rpm for a further 10 minutes. The supernatant was discarded and gDNA pellets washed with 700µl of 70% ethanol. The tubes were again centrifuged at 13,000 rpm for 10 minutes, the supernatant discarded. The gDNA pellets left to air dry at room temperature for 1 hour and then suspended in 200µl TER, incubated at 50^{o}C for 1 hour and stored at -20^{o}C. gDNA concentrations

were quantified using a Nanodrop™ ND-1000 spectrophotometer (LabTech International Ltd, U.K.). Constituents of all the buffers used are below:

DNA Extraction Buffer (1L), final concentrations:
1M KCl
10mM EDTA pH 8.0
pH adjusted to 9.5 using 1M NaOH
0.18mM PVP-40
34.6mM Sodium bisulphite
100mM Trizma Base (Tris Base)

1 X TE buffer final concentrations (1L):

10mM Tris-HCl pH7.5
1mM EDTA

2.4.2 Polymerase Chain Reaction (PCR)

Unless otherwise stated, 20µl reactions containing HotShot Diamond Mastermix (Clent Life Science, Stourbridge, United Kingdom) were used to amplify target DNA sequences from gDNA:

- 10µl HotShot Diamond Mastermix
- 7µl Distilled, sterile water
- 0.5µl 10µM Forward primer
- 0.5µl 10µM Reverse primer
- 2µl DNA template (25ng/µl)

Reactions were carried out in a DNA Engine Tetrad 2 thermal cycler (Bio-Rad Laboratories, Hercules, California, U.S.A.) using the following reaction conditions:

- 98°C – 300 seconds
- 97°C – 30 seconds
- 58-69.2°C – 30 seconds
- 72°C – 60 seconds per kb

(43 Cycles)

- 72°C – 420 seconds
- 12°C – Hold

2.4.3 Sequencing Optimisation for *Rht-A1*

Genomic DNA was extracted from leaf samples using the method described in 2.4.1. To establish whether the sampled individuals contained intragenic mutations in the *Rht-A1b* sequence, PCR amplification and Sanger sequencing (section 2.4.6) was

used to examine the C-terminal GRAS coding domain. The presence of the *Rht-A1b* mutation was also confirmed by sequencing. The homoeologues are GC rich; 65.7%, 66.7% and 66.2% for *Rht-A, B* and *D* respectively. *Rht-A1* is also very similar to *Rht-B1* (89.1%) and *Rht-D1* (92.4%).

The primers used for *Rht-A1* sequencing are described in Table 2.1. PCRs were set up as described in section 2.4.2 with a temperature gradient (55-70^{o}C) for the annealing stage of the PCR cycle.

Table 2.1: PCR Primers Tested for Sequencing the N-terminal Rht Domain

Primer Name	Targeted Gene	Primer Position in CDS (bp)	Primer Sequence	Sequencing Primer
Rht-A1F	*Rht-A1*	-11 to -33	AGCGAGGCAGCTCGCTCGCGGT	Yes
Rht-A1R	*Rht-A1*	557 to 575	CGTCGTCATCCTCCTCGTC	-
Rht3F20	*Rht-1*	664 to 681	GTGGTCGACACGCAGGAG	Yes
Rht-A1R3	*Rht-A1*	+96 to +118	CCTCTGAAGAAGAAGCTAAATG	Yes

2.4.4 Gel Electrophoresis and Documentation

PCR reactions were mixed with 5X loading dye (Thermo Scientific, Hemel Hempstead, U.K.) and run on 1-2% (w/v) agarose (Fisher Scientific, Loughborough, U.K.)/ TBE (45 nM Tris-borate, 1 mM EDTA, pH 8.3) gels, containing 0.5 µg/µl ethidium bromide. To assist in product size estimation, 100 bp DNA ladder or 1 kb GeneRuler^{TM} DNA ladder (Thermo Scientific, Hemel Hempstead, U.K.) were run alongside the products. Electrophoresis was carried out at 100mV for 40 minutes unless otherwise stated. PCR products were visualised through ethidium bromide fluorescence under UV light, using SynGene GelDoc imaging equipment (Synoptics Ltd, Cambridge, U.K.).

2.4.5 Purification of PCR products for Sequencing

Amplified DNA sequences were purified using the QIAquick®PCR Purification kit (QIAgen, Hilden, Germany) per the manufacturer's instructions. DNA concentrations were quantified using a Nanodrop™ ND-1000 spectrophotometer (LabTech International Ltd., U.K.).

2.4.6 Sequencing and Genotyping

Eurofins Genomics (Wolverhampton, U.K.) was used for sequencing. The value read tube sequencing service was used to sequence purified PCR products (5 ng/µl 1), premixed with their appropriate sequencing primer (10 pmol/µl). Unpurified PCR products were sequenced from 96 well PlateSeq Kits with the appropriate sequencing primers (10 pmol/µl) attached. Geneious software (v10.0.02, Biomatters Ltd, Auckland, New Zealand) (Kearse et al. 2012) was used to assess the sequencing results.

2.4.7 RNA Extraction

Seedling material was harvested into liquid nitrogen and ground into a fine powder using liquid nitrogen and a pestle and mortar. Up to 100mg of plant material was transferred into a sterile 2ml tube and the material was stored at -70^{o}C until required. RNA was then extracted using the QIAgen RNeasy Kit (QIAgen, Hilden, Germany) with an on-column DNase treatment, per the manufacturer's instructions. The quantity and quality of the extracted RNA was tested using an Agilent Nano RNA Kit (Agilent, Santa Clara, California, USA) and Agilent 2100 Bioanalyzer (Agilent, Santa Clara, California, USA) as per the manufacturer's instructions.

2.4.7 RNAseq

Rht-A1b, Rht-D1b, Rht-B1c and *Rht-1* seeds were germinated and grown in randomised vermiculite trays under the same growth conditions as the seedlings used for GA content analysis (Section 2.5.8). Seven days post-germination seedlings were treated with 5µM GA_3 or water and 8-hours later material was harvested in pools of 10 seedlings per genotype, with 3 replicates per genotype produced. RNA samples were then sent to Novogene Bioinformatics Technology Co. Ltd., Beijing,

China (http://www.novogene.cn) for further processing and sequencing to a depth of 30 million reads (Appels et al. 2018).

Data was analysed using the following tools:

1) Reads were QCed using FastQC (https://www.bioinformatics.babraham.ac.uk/projects/fastqc/),

2) Data was mapped using HiSAT2 (v2.1.0, https://ccb.jhu.edu/software/hisat2/index.shtml)

3) Gene counts were calculated using featureCounts, part of the SubRead package (https://bioconductor.org/packages/release/bioc/html/Rsubread.html) in R Bioconductor (v3.7 https://www.bioconductor.org/). (Liao, Smyth, and Shi 2014)

4) Differential expression was calculated using the DESeq package (https://bioconductor.org/packages/release/bioc/html/DESeq.html) (Anders and Huber 2010) in R (v3.6.1) software (R Core Team 2019)

2.4.8 GA Hormone Extraction and Analysis

Gibberellin was extracted and purified using an adapted protocol (Šimura et al. 2018) by colleges in Laboratory of Growth Regulators at Palacký University Olomouc.

Extraction: The leaf sheaths of 7-day old wheat seedlings samples were harvested between the grain crown and ligule of the 1st leaf leaf (Figure 2.7) and freeze dried for 1 week.

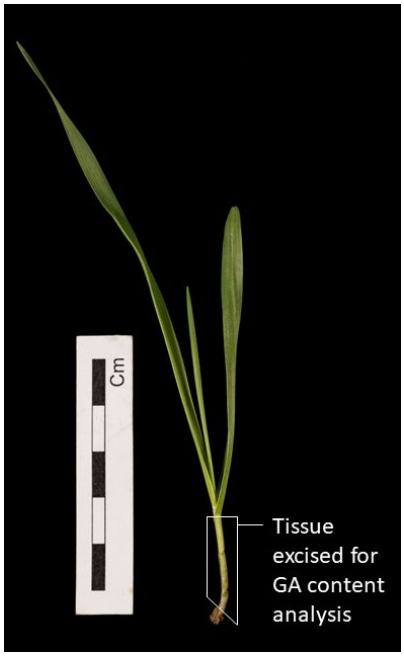

Figure 2.7: Photograph of *Rht-A1b* seedling 7-days post-germination, grown in vermiculite and water. The whole area harvested for gibberellin content analysis is highlighted with a white box. Scale (cm) shown.

Samples where homogenised in 1ml 60% acetonitrile using silica beads and a Retsch MM400 bead mill at a frequency of 27/s for 5 minutes. Samples were then sonicated for 3 minutes and rotated for 20 rotations/minute for 30 minutes at 4 °C, then centrifuged in a Beckman Avanti 30 Centrifuge at 20,000 RPM, for 15 minutes at 4 °C. The supernatant was removed and stored in a 2ml tube. 1 ml of pre-cooled extraction solution was added to the pellet, which was vortexed and rotated at 4°C for 60 min. The re-extracted samples were centrifuged at 20 000 rpm for 10 min and the supernatant combined with the same from the first centrifugation.

Purification: Samples were purified using MAX SPE columns (Oasis®) in a 60 mg Oasis® MAX anion exchanger. The columns were activated using 100% MeOH followed by ddH_2O and then equilibrated using 100% ACN (1ml for 30mg HLB tube and 2 ml for 60mg HLB tube). The sample was passed through the column and eluted using 60% ACN and 30% ACN (500µl for 30mg HLB tube and 1ml for 60mg HLB tube). A nitrogen evaporator was used to completely dry out samples, which

were then dissolved in 50µl 30% ACN, by vortexing and 5 minutes of sonification. The volume was transferred to a 1.5ml centrifuge tube and centrifuged for 5 mins, 8500rpm to remove debris. The samples were transferred to insert-equipped vials and centrifuged again to removed remaining debris.

Analysis: Using a triple quadrupole mass spectrometer Xevo® 581 TQ-S MS (Waters, Manchester, UK). Samples should be spun down for 5 mins to avoid any remaining particulates. On the day of use 0.01% Formic Acid in ACN was used for Mobile Phase A and 0.01% Formic Acid in H_2O was used for Mobile Phase B. MassLynxTM 584 software (version 4.1, Waters, Milford, MA, USA) 585 was used to control the instrument and to acquire and process the MS data. MassLynxTM 584 software was used to assess the abundance of each gibberellin. GenStat (v18, VSNI, Hemel Hempstead, U.K.) was used to statistically assess this data.

2.5 GA Dose Response Assays

Wheat seeds were surface sterilised prior to germination. Initially seeds were soaked in 70% ethanol for 5 minutes and rinsed twice with sterile water. Then seeds were soaked in 10% commercial bleach with 0.1% (v/v) Tween 20 for 10 minutes and rinsed six times with sterile water.

Seeds were transferred to petri dishes containing sterile filter paper, where they were imbibed in water or 25µM paclobutrazol and stored for 3 days at 4^{o}C in darkness. On the fourth day, seeds were transplanted into moist vermiculite containing water or a GA_3 solution. Where more than one genotype was tested, three replicates of 5 seeds per genotype were planted in randomly distributed rows in the vermiculite tray. Unless otherwise stated trays were stored in a controlled environment (Section 2.1) for the duration of the experiment. Trays were randomly distributed on CE shelves. On the fifteenth day, seedlings were removed from the vermiculite and the leaf sheath and first leaf lengths were measured (Figure 2.8).

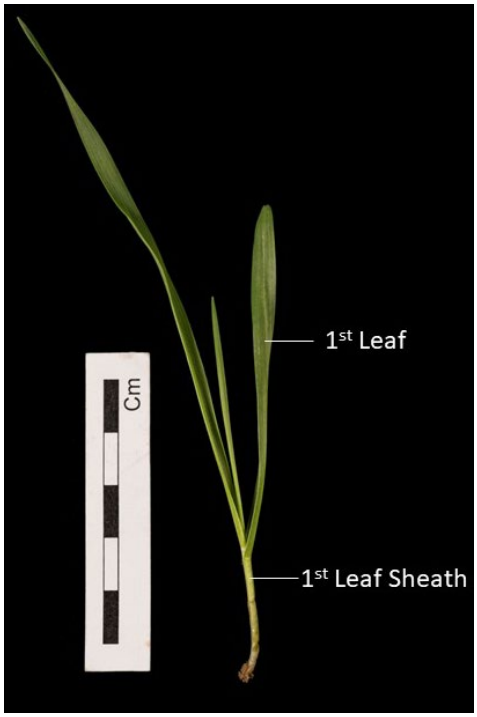

Figure 2.8: Photograph of *Rht-A1b* seedling 7-days post-germination, grown in vermiculite and water. First leaf and first leaf sheath are annotated.

Unless otherwise stated the following lines were used for the GA dose response assays; *Rht-A1b* (BC_6F_3), *Rht-B1c* (BC_6F_3), *Rht-D1b* (BC_6F_3), *Rht-1* (WT Cadenza).

GA dose response data was assessed using GenStat (v18, VSNI, Hemel Hempstead, U.K.),

2.6.1 24Hour GA Response Assay

To determine the time-point to harvest GA_3 treated seedlings, 40 *Rht-1* seeds were germinated and grown under the conditions described in Section 2.6. Seven days post germination, seedling first leaf sheaths were measured, and 20 seedlings were then treated either 5µM GA_3 or water. Leaf sheath measurements were then taken every 4 hours for 24hours. Leaf sheath elongation between the two-time points (e.g. 0-4 hours, 4-8 hours, 8-12 hours) was then calculated to determine when seedling leaf sheath elongation was significantly responding to GA_3 treatment.

2.6 Statistical Analysis

The mean for each measurement was calculated and used in an analysis of variance (ANOVA). The ANOVA was applied to individual measurements for all the genotypes together from the experiment, considering the variation due to replication, blocking and the difference between all individual lines in consecutive order using a nested treatment structure. The standard error of the difference (SED) or the residual degrees of freedom (DF) from the ANOVA were output along with the F-statistics and p-values. The least significant difference (LSD) at the 5% level of significance was used to compare between lines. The GenStat statistical package (17th edition, 2014, ©VSN International, Hemel Hempstead, UK) was used for the analysis. No transformation of data was required, plots of residuals were produced showing that there was good conformation to the assumptions of the analysis (normal distribution, additivity of effects and constant variance over the lines).

2.6.1 Principle Component Analysis (PCA)

RNASeq data was analysed using the DESeq package (Anders and Huber 2010) in R (v3.6.1) software (R Core Team 2019). The data contained 120,744 genes reads, which was filtered down to 74,957 by removing genes where there are less than 3 samples with normalised counts greater than or equal to 5. A principle component analysis (PCA) plot was then generated (Figure 3.17) to establish that there was separation of the gene expression data according to genotype and GA_3 treatment.

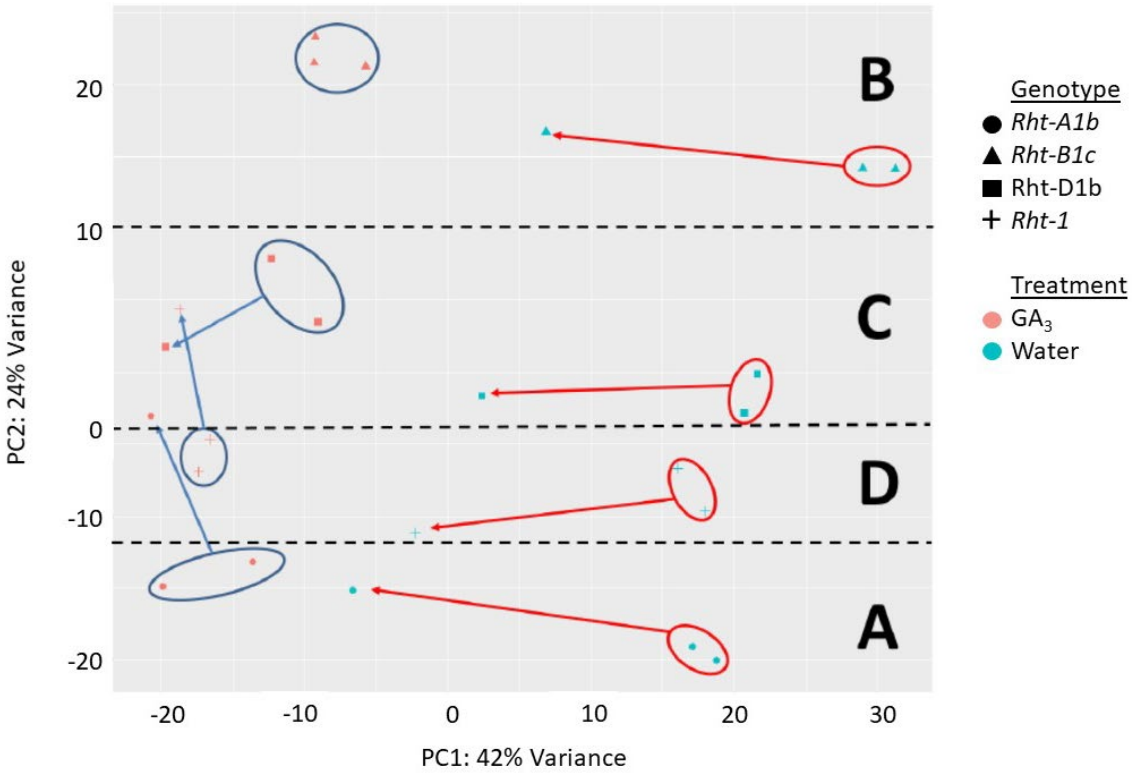

Figure 3.17: Principal Component Analysis (PCA) Plot of Gene Expression in *Rht-1* mutants and *Rht-1*. Sections (top to bottom): B = *Rht-B1c* (▲), C = *Rht-1* (+), D = *Rht-D1b* (▪) and A = *Rht-A1b* (•). Right (pink symbols) = GA_3 treated seedlings. Left (blue symbols) = water (control) treated seedlings.

The PCA shows that the results group separately according to genotype and GA_3 treatment, although here is some overlap between *Rht-A1b, Rht-D1b* and *Rht-1* GA_3 treated seedlings. Additionally, one control replicate for each genotype shows an intermediate expression profile between the treated and untreated clusters (Figure 3.17). This suggests that there may have been some GA_3 contamination in the samples, however due to the limited number of replicates, these data points cannot be removed from the analysis.

2.6.2 Hierarchical Clustering Analysis (HCL) and Pearson Correlations

Genotypes were classified into groups based on the relative performance of each mutant line compare to the WT (*Rht-1)*. The following equation was used to transform the data to allow this analysis:

$$\text{relative performance} = \frac{mut - \text{wt}}{\text{wt}}$$

in which “mut” denotes the mutant line and “wt” wild type. Calculations were performed on the trait averages for each mutant line. The relative performance values were used to cluster the different mutants using a hierarchical cluster analysis (HCL). The HCL analysis was done using the MeV multiple experiment viewer (http://www.tm4.org/mev.html), with default settings that apply a Pearson correlation as distance measure and average linking for clustering.

Individual Pearson Correlations were also performed to establish whether there was a correlation between traits that was not immediately obvious in the correlation matrix. This was performed using the untransformed trait averages for each mutant line. The analysis was performed in GenStat.

Chapter 3: Characterisation of *Rht-A1b*

3.1 Introduction

The hexaploid bread wheat genome contains three *Rht-1* homoeologues: *Rht-A1, Rht-B1* and *Rht-D1*, which demonstrate similar expression profiles in the elongating stem. Despite this, *Rht-A1* alleles that produce a GA-insensitive phenotype have not yet been characterised (Pearce et al. 2011). High throughput sequencing of the wheat variety Quarrion was believed to have identified a nonsense mutation in *Rht-A1* in a similar location to *Rht-B1b* (Tan, Koval, and Ghalayini 2013); however this was later confirmed to be a chimeric sequence (Tan, Koval, and Ghalayini 2014). Prior to the start of this project a Cadenza population containing only WT *Rht-1* alleles (*Rht-A1a, Rht-B1a* and *Rht-D1a*) was mutagenised using ethyl methanesulfonate (EMS). An M2 population, consisting of 2200 individuals was screened to identify novel *Rht-1* mutations using a TILLING based approach (Chen et al. 2014). This resulted in the identification of multiple mutations in the *Rht-A1* and *Rht-D1* genes. One of these mutants contained a nonsense mutation (predicted to cause a Q59* amino acid substitution) in *Rht-A1* in a similar location to those in the Green Revolution alleles *Rht-B1b* (predicted Q65* substitution) and *Rht-D1b* (predicted E62* substitution) and an identical location to the *Rht-B1* mutant, *Rht-B1p* (predicted Q60* substitution) (Bazhenov et al. 2015). This mutation was subsequently designated *Rht-A1b* (personal comm. Dr Stephen Thomas) (Figure 3.1 and Table 3.1).

Table 3.1: Rht-1 Nonsense Mutations

Allele	Nucleotide Change	Amino Acid Change	Predicted Height Change (Compared to *Rht-1*)
Rht-B1b	C190T	Q65*	12-15% (Flintham et al. 1997)
Rht-B1e	G181T	E62*	20% (Worland 1986)
Rht-B1p	C176T	Q60*	33% (Bazhenov et al. 2015)
Rht-D1b	G181T	E62*	16-20% (Flintham et al. 1997)
Rht-A1b	C169T	Q59*	25-41% (Dr. Stephen Thomas, personal comms.)

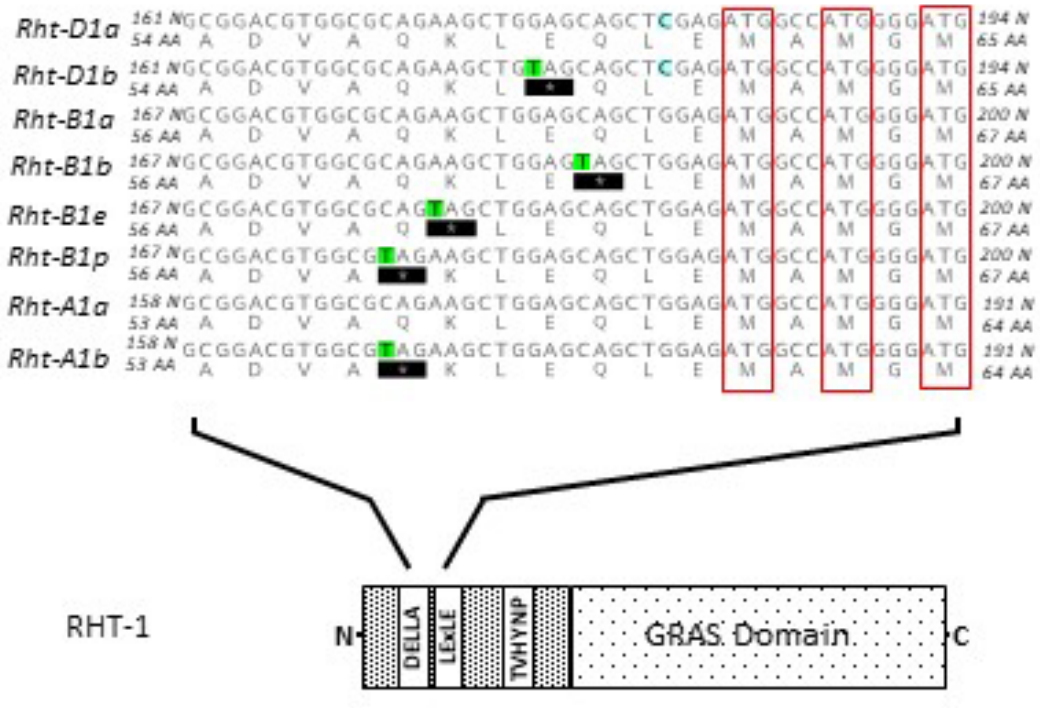

Figure 3.1 Nonsense Mutations in *Rht-1* Resulting in a GA Insensitive Phenotype. A schematic diagram of RHT-1 is shown, with the conserved motifs in the N-terminal region (DELLA, LExLE, TVHYNP) and the GRAS domain. The partial nucleotide and amino acid sequence in DELLA and LExLE motifs is shown. The nucleotide (green) and amino acid (black *) substitutions for *Rht-1* alleles are shown. *Rht-D1a/Rht-B1a/Rht-A1a* = WT, *Rht-D1b* = E61*, *Rht-B1b* = Q64*, *Rht-B1e* = K61*, *Rht-B1p* = Q60* and *Rht-A1b* = Q57*. * = a predicted nonsense mutation. Methionine (AUG) codons believed to induce translation reinitiation are shown in red rectangles.

The *Rht-B1p* mutation results in a 33% height reduction compared to WT control (Bazhenov et al. 2015). Similarly, *Rht-A1b* results in a 25-41% height reduction compared to WT control (personal comm. Dr Stephen Thomas). These are both more severe than the classic Green Revolution semi-dwarfing alleles, *Rht-B1b* and *Rht-D1b* that cause a 12-15% or 16-20% height reduction, respectively (Table 3.1.).

The three alleles *Rht-B1b, Rht-D1b* and *Rht-B1p* potentially result in GA-insensitive phenotypes due to translational re-initiation producing functional N-terminally truncated RHT proteins (Section 1.4) that constitutively repress GA mediated growth (Peng et al. 1999; Pearce et al. 2011).

By contrast, a more severe GA-insensitive phenotype in the mutant *Rht-B1c* is caused by a 30-amino acid insertion in the 'DELLA' region of (Figure 1.3.1) that potentially inhibits GA mediated degradation of the RHT-B1C protein (Wu et al. 2011; Pearce et al. 2011). It is conceivable that the *Rht-1* nonsense mutants produce a less severe GA-insensitive phenotype because the efficiency of translational re-initiation produces reduced levels of the constitutively active RHT-1 repressor than the insertion mutant Rht-B1c (Chandler and Harding 2013; Derkx et al. 2017; Phillips 2016).

The similarity of the *Rht-A1b* mutation to *Rht-B1b, Rht-D1b* and *Rht-B1p* suggests that it may be the first GA-insensitive allele identified in *Rht-A1.* To confirm whether this is the case and determine the effect of *Rht-A1b* on plant phenotype and GA sensitivity, detailed characterisation experiments were performed using *Rht-D1b, Rht-B1c* and WT Cadenza (*Rht-1)* controls. These genotypes have been extensively characterised and represent a spectrum of *GA in/*sensitive phenotypes, thus providing a background for comparison with the *Rht-A1b* mutations (Derkx et al. 2017; Chandler and Harding 2013). *Rht-A1b* was backcrossed extensively (BC_6F_4 generation), reducing the number of background mutations, ensuring the plant material is robust for phenotyping. *Rht-D1b* and *Rht-B1c* are Cadenza near isogenic lines. *Rht-B1p* was not included in these characterisation experiments as it has not been introgressed into the Cadenza (var.) background.

This chapter will describe a detailed characterisation of *Rht-A1b* and comparison with *Rht-D1b, Rht-B1c* and WT Cadenza (*Rht-1*) to determine the impact of *Rht-A1b* on GA sensitivity.

3.2 Phenotypic Characterisation of *Rht-A1b*

Gibberellin signalling plays a crucial role in plant growth and development from stem and leaf elongation to floral development, fertility and grain set (Section 1.3). The *Rht-1* dwarf and semi-dwarf alleles repress GA signalling (Peng et al. 1999). The most noticeable effect of this is reduced stem elongation (Lenton, Hedden, and Gale 1987), although pleiotropic effects on fertility, grain number, and stress responses have been noted (Ikeda et al. 2001) (Section 1.4). To quantify the effect of *Rht-A1b*

on mature plant phenotype, the line was grown alongside *Rht-D1b, Rht-B1c* and WT Cadenza (*Rht-1)* controls. Five individuals per line were grown up to maturity under standard glasshouse conditions (Section 2.1) in a randomised block design. Phenotypic measurements were taken during plant development and at maturity.

3.2.1 Heading date

GA insensitivity in *Rht-1* dwarfing alleles limits peduncle elongation (Keyes 1987; Keyes, Paolillo, and Sorrells 1989), which is key for heading date (Gardner, Hess, and Trione 1985). There is not much evidence to suggest that the *Rht-1* alleles affects heading date (Fischer and Stockman 1986; Youssefian, Kirby, and Gale 1992b), with the exception of one study that suggests a 5-10 day delay in flowering in *Rht-B1c* (Wu et al. 2011). Additionally, the mutant *sdw1* in barley (caused by a 7-bp deletion in exon 1 of *HvGA20ox2*) has been shown to delay flowering by 3-5 days (Teplyakova et al. 2017) . As heading date is strongly correlated to final grain yield in cereals it is important to assess whether the *Rht-A1b* mutation, which is more severe than *Rht-D1b* and *Rht-B1b*, has an effect on heading date. To assess this, the number of days between germination and first heading date was recorded. Residual plots for this data were assessed in GenStat, which confirmed that the data was Normal and did not require transformation. A General Analysis of Variance (ANOVA) was conducted, the output of which is presented in Table 3.2 and Figure 3.2.

Table 3.2: ANOVA output for Heading date in Rht-1 Dwarf and Control Lines

Line	Heading date (Days)	Days Difference Compared to *Rht-1*	P-Value	SED	LSD 5%
Rht-B1c	**63.6 ± 0.9**	6.8	<0.001	0.8	1.8
Rht-A1b	**59.4 ± 1.1**	2.6			
Rht-D1b	**59 ± 0.3**	2.2			
Rht-1	56.8 ± 0.4				

The mean value is shown with its standard deviation, along with the standard error of differences (SED) and 5% least significant difference of means (LSD 5%). Means shown in bold are significantly different from *Rht-1,* underlined means are significantly different from *Rht-A1b.*

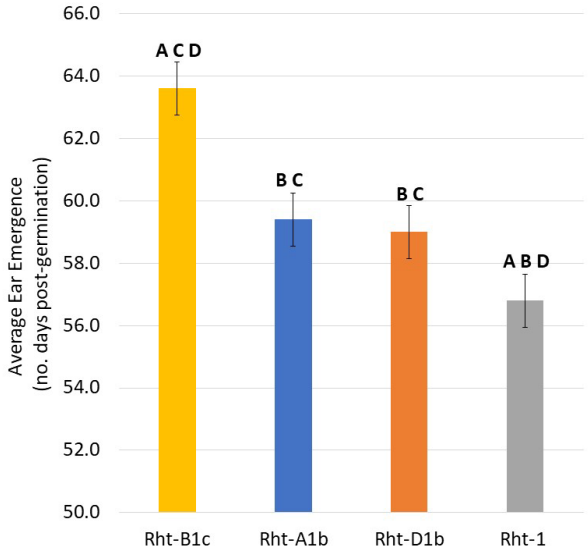

Figure 3.2: Average Time for Heading date in Rht-1 Dwarf and Control Lines. Shown as number of days post-germination. Yellow = *Rht-B1c,* blue = Rht-A1b, orange = *Rht-D1b,* grey = *Rht-1.* All mutations are backcrossed into Cadenza (var). P-value = <0.001. Error bars = standard error of means (0.8). Significantly different from: A = *Rht-A1b,* B = *Rht-B1c,* C = *Rht-1,* D = *Rht-D1b*.

The ANOVA confirmed a highly significant interaction between genotype and the time taken for first flowering ($p<0.001$). The 5% least significant difference of means (5% LSD) (1.8) was used to assess significantly different heading dates between the genoptypes. emergence of the wild-type control *Rht-1* occurred significantly earlier than those lines containing the *Rht-1* dwarfing alleles. There was no significant difference between the heading dates of *Rht-A1b* and *Rht-D1b* which flowered 2.2-2.8 days later than *Rht-1*. Meanwhile, *Rht-B1c* ears emerged significantly later than in the other lines, with an average heading date 6.8 days later than *Rht-1*.

These results suggest that *Rht-A1b* displays an intermediate heading date, similar to *Rht-D1b*, with ears emerging faster than the severe dwarf *Rht-B1c* and later than WT *Rht-1.*

3.2.2 Plant Height

As discussed in Section 1.3.1, the most notable effect of *Rht-1* alleles is a reduction in plant height, caused by reduced cell elongation (Keyes 1987; Keyes, Paolillo, and Sorrells 1989), which strongly correlates to reduced GA responsiveness (Lenton, Hedden, and Gale 1987). Previous studies in which the classical *Rht-1* dwarfing mutations were present (as NILs) in the wheat varieties April Bearded, Bersée, Maris Widegeon and Maris Huntsman have also demonstrated this correlation, with the severely GA insensitive *Rht-B1c* allele resulting in a 50% height reduction compared to the relevant tall control and *Rht-D1b* causing a 14% height reduction (Flintham et al. 1997). To assess the effect of *Rht-A1b* on plant height and to establish the effects of *Rht-B1c* and *Rht-D1b* on height in the variety Cadenza, plants were grown to maturity in the glasshouse alongside the control *Rht-1* (Figure 3.3).

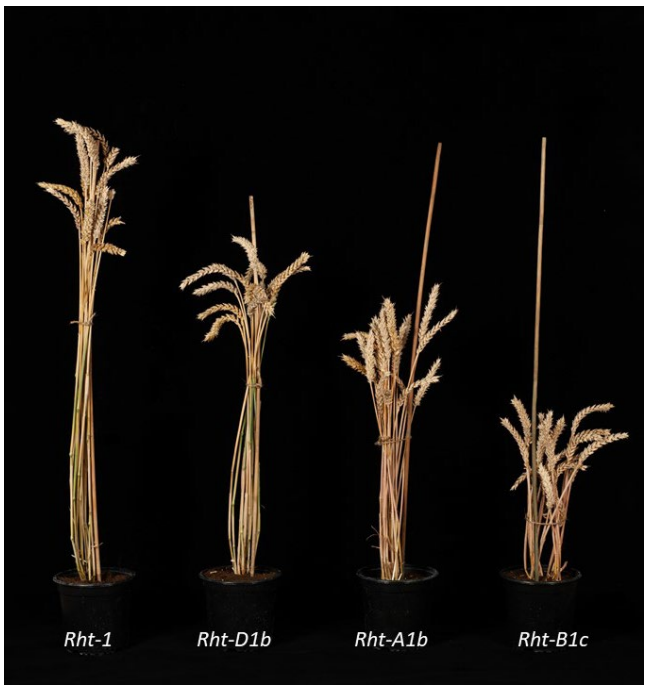

Figure 3.3: Photograph of *Rht-1* Mutant Lines. Plants were grown to maturity in the glasshouse before being photographed. All alleles are in Cadenza (var.), *Rht-A1b* is BC_6F_4 whilst *Rht-D1b* and *Rht-B1c* are near isogenic lines.

To confirm the effect of the *Rht-1* alleles on plant height, ear and internode measurements were taken for three shoots per plant. *Rht-A1b* was grown alongside controls of *Rht-D1b, B1c* and *Rht-1* and the Residual plots for the data were assessed in GenStat, which confirmed that the data was Normal and did not require

transformation. A General Analysis of Variance (ANOVA) was conducted on each data set, the output of which is described in Table 3.3, and Figure 3.3.

Table 3.3: ANOVA output for Total Shoot Length in Rht-1 Mutant and Control Lines

Line	Total Shoot Length (mm)	% Height Reduction from *Rht-1*	P-value	SED	LSD 5%
Rht-B1c	**349.5 ± 2.98**	55.4%	<0.001	13.83	29.76
Rht-A1b	**520.5 ± 2.98**	33.5%			
Rht-D1b	**647.1 ± 1.26**	17.4%			
Rht-1	783.1 ± 1.67	NA			

The mean value is shown with its standard deviation, along with the standard error of differences (SED) and 5% least significant difference of means (LSD 5%). Means shown in bold are significantly different from *Rht-1,* underlined means are significantly different from *Rht-A1b.*

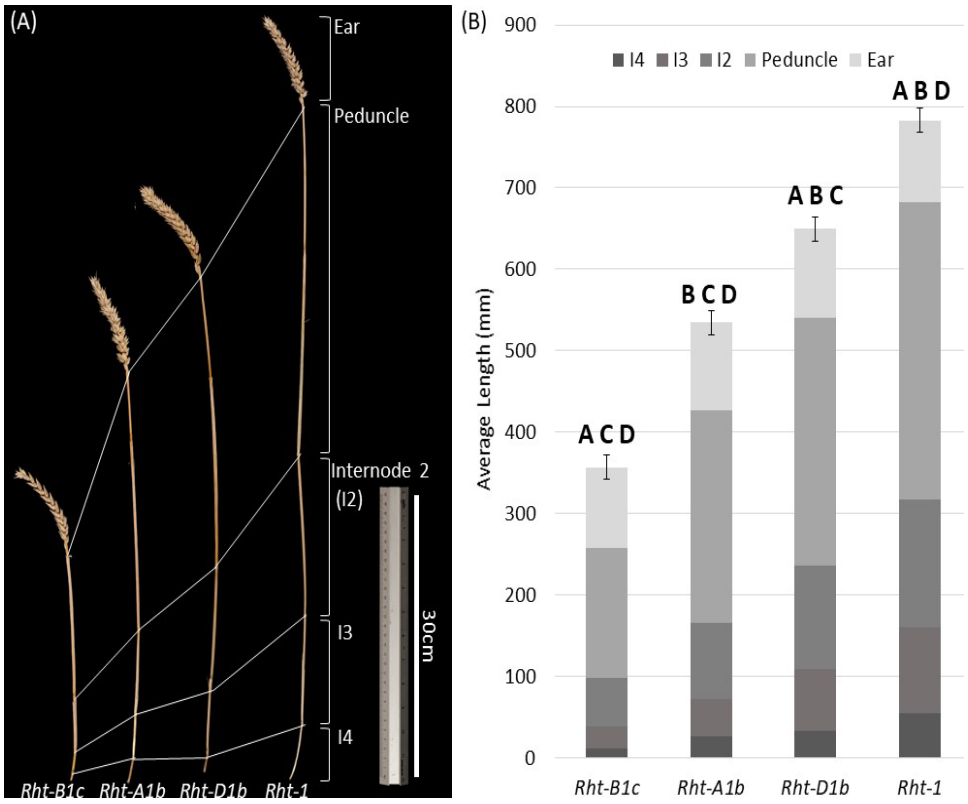

Figure 3.4: Phenotyping Shoots to Determine the Effect of *Rht-A1b* on Plant Height. (A) Photograph of a single mature shoot from *Rht-B1c, Rht-A1b, Rht-D1b and Rht-1*. Ear and internode segments are shown. **(B) ANOVA output comparing total shoot length for each line.** p<0.001, error bars = standard error of means (SED) 13.83. * denotes a value significantly different than *Rht-A1b*. The average length of the different shoot segments: ear, peduncle, internode 2 (I2), internode 3 (I3) and internode 4 (I4), for each line are shown. All lines are in Cadenza (var.) Significantly different from: A = *Rht-A1b,* B = *Rht-B1c,* C = *Rht-1,* D = *Rht-D1b*.

A ANOVA confirmed that there was a significant interaction between genotype and total shoot length ($p<0.001$), as shown in Figure 3.4 (A). The 5% LSD (29.76) confirmed that the shoot lengths of all genotypes were significantly different from one another. *Rht-1* produced the longest shoots, which reduced in length by 17.4% in *Rht-D1b,* 33.5% in *Rht-A1b* and 53.5% in *Rht-B1c*.

The difference in shoot length between genotypes is the result of differences in the lengths of each shoot segment (internode 4, 3, 2, peduncle and ear). The *Rht-1* dwarfing alleles have been shown to reduce internode elongation by up to 50% (Miralles et al. 1998), by limiting cell wall extensibility and cell elongation (Tonkinson et al. 1995; Keyes, Paolillo, and Sorrells 1989). To determine the effect of *Rht-A1b, Rht-D1b* and *Rht-B1c* on internode elongation, these measurements (defined in Section 2.3.1) were taken for the three tallest shoots per plant. In addition, although there is no evidence that the *Rht-1* alleles influence ear length, this characteristic was measured as this is also a component in total shoot length.

To determine the effect of genotype on the length of different internode segments additional ANOVAs were conducted, described in Table 3.4 and Figure 3.5.

Table 3.4: ANOVA output for Shoot Components(mm) in Rht-1 Mutant and Control Lines

	Internode 4		Internode 3		Internode 2		Peduncle		Ear	
	ANOVA	%	ANOVA	%	ANOVA	%	ANOVA	%	ANOVA	%
Rht-B1c	**11.6 ± 3.4**	-79%	**27.1 ± 6.4**	-74%	**59.5 ± 11.3**	-62%	**160 ± 32.8**	-56%	**99 ± 9.5**	-1%
Rht-A1b	**27.1 ± 6.4**	-50%	**45.6 ± 10.1**	-57%	**92.6 ± 17.5**	-40%	**261.1 ± 33.1**	-29%	**108.5 ± 6.4**	+8%
Rht-D1b	**33.6 ± 15.6**	-38%	**75.2 ± 10.8**	-29%	**127.1 ± 15**	-18%	**303.9 ± 17.6**	-17%	**108.6 ± 3.4**	+8%
Rht-1	53.5 ± 25.5	NA	106. ± 18.4	NA	155.8 ± 33.5	NA	365.9 ± 23.4	NA	100.2 ± 8.7	NA
P-Value	<0.001		<0.001		<0.001		<0.001		<0.001	
SED	6.62		3.33		7.95		6.14		2.56	
LSD 5%	13.45		8.68		15.96		12.32		5.14	

The mean value (measured in mm) is shown with its standard deviation, along with the standard error of differences (SED) and 5% least significant difference of means (LSD 5%). Means shown in bold are significantly different from *Rht-1,* underlined means are significantly different from *Rht-A1b.* Percentage length is calculated against the control *Rht-1*, - = reduction in length, + = increase in length.

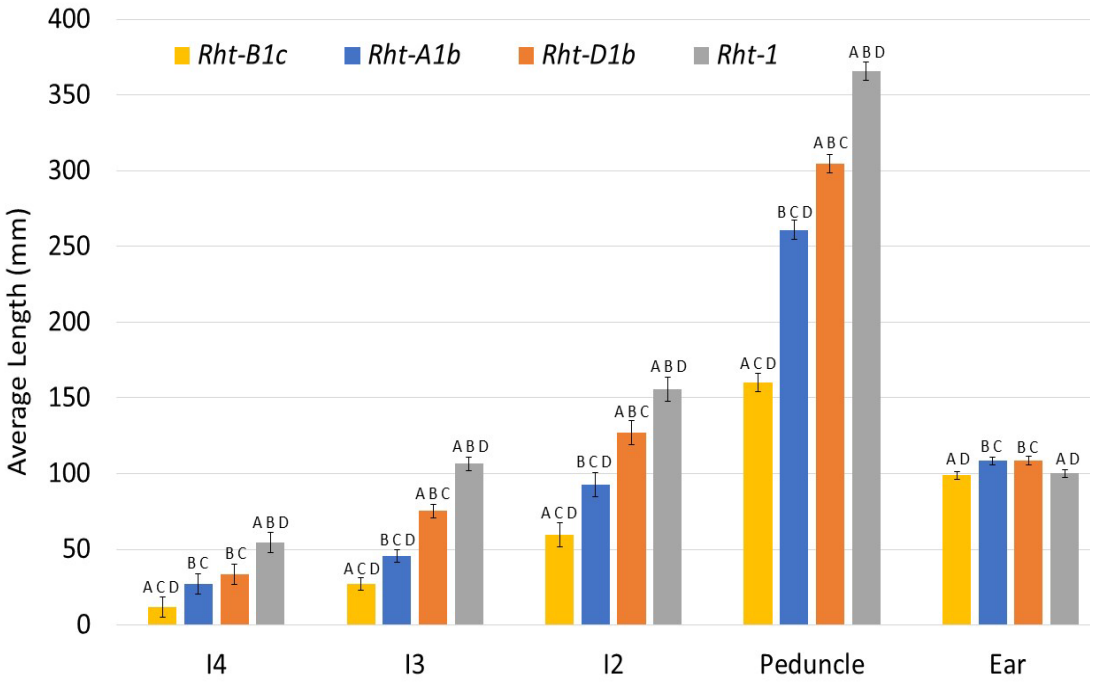

Figure 3.5: ANOVA outputs for different shoot segment lengths for in Rht-1 Mutant and Control Lines. Error bars = standard error of differences (SED) **(I4)** Internode 3. P<0.001, error bars = SED 6.62. **(I3)** Internode 3. P<0.001, error bars = SED 3.33. **(I2)** Internode 2. P<0.001, error bars = SED 7.95. **(Peduncle)** P<0.001, error bars = SED 6.13. **(Ear)** P<0.001, error bars = SED 2.561. All lines are in Cadenza (var.) Significantly different from: A = *Rht-A1b,* B = *Rht-B1c,* C = *Rht-1,* D = *Rht-D1b*.

As described in previous studies, there was no difference in the number of internodes in each shoot (Borrell, Incoll, and Dalling 1991). A ANOVA confirmed that there was a significant interaction between genotype and each of the shoot segment lengths: internode 4 ($p<0.001$), internode 3 ($p<0.001$), internode 2 ($p<0.001$), peduncle ($p<0.001$) and ear ($p<0.001$) (Table and Figure 3.5). The 5% LSD value was then used to confirm which genotypes produced significantly different segment lengths.

For internode 4 (LSD 13.45), *Rht-B1c, A1b* and *D1b* produced significantly shorter lengths than *Rht-1,* representing a length reduction of 78.7%, 50.3% and 38.3%, respectively. There was no significant difference between *Rht-A1b* and *Rht-D1b.*

For internode 3 (LSD 8.68), all the genotypes produced significantly different internode lengths from one another. *Rht-B1c, A1b* and *D1b* produced significantly shorter internode 3s than *Rht-1,* representing a length reduction of 73.4%, 57% and 29.1%, respectively.

For internode 2 (LSD 7.95), all the genotypes produced significantly different internode lengths from one another. *Rht-B1c, A1b* and *D1b* produced significantly shorter second internode than *Rht-1,* representing a length reduction of 61.8%, 40.6% and 18.4%, respectively.

For the peduncle (LSD 6.14), all the genotypes produced significantly different internode lengths from one another. *Rht-B1c, A1b* and *D1b* produced significantly shorter peduncles than *Rht-1,* representing a length reduction of 56.3%, 28.6% and 16.7%, respectively.

For ear length (LSD 2.56), there was no significant difference between *Rht-B1c* and *Rht-1. Rht-A1b* and *Rht-D1b* produced ears that were significantly longer than *Rht-1,* by 8.3% and 8.4% respectively, and that were not significantly different from each other.

These results suggest that *Rht-A1b* produces a dwarf phenotype, intermediate to *Rht-D1b* and *Rht-B1c*, and that this phenotype is caused by the intermediate length of the peduncle, internode 2 and internode 3 (Figure 3.5).

3.2.3 Tillering

In rice, GA mediated degradation of the DELLA, SLR1, triggers stem elongation and the degradation of the shoot regulator MONOCULM 1, resulting in a decrease in shoot number (Liao et al. 2019). As a result GA-deficient (*sdg*) and GA-signalling mutants (*sd1* and *slr1-d1*) have a greater number of shoots than WT plants (Liao et al. 2019). As the *Rht-1* dwarfing alleles are hypothesised to be resistant to GA-mediated degradation (Peng et al. 1999), shoot number for each plant was counted to see if there was an increase in shoot number in the *Rht-1* alleles. Residual plots for this data were assessed in GenStat, which confirmed that the data was Normal and did not require transformation. A General Analysis of Variance (ANOVA) was conducted on each data set, the output of which is described in Table 3.5.

Table 3.5: ANOVA output for Shoot Number in Rht-1 Mutant and Control Lines

Line	Total Shoot Number	P-value
Rht-B1c	19.8 ± 3.1	0.051
Rht-A1b	18 ± 3.4	
Rht-D1b	15.2 ± 3.2	
Rht-1	13.8 ± 5.8	

The mean value is shown with its standard deviation, along with the ANOVA p-value.

The ANOVA determined that there was no significant interaction between genotype and shoot number (P-value = >0.05), therefore no further analysis was taken.

3.2.4 Spikelet Number

There is no recorded association between *Rht-1* dwarfs and spikelet number in wheat (Villareal, Rajaram, and Deltoro 1992). However, in barley, the dwarf DELLA mutant, *sln1-d,* 3D imaging of the inflorescence meristem during the double ridge stage when spikelet are initiated (Section 1.3.5) has demonstrated that significantly fewer spikelets are initiated at this stage, resulting in a lower spikelet number per ear than in WT ears (Serrano-Mislata et al. 2017). To see whether this is the case in *Rht-D1b* and *Rht-A1b,* which had ears 8.4% and 8.3% respectively longer than *Rht-1,* the number of spikelets per ear were counted to see whether increased ear length translated into increased spikelet number.

Residual plots for this data were assessed in GenStat, which confirmed that the data was Normal and did not require transformation. A General Analysis of Variance (ANOVA) was conducted on each data set, the output of which is described Table 3.6.

Table 3.6: ANOVA output for Spikelet Number in Rht-1 Mutant and Control Lines

Line	Spikelet Number	P-value
Rht-B1c	19.1 ± 1.8	0.177
Rht-A1b	19.3 ± 1.4	
Rht-D1b	19.7 ± 1.8	
Rht-1	18.47 ± 1.8	

The mean value is shown with its standard deviation and the ANOVA P-value.

The ANOVA determined that there was no significant interaction between genotype and shoot number (P-value = >0.05), therefore no further analysis was taken.

3.2.5 Grain Number Per Ear

In lines containing the *Rht-1* dwarfing alleles, increased grain number is associated with improved assimilate partitioning to the developing ear, resulting in an increased number of viable florets at anthesis (Section 1.3.2) (Youssefian, Kirby, and Gale 1992a, 1992b). The ability of *Rht-1* alleles to improve yield is closely associated with the general height of the wheat variety in which they are introduced. Previous studies suggest that taller wheat varieties such as April Bearded show improved yields when more severe dwarfing alleles (e.g. *Rht-B1c*) are introduced, whilst shorter varieties such as Maris Huntsman benefit from semi-dwarfing alleles such as *Rht-B1b* and *Rht-D1b* (Section 1.3.2) (Flintham et al. 1997). To assess the effect of each allele in a Cadenza (var.) background, the total number of grain per plant was counted and then divided by the number of shoots per plant to provide an estimate of the number of grains per ear. This measure allows us to compare whether there are an increased number of viable florets per spikelet in the *Rht-1* alleles. Residual plots for this data were assessed in GenStat, which confirmed that the data was Normal and did not require transformation. A General Analysis of Variance (ANOVA) was conducted on each data set, the output of which is described in Table 3.7 and Figure 3.6.

Table 3.7: ANOVA output for Number of Grains per Ear in Rht-1 Mutant and Control Lines

Line	Number of Grains Per Ear	P-value	SED	LSD 5%
Rht-B1c	**<u>12.7 ± 8.3</u>**	<0.001	5.62	12.25
Rht-A1b	42.5 ± 5.5			
Rht-D1b	50.1 ± 8.4			
Rht-1	51.7 ± 10.6			

The mean value is shown with its standard deviation, along with the standard error of differences (SED) and 5% least significant difference of means (LSD 5%). Means shown in bold are significantly different from *Rht-1,* underlined means are significantly different from *Rht-A1b.*

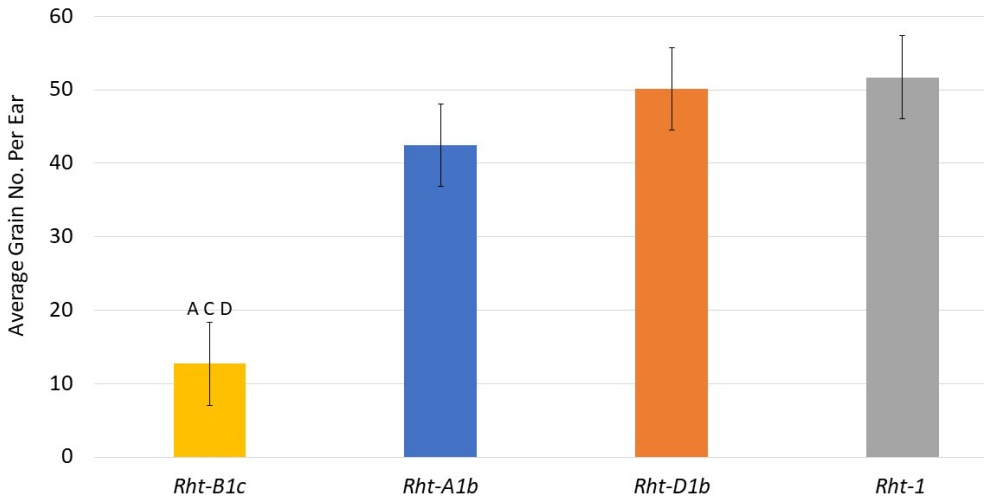

Figure 3.6: Number of Grains Per Ear in Rht-1 Mutant and Control Lines. Yellow = *Rht-B1c,* blue = Rht-A1b, orange = *Rht-D1b,* grey = *Rht-1.* All mutations are backcrossed into Cadenza (var). P-value = <0.001. Error bars = standard error of differences (SED) 5.62. Significantly different from: A = *Rht-A1b,* C = *Rht-1,* D = *Rht-D1b*.

The ANOVA confirmed that there was a highly significant interaction between genotype and the number of grains per ear (P<0.001). The 5% LSD (12.25) was used to confirm which genotypes produced significantly different number of grains per ear. This identified that there was no significant difference between *Rht-A1b, Rht-D1b* and *Rht-1* and that *Rht-B1c* produced significantly fewer (75.4% reduction) grains than *Rht-1.*

These results suggest that *Rht-A1b* may be a higher yielding allele, like *Rht-D1b,* and that the *Rht-A1b* mutation is not so severe as to reduce yield as seen in *Rht-B1c*.

3.2.6 Grain Characteristics

Increased grain number in *Rht-1* dwarfing alleles is often associated with reduced grain size in wheat, potentially due to increased inter-floret competition for assimilates and space (Gooding, Addisu, et al. 2012; Flintham et al. 1997). To assess the effect of the *Rht-1* alleles on grain size in Cadenza, a Marvin grain analyser (INDOSAW, India) was used to measure the length (mm), width (mm) and area (mm^2) of all the grain collected from each genotype. Residual plots for this data were assessed in GenStat, which confirmed that the data was Normal and did not require transformation. An Unbalanced Analysis of Variance (ANOVA) was

conducted on the data set, the output of which is described in Table 3.8 and Figure 3.7.

Table 3.8: ANOVA output 1 for Individual Grain Components in Rht-1 Mutant and Control Lines

	Grain Area (mm^2)	Grain Length (mm)	Grain Width (mm)
Rht-B1c	**18.9 ± 3.27**	**6.81 ± 0.58**	**3.52 ± 0.62**
Rht-A1b	**16.6 ± 3.57**	**6.64 ± 0.62**	**3.21 ± 0. 54**
Rht-D1b	**17.9 ± 3.6**	**6.72 ± 0.51**	**3.42 ± 0.56**
Rht-1	19 ± 3.85	6.92 ± 0.52	3.54 ± 0.59
P-Value	<0.001	<0.001	<0.001
SED	0.13	0.02	0.02
LSD 5%	0.25	0.04	0.04

The mean value (measured in mm) is shown with its standard deviation, along with the standard error of differences (SED) and 5% least significant difference of means (LSD 5%). Means shown in bold are significantly different from *Rht-1,* underlined means are significantly different from *Rht-A1b.*

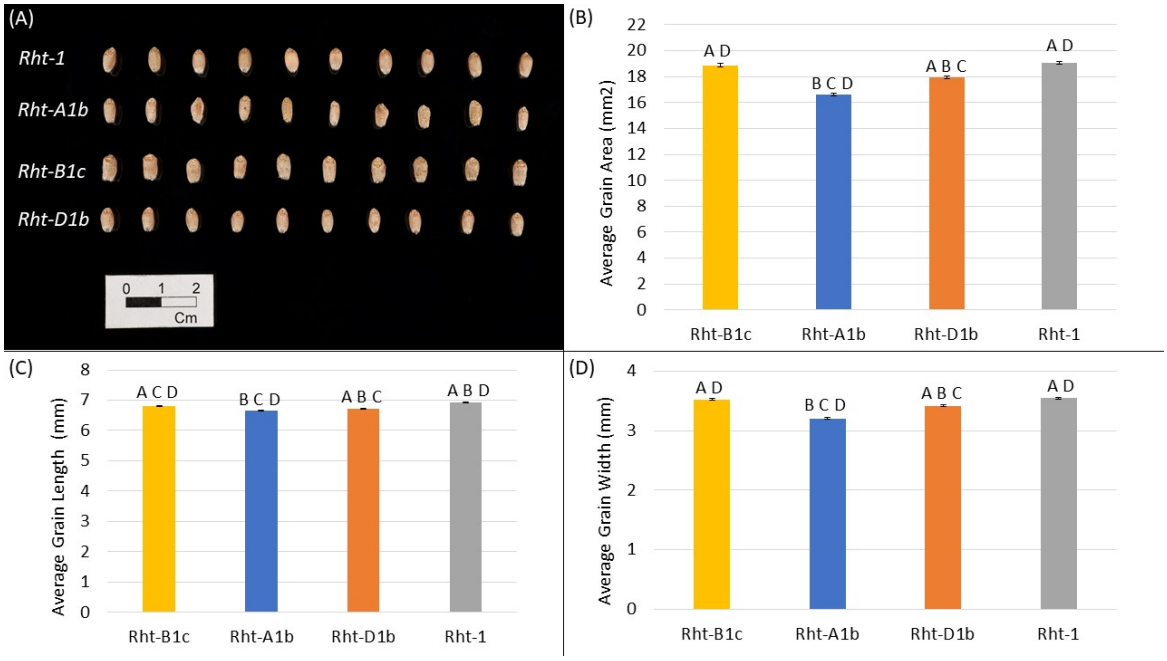

Figure 3.7: Grain Size Characteristics for *Rht-1* dwarfing mutants and Cadenza. (A) Photograph of 10 mature seed for each line. (B) Average Grain Area (mm^2). P=<0.001, error bars = SED 0.13. **(C) Average Grain Length (mm).** P=<0.001, error bars = SED (0.02). **(D) Average Grain Width (mm).** P=<0.001, error bars = SED (0.02). Yellow = *Rht-B1c,* blue = *Rht-A1b*, orange = *Rht-D1b,* grey = *Rht-1.* All mutations are backcrossed into Cadenza (var). A = *Rht-A1b,* B = *Rht-B1c,* C = *Rht-1,* D = *Rht-D1b*.

The ANOVAs confirmed that there is a significant interaction between grain area (p=<0.001), grain length (p=<0.001) and grain width (p=<0.001) and genotype. The least significant difference of means for grain area (0.25) determined that there was no significant difference between *Rht-1* and *Rht-B1c,* that *Rht-D1b* produced intermediate grain size significantly larger than *Rht-A1b* and smaller than *Rht-1* and *Rht-B1c.*

Rht-A1b produced the smallest grains, despite not producing significantly more grains that the other phenotypes. The least significant difference of means for grain length (0.04) and grain width (0.04) determined that this was because *Rht-A1b* produced significantly shorter and narrower grains than *Rht-D1b, Rht-B1c* and *Rht-1*.

3.3 Determining GA Sensitivity in *Rht-A1b*

Early studies of *Rht-1* mutants demonstrated that their dwarf and semi-dwarf phenotype was due to GA insensitivity (Gale and Marshall 1973), which limits cell elongation resulting in reduced stem length (Keyes 1987; Keyes, Paolillo, and Sorrells 1989). Additional studies demonstrated that application of exogenous GA to wheat seedlings in culture could be used to identify seedlings containing *Rht-1* dwarfing alleles (Gale et al. 1975). The Minister Dwarf variety, containing *Rht-B1c* (formerly *Rht3*), was crossed to Chinese Spring. In the F_2 generation seedling coleoptile lengths were measured one-week post-germination and then their culture solution was supplemented with GA_3. Ten days later, only seedlings with long coleoptiles at a week old had responded to the GA_3 treatment. The short coleoptile seedlings did not elongate in response to GA treatment, demonstrating GA insensitivity. Thirty 'short' seedlings were identified compared to 10 'long' seedlings, indicating the segregation of a single dominant gene (Gale et al. 1975). Subsequently, measuring plant response to the application of exogenous GA has widely been used to aid in the characterisation of GA-response mutants (Weyers et al. 1995; Swain and Olszewski 1996).

GA response assays were then developed to characterise DELLA mutants in cereals. In barley, mutants of the DELLA SLN1 where characterised by growing seedlings in filter paper 'envelopes' held vertically in culture solutions containing different GA_3 concentrations for 10 days. At 24-hour intervals the position of the 1st leaf tip was marked on a plastic sheet, enabling the growth rate per day to be recorded. The maximal millimetre-per-day rate at each GA_3 concentration was then plotted, generating a GA-dose response curve (Chandler and Robertson 1999) (Figure 3.8).

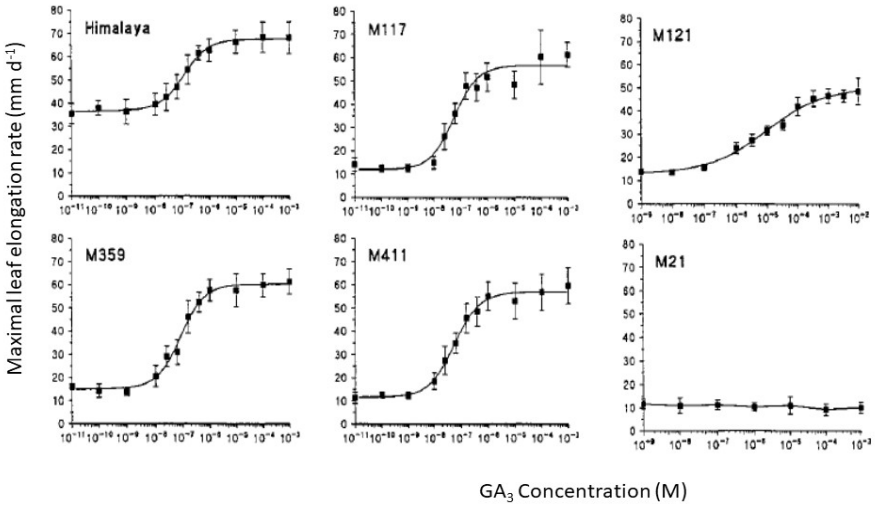

Figure 3.8: GA Dose Response Assays for *Sln1* and *Sln1* mutants in Himalaya (var.) barley seedlings. Maximal daily growth rates (mm d^{-1}) are shown for each line in each GA_3 treatment. WT *Sln1* = Himalaya, *Sln1* mutants = M117, M121, M359, M411 and M21. Adapted from (Chandler and Robertson 1999).

M21 the mutant which exhibited no GA_3 response was identified as an *Sln1* dwarf mutation. Similar GA dose response assays have also been developed to characterise DELLA *(Slr1)* mutants in rice, with seedlings sown onto 1% agar plates containing different concentrations of GA_3. After 10 days, the length of the second leaf sheath for each plant was measured to assess plant responsiveness to GA_3 (Asano et al. 2009).

Seedling elongation is used for GA dose response assays, as GA insensitivity in DELLA mutants affects all organ expansion processes (Ikeda et al. 2001; Chandler et al. 2002). Reduced cell wall extensibility (Tonkinson et al. 1995; Keyes, Paolillo, and Sorrells 1989), limits cell elongation (Keyes 1987; Keyes, Paolillo, and Sorrells 1989),

resulting in shorter seedling leaf sheaths and leaves. The severity of GA insensitivity is correlated with decreased seedling elongation and mature plant height (Sojka, Stolzy, and Fischer 1981), therefore these studies provide a convenient measure of GA responsiveness.

Using the method detailed in Section 2.5, GA_3 dosage response assays were conducted to compare *Rht-A1b* seedlings to *Rht-D1b, Rht-B1c* and WT (*Rht-1*) Cadenza. Seedlings were surface sterilised, germinated on filter paper and then transferred to vermiculite trays containing different GA_3 treatments. 10 days post germination, the lengths of the first leaf and first leaf sheath of 15 seedlings per genotype, per GA_3 treatment were measured (Figure 3.9). Leaf sheath and first leaf measurements were taken to optimise this protocol for wheat seedlings. Previous GA dose response assays in rice (Asano et al. 2009) and barley (Chandler and Robertson 1999) have respectively measured the second leaf sheath and first leaf length. Both measurements were therefore taken to determine which is most suitable for wheat seedling assays. The experiment was replicated 3 times using a randomised block method.

Leaf Sheath Data

The residual plots for the raw leaf sheath data was assessed in GenStat (v18, VSNI, Hemel Hempstead, U.K.), this confirmed that the data was Normal and did not require transformation. A General Analysis of Variance (ANOVA) was conducted on the leaf sheath data to assess the effect of GA concentration on the growth of *Rht-A1b, Rht-B1c, Rht-D1b* and *Rht-1* seedlings. The output of this ANOVA is described in Tables 3.9 and Figure 3.9.

Table 3.9: ANOVA Output for Leaf Sheath (mm) Data in Untreated Rht-1 Mutant and Control Lines 10 days post-germination

	[GA_3] (M)						
	0	10^{-9}	10^{-8}	10^{-7}	10^{-6}	10^{-5}	10^{-4}
Rht-A1b	**33.84 ± 3.81**	**36.24 ± 2.78**	**36.55 ± 2.85**	**37.59 ± 3.2**	**40.3 ± 2.3**	**40.61 ± 3.12**	**41.19 ± 2.8**
Rht-B1c	**20.41 ± 1.6**	**19.95 ± 1.46**	**20.15 ± 1.49**	**20.33 ± 1.77**	**20.52 ± 3.87**	**20.93 ± 1.42**	**21.55 ± 1.62**
Rht-D1b	**36.46 ± 3.1**	**39.48 ± 3.75**	**39.96 ± 3.11**	**40.95 ± 2.58**	**41.82 ± 3.39**	**43.44 ± 8.06**	**42.84 ± 2.13**
Rht-1	56.49 ± 3.04	58.28 ± 3.11	61.06 ± 9.57	70.53 ± 5.23	81.46 ± 7.75	80.73 ± 9.57	80.84 ± 8.47
P-Value	Genotype <0.001						
	[GA_3] <0.001						
	Genotype * [GA_3] <0.001						
SED	0.87						
5% LSDa	1.71						
5% LSDb	2.45						

The mean value is shown with standard deviation, along with the P-values for the effect of genotype, GA_3 concentration and the interaction between both (genotype*concentration). The standard error of differences (SED) is shown and 5% least significant difference of means (LSD 5%). LSDa = tests for significance between different genotypes with the same GA treatment. LSDb = tests for significance in the response of a genotype to different GA treatments. Means shown in bold are significantly different

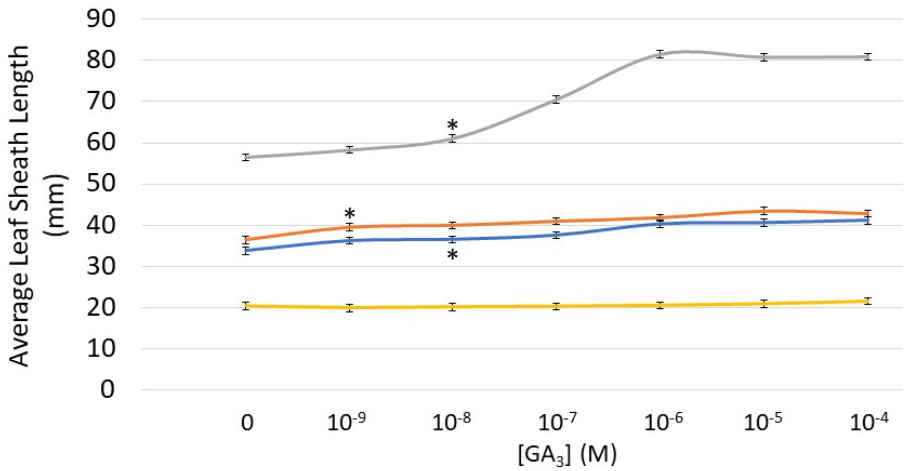

Figure 3.9: GA Dose Response Assays for *Rht* mutants and *Rht-1* controls.
Measurements of seedlings first leaf sheaths (mm) grown under different GA_3 concentrations [M]: 0 = water, 10^{-9}, 10^{-8}, 10^{-7}, 10^{-6}, 10^{-5} and 10^{-3}. Yellow = *Rht-B1c,* blue = *Rht-A1b*, orange = *Rht-D1b,* grey = *Rht-1.* All mutations are backcrossed into Cadenza (var). Data was assessed using a ANOVA.P=<0.001, error bars = standard error of differences (SED) 0.87. The first significant response to a GA_3 treatment (LSDb 2.45), compared to the control (0) is denoted with a *.

The ANOVA confirmed that both genotype ($P<0.001$) and GA_3 treatment ($P<0.001$) have a significant effect on leaf sheath elongation and that there is a significant interaction between genotype and GA_3 concentration ($P<0.001$).

The 5% LSDa (1.71) was then used to assess whether there was a significant difference between the leaf sheath lengths of genotypes for the same GA treatment. This confirmed that each genotype produced significantly different leaf sheath lengths from one another, although *Rht-A1b* and *Rht-D1b* produced very similar results and were not significantly different at 100 nm and 100 µM GA_3 (Table 3.9).

The 5% LSDb (2.4) was then used to assess when each genotype produced a significant response to GA_3 treatment, compared to the water (0) control. This identified that *Rht-D1b* produced a significant response to GA_3 following the 1 nM GA_3 treatment, elongating by 3.02 mm. *Rht-1* and *Rht-A1b* produced a significant response to GA_3 following the 10 nM GA_3 treatment elongating by 3.57 mm and 2.71 mm, respectively. *Rht-B1c* did not produce a significant response to any of the GA_3 treatments (Figure 3.9).

First Leaf Data

The residual plots for the raw first leaf data was assessed in GenStat (v18, VSNI, Hemel Hempstead, U.K.), this confirmed that the data was Normal and did not require transformation. A General Analysis of Variance (ANOVA) was conducted on the leaf length data to assess the effect of GA concentration on the growth of *Rht-A1b, Rht-B1c, Rht-D1b* and *Rht-1* seedlings. The output of this ANOVA is described in Tables 3.10 and Figure 3.10.

Table 3.10: ANOVA Output for First Leaf lengths (mm) in Untreated Rht-1 Mutant and Control Lines 10 days post-germination

	[GA_3] (M)						
	0	10^{-9}	10^{-8}	10^{-7}	10^{-6}	10^{-5}	10^{-4}
Rht-A1b	**101.41 ± 16.27**	**103.63 ± 16.07**	**101.49 ± 20.2**	**107.27 ± 12.43**	**109.80 ± 13.28**	**106.56 ± 13.87**	**102.89 ± 19.38**
Rht-B1c	**86.47 ± 8.74**	**86.81 ± 8.68**	**87.61 ± 6.3**	**88.03 ± 9.48**	**90.12 ± 7.65**	**90.78 ± 8.72**	**91.54 ± 7.31**
Rht-D1b	**107.36 ± 8.57**	**116.36 ± 11.09**	**113.07 ± 15.88**	**107.96 ± 16.73**	**110.78 ± 23.87**	**108.57 ± 17.82**	**106.01 ± 16.83**
Rht-1	125.32 ± 8.47	139.36 ± 12.9	148.08 ± 26.14	167.29 ± 20.91	177.47 ± 22.84	185.03 ± 13.78	176.81 ± 19.36
P-Value	Genotype <0.001						
	[GA_3] 0.002						
	Genotype * [GA_3] <0.001						
SED	3.13						
LSDa	6.28						
LSDb	8.79						

The mean value is shown with its standard deviation, along with the P-values for the effect of genotype, GA_3 concentration and the interaction between both (genotype*concentration). The standard error of differences (SED) is shown and 5% least significant difference of means (LSD 5%). LSDa = tests for a significant difference between different genotypes for the same GA treatment. LSDb = tests for a significant difference for the response to GA treatments for a genotype. Means shown in bold are significantly different (LSDa) from *Rht-1,* underlined means are significantly different from *Rht-A1b.*

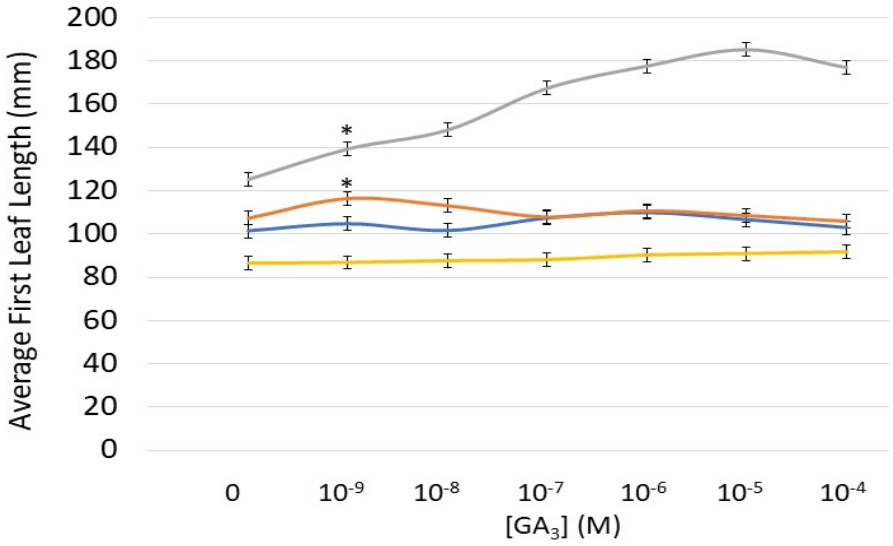

Figure 3.10: GA Dose Response Assays for *Rht* mutants and *Rht-1* controls. Measurements of seedlings first leaf lengths (mm) grown under different GA_3 concentrations: 0 = water, 10^{-9}, 10^{-8}, 10^{-7}, 10^{-6}, 10^{-5} and $10^{-3.}$ Yellow = *Rht-B1c,* blue = *Rht-A1b*, orange = *Rht-D1b,* grey = *Rht-1.* All mutations are backcrossed into Cadenza (var). Data was assessed using a ANOVA. P=<0.001, error bars = SED (3.13). The first significant response to a GA_3 treatment (LSDb 8.79), compared to the control (0) is denoted with a *.

The ANOVA confirmed that both genotype (P<0.001) and GA_3 treatment (P<0.001) have a significant effect on leaf elongation and that there is a significant interaction between genotype and GA_3 concentration (P<0.001). The 5% LSDa (6.38) was then used to assess whether there was a significant difference between the first leaf lengths of genotypes for the same GA treatment. This confirmed that *Rht-1* gave a significantly greater growth response than the other genotypes and that *Rht-B1c* produced a significantly lower response. *Rht-A1b* and *Rht-D1b* that same responses, that were only significantly different at 1 nM and 10 nM (Table 3.10).

The 5% LSDb (8.79) was then used to assess when each genotype produced a significant response to GA_3 treatment, compared to the water (0) control. This identified that *Rht-1* and *Rht-D1b* produced a significant response to GA_3 following the 1 nM GA_3 treatment, elongating by 13.04 mm and 9 mm, respectively. Neither *Rht-A1b* or *Rht-B1c* produced a significant response (Figure 3.10).

.

3.3.1 Optimising Paclobutrazol Treatment for GA Dose Response Assays

GA insensitive mutants such as *Rht-B1b* and *Rht-D1b* have altered GA feedback regulation that results in the overaccumulation of bioactive GAs (Lenton, Hedden, and Gale 1987). Therefore, to ensure that the measured seedling response to applied GA_3 is not influenced by the overaccumulation of endogenous GAs in the mutants, the GA dose response assay described in 3.3 was repeated using seeds imbibed in paclobutrazol (PAC) to eliminate the endogenous GA. PAC inhibits the oxidation steps that convert *ent*-kaurene into *ent*-kaurenoic acid early in the GA biosynthesis pathway, preventing the production of bioactive GAs *in planta* (Fletcher, Hofstra, and Gao 1986; Dalziel and Lawrence 1984).

To determine the appropriate PAC treatment for this experiment, Cadenza (*Rht-1)* seeds were imbibed in either 5 µM, 10 µM, 25 µM or 50µM paclobutrazol or a water control. These seeds were then germinated using the protocol described in Section 2.5 and 3.3. Seedlings were grown in vermiculite containing either sterile water or 1 µM GA_3 to confirm that leaf sheath length could be rescued following application of GA_3. 1 µM GA_3 was chosen as the GA treatment as this was the

lowest concentration that produced a near maximal growth response in the previous GA dose response assays (Section 3.3). Eleven days post-germination seedling first leaf sheaths were measured for 10 seedlings per treatment.

Residual plots for the raw leaf sheath measurements were assessed in GenStat, which confirmed that the data was Normal and did not require transformation. A Two-way ANOVA was used to assess the interaction between PAC treatment and GA_3 concentration on leaf sheath length. The output of the Two-way ANOVA is shown in Table 3.11 and Figure 3.12

Table 3.11: Two-Way ANOVA Output for Leaf Sheath lengths

[GA_3]	0					1µM				
[PAC]	0	5 µM	10 µM	25 µM	50 µM	0	5 µM	10 µM	25 µM	50 µM
Average Leaf Sheath Length (mm)	71.4 ± 3.0	77.5 ± 8.1	71.8 ± 5.4	43.2 ± 6.1	42.6 ± 12.6	97.7 ± 9.1	103.9 ± 7.0	96.3 ± 10.5	100.7 ± 3.5	97.5 ± 3.3
P-Value	[GA_3] <0.001									
	[PAC] <0.001									
	[GA_3]*[PAC] <0.001									
SEDa	2.32									
5% LSDa	3.6									
SEDb	3.29									
5% LSDb	6.6									

The mean value is shown with its standard deviation, along with the P-values for the effect of [GA_3], [PAC] and the interaction between both ([GA_3]*[PAC]), standard error of differences (SED) and 5% least significant difference of means (5% LSD). SEDa = for seedlings treated with the same [PAC], 5% LSDa = assess the significant difference between seedlings treated with the same [PAC], SEDb = for seedlings treated with the same [GA_3], 5% LSDa = assess the significant difference between seedlings treated with the same [GA_3].

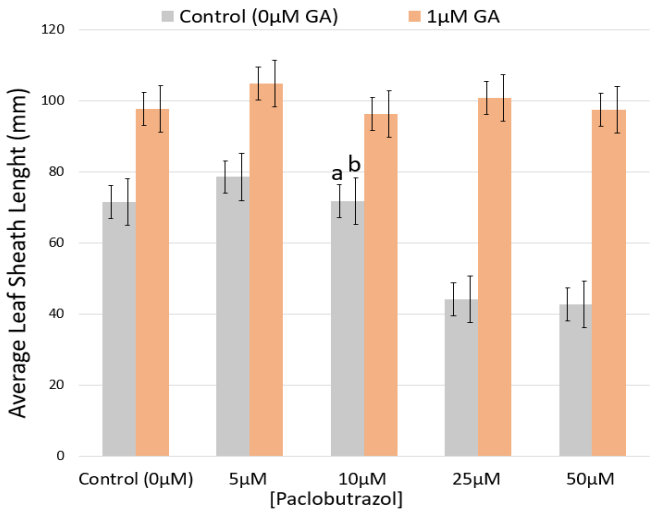

Figure 3.11: Leaf Sheath elongation in Cadenza Seedlings Treated with Paclobutrazol and GA_3. Average leaf sheath length (mm) of Cadenza (*Rht-1)* seedlings treated with different paclobutrazol (PAC) concentrations; 1µM, 5µM, 10µM, 25µM, 50µM and control (water) and grown under different GA_3 concentrations; 1µM (orange) and control (grey). Leaf sheaf measurements were taken 11 days post-germination. Error bars; a= standard error of means (SEDa) for seedlings treated with the same PAC concentration (2.46), b= SEDb for seedlings with the same GA_3 treatment, across the different PAC concentrations, 3.47.

The Two-way ANOVA confirmed a highly significant interaction between PAC treatment and response to GA_3 ($p<0.001$) (Figure 3.11).

The LSDb value (6.6) was used to assess whether there was a significant difference between seedlings with the same GA_3 treatment, across the different PAC concentrations. The leaf sheaths of seedlings not treated with GA_3 did not respond to the PAC treatments until 25µM, where there was a significant decline (27.2mm) in leaf sheath length. Across the different PAC treatments there was no significant difference in the leaf sheath lengths of seedlings treated with 1µM GA_3, demonstrating that application of GA_3 can fully rescue leaf sheath length. Therefore, it was determined that seeds treated with 25µM PAC would be used for further GA dose response experiments, as this was the lowest concentration to produce a significant decrease in leaf sheath lengths.

3.3.2 GA Dose Response Assay with Paclobutrazol Treated Seeds

To assess seedling response to only the application of exogenous GA, GA dose response assays were conducted on *Rht-A1b, Rht-D1d, Rht-B1c* and WT (*Rht-1*) Cadenza seeds using the same protocol as described in Section 2.5 and 3.3, using the optimised concentration of PAC (25µM). 10 days post-germination seedling leaf sheaths and first leaves were measured for 15 seedlings per genotype, per treatment. The experiment was repeated 3 times using a randomised block method. The raw data was assessed in GenStat and the residual plots confirmed that the data was Normal and did not require transformation.

An ANOVA was conducted on the raw leaf sheath data to assess if the application of exogenous GA significantly increased the growth of *Rht-A1b, Rht-B1c, Rht-D1b* and *Rht-1* seedlings treated with PAC. The output of these ANOVAs is described in Table 3.12 and Figure 3.13

Table 3.12: ANOVA Output for Leaf Sheath length (mm) of seedlings treated with PAC, 10 days posy-germination

	$[GA_3]$ (M)						
	0	10^{-9}	10^{-8}	10^{-7}	10^{-6}	10^{-5}	10^{-4}
Rht-A1b	**20.31 ± 1.59**	**23.66 ± 2.32**	**26.35 ± 1.49**	**32.93 ± 2.69**	**37.66 ± 2.02**	**38.21 ± 2.09**	**36.57 ± 1.88**
Rht-B1c	**12.93 ± 1.42**	**12.93 ± 1.42**	**12.82 ± 1.1**	**12.93 ± 1.42**	**13.91 ± 1.32**	**13.44 ± 1.86**	**13.73 ± 1.32**
Rht-D1b	**21.53 ± 2.57**	**23.8 ± 3.29**	**27.37 ± 1.74**	**33.02 ± 2.44**	**39.57 ± 2.51**	**39.97 ± 3.33**	**37.7 ± 2.37**
Rht-1	23.06 ± 3.11	27.37 ± 2.93	32.62 ± 3.25	52.53 ± 3.85	71.8 ± 6.87	82.28 ± 5.2	78.88 ± 3.32
P-Value	$[GA_3]$ <0.001						
	Genotype <0.001						
	$[GA_3]$*Genotype <0.001						
SED	1.15						
LSDa	1.82						
LSDb	2.32						

The mean with standard deviation is shown, along with the P-values for the effect of genotype, GA_3 concentration and the interaction between both (genotype*concentration). The standard error of differences (SED) is shown and 5% least significant difference of means (LSD 5%). LSDa = tests significant between different genotypes in the same GA treatment. LSDb = tests significant in a genotypes response to GA treatments. Means shown in bold are significantly different (LSDa) from *Rht-1,* underlined are significantly different from *Rht-A1b.*

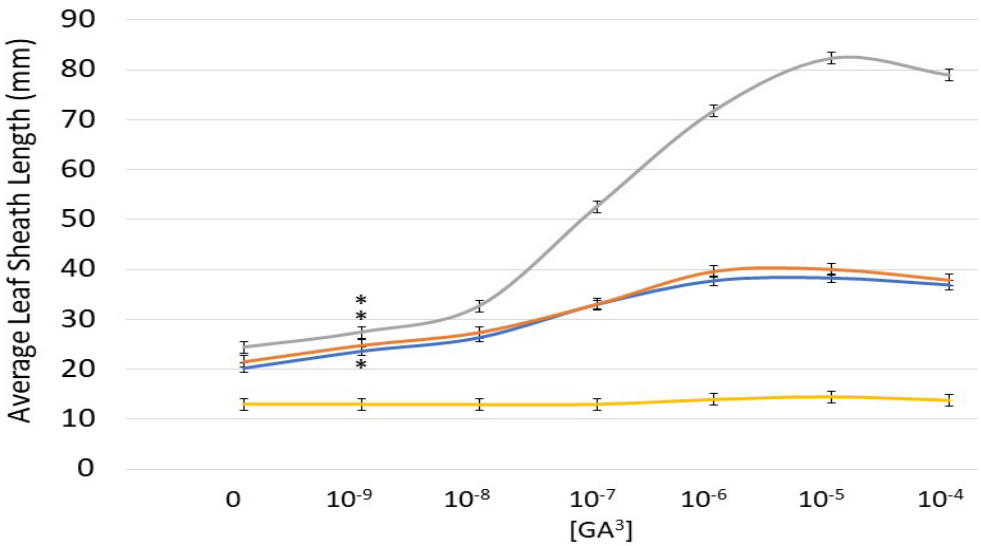

Figure 3.13: GA Dose Response Assays for *Rht* mutants and *Rht-1* controls treated with PAC. Measurements of seedling leaf sheath lengths (mm) following 25µM paclobutrazol treatment and grown under different GA_3 concentrations: : 0 = water, 10^{-9}, 10^{-8}, 10^{-7}, 10^{-6}, 10^{-5} and $10^{-3.}$ Yellow = *Rht-B1c,* blue = *Rht-A1b*, orange = *Rht-D1b,* grey = *Rht-1.* All mutations are backcrossed into Cadenza (var). Data was assessed using a ANOVA. P=<0.001, error bars = standard error of differences (1.15). The first significant response to a GA_3 treatment (LSDb 2.32), compared to the control (0) is denoted with a *.

The ANOVA confirmed that both genotype (P<0.001) and GA_3 treatment (P<0.001) have a significant effect on leaf sheath elongation and that there is a significant interaction between genotype and GA_3 concentration (P<0.001). The 5% LSDa (1.82) was then used to assess whether there was a significant difference between the leaf sheath lengths of genotypes with the same GA treatment. This confirmed that *Rht-1* produced significantly longer leaf sheaths than the other genotypes and that *Rht-B1c* produced significantly shorter leaf sheaths. Excluding the 1 µM GA_3 treatments, there was no significant difference between the growth of the *Rht-A1b* and *Rht-D1b* leaf sheaths, which produced very similar responses (Table 3.12).

The 5% LSDb (2.32) was then used to assess when each genotype produced a significant response to GA_3 treatment, compared to the water (0) control. This identified that *Rht-1, Rht-A1b* and *Rht-D1b* produced a significant response to GA_3 following the 1nM GA_3 treatment, elongating 3.31mm, 3.35mm and 3.27mm. *Rht-B1c* did not produce a significant response (Figure 3.13).

An ANOVA was also conducted on the raw first leaf data to assess if the application of exogenous GA significantly increased the growth of *Rht-A1b, Rht-B1c, Rht-D1b* and *Rht-1* seedlings treated with PAC. The output of these ANOVAs is described in Table 3.14 and Figure 3.14.

Table 3.13: ANOVA Output for First Leaf length (mm) for Paclobutrazol Treated Seedlings

	$[GA_3]$ (M)						
	0	10^{-9}	10^{-8}	10^{-7}	10^{-6}	10^{-5}	10^{-4}
Rht-A1b	**63.66 ± 8.63**	**73.48 ± 18.25**	**73.86 ± 17.52**	**88.11 ± 13.4**	**93.37 ± 13.06**	**100.8 ± 13.71**	**87.35 ± 8.08**
Rht-B1c	**60.68 ± 7.95**	**63.68 ± 8.03**	**67.77 ± 3.55**	**70.68 ± 6.32**	**78.57 ± 7.42**	**82.6 ± 9.09**	**70.6 ± 9.1**
Rht-D1b	69.71 ± 7.73	**75.6 ± 13.2**	**78.26 ± 11.91**	**88.53 ± 11.85**	**96.93 ± 13.69**	**93.71 ± 11.65**	**92.45 ± 13.41**
Rht-1	76.35 ± 9.16	85.26 ± 16.82	86.95 ± 9.25	113.91 ± 12.55	139.57 ± 19.23	150.06 ± 19.43	136.84 ± 17.01
P-Value	$[GA_3]$ <0.001						
	Genotype <0.001						
	$[GA_3]$*Genotype <0.001						
SED	3.77						
LSDa	7.13						
LSDb	9.67						

The mean value is shown with its standard deviation, along with the P-values for the effect of genotype, GA_3 concentration and the interaction between both (genotype*concentration). The standard error of differences (SED) is shown and 5% least significant difference of means (LSD 5%). LSDa = tests for significant between different genotypes in the same GA treatment. LSDb = tests for significant in a genotypes response to GA treatments. Bold means are significantly different (LSDa) from *Rht-1,* underlined means are significantly different from *Rht-A1b.*

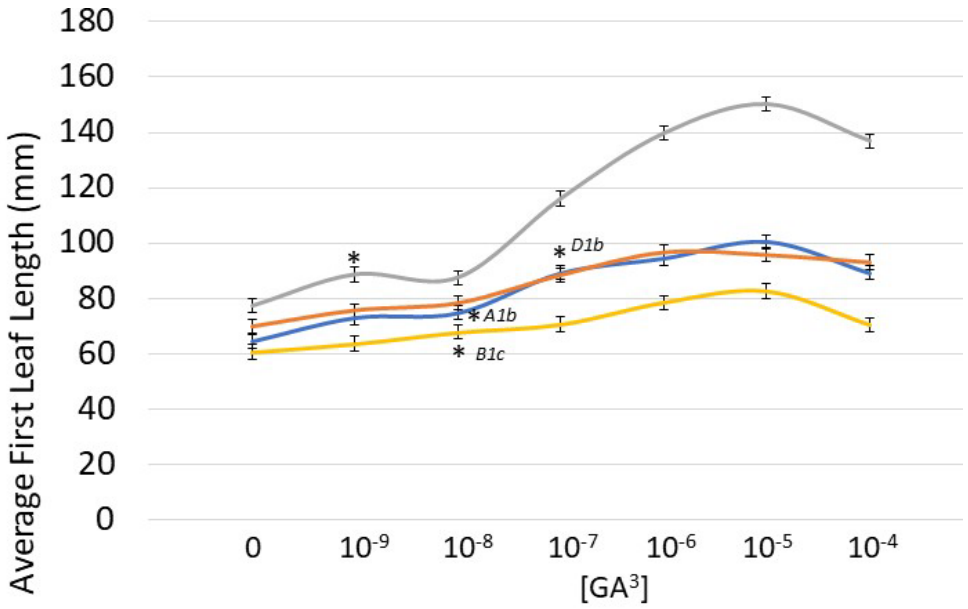

Figure 3.14: GA Dose Response Assays for *Rht* mutants and *Rht-1* controls Treated with PAC. Measurements of seedlings first leaf lengths (mm) grown under different GA_3 concentrations: 0 = water, 10^{-9} = 1nM GA_3, 10^{-8} = 10nM GA_3, 10^{-7} = 100nM GA_3, 10^{-6} = 1µM GA_3, 10^{-5} = 10µM GA_3 and 10^{-4} = 100µM GA_3. Yellow = *Rht-B1c,* blue = *Rht-A1b*, orange = *Rht-D1b,* grey = *Rht-1.* All mutations are backcrossed into Cadenza (var). Data was assessed using a two-way ANOVA. P=<0.001, error bars = SED (2.547). The first significant response to a GA_3 treatment (LSDb 2.32), compared to the control (0) is denoted with a *.

The ANOVA confirmed that both genotype (P<0.001) and GA_3 treatment (P<0.001) have a significant effect on leaf sheath elongation and that there is a significant interaction between genotype and GA_3 concentration (P<0.001).

The 5% LSDa (7.13) was then used to assess whether there was a significant difference between the leaf sheath lengths of genotypes in the same GA treatment. This confirmed that *Rht-1* produced significantly longer leaf sheaths than the other genotypes and that *Rht-B1c* produced significantly shorter leaf sheaths. Although, there was no significant difference between the pairs: *Rht-A1b* and *Rht-B1c, Rht-D1b* and *Rht-1*, in the control treatment. There was no significant difference between *Rht-A1b* and *Rht-D1b* first leaf lengths for any GA_3 treatment, which produced very similar responses (Table 3.13).

The 5% LSDb (9.67) was then used to assess when each genotype produced a significant response to GA_3 treatment, compared to the water (0) control. This identified that *Rht-1* produced a significant response to GA_3 following the 1nM GA_3

treatment*, Rht-A1b* and *Rht-B1c* for the 10nM treatment and *Rht-D1b* for the 100nM treatment (Figure 3.13).

Overall *Rht-A1b* displayed an intermediate response to exogenous GA, like the *Rht-D1b* response, across both (PAC and no PAC) seedling assays. This suggests that DELLA function at the seedling stage may not correlate to final plant height. If this was the case then *Rht-A1b* would have produced a more muted response.

3.3.3 Assessing the Robustness of Wheat Seedling GA Dose Response Assays

Dose response assays have been used widely to assess barley (Chandler et al. 2002; Chandler and Robertson 1999) and rice (Asano et al. 2009) DELLA mutants, by characterising seedling response to the application of exogenous GA. In barley, these assays measured elongation rates of the first leaf, whilst in rice the second leaf sheath was used as a measure of the response to GA. As GA-dose response assays have not been optimised for wheat DELLA mutants, both first leaf and leaf sheath measurements were taken during the assays described above. As a result, this section discusses four different GA dose response assays, involving combinations of measuring seedling leaf sheath and first leaf and treating seeds with or without paclobutrazol. ANOVAs for each of these combinations confirmed that there was a significant interaction between genotype and GA_3 concentration in seedling elongation ($p<0.001$). To assess which dose response assay would be most suitable for future experiments, the seedling-to-seedling variation (variance) for each ANOVA was assessed (Table 3.14)

Table 3.14: Seedling-to-seedling variation (variance) from each GA response assay

[PAC]	Measurement	Variance
0	Leaf Sheath	11.85 on 1259 d.f
	First Leaf	165.6 on 1259 d.f.
25µM	Leaf Sheath	3.19 on 1255 d.f
	First Leaf	82.17 on 1255 d.f.

The ANOVAs determined that the leaf sheath data had smaller variance (11.85 and 3.19 in untreated and PAC treated seedlings, respectively) in comparison to the first leaf data (165.6 and 82.17 in untreated and PAC treated seedlings respectively). Therefore, leaf sheath measurements provide a more precise means to assess seedling response to GA_3 in wheat. Additionally, seedling-to-seedling variation was reduced following PAC treatments, suggesting that the inhibition of GA biosynthesis (Dalziel and Lawrence 1984) provides a more precise method for monitoring seedling response to GA_3 during wheat seedling development.

3.4 Gibberellin Content in *Rht-1, Rht-A1b, Rht-D1b* or *Rht-B1c* Seedlings

The absence of GA results in the accumulation of DELLAs, which act to repress GA-dependent growth (Peng et al. 1997) and also control the homeostatic regulation of GA metabolism (Section 1.5.5) (Martin, Proebsting, and Hedden 1999). In model plants it has been demonstrated that DELLAs promote the expression of *GA20ox* and *GA3ox,* GA biosynthesis genes that catalyse the final steps in bioactive GA biosynthesis, while downregulating *GA2ox* genes which inactivate bioactive GAs (Hedden and Phillips 2000; Zentella et al. 2007). Gain-of- function DELLA mutants in *Arabidopsis (rga-Δ17)* (Zentella et al. 2007) and rice (*sd1*) (Wu et al. 2018) have been shown to upregulate *GA20ox* and *GA3ox* expression and it is expected that the same situation occurs with *Rht-1* dwarfs in wheat.

The first record of GA overaccumulation in *Rht-1* mutants was noted in (1970), when chromatography and bioassays identified that GA-like substances accumulated in higher levels in the seedlings of dwarf varieties such as Norin-10 (the source of *Rht-B1b* and *Rht-D1b*) compared to tall wheat varieties (Radley 1970). Later, gas chromatography (GC) mass spectrometry of near isogenic lines of Maris Huntsman (var.) identified that there was a 4- and 24-fold increase in GA_1 levels in the seedling leaf expansion zone of *Rht-D1b* and *Rht-B1c* seedlings, respectively, when compared to *Rht-1* seedlings (Lenton and Appleford 1991). Additionally, GC-mass spectrometry has demonstrated that GA_1 accumulates in vegetative stems of *Rht-B1c* and *Rht-B1b* (Maris Huntsman var.) during linear phase expansion. Again, GA_1 levels were most highly elevated in *Rht-B1c* than in *Rht-B1b,* compared to *Rht-1*

(Webb et al. 1998). The focus on GA_1 accumulation is because in wheat the 13-hydroxylation GA biosynthesis pathway is dominant. GA13ox converts GA_{12} to GA_{53} more efficiently than GA20ox converts GA_{12} to GA_{15}, resulting in higher levels of C_{19} GAs (Lenton, Hedden, and Gale 1987; Lenton and Appleford 1991). Studies also suggested that C_{20} GAs such as GA_{19} were at reduced levels in *Rht-1* dwarfs compared to the tall controls (Appleford and Lenton 1991).

To characterise *Rht-A1b* and determine whether similar GA content profiles are observed in *Rht-1* lines in Cadenza (var.), *Rht-A1b, Rht-D1b, Rht-B1c* and *Rht-1* seeds were germinated (Section 2.5) and grown in randomised vermiculite trays under standard conditions in 24-hour light. Seven days post-germination seedling material was harvested in pools of 10 seedlings per genotype. This time point was chosen as seedling tissue is still elongating (Lenton and Appleford 1991), enabling identification of bioactive GAs that are likely controlling this growth process (Section 1.3.2). Seedlings were removed from the vermiculite and cut between the crown and the first leaf ligule (Section 2.5.8) Five replicates per genotype were analysed.

Gibberellins were extracted from freeze dried seedling tissues and analysed using a triple quadrupole mass spectrometer (further details provided in Section 2.5.8).

Concentration profiles were generated for GAs from both the 13-hydroxylation and non-13-hydroxylation pathways. Residual plots for this data were assessed in GenStat, which confirmed that the data was Normal and did not require transformation. A series of one-way ANOVAs were than used to assess whether individual GA concentrations varied significantly between the genotypes, the output is shown Table 3.15 and Figure 3.15. The fold-change of GA content in *Rht-A1b, Rht-B1c,* and *Rht-D1b* compared to *Rht-1* is shown in Table 3.15.

Table 3.15: One-Way ANOVA Output for the concentration of GAs in wheat containing different Rht-1 *alleles*

		Rht-A1b	*Rht-B1c*	*Rht-D1b*	*Rht-1*	P-Value	SED	5% LSD
Gibberellin Content (pg/mg DW)	***GA1***	8.00 ± 0.54	10.45 ± 2.29	6.36 ± 0.88	3.34 ± 0.96	<0.001	0.67	1.46
	GA3	2.81 ± 0.77	2.00 ± 0.59	1.73 ± 0.38	1.76 ± 0.26	0.02	0.33	0.72
	GA4	5.16 ± 0.57	10.08 ± 0.78	3.13 ± 0.53	0.63 ± 0.14	<0.001	0.42	0.92
	GA6	0.18 ± 0.03	0.12 ± 0.01	0.35 ± 0.2	0.12 ± 0.01	0.03	0.07	0.16
	GA7	0.46 ± 0.13	0.66 ± 0.13	0.31 ± 0.04	0.20 ± 0.04	<0.001	0.07	0.15
	GA8	6.76 ± 0.92	6.97 ± 0.99	7.42 ± 1.13	8.93 ± 0.76	0.045	0.73	1.59
	GA9	0.04 ± 0.03	0.08 ± 0.03	0.02 ± 0.02	0.04 ± 0.02	0.02	0.01	0.03
	GA13	0.10 ± 0.02	0.04 ± 0.02	0.12 ± 0.03	0.06 ± 0.03	0.004	0.02	0.04
	GA15	0.36 ± 0.1	0.08 ± 0.02	0.14 ± 0.02	0.01 ± 0.00	<0.001	0.03	0.06
	GA19	3.38 ± 0.32	1.41 ± 0.28	3.1 ± 0.41	6.95 ± 0.67	<0.001	0.18	0.4
	GA20	1.63 ± 0.25	1.45 ± 0.32	1.67 ± 0.27	1.45 ± 0.29	0.055	0.19	0.42
	GA29	2.29 ± 0.51	2.62 ± 0.58	2.74 ± 0.32	2.84 ± 0.49	0.51	0.38	0.83
	GA34	0.89 ± 0.09	0.78 ± 0.08	0.69 ±0.09	0.76 ± 0.11	0.11	0.07	0.15
	GA44	2.04 ± 0.62	1.33 ± 0.4	3.04 ± 0.35	6.30 ± 0.68	<0.001	0.33	0.72
	GA51	0.02 ± 0.01	0.04 ± 0.03	0.02 ± 0.01	0.02 ± 0.01	0.23	0.01	0.03
	GA53	0.33 ± 0.03	0.32 ± 0.04	0.34 ± 0.04	0.14 ± 0.03	<0.001	0.01	0.03
	GA54	0.004 ± 0.0008	0.002 ± 0.001	0.002 ± 0.001	0.002 ± 0.001	0.02	0.0007	0.001

The mean value is shown with its standard deviation, along with the P-values, standard error of differences (SED) and 5% least significant difference of means (LSD 5%).

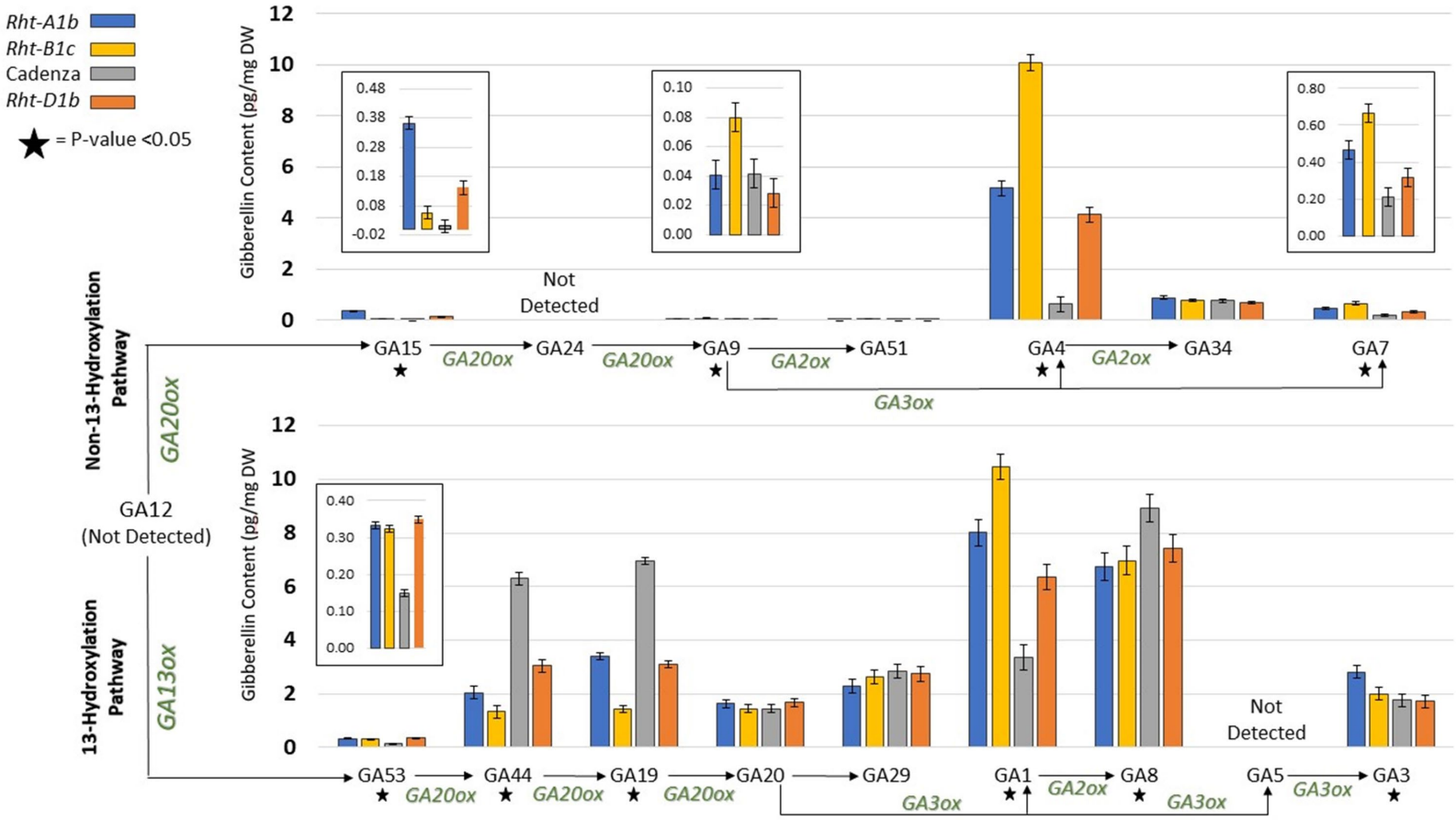

Figure 3.15: GA Hormone Analysis in *Rht-1* Mutants and *Rht-1* Controls. Gibberellin (GA) profiles for *Rht-A1b* (blue), *Rht-B1c* (yellow) and Cadenza (grey) and *Rht-D1b* (orange), GA biosynthesis enzymes are shown in green. Gibberellin content (pg/mg DW) was measured from seedling first leaf sheath tissue, collected 6 days post-germination. GA profiles have been ordered according to the GA biosynthesis pathway. Error bars = standard error of means. Significant results are denoted with a black star. **Non-13-Hyproxylation Pathway: GA12** not measured , **GA15** ($p<0.001$), error bar = 0.0314, **GA24** not detected, **GA9** ($p=0.016$) error bar = 0.0141, **GA51** ($p=0.23$) error bar =0.0134, **GA4** ($p<0.001$) error bar = 0.424, **GA34** ($p=0.107$) error bar = 0.0727, **GA7** ($p<0.001$) error bar = 0.0685. **13-Hydroxylation Pathway: GA12** not detected, **GA53** ($p<0.001$) error bar = 0.0161, **GA44** ($p<0.001$) error bar = 0.333, **GA19** ($p<0.001$) error bar = 0.1845, **GA20** ($p=0.556$) error bar = 0.1945 , **GA29** ($p=0.514$) error bar = 0.381, **GA1** ($p<0.001$) error bar = 0.671 , **GA8** ($p=0.045$) error bar = 0.73, **GA5** not detected , **GA3** ($p=0.022$) error bar = 0.332.

Table 3.16: Fold Change Difference in Gibberellin Content in Rht-1 dwarfing alleles compared to Rht-1

		Rht-B1c	*Rht-A1b*	*Rht-D1b*
Gibberellin Content Fold Change Compared to *Rht-1*	GA1	3.1	2.4	1.9
	GA3	1.1	1.6	1.0
	GA4	15.9	8.2	6.5
	GA6	1.1	1.4	2.8
	GA7	3.2	2.2	1.5
	GA8	1.3	1.3	1.2
	GA9	1.9	1.0	1.5
	GA13	1.7	1.7	2.0
	GA15	5.4	33.4	13.5
	GA19	3.9	2.1	2.2
	GA20	1.0	1.1	1.2
	GA29	1.1	1.2	1.0
	GA34	1.0	1.2	1.1
	GA44	3.7	3.1	2.1
	GA51	1.8	1.2	1.0
	GA53	2.2	2.3	2.4
	GA54	1.0	2.1	1.0

Coloured boxes highlight the fold increase (green) or decrease (pink) in gibberellin content (pg/mg DW) compared to *Rht-1*.

There is a significant interaction between genotype and GA content for the 4 bioactive GAs in the 13-hydroxylation (GA_1 and GA_3) and non-13 hydroxylation pathway (GA_4 and GA_7) ($p = 0.02$ or <0.001) (Table 3.15). The 5% LSDs were then used to assess which genotypes produced significantly different contents for each GA. For GA_1 (5% LSD = 1.46), each genotype produced significantly different hormone levels. These GA_1 levels correlated to dwarfing severity, with *Rht-B1c* accumulating the most GA_1 followed by *Rht-A1b, Rht-D1b* and *Rht-1*. This accumulation represented a 3.1, 2.4 and 1.9-fold increase in *Rht-B1c, Rht-A1b* and *Rht-D1b*, respectively, compared to *Rht-1* (Table 3.16).

For GA_3 (5% LSD = 0.72), *Rht-A1b* and *Rht-B1c* accumulated significantly different hormone levels from the other genotypes, whilst there was no significant difference between *Rht-1* and *Rht-D1b* (Table 3.15). *Rht-A1b* accumulated the highest levels of

GA_3, representing a 1.6-fold increase in hormone compared to *Rht-1,* whilst *Rht-B1c* saw a 1.1-fold increase (Table 3.16).

For GA_4 (5% LSD = 0.15), each genotype produced significantly different hormone levels. These GA_4 levels correlated to dwarfing severity, with *Rht-B1c* accumulating the most GA_4 followed by *Rht-A1b, Rht-D1b* and *Rht-1*. This accumulation represented a 15.9, 8.2 and 6.5-fold increase in *Rht-B1c*, *Rht-A1b* and *Rht-D1b*, respectively, compared to *Rht-1* (Table 3.16).

For GA_7 (5% LSD = 0.72), *Rht-A1b* and *Rht-B1c* accumulated significantly different hormone levels compared to *Rht-1* and *Rht-D1b,* which were not significantly different from one another (Table 3.15). *Rht-B1c* accumulated the highest levels of GA_7, representing a 3.2-fold increase in hormone compared to *Rht-1,* whilst *Rht-A1b* saw a 2.2-fold increase (Table 3.16).

In wheat the 13-hydroxylation pathway is dominant (Appleford and Lenton 1991) as GA13ox converts GA_{12} to GA_{53} more efficiently than GA20ox converts GA_{12} to GA_{15} (Lenton, Hedden, and Gale 1987; Lenton and Appleford 1991). Previous studies have demonstrated that GA_1 accumulates in wheat, perhaps due to high levels of *GA13ox* expression in vegetative organs (Webb et al. 1998). The 15.9, 8.2 and 6.5-fold increase in GA_4 from the non-13-hydroxylation pathway in *Rht-B1c, Rht-A1b* and *Rht-D1b*, is therefore surprising and has not been observed previously. It suggests that *GA20ox* may be upregulated in lines containing the *Rht-1* alleles, enabling greater conversion of GA_{12} to GA_{15} and ultimately higher levels of GA_4.

Upregulation of both the 13-hydroxylation and non-13-hydroxylation pathways is also reflected in the levels of GA precursors. In the non-13-hydroxylation pathway, there is a significant interaction between GA_{15} accumulation and genotype - ($p<0.001$), with *Rht-A1b*, *Rht-D1b* and *Rht-B1c* having significantly higher levels of GA_{15} than *Rht-1* (5% LSD 0.06), representing a 33.5, 13.5 and 5.4-fold increase respectively. This suggests an upregulation in the GA20ox activity and increased conversion of GA_{12} to GA_{15}. In the 13-hydroxylation pathway, there is a significant interaction between GA_{53} accumulation and genotype ($p<0.001$). There is a significant increase in GA_{53} levels in *Rht-A1b, Rht-B1c* and *Rht-D1b* compared to *Rht-*

1, although there is no significant difference between the three alleles (5% LSD 0.03). This increase accounts for a 2.3, 2.2 and 2.4-fold increase in GA_{53} respectively. In the following precursors of the pathway, GA_{44} and GA_{19}, this is switched with *Rht-1* significantly accumulating precursors compared to the *Rht-1* alleles ($p<0.001$, 5% LSD 0.72 and 0.4 respectively). There is a significant decrease in GA_{44} and GA_{19} with increased dwarfing severity. *Rht-B1c* has the lowest levels, followed by *Rht-A1b* and *Rht-D1b,* although there is no significant difference between *Rht-A1b* and *Rht-D1b* levels of GA_{19}. For GA_{44} this represents a 3.7, 3.1 and 2.1-fold decrease in content compared to *Rht-1* in *Rht-B1c, Rht-A1b* and *Rht-D1b*, respectively, while for GA_{19} this represents a 3.9, 2.1 and 2.2-fold decrease. These results suggest that both GA13ox and GA20ox are upregulated in the *Rht-1* alleles. Conversion of GA_{12} to GA_{53} by GA13ox is more efficient in the *Rht-1* allele lines resulting in higher levels of GA_{53}. The conversion of GA_{53} to GA_{44} and GA_{19} is also slower in *Rht-1,* hence the accumulation of these GAs, suggesting that in *Rht-A1b, -B1c* and *D1b*, GA20ox is also upregulated.

Overall *Rht-A1b* displayed an intermediate accumulation of endogenous bioactive GAs compared to *Rht-D1b* and *Rht-B1c,* which may be correlated to its intermediate height phenotype (section 3.2.2). This further demonstrates that RHT-A1B protein may produce a more efficient repression of GA responses than *Rht-D1b.*

3.5 Transcription Analysis of Gibberellin Biosynthesis Pathway Components

The gibberellin content analysis suggests that the bioactive gibberellins GA_1 and GA_4 accumulate in *Rht-B1c, Rht-A1b* and *Rht-D1b* (Section 3.4). To test the hypothesis that accumulation of GA_1 and GA_4 is due to enhanced GA biosynthesis, potentially through the upregulation of *GA13ox* and *GA20ox* genes, a RNA-seq experiment was conducted (Wang, Gerstein, and Snyder 2009) to assess transcription changes induced by GA treatment in the *Rht-1, Rht-A1b, Rht-B1c* and *Rht-D1b* lines. Identical tissue samples as used for GA analysis were used for this transcript profiling experiment (Section 3.4). Measuring the transcription of specific genes is often conducted using qRT-PCR (Quantitative Reverse Transcriptase PCR) (Gibson, Heid, and Williams 1996), however this is challenging for hexaploid wheat involving

optimisation and individual analysis of each homoeologous gene and was not feasible late in the project (Costa et al. 2013). By contrast, RNA-seq could examine transcription of all the components of the GA biosynthesis pathway to be analysed from a single experiment (Costa et al. 2013) (Supplementary Table 1).

To assess whether the biosynthesis components were regulated by GA, seedlings were also harvested following a GA_3 treatment. In *Arabidopsis GA3ox* and *GA20ox* transcription is noticeably downregulated 15 mins after treatment with 2µM GA_4 (Zentella et al. 2007). To establish how quickly wheat seedlings respond to GA (as indicated by a significant growth response) a 24 hour GA response assay was conducted (Section 2.6.1). To determine the time-point to harvest GA_3 treated seedlings, 40 *Rht-1* seeds were germinated and 7-days post germination where treated with either 5µM GA_3 or water. Leaf sheath measurements were then taken every 4 hours over a 24hour period. Leaf sheath elongation between time points (e.g. 0-4 hours, 4-8 hours, 12-16 hours) was then calculated to determine when seedling leaf sheath elongation was significantly responding to GA_3 treatment. The residual plots for the data was assessed in GenStat (v18, VSNI, Hemel Hempstead, U.K.), this confirmed that the data was Normal and did not require transformation. A General Analysis of Variance was (ANOVA) was then conducted to assess the effect of the GA treatment of *Rht-1* leaf sheath elongation. The output of this ANOVA is described in Table 3.17 and Figure 3.16.

Table 3.17: ANOVA Output - Leaf Sheath Elongation in Water and GA_3 Treated Rht-1 Seedlings

Time	Mean Growth (mm)		ANOVA Output		
	Control (water)	[5µM GA_3]	P-Value	SED	5% LSD
0-4hr	2.9 ± 2.2	3.9 ± 2.0	<0.001	0.6	1.1
4-8hr	1.8 ± 1.1	**3.8 ± 1.4**			
8-12hr	1.9 ± 1.1	**3.4 ± 1.6**			
12-16hr	2.6 ± 1.4	**5.4 ± 2.1**			
16-20hr	2.1 ± 0.7	**3.1 ± 1.6**			
20-24hr	2.6 ± 1.1	**3.5 ± 2.0**			

The mean value (measured in mm) is shown with its standard deviation, along with the standard error of differences (SED) and 5% least significant difference of means (LSD 5%). Means shown in bold are significantly different from their equivalent control.

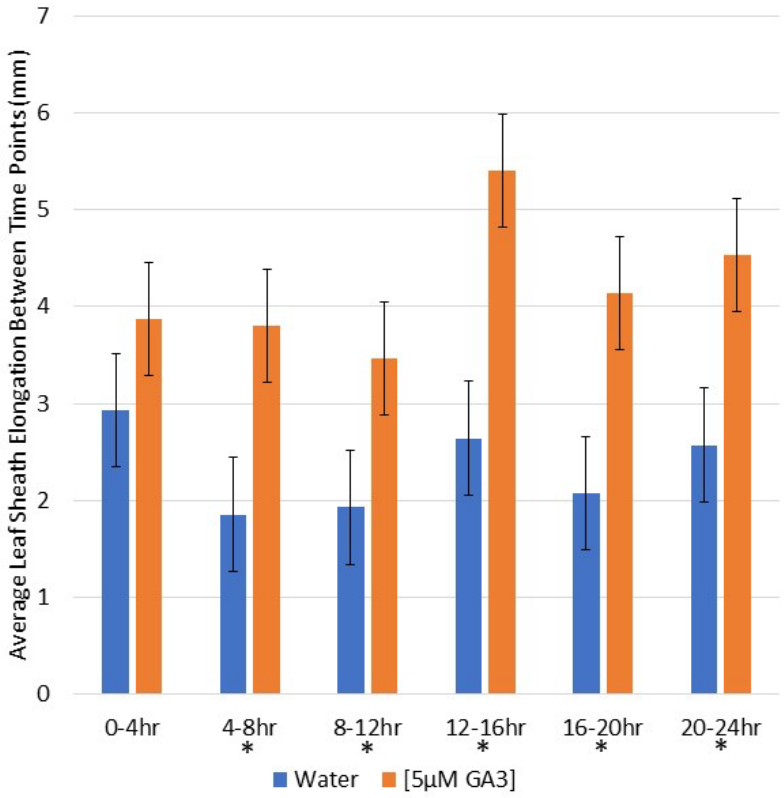

Figure 3.16: *Rht-1* First Leaf Sheath Elongation (mm) Between Time Points. Blue = water (control) and orange = 5µM GA_3. P=<0.001, error bars = standard error of differences (0.6). Significantly different elongation between 5µM GA_3 seedlings and controls is calculated using the least significant difference of means (1.1) and denoted with a *.

The ANOVA confirmed that GA_3 treatment had a significant effect on leaf sheath elongation (p=<0.001). The least significant difference of means (1.1) was used to determine when there was a significant difference between sheath elongation in 5µM GA_3 and water treated seedlings. This determined that between 4-8 hours, the leaf sheaths of 5µM GA_3 seedlings began to elongate significantly more than water treated seedlings (Figure 3.16). As a result, it was decided that for the RNA-seq analysis, GA_3 treated seedlings would be harvested 8 hours post-treatment.

For the RNAseq experiment, *Rht-1, Rht-A1b, Rht-D1b* and *Rht-B1c* seedlings were grown up and the RNA samples prepared as described in Section 2.5.7. Three replicates containing RNA from a pool of 10 seedlings were generated for each genotype, GA/water treatment combo. The samples were sent to Novogene Bioinformatics Technology Co. Ltd. (Beijing, China) for paired end sequencing to a depth of 30 million reads (Appels et al. 2018).

FastQC confirmed that the data and the read quality was good, and the data was mapped to the reference bread wheat genome (IWGSC RefSeq v2.0) using HiSAT2 (Kim, Langmead, and Salzberg 2015). Gene counts were calculated using featureCounts in R bioconductor (Liao, Smyth, and Shi 2014), which identified that the number of reads varied from 44,675,770 (Cadenza2_H20.bam) to 74,397,474 (*Rht-D1b*3_GA.bam).

Differential gene expression was then calculated using DESeq. This determined that out of the 75,957 genes, 257 were differentially expressed (75 upregulated, 182 downregulated). Out of these 257 genes, only 5 (all *GA2oxs*) were associated with GA biosynthesis. These genes were all upregulated in response to the GA treatment across the four genotypes (Table 3.18 and Figure 3.18).

Table 3.18: Differentially Expressed GA Biosynthesis Components

Gene Name	Geneid	Basemean	log2foldchange	P-value	padj
GA2ox10-D	TraesCS1D02G127000	343.6092	2.3939	1.69E-10	3.69E-07
GA2ox10-A	TraesCS1A02G126400	399.8741	1.8992	2.91E-10	7.02E-07
GA2ox10-B	TraesCS1B02G145600	321.9060	2.4954	1.24E-07	0.0001
GA2ox3-D	TraesCS3D02G293800	170.9177	1.9406	2.27E-07	0.0002
GA2ox7-D	TraesCS3D02G149600	425.6985	1.7690	5.09E-06	0.0028

The gene name (*GA2ox*X*)* and genome (A/B/D) of differentially expressed genes is shown. The RefSeqv1.1 Gene ID for each gene is also shown. Basemean is the mean of normalized counts of all samples, normalizing for sequencing depth. Log2 foldchange refers the difference in expression between the GA treatment and control across all 4 genotypes. P-value is shown, the Padj = the adjust P-value which considers the 5% false discovery rate.

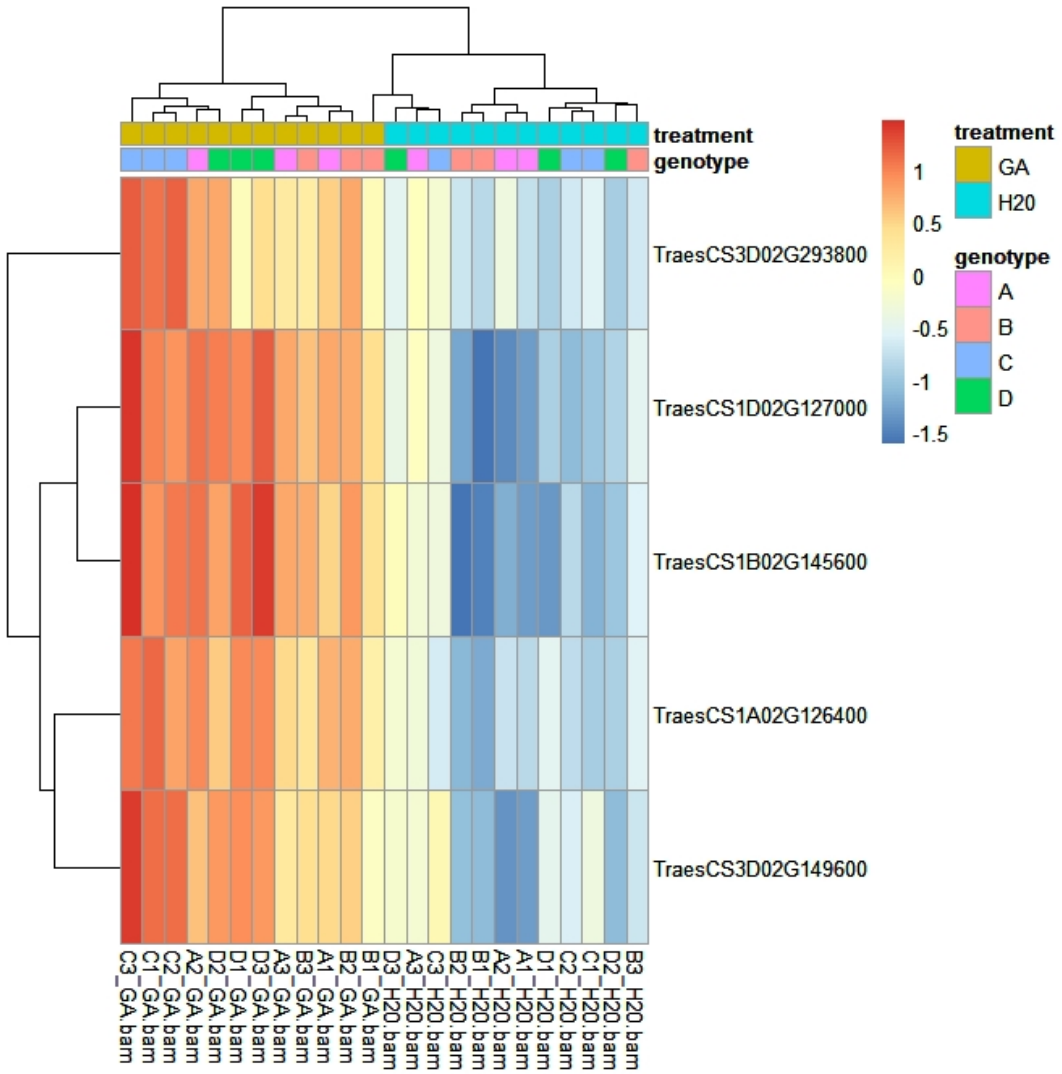

Figure 3.18: Heatmap Showing Significantly Differentially Expressed GA Biosynthesis Components. Genotype: A = *Rht-A1b,* B =*Rht-B1c,* C = *Rht-1* (WT Cadenza), D = *Rht-D1b*. GA = GA_3 treated, H20 = control. TRAESCS1A02G126400 (*GA2ox10-A),* TRAESCS1B02G145600 (*GA2ox10-B)*, TRAESCS1D02G127000 (*GA2ox10-D)*, TRAESCS3D02G293800 (*GA2ox3-D)* and TRAESCS3D02G149600 (*GA2ox7-D*). Upregulation is shown in red, down regulation shown in blue.

The four genotypes display similar expression profiles for the five *GA2ox* genes, upregulated in following the application of GA and downregulated in the absence of GA. The exact differences in expression between the genotypes cannot be discerned as the heatmaps show overlapping responses between genotypes and the bioinformatics performed by the statistician analysed the difference in gene expression with/without GA treatment, not between genotypes. GA2oxs are gibberellin inactivators that catabolise bioactive GAs and their precursors into non-active forms (Lester et al. 1999; Schomburg et al. 2003). Their expression is

upregulated in response to increased GA levels, in a mode that is DELLA dependent (Thomas, Phillips, and Hedden 1999; Lo et al. 2008). Therefore, *GA2ox* transcription would be predicted to be low in GA treated and untreated *Rht-B1c, Rht-D1b* and *Rht-A1b* as their proteins are not degraded. However, the upregulation of the *GA2oxs* was seen in all four genotypes following GA treatment, and downregulation seen in water controls for all four genotypes (Figure 3.18). This suggests that regulation of *GA2oxs* may also be under the control of additional components.

Although not identified as differentially expressed in the analysis performed by the statistician, the expression of the *Rht-A1, -B1* and *-D1* is interesting in the mutant lines *Rht-A1b, Rht-B1c* and *Rht-D1b* respectively (Figure 3.19).

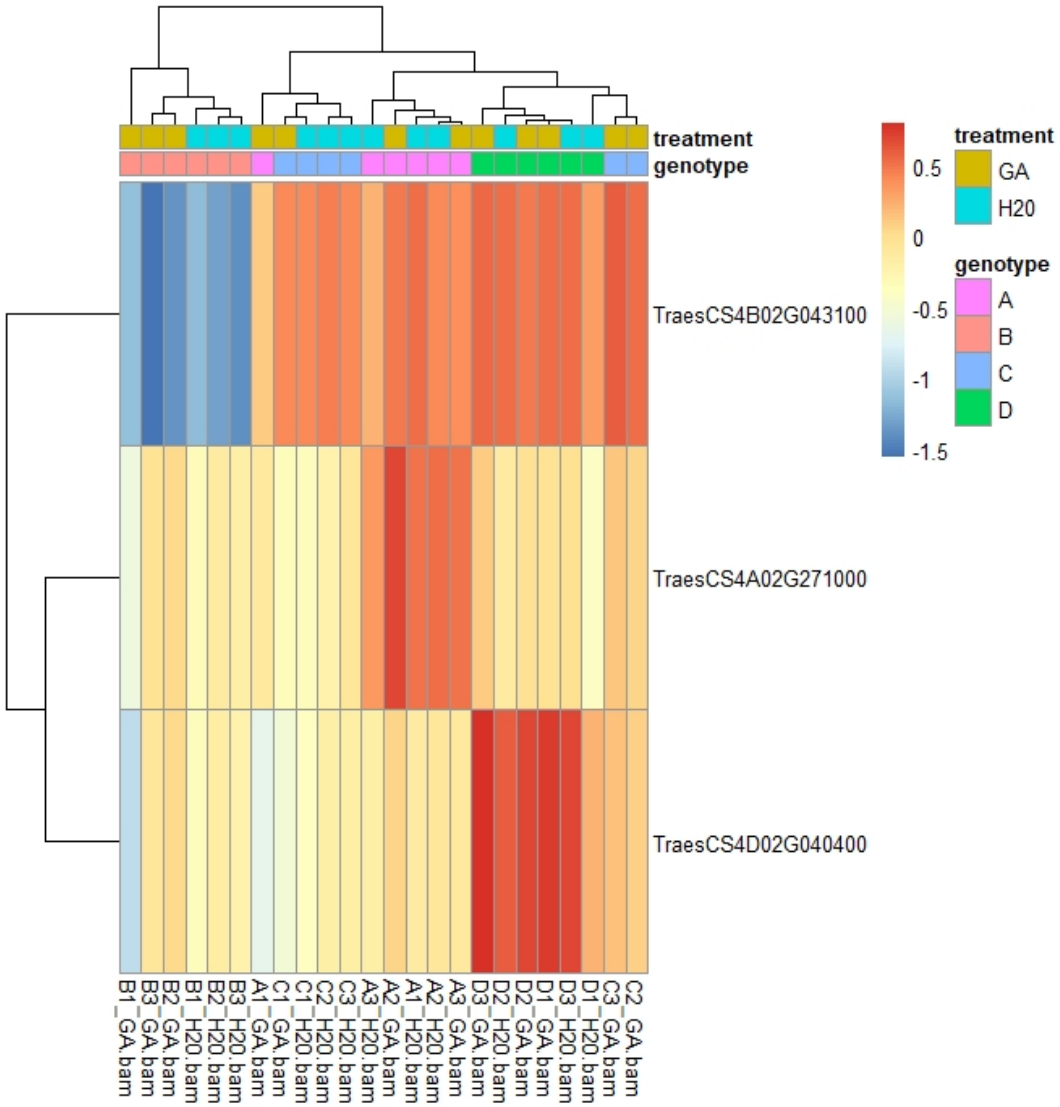

Figure 3.19: Individual Plots for *Rht-A, -B* and *-D* Expression. TraesCS4A02G271000 *(Rht-A1),* TraesCS4B02G043100 (*Rht-B1)* and TraesCS4D02G040400 (*Rht-D1)*. Upregulation is shown in red, down regulation shown in blue.

The heatmap suggests that *Rht-A1* and *Rht-D1* are only upregulated in the *Rht-A1b* and *Rht-D1b* mutants respectively, whilst *Rht-B1* is downregulated in the *Rht-B1c*. The current hypothesis for the differing dwarfing severity of *Rht-A1b, Rht-B1c* and *Rht-D1b* suggests that *Rht-B1c* produces a more severe dwarf mutant because the *Rht-B1c* insertion has less of an inhibitory effect on protein translation than the *Rht-A1b* and *Rht-D1b* nonsense mutations (Chandler and Harding 2013; Derkx et al. 2017; Phillips 2016). Therefore, transcription of *Rht-B1* in *Rht-B1c* would be expected to be high, whilst *Rht-A1* and *Rht-D1* are expected to be low in *Rht-A1b* and *Rht-D1b* respectively. The RNAseq data suggests that the opposite may be true, as there are very low transcript levels of *Rht-B1* in the *Rht-B1c* mutant and high levels of *Rht-A1* and *Rht-D1* in the *Rht-A1b* and *Rht-D1b* mutants compared to the other genotypes. In a study examining *Rht-1* expression levels in the stems of dwarf mutants, a similar trend was identified, with higher levels of *Rht-A1* and *Rht-D1* compared to *Rht-B1* in the mutant *Rht-B1c.* There was no significant upregulation of *Rht-D1* in the *Rht-D1b* mutant, although this may have been because the *Rht-D1c* mutant, which has a four-fold copy number, was also analysed in this study (Pearce et al. 2011). To further analyse this pattern, RT-PCR will need to be carried out to quantify the levels of *Rht* transcript in each of the mutants.

The limited identification of differentially expressed GA biosynthesis components could be down to two separate factors. The first involves the seedling tissue sampled. Seedlings were cut between the grain crown and the first leaf ligule, as this was the tissue sampled for the gibberellin content analysis (Section 3.4). However, gibberellin biosynthesis occurs predominantly in the seedling expansion zone (Coolbaugh 1985). Sampling all the tissue between the grain crown and the first leaf ligule may dilute the RNA for GA biosynthesis genes, resulting in them not being identified. The second factor involves the time point chosen for the GA treatment. The point chosen (8 hours post treatment) was selected as this was when the seedlings where shown to be significantly responding to the exogenous GA (Figure 3.16). However previous studies in *Arabidopsis* demonstrate that transcription can be down-regulated 15 minutes after the application of exogenous

GA_4 (Zentella et al. 2007), therefore conducting a timecourse experiment ijcluding earlier timepoints is likely to be more informative.

Additionally, there appears to be some GA_3 contamination in one of the water controls (Figure 3.17). This could act to skew the results, reducing the identification of differentially expressed GA biosynthesis components, which often are at low levels (Zentella et al. 2007). If the experiment was repeated, having more replicates per genotype per treatment and keeping the treatment trays well separated would mitigate this problem,

3.6 Discussion

The objective of the work presented in this chapter was to determine whether *Rht-A1b* is a GA insensitive mutant and to provide a detailed phenotypic characterisation of the effects of this mutation in the Cadenza (var.) background. Phenotyping in the glasshouse suggests that *Rht-A1b* produces a shorter semi-dwarf phenotype than *Rht-D1b,* although not as short as the severe dwarf *Rht-B1c* (Section 3.2). This reduced height phenotype is likely due to GA insensitivity, as GA response assays demonstrate that *Rht-A1b* seedlings only respond minimally to increasing doses of exogenous GA_3. Therefore *Rht-A1b* is the first characterised *Rht-A1* GA insensitive mutant in wheat (Pearce et al. 2011) (Section 3.3). Liquid chromatography-mass spectrometry has also demonstrated that like other *Rht-1* dwarf and semi-dwarf mutants, *Rht-A1b* seedlings accumulate bioactive GA (particularly GA_1 and GA_4) compared to WT *Rht-1* seedlings (Section 3.4). Evidence for the accumulation of the non-13-hydroxylated C_{19} GA, GA_4, in wheat is a novel finding which has potential implications for understanding the physiological consequences of *Rht-1* dwarfing alleles. Additional transcription analysis need to be performed to establish which steps in the GA metabolic pathway are regulated in the *Rht-1* mutants, however the RNAseq does suggest that there may be additional mechanisms controlling GA biosynthesis regulation, as *GA2ox* expression appears to independent of DELLA.

3.6.1 *Rht-A1b* is a GA Insensitive Mutant

Gibberellin dose response assays where conducted on the *Rht-1* mutants and *Rht-1* to establish the effect of the mutations on seedling response to exogenous GA_3 (Weyers et al. 1995; Swain and Olszewski 1996). These assays have been used in previous studies assessing barley (Chandler et al. 2002; Chandler and Robertson 1999) and rice (Asano et al. 2009) DELLA mutants, with first leaf elongation and second leaf sheath elongation, respectively, used to quantify GA responsiveness.

To optimise the assays for wheat seedlings, both first leaf and leaf sheath measurements were taken for *Rht-A1b, Rht-B1c, Rht-D1b* and *Rht-1* seedlings grown under different GA treatments. Additional response assays were also conducted on paclobutrazol (PAC) treated seedlings. Paclobutrazol has been used in previous studies to assess how the absence of endogenous GA effects hypocotyl growth in *Arabidopsis* DELLA mutants (Cowling and Harberd 1999), but with DELLA mutants in rice (Asano et al. 2009) and barley (Chandler et al. 2002; Chandler and Robertson 1999).

Across the GA-dose response experiments (untreated or PAC treated), both sets of data (first leaf and leaf sheath length) confirmed that there was a significant interaction between genotype and response to exogenous GA ($P<0.001$) (Sections 3.3 and 3.3.2). However, seedling-to-seedling variation was lowest when seeds were treated with 25µM PAC and the length of the first leaf sheath length was used to determine GA response, suggesting that this is the most robust protocol for conducting wheat seedling GA-response assays (Section 3.3.3). At present there is no robust wheat GA response assay protocol, as wheat growth responses can be quite strikingly affected by environmental changes (Tonkinson et al. 1997). For example, reduced extension zones have been reported for wheat seedlings grown at 10^{o}C compared to 20^{o}C (Tonkinson et al. 1997). As such this work is important towards establishing a robust working protocol.

The *Rht-1* mutants showed a reduced response to exogenous GA compared to *Rht-1*, with the most severe dwarfing allele, *Rht-B1c*, showing the smallest response to the GA treatments, followed by *Rht-A1b* and *Rht-D1b*. This echoes the results of

previous GA dose-response experiments with *Rht-1* alleles (Pinthus et al. 1989) and other gain-of-function DELLA mutants (e.g. barley (*Sln1*) and rice (*Slr1*)) (Chandler et al. 2002; Chandler and Robertson 1999; Asano et al. 2009), which found that mutants with more severe dwarf phenotypes showed the smallest response to exogenous GA. The GA responsiveness of *Rht-A1b* most closely mirrored the response of *Rht-D1b* lines. Overall, this confirms that *Rht-A1b* is the first characterised *Rht-A1* GA insensitive mutant (Pearce et al. 2011).

Previous studies have demonstrated that the 13-hydroxylation pathway is upregulated in the *Rht-1* mutants; *Rht1* (*Rht-B1b*) and *Rht3* (*Rht-B1c*) seedlings, resulting in the accumulation of GA_1 (Appleford and Lenton 1991). Analysis of GA

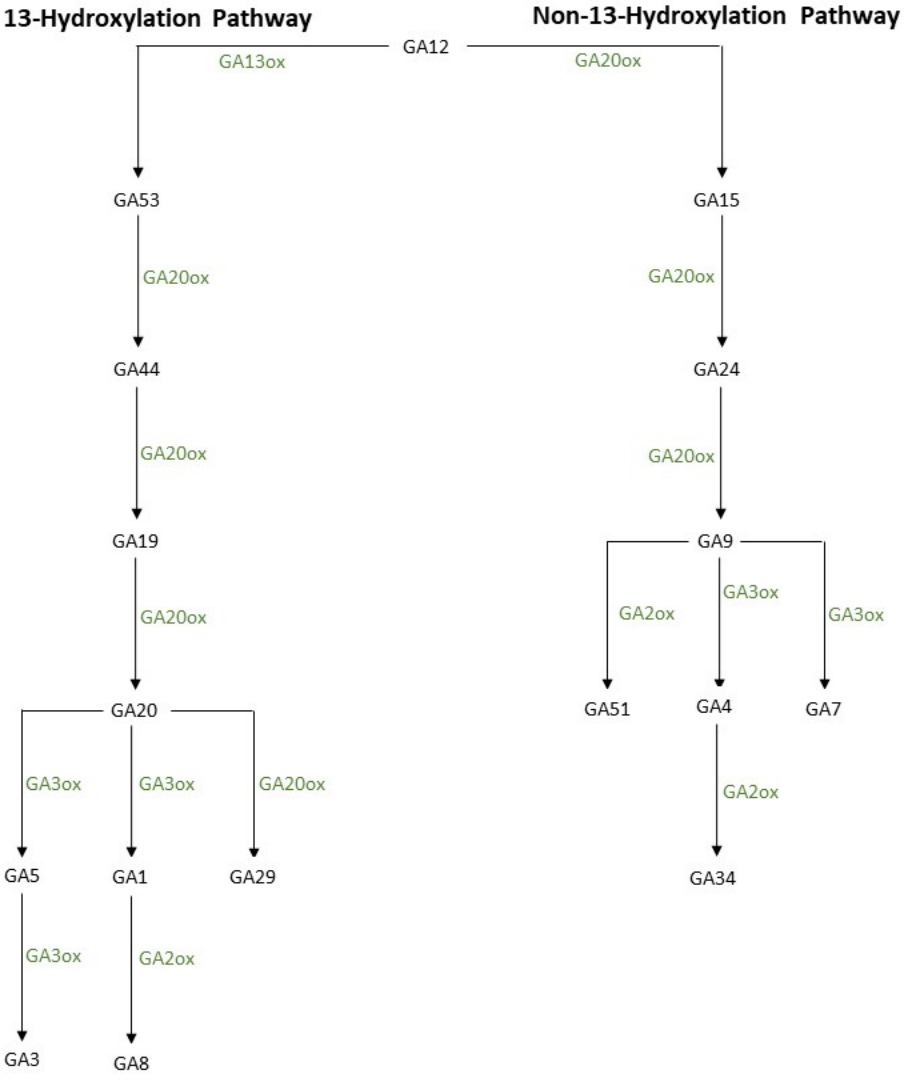

Figure 3.20: The 13-Hydroxylation and Non-13-Hydroxylation Gibberellin Metabolic Pathways. Gibberellins are shown in black. The enzymes involved in each step of the pathway are written in green.

levels using liquid chromatography-mass spectrometry (Section 3.4) confirmed these findings and demonstrated that the non-13-hydroxylation pathway is also upregulated in the *Rht-1* mutants; *Rht-D1b, Rht-A1b* and *Rht-B1c*, shown by the accumulation of GA_4 in comparison to WT *Rht-1* (biosynthesis pathways shown in Figure 3.20).

In the dominant GA-biosynthesis pathway in wheat, the 13-hydroxylation pathway (Appleford and Lenton 1991), the precursor GA_{53} accumulates in significantly high levels in the *Rht-1* mutants compared to the Cadenza control. However, the proceeding two precursors in this pathway, GA_{44} and GA_{19}, accumulate in higher quantities in *Rht-1.* This suggests that *GA20ox* is upregulated in the *Rht-1* mutants as the conversion of GA_{53} to GA_{20} is pushed through more efficiently. Additionally, the high accumulation of GA_4 in *Rht-1* mutants also suggests that *GA20ox* is upregulated. The 13-hydroxylation pathway dominates in wheat because GA13ox dominates over GA20ox activity in respect to GA_{12} conversion to GA_{53} than GA_{15} (Lenton, Hedden, and Gale 1987; Lenton and Appleford 1991). Therefore, high accumulation of GA_4 suggests that GA20ox exists in higher concentrations to compete effectively with GA13ox.

The most important bioactive GAs of either pathway, GA_1 and GA_4 (Talon, Koornneef, and Zeevaart 1990), accumulate at higher levels in the *Rht-1* mutants than in WT Cadenza. This suggests that in addition to *GA20ox, GA3ox* is also upregulated in the *Rht-1* mutants enabling more efficient production of bioactive GAs. These results reflect current evidence in *Arabidopsis* that the GA biosynthesis genes *GA20ox2* and *GA3ox1* are upregulated by DELLAs (Zentella et al. 2007). However, the RNAseq analysis conducted for this project is inconclusive as to whether this is the case in wheat (Section 3.5). Repeating the analysis with either qRT-PCR or using tissue harvesting solely from the seedling elongation zone may provide more information (Coolbaugh 1985). Differences in the levels of GA identified in the *Rht-1* mutants in this study compared to previously published reports could be due to the tissues analysed. The tissue assessed in this study, leaf sheath material harvested at the height of leaf 1' ligule from 7 day old seedlings is

different from plant material used in the previous studies 'leaf 2 together with the enclosed leaf 3 and shoot apex was cut at the height of the ligule of leaf 1' of 11 day old seedlings in a Maris Huntsman background (Appleford and Lenton 1991). As both studies demonstrate an accumulation of GA, it implies a robustness to the experiments and that bioactive GAs are likely to accumulate more highly in *Rht-1* mutant seedlings. The accumulation of bioactive GAs in *Rht-1* mutants is likely due to the disruption to the N-terminal DELLA motif, which prevents DELLA degradation (Dill, Jung, and Sun 2001), resulting in upregulation of the feedback regulated *GA20ox* and *GA3ox* biosynthesis genes (Lenton, Hedden, and Gale 1987). *Rht-A1b* which produces an intermediate phenotype to *Rht-B1c* and *Rht-D1b,* produced an intermediate concentration of GA_1 and GA_4 compared to the other two *Rht-1* mutants. This is consistent with GA accumulation being linked to mutational severity (and therefore dwarfing severity) in *Rht-1* lines.

In the 13-hydroxylation pathway, inactive GA_8 accumulated highest in *Rht-1* despite this line having the lowest amount of its precursor, GA_1. This suggests that the GA inactivation genes *GA2ox* may be downregulated in the *Rht-1* mutants. The RNAseq data provides additional evidence for this idea, as multiple *GA2oxs* (*-10oxA/B/D, -3oxD* and *-7oxD*) were downregulated in the *Rht-1* treated with water (Figure 3.18). However, *GA2ox* expression was also upregulated in all genotypes following GA treatment (Figure 3.18) which suggests that these genes may be independent of GA control. This is in contrast to other GA signalling genes which have been found to mediated by DELLA (e.g. *GA20ox, GA3ox* and *GID1*) (Zentella et al. 2007; Middleton et al. 2012)

3.6.2 *Rht-A1b* is a more severe dwarf than *Rht-D1b*

Gibberellin insensitivity disrupts a range of plant developmental processes from flowering to grain development (Willige et al. 2007; Kondhare et al. 2014), however the most noticeable phenotypic change observed in *Rht-1* GA insensitive mutants is reduced stem elongation (Koornneef and Vanderveen 1980). Reduced plant stature is the result of reduced stem cell wall extensibility and elongation (Keyes, Paolillo, and Sorrells 1989). When phenotyped in the glasshouse, *Rht-A1b* demonstrated a reduced height phenotype, more severe than *Rht-D1b*, but less severe than *Rht-B1c*.

This intermediate phenotype is consistent with the intermediate response *Rht-A1b* exhibits to application of GA, discussed above. Reduced height is due to the cumulative effect of the *Rht-A1b* stem components (internode 4 – peduncle) being longer than *Rht-B1c* and shorter than *Rht-D1b* and *Rht-1* (Section 3.2.2). This reduction in height is also observed in *Rht-A1b* material grown in the field. In 2016 and 2017 field grown *Rht-A1b* plants were 49.8 cm (SE +/-0.33 cm) and 65.2 cm (SD +/- 2.6 cm) tall, compared to 80.2 cm (SE +/- 1.02 cm) and 82.7 cm (SD +/- 0.7 cm) Cadenza (*Rht-1)* plants (Dr Stephen Thomas, personal communication). This demonstrates that the phenotype observed in the glasshouse is not solely due to the plants being grown in controlled conditions.

Heading date is partially regulated by GA and DELLA , with quantitative trait loci analysis demonstrating that in several wheat varieties, *Rht-D1* has a strong significant effect on heading date (Holzapfel et al. 2008). Additionally in rice, the mutant (*el1*), has enhanced DELLA degradation that enhances GA signalling causing early heading date compared to *ER1* (Dai and Xue 2010). Therefore, it is unsurprising that GA insensitivity and reduced DELLA degradation in the *Rth-1* alleles results in results in longer heading dates than Cadenza. As these delayed floral development and ear emergence through peduncle elongation (Holzapfel et al. 2008; Dai and Xue 2010)

GA insensitivity did not affect ear length in *Rht-A1b* and *Rht-D1b* with the two mutants producing slightly longer ears than *Rht-1,* although this did not translate into improved grain number per ear, as there was no significant difference in floret numbers. These results vary from studies that show that *Rht-D1b* lines produce more grain due to improved assimilate partitioning increasing the number of viable florets in the ear (Youssefian, Kirby, and Gale 1992a, 1992b). This may be due to phenotypic measurements being taken from only 5 plants per genotype grown in the glasshouse. Conducting a larger phenotypic study in the field, as in the Youssefian *et. al* studies may demonstrate variation in grain and floret number. *Rht-A1b* produced significantly smaller grain than *Rht-D1b* or *Rht-1,* despite there being no significant difference in the number of grain per plant produced by the three genotypes. The reduced grain size is therefore unlikely to be due to increased inter-

floret competition for space and nutrients (Gooding, Addisu, et al. 2012; Flintham et al. 1997). Reduced grain size may be due to a more severe GA-insensitivity than *Rht-D1b* and *Rht-1,* as increased GA content and signalling is associated with larger, heavier seed due to increased endosperm development (Kondhare et al. 2014). Reduced seed size is not reflected in the severe GA-insensitive mutant *Rht-B1c* as these plants produced significantly less seed than the other genotypes, as seen previously when *Rht-B1c* is introduced into a shorter wheat variety (Flintham et al. 1997).

The GA insensitive phenotypes of *Rht-A1b* and *Rht-D1b* reflect the current hypothesis that their premature nonsense mutations result in functional N-terminally truncated RHT-1 proteins (Peng et al. 1999). These truncated proteins are not recognised for degradation in the presence of GA and continue to repress GA signalling, resulting in plant GA-insensitivity (Chandler et al. 2002; Peng et al. 1999; Pearce et al. 2011). Although *Rht-D1b* and *Rht-A1b* are very similar nonsense mutations in the same DELLA region of *Rht-1* genes, adult *Rht-A1b* plants appear to be more severely dwarfed. Similarly, *Rht-B1p* a *Rht-B1* nonsense mutation in the same location as *Rht-A1b,* produced a more severe phenotype, suggesting that the phenotype is likely caused by a positional effect as opposed to homoeologue specificity (Bazhenov et al. 2015). Unfortunately, *Rht-B1p* has not been introgressed into a Cadenza for comparison to *Rht-A1b*. Future studies comparing the *Rht-B1p* and *Rht-A1b* would establish whether the severity of the *Rht-A1b* phenotype is due to the position of the nonsense mutation, or due to the nonsense mutation occurring in *Rht-A1b*.

3.6.3 *Rht-A1b* - a Potential Dwarfing Allele for Wheat Breeding?

Rht-A1b is a GA insensitive mutant that on its own may be useful as a dwarfing allele for taller wheat varieties (e.g. Bearded April) (Flintham et al. 1997). Across the GA treatments in the GA-dose assays there was minimal difference between the first leaf or leaf sheath lengths of *Rht-A1b* and *Rht-D1b*. This suggests that *Rht-A1b* may have more of an effect on final height than seedling growth in comparison to *Rht-D1b*. Therefore, *Rht-A1b* may have more severe GA insensitivity later in development, suggesting that *Rht-A1b* mutants may suitable for reducing height of

more vigorous cultivars without a detrimental effect on seedling vigour (Lenton, Hedden, and Gale 1987; Lenton and Appleford 1991), which would be desirable from an agronomic perspective (Ellis et al. 2004). Seedling vigour is often a problem for more severe *Rht-1* dwarfs (e.g. *Rht-B1c*) during drought, when deep sowing practices are deployed (Rebetzke et al. 1999). The shorter coleoptiles are less able to emerge and establish, resulting in yield losses (Sojka, Stolzy, and Fischer 1981; Nizam Uddin and Marshall 1989; Amram et al. 2015). Additional experiments, assessing the growth rate of *Rht-A1b* seedlings compared to other *Rht-1* alleles, either the time taken to reach a certain height or growth rate per day (Chandler and Robertson 1999), would help to establish whether *Rht-A1b* has improved seedling vigour.

Studies on the severe dwarf *Rht-B1c* suggest that the introduction of intragenic mutations through mutagenesis, can result in a partial loss-of-function (taller) phenotype (Chandler and Harding 2013; Derkx et al. 2017). Using a similar process on *Rht-A1b* it may be increased the range of *Rht-A1b* dwarfing alleles with different effects that can be selected for different cultivars and environments (Ellis et al. 2004).

3.6.4 Future Experiments

Characterisation of *Rht-A1b* and *Rht-B1p* – To establish why *Rht-A1b* produces a significantly shorter mature plant than *Rht-D1b,* this line will need to be characterised with *Rht-B1p* which has the same nonsense mutation except in *Rht-B1* (Bazhenov et al. 2015). This will determine whether the height phenotype is due to a positional effect of the mutation (in which case *Rht-A1b* and *Rht-B1p* will produce the same phenotype), or whether it is due to the nonsense mutation occurring in *Rht-A1* (in which case *Rht-A1b* and *Rht-B1p* will produce different phenotypes). This characterisation will require the two mutations to be in the same variety, which could be achieved through introgression or gene editing (Li et al. 2018). Once in the same variety, the mutations should be characterised on their GA sensitivity through GA dose response assays as well as their effect on phenotype, preferably in the field as this will simulate the effect the mutations could have in commercial lines.

Additional RNAseq Analysis - Further bioinformatics to analyse the difference in gene expression between the genotypes instead of between GA treatments will more accurately highlight differences in each genotype's expression profile. For example, differences in GA biosynthesis gene expression that may explain the results in Section 3.4.

on further bioinformatics analysis to examine differences in expression among genotypes rather than between GA treatments.

Chapter 4: Identification of Intragenic *Rht-A1b* Mutants

4.1 Introduction

4.1.1 Rht-A1b

Over 70% of modern wheat varieties carry at least one of the 'Green Revolution' semi-dwarf alleles, *Rht-B1b* and *Rht-D1b* (Hedden 2003; Walton 2000). Despite *Rht-A1* having a similar expression profile in the elongating stem, semi-dwarf alleles in *Rht-A1* have not yet been identified for use in commercial wheat lines (Pearce et al. 2011). Prior to the start of this project, a Cadenza population containing only WT *Rht-1* alleles *(Rht-A1a, Rht-B1a* and *Rht-D1a*) was mutagenised using EMS and screened using a TILLING based approach (Chen et al. 2014). From this screen, a nonsense mutation (C169T) in *Rht-A1* was identified that resulted in the creation of a stop codon (Q57*) at a similar location to those in *Rht-B1b* (Q65*) and *Rht-D1b* (E62*) (Figure 4.2.1). This mutation, designated *Rht-A1b,* is the first identified GA-insensitivity mutation in *Rht-A1* and produces a more dramatic height reduction than *Rht-B1b* and *Rht-D1b*, despite occurring at a similar location (Chapter 3). In the wheat variety Cadenza, *Rht-A1b* produces shoots significantly shorter than those in *Rht-D1b;* 52.1 cm (SE +/- 14.7 cm) compared to 64.7 cm (SE +/-12.0 cm) (Chapter 3), which is below the optimum height for commercial wheat (70-100 cm), associated with maximal grain yield (Flintham et al. 1997). As taller wheat varieties require more potent *Rht* alleles to achieve maximal grain yield, *Rht-A1b* could be introduced to improve yield in tall varieties such as Bearded April (Flintham et al. 1997). Additionally, *Rht-A1b* may have differential growth rates to *Rht-D1b*, a potentially advantageous agronomic trait. Therefore, Rht-A1b represents a potential target for the development of alternative GA-insensitive alleles.

4.1.2 Generating and Identifying Novel *Rht-B1c* Derived Alleles

A study by Peter Chandler and colleagues at the Commonwealth Scientific and Industrial Research Organisation (CSIRO) in Australia demonstrated that intragenic suppressor mutations, introduced by sodium-azide mutagenesis (Figure 4.1),

rescued stem elongation in Maringá wheat containing the severe *Rht-1* dwarfing allele, *Rht-B1c* (Chandler and Harding 2013; Derkx et al. 2017).

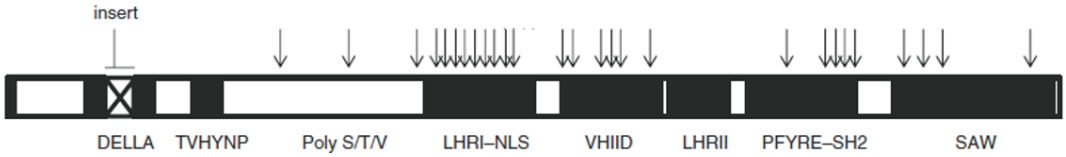

Figure 4.1: Sites of amino acid substitutions in *Rht-B1c* following sodium-azide mutagenesis. Arrows mark the locations of amino acid substitutions. Conserved regions are shown in black and non-conserved regions shown in white. The 30-amino acid insertion in Rht-B1c is shown as a crossed box. Taken from Derx, Harding et al. 2017.

The *Rht-B1c* mutant contains a 2-kb retrotransposon insertion that is partially removed during splicing resulting in a 90-bp in-frame insertion in the transcript (Wu et al. 2011; Pearce et al. 2011). This insertion is predicted to cause a 30-amino acid insertion in the 'DELLA' region, which likely prevents RHT-B1C from interacting with the GID1 receptor and being recognised for GA-mediated degradation (Chapter 1.4.1), resulting in constitutive repression of GA signalling.

Following sodium-azide mutagenesis, an M2 population was screened in the field and intragenic *Rht-B1c* suppressor mutants were identified by their taller phenotype. Subsequent characterisation of backcrossed lines revealed that nucleotide substitutions resulted in rescued stem growth, with mutant stem lengths varying from 72-107% of those in *Rht-B1a* (Chandler and Harding 2013; Derkx et al. 2017). The missense mutations in *Rht-B1c,* were all associated with amino acid substitutions in the C-terminal GRAS domain (Figure 4.2.1). The restored stem height in the intragenic mutants is therefore associated with disrupted function of the RHT-B1C protein (Chapter 1.4.3) (Chandler and Harding 2013; Derkx et al. 2017).

4.1.3 Generating Novel *Rht-A1b*-Derived Alleles

Unlike *Rht-B1c*, the lesions that cause GA-insensitivity in *Rht-B1b*, *Rht-D1b* and *Rht-A1b* are the result of nonsense mutations in the N-terminal coding region of the *Rht-1* genes (Figure 4.2).

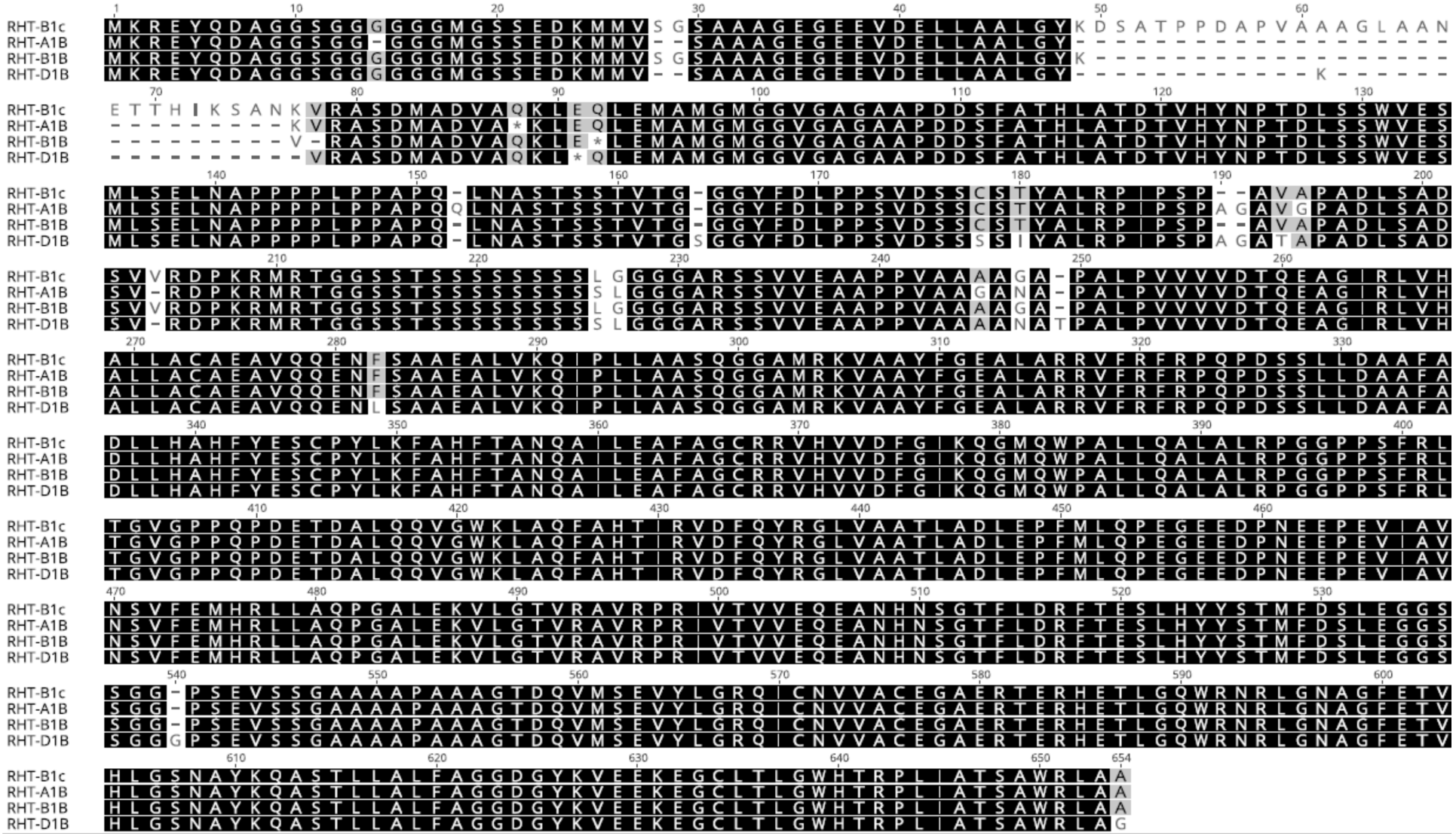

Figure: 4.2: Amino Acid Alignment of reducted height (RHT) alleles: RHT-B1C, RHT-A1B, RHT-B1B and RHT-D1B. Numbering refers to amino acid number for the consensus sequence. Black shading marks identical amino acid residues, grey shading marks where three proteins have identical amino acid residues and no shading refers to amino acids only present in one protein. An '-' marks where an amino acid insertion not present in the protein. The 30-amino acid insertion in RHT-B1C is shown, alongside the premature terminal mutations in RHT-A1B (Q59*), RHT-B1B(Q65*) and RHT-D1B (E62*).

These are hypothesized to produce functional N-terminally truncated proteins that lack the full 'DELLA' domain, preventing recognition by GID1 and GA-mediated degradation (Peng et al. 1999). Like *Rht-B1c,* the N-terminally truncated proteins are predicted to contain a full C-terminal GRAS domain, resulting in constitutive repression of GA signalling (Pearce et al. 2011). As the *Rht-B1c* suppressor mutants were the result of mutations in the GRAS domain, this suggests that mutagenesis could also be used to introduce missense mutations into the GRAS domain of *Rht-A1b*, resulting in alleles that produce a taller height phenotype (Chandler and Harding 2013; Pearce et al. 2011). Note, that if repression of GA signalling is actually the result of the N-terminal peptide, produced by the truncated mutations in *Rht-B1b*, *Rht-D1b* and *Rht-A1b,* then mutagenesis of in the GRAS domain will not result in generation of *Rht-A1b* suppressors (Pearce et al. 2011). However, an intragenic substitution (E529K) in the C-terminal PYFRE motif of *Rht-B1b* resulted in taller plants with longer coleoptiles, which suggests that intragenic mutations in *Rht-A1b* will also produce taller phenotypes (Mo, Pearce, and Dubcovsky 2018).

Prior to the start of this PhD project, *Rht-A1b* seed was treated with ethyl methanosulfonate (EMS) (Section 2.4), which was expected to introduce mutations at a density of at least one per 34-47kb (Chen et al. 2012; Uauy et al. 2009). EMS mutagenesis was chosen for this experiment as it has been shown to introduce random point mutations in polyploid plants such as rice and wheat, resulting in the generation of multiple alleles in a single gene of interest (Till et al. 2007; Till, Comai, and Henikoff 2008; Chen et al. 2012).

4.1.4 Identifying Novel *Rht-A1b* Derived Alleles

M2 seed from *Rht-A1b* populations mutagenised with EMS (Chapter 2.2) were used for two suppressor screens. A pilot screen (Suppressor Screen 1) in 2016 that screened ~20,000 M_2 individuals and a larger screen (Suppressor Screen 2) in 2017 that screened approximately ~468,000 M_2 plants. The aim of this was to identify intragenic *Rht-A1* suppressor mutations that could potentially provide the basis of improved dwarfing alleles. Tall plants with a similar height to the Cadenza controls were expected to possess loss-of-function *Rht-A1* mutations. These are unlikely to be useful as alternative dwarfing genes as they retain the presence of *Rht-B1a* and

Rht-D1a homoeologues and are therefore expected to be phenotypically identical to the wild type Cadenza. 'Semi-dwarf' plants are more likely to be the result of a missense mutation in the C-terminal GRAS coding region, resulting in a partial reduction in the repressive activity of RHT-A1B protein (Chandler and Harding 2013; Derkx et al. 2017). The intragenic mutants identified in these screens are discussed in this chapter and their subsequent characterisation is described in Chapter 6.

4.2. *Rht-A1b* Suppressor Screen One (2016)

In late March 2016, twelve pools of M_2 EMS-mutagenised *Rht-A1b* seed were sown with Cadenza (*Rht-1)* controls into randomly distributed plots in the field (Chapter 2.1.1). The weather conditions during the growing season are described in Table 4.1.

Table 4.1: Weather Conditions During Suppressor Screen One

Month	Sunshine		Mean Temperatures				Rainfall		
			Maximum		Minimum		Total		Duration days**
	Total Hours	( )	ºC	( )	ºC	( )	mm	( )	
March	133.4	+18.45	9.2	-0.65	1.8	-0.92	84.3	+33.52	16
April	167.6	+6.37	11.9	-0.73	3.5	-0.52	62	+6.96	24
May	197	+2.40	17.4	+1.34	7.9	+0.99	39.4	-14.30	11
June	141	-57.17	19	-0.11	11.2	+1.45	84.8	+31.58	22
July	210.3	+4.09	22.2	+0.43	12.8	+0.89	27.1	-22.80	16
August	217.6	+21.38	22.7	+1.17	12.9	+1.02	30.1	-33.58	12

Numbers in the columns marked ( ) refer to variations from the 30 year means (1981-2010) for that month. Duration days **, refers to the number of days where there was >0.2mm rainfall. Data is from: http://resources.rothamsted.ac.uk/environmental-change-network/yearly-weather-summaries#loaded

In June, when the crop was booting, there were 57.17 fewer sunshine hours than the 30-year average and 31.58 mm more rainfall than the 30-year average.

4.2.1 Identification of *Rht-A1b* Suppressor Mutants

Once plants had reached maturity, height measurements were taken from 10 plants per plot to establish the average M2 *Rht-A1b* height 64.2 cm (SD +/- 2.6 cm) and Cadenza control height 82.7 cm (SD +/- 0.7 cm). A separate field characterisation experiment of *Rht-A1b* and Cadena (*Rht-1a*) in plots neighbouring the suppressor screen one, established the average heights to be 61.9 cm (SD +/- 0.82 cm) and 84.5

cm (SD +/- 2.92 cm), respectively. Potential *Rht-A1b* suppressor mutants were screened by eye and tagged and sampled if they produced three or more semi-dwarf shoots approximately 68-78 cm in length (Figure 4.3).

4.2.2 Genotyping Intragenic *Rht-A1b* Mutations

Genomic DNA was extracted from leaf samples using the method described in 2.4.1. To establish whether the sampled individuals contained intragenic mutations in the *Rht-A1b* sequence, PCR amplification and Sanger sequencing (section 2.4.6) was used to examine the C-terminal GRAS coding domain. The presence of the *Rht-A1b* mutation was also confirmed by sequencing. The primers used are described in Table 4.2 and Figure 4.3.

Figure 4.3: Photograph of a *Rht-A1b* Suppressor in the Field. By Steve Thomas.

Table 4.2: Primers for Genotyping Potential Rht-A1b Mutants

Primer Name	Targeted Gene	Primer Position in CDS (bp)	Primer Sequence	Sequencing Primer
Rht-A1F	*Rht-A1*	-11 to -33	AGCGAGGCAGCTCGCTCGCGGT	Yes
Rht-A1R	*Rht-A1*	557 to 575	CGTCGTCATCCTCCTCGTC	-
Rht3F20	*Rht-1*	664 to 681	GTGGTCGACACGCAGGAG	Yes
Rht-A1R3	*Rht-A1*	+96 to +118	CCTCTGAAGAAGAAGCTAAATG	Yes

Two sets of primers Rht-A1F/Rht-A1R and Rht3F20/Rht-A1R3 designed to sequence most of the *Rht-A1b* coding sequence (CDS), confirming the presence of the *Rht-A1b* mutation and identifying additional intragenic mutations Their position relative to the CDS is shown.

Figure 4.4: Locations of PCR primers in the *Rht-A1* gene. Coding sequence written in black, conserved DELLA protein domain coding sequences are highlighted in black with white lettering. The nucleotide site of the *Rht-A1b* mutation is highlighted in yellow in the DELLA motif. Primers for sequencing the *Rht-A1b* mutation are highlighted in yellow. Primers for sequencing the functional C-terminal GRAS domain are highlighted in orange.

To check that the sampled plants were not contaminants or volunteers (left over wheat from past crops), the presence of the *Rht-A1b* mutation was confirmed using the *Rht-A1* specific primers Rht-A1F and Rht-A1R. These primers produced a 567-bp PCR product, that included the three conserved motifs, 'LExLE', 'TVHYNP' and 'DELLA', within the N-terminal region where the *Rht-A1b* mutation is located.

To identify intragenic mutations in the C-terminal domain, a generic *Rht-1* primer, Rht-3F20 (Chandler and Harding 2013) was used with the *Rht-A1* specific reverse primer, Rht-A1R3. These produced a 1316-bp PCR product that contained the five C-terminal conserved motifs: LHR1, VHIID, LHR2, PYFRE and SAW. These motifs contained the majority of intragenic *Rht-B1c* mutations that were previously identified in (Derkx et al. 2017). As the resulting PCR product was >1000 bp in size, both primers were used to sequence the entire length of the product.

It is conceivable that that this screen could identify different classes of suppressor mutations that are not linked to *Rht-A1*. For example, mutations in genes encoding other GA signalling components. However, this is unlikely to be the case. The *Rht-B1c* suppressor screen performed by Chandler and colleagues (2013) did not identify any alleles that were not linked to *Rht-B1* (Chandler and Harding 2013; Derkx et al. 2017). Similarly, in the equivalent barley suppressor screen all of the mutations occurred in the DELLA gene *Sln1,* with the exception of a single recessive mutation in *Spindly1 (SPY1)* a negative regulator of GA signalling (Chandler and Harding 2013; Robertson et al. 1998). Mutations in SPY are not expected to be identified in the *Rht-A1b* suppressor screens as recessive loss-of-function mutations should not cause a phenotypic change in hexaploid wheat (Chandler and Harding 2013).

4.2.3 Intragenic *Rht-A1b* Mutations Identified in Suppressor Screen One

A total of 68 plants with a height of greater that 68 cm were genotyped from the suppressor screen. From these plants, 7 intragenic *Rht-A1b* mutations were identified in 11 individual M_2 plants, the equivalent of 1 mutant in 363 M_1 plants. These are detailed in Table 4.3

Table 4.3 Intragenic Rht-A1b Mutations Identified in Suppressor Screen One

Allele	Intragenic Mutation		Zygosity	Pool (No. Individuals)
	Nucleotide	Amino Acid		
Rht-A1b.1	C787T	**A262A**	Homozygous	F4 (1)
Rht-A1b.2	C836T	**A279V**	Homozygous	F1 (1)
Rht-A1b.3	G1047A	**W349***	Heterozygous	GH5 (1)
Rht-A1b.4	C1479T	**T493I**	Homozygous	F4 (3) and F5 (1)
Rht-A1b.5	C1591T	**L513F**	Homozygous	F6 (1)
Rht-A1b.6	G1812A	**W604***	Homozygous	GH5 (1) and F2 (1)
Rht-A1b.7	G1845A	**W615***	Heterozygous	F4 (1)

Table describing the 7 intragenic *Rht-A1b* mutations (*Rht-A1b.x)* identified in Suppressor Screen One; the nucleotide substitution, resulting amino acid substitution and zygosity of the mutation. The pool the mutations was identified in 'X' and the number of individuals containing that mutation in the pool 'Y' are shown as X (Y).

Of the seven mutations identified, three encoded premature stop codons (*Rht-A1b.3, Rht-A1b.6* and *Rht-A1b.7),* three encoded amino acid substitutions (*Rht-A1b.2, Rht-A1b.4* and *Rht-A1b.5)* and one was a silent (*Rht-A1b.1)*. All mutations occurred in the coding region for conserved motifs in the C-terminal domain of the protein (Figure 4.5).

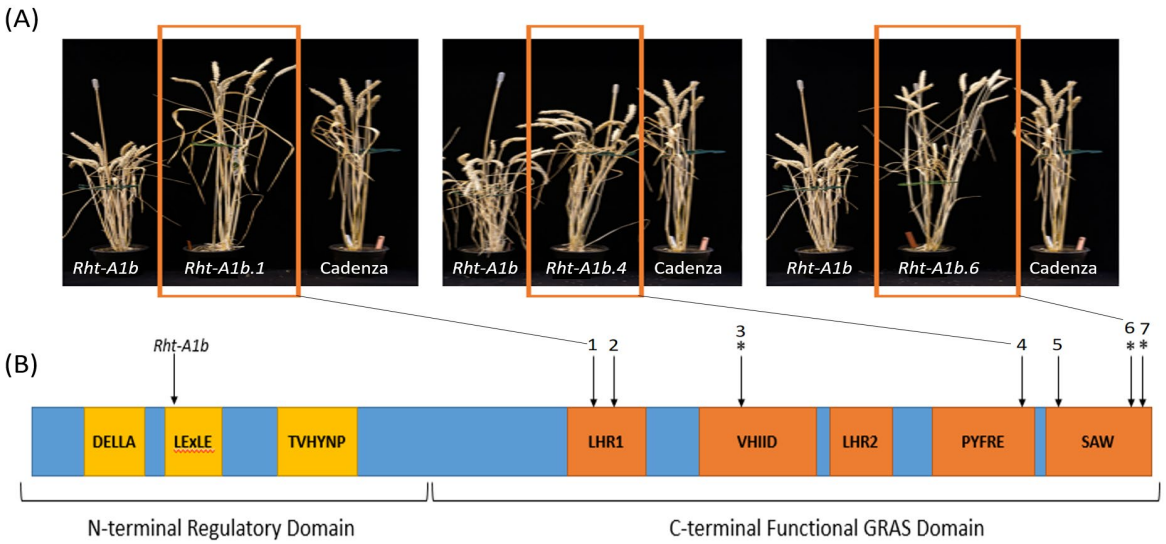

Figure 4.5: *Rht-A1b* Suppressors Identified in Suppressor Screen 1. (A) Photographs of Three M3 *Rht-A1b* Suppressor Mutants Identified in Screen One. Intragenic mutants are shown between *Rht-A1b* (left) and Cadenza (right). Plants were photographed at maturity. **(B) Position of Intragenic *Rht-A1b* Premature Terminations and Amino Acid Substitutions Identified in Suppressor Screen One.** Shown on a schematic diagram of RHT-A1 protein, including conserved domains. Yellow boxes represent conserved regulatory domains. Orange boxes represent conserved functional domains. Plain arrows show the mutation locations on the Rht-A1b protein. * = stop codon mutation. 1 = *Rht-A1b.1* (A262A), 2 = *Rht-A1b.2* (A279V), 3 = *Rht-A1b.3* (W349*), 4 = *Rht-A1b.4* (T493I), 5 = *Rht-A1b.5* (L513F), 6 = *Rht-A1b.6* (W604*), 7 = *Rht-A1b.7* (W615*).

4.3 *Rht-A1b* Suppressor Screen Two (2017)

In late March 2017, a larger scale suppressor screen, consisting of thirteen pools of M_2 EMS-mutagenised *Rht-A1b* seed was sown (Chapter 2.1.2). The weather conditions during the growing season are described in Table 4.4.

Table 4.4: Weather Conditions During Suppressor Screen Two

Month	Sunshine		Mean Temperatures				Rainfall		
			Maximum		Minimum		Total		Duration days**
	Total Hours	( )	°C	( )	°C	( )	mm	( )	
March	139.9	(+24.97)	12.7	(+2.76)	5	(+2.33)	40.4	(-10.42)	21
April	197.4	(+36.17)	13.8	(+1.20)	4.2	(+0.13)	10.9	(-44.19)	14
May	184.1	(-9.57)	17.7	(+1.65)	8.6	(+1.79)	70.5	(+14.82)	16
June	229.1	(+30.91)	21.5	(+2.38)	12	(+2.25)	39.1	(-14.12)	12
July	187.4	(-17.77)	21.8	(+0.00)	13.2	(+1.31)	72.6	(+22.69)	16
August	170.2	(-26.04)	20.2	(-1.39)	11.8	(-0.03)	66.6	(+2.89)	14

Numbers in the columns marked ( ) refer to variations from the 30 year means (1981-2010) for that month. Duration days **, refers to the number of days where there was >0.2mm rainfall. Data is from: http://resources.rothamsted.ac.uk/environmental-change-network/yearly-weather-summaries#loaded

In June, when the crop was booting, there was an additional 30.91 hours of sunshine, average temperature was 2.38°C to 2.25°C higher and there was 14.12 mm less rainfall compared to the 30-year average.

4.3.2 Identification of Intragenic *Rht-A1b* mutations in Suppressor Screen Two

Average height measurements for Cadenza 80.2 cm (SE +/- 1.02 cm) and *Rht-A1b* 49.8 cm (SE +/- 0.33 cm) were taken from a characterisation experiment next to suppressor screen two (Dr Stephen Thomas, personal communication).

Potential suppressor mutants were screened by eye and tagged and sampled if they produced three or more shoots that were between 55-75cm. In total, 285 individuals were tagged and sampled across the 13 pools. Genomic DNA was extracted from leaf samples (section 2.4.1) and the *Rht-A1* gene sequenced as described in section 4.2.2. From the 285 individuals sequenced, 28 different

intragenic mutations were identified in 59 plants, the equivalent of 1 mutant in 220 M1 plants. These mutants are described in Table 4.5.

Table 4.5 Intragenic Rht-A1b Mutations Identified in Suppressor Screen Two

Allele	Intragenic Mutation		Zygosity	Pool (No. individuals)
	Nucleotide	Amino Acid		
Rht-A1b.8	C785T	A262V	Homozygous	16 (1)
Rht-A1b.9	G800A	G267D	Homozygous	14 (2) and 20 (1)
Rht-A1b.10	C803T	A268V	Heterozygous	14 (1)
Rht-A1b.11	G809A	R270H	Homozygous	8 (3)
Rht-A1b.12	C808T	R270C	Homozygous	9 (1)
Rht-A1b.13	C821T	A274V	Homozygous	14 (2)
Rht-A1b.14	G830A	G277D	Homozygous (3) Heterozygous (1)	9 (1), 17 (2) and 18 (1)
Rht-A1b.15	G878A	S293N	Heterozygous	20 (1)
Rht-A1b.16	C965T	A322V	Homozygous	10 (1)
Rht-A1b.17	C1033T	Q345*	Heterozygous	10 (1)
Rht-A1b.18	C1150T	Q384*	Homozygous	20 (1)
Rht-A1b.19	G1162A	W387*	Homozygous (7) Heterozygous (1)	8 (6) and 18 (2)
Rht-A1b.20	C1201T	Q401*	Homozygous (1) Heterozygous (1)	11 (1) and 14 (1)
Rht-A1b.21	G1222A	A408T	Homozygous	20 (1)
Rht-A1b.22	C1256T	Q419*	Homozygous	16 (1)
Rht-A1b.23	C1301T	A434V	Heterozygous	20 (1)
Rht-A1b.24	G1408A	E470K	Heterozygous	11 (1)
Rht-A1b.25	C1460T	S487F	Homozygous (2) Heterozygous (2)	11 (4)
Rht-A1b.26	C1475T	S492F	Homozygous	18 (1)
Rht-A1b.4	C1478T	T493I	Homozygous (1) Heterozygous (2)	8 (1), 9 (1) and 14 (1)
Rht-A1b.27	G1487A	D496N	Homozygous	11 (2)
Rht-A1b.28	G1491A	S497F	Homozygous (1) Heterozygous (1)	8 (1) and 14 (1)
Rht-A1b.29	C1580T	S527F	Homozygous	10 (2), 11 (1) and 17 (1)
Rht-A1b.30	C1663T	Q555*	Homozygous	8 (2)
Rht-A1b.31	G1668A	W556*	Homozygous	14 (1) and 20 (1)
Rht-A1b.32	G1762A	W587*	Homozygous	8 (1)
Rht-A1b.6	G1812A	W604*	Homozygous (1) Heterozygous (1)	8 (1) and 10 (1)
Rht-A1b.7	G1845A	W615*	Homozygous	14 (1) and 20 (1)

Table describing the 28 intragenic *Rht-A1b* mutations (*Rht-A1b.x)* identified in Suppressor Screen Two; the nucleotide substitution, resulting amino acid substitution and zygosity of the mutation. The pool in which the mutations were identified, X, and the number of individuals containing that mutation in the pool, Y are shown as X (Y).

Of the 28 independent mutations, 10 introduce premature stop codon and 18 result in amino acid substitutions. The majority of these occurred in the conserved motifs of the C-terminal GRAS domain of the RHT-A1 protein, except for *Rht-A1b.15* and *Rht-A1b.22,* which occurred outside these domains (Figure 4.6).

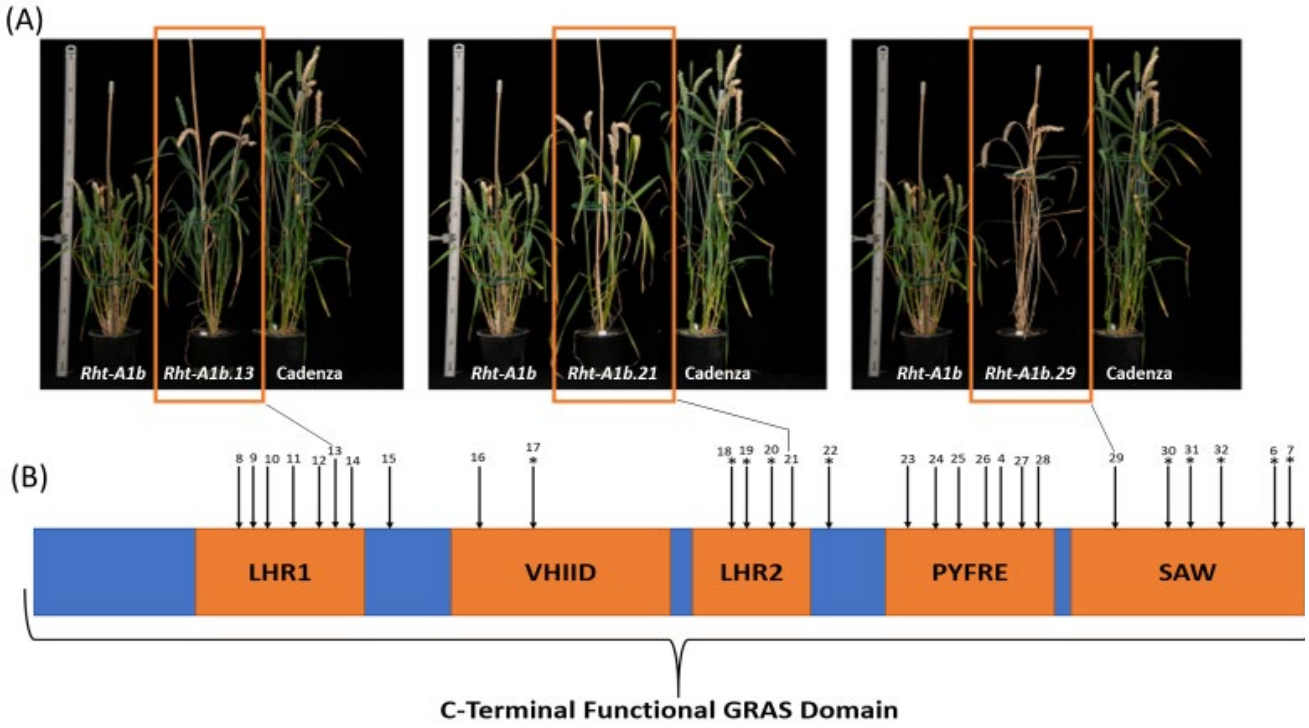

Figure 4.6: *Rht-A1b* Suppressor Mutants Identified in Suppressor Screen 2. (A) Photographs of Three M3 Intragenic Mutants Identified in Suppressor Screen Two. Intragenic mutants are shown between *Rht-A1b* (left) and Cadenza (right). Plants were photographed at maturity. **(B) Position of Intragenic *Rht-A1b* Premature Terminations and Amino Acid Substitutions Identified in Suppressor Screen Two.** Shown on a schematic diagram of RHT-A1 protein, including conserved domains. Yellow boxes represent conserved regulatory domains. Orange boxes represent conserved functional domains. Plain arrows show the mutation locations on the Rht-A1b protein. * = stop codon mutation. 8 = *Rht-A1b.8* (A262V), 9 = *Rht-A1b.9* (G267D), 10 = *Rht-A1b.10* (A268V), 11 = *Rht-A1b.11* (R270H), 12 = *Rht-A1b.12* (R270C), 13 = *Rht-A1b.13* (A274V), 14 = *Rht-A1b.14* (G277D), 15 = *Rht-A1b.15* (S293N), 16= *Rht-A1b.16* (A322V), 17 = *Rht-A1b.17* (Q345*), 18 = *Rht-A1b.18* (Q384*), 19= *Rht-A1b.19* (W387*), 20 = *Rht-A1b.20* (Q401*), 21 = *Rht-A1b.21* (A408T), 22 = *Rht-A1b.22* (Q419*), 23 = *Rht-A1b.23* (A434V), 24 = *Rht-A1b.24* (E470K), 25 = *Rht-A1b.25* (S487F), 26 = *Rht-A1b.26* (S492F), 4 = *Rht-A1b.4* (T493I), 27 = *Rht-A1b.27* (D496N), 28 = *Rht-A1b.28* (S497F), 29 = *Rht-A1b.29* (S527F), 30 = *Rht-A1b.30* (Q555*), 31 = *Rht-A1b.31* (W556*), 32 = *Rht-A1b.32* (W587*), 6 = *Rht-A1b.6* (W604*), 7 = *Rht-A1b.7* (W615*).

4.4.1 Identification of *Rht-A1b* Intragenic Mutants

In this chapter I have discussed the successful use of EMS mutagenesis suppressor screens to generate and identify derivative *Rht-A1b* alleles. Identification of intragenic *Rht-A1b* suppressor mutations increased from 1 in 363 M_1 plants in screen one, to 1 in 220 M_1 plants in screen two. This is most likely linked to the increased difference between the *Rht-A1b* and Cadenza shoot heights in suppressor screen two (30.4 cm), compared to suppressor screen one (24.6 cm). This is likely a result of the warmer, sunnier and drier weather during suppressor screen two (Table. 4.3), Dr Stephen Thomas, personal communication). At higher temperatures the differences in GA responses between tall and dwarf *Rht* lines are more extreme, resulting in more severe dwarfing phenotypes in dwarf and semi-dwarf *Rht* lines (Stoddart and Lloyd 1986; Pinthus et al. 1989; Lenton and Appleford 1991). Additionally, hot dry growing conditions have been shown to result in smaller shoots and leaves in shorter *Rht* lines (Bush and Evans 1988). As a result, less severe *Rht-1* alleles such as *Rht8* and *Rht-D1b,* which are more resistant to drought and temperatures are present in Mediterranean commercial wheat varieties (Worland 1986; Börner et al. 1991; Grover et al. 2018).

The greater variation in *Rht-A1b* and Cadenza heights during suppressor screen two made the potential *Rht-A1b* suppressors more striking and easily identifiable in the field, suggesting that carrying out future screens in warmer, drier climates may aid the identification of tall suppressor mutants in future screens (Bush and Evans 1988; Chandler and Harding 2013). Additionally, although the same EMS treatment protocol (Section 2.2) was used to generate both M1 population, it is possible that the two treatments resulted in different levels of mutagenesis. Therefore, there is a possibility that a higher level of mutagenesis occurred during the generation of the population used in screen two, resulting in an increased number of *Rht-A1b* suppressor mutants.

If this screen was repeated, a better starting point may be a different, more severe *Rht-A1* allele. Seventeen nonsense mutation were identified in *Rht-A1* during the initial TILLING screen, some of which produced a more severe GA insensitive phenotype. These would provide a better starting point for an EMS mutagenesis

screen, as loss of function mutants would be more easily identifiable (Chandler and Harding 2013).

4.4.2 *Rht-A1b* Intragenic Mutations

All the intragenic *Rht-A1b* mutations that were identified in the two screens were the result of G/C to A/T transitions caused by alkylation of guanine bases during EMS mutagenesis (Henikoff and Comai 2003). Across the two *Rht-A1b* suppressor screens these transitions resulted in 32 different intragenic mutations: 11 nonsense mutations, 20 missense mutations and one silent mutation. Truncated mutations therefore accounted for 34.4% of mutations identified, missense mutations 62.5% and silent mutations 4.1%. This varies from the proportion of truncated, missense and silent mutations identified in other EMS mutagenesis experiments in hexaploid wheat. These mutations ranged from 34.2-46% missense, 30.3-38.6% silent and 1-9.2% truncated (Slade et al. 2005; Dong et al. 2009; Sestili et al. 2010). The variation is due to these experiments using high-throughput TILLING to analyse hundreds of individuals (Till et al. 2006), whilst potential *Rht-A1b* mutants were selected on their phenotype. Therefore, significantly fewer silent mutations were identified as these are unlikely to produce a taller mutant, resulting in a skewed higher proportion of missense and truncated mutations being identified. Similarly, in the *Rht-B1c* suppressor screen which used the same methodology, but a different mutagenesis treatment (sodium azide instead of EMS) truncated mutations accounted for 28.6%, 57.1% missense and 14.3% splice site mutations (Derkx et al. 2017). Splice site mutations were only identified in the *Rht-B1c* suppressor screen because *Rht-A1b* does not contain introns. In contrast, *Rht-B1c* contains a 2-kb retrotransposon insertion (Wu et al. 2011; Pearce et al. 2011) that is partially spliced. Splice site mutations also resulted in a taller phenotype as these are predicted to affect the amount of RHT-B1C repressor produced, depending on the efficiency of splicing (Talerico and Berget 1990; Chandler and Harding 2013).

As was previously demonstrated in the *Rht-B1c* suppressor screens (2013; 2017), the majority of *Rht-A1b* suppressor mutations that were identified caused amino acid substitutions in conserved motifs (LHR1, VHIID, LHR2, PYFRE and SAW) of the C-

terminal GRAS domain (Figure 4.7). Disruption to these domains results in a reduction of DELLA repressive activity (Li et al. 2016; Derkx et al. 2017).

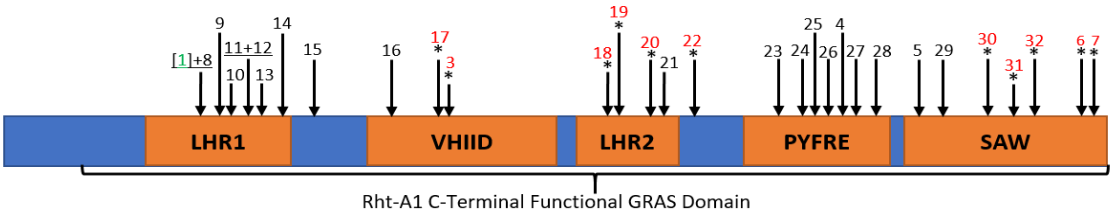

Figure 4.7: Locations of Mutations in the Rht-A1 C-terminal GRAS Domain, Identified in the Suppressor Screens. Orange boxes represent the conserved motifs; LHR1, VHIID, LHR2, PYFRE and SAW. Arrows depict the approximate mutation site. Numbers correspond to allele number. [X] = silent mutation, X* = terminal mutation, plain arrow = missense mutation.

The *Rht-A1b* intragenic mutations most commonly occurred in the LHR1, PYFRE and SAW motifs, which are integral for RHT function, e.g. binding to protein partners (Li et al. 2016). In rice, the LHR1 motif is composed of three α-helices important for protein interactions (Pysh et al. 1999; Li et al. 2016) with proteins such as BZR1, MYC2, JAZ1 and EIN3, (Hou et al. 2010; An et al. 2012; Gallego-Bartolome et al. 2012; Hong et al. 2012). The PYFRE and SAW motifs consist of α-helices and a β-strands, which form part of the Rossmanfold α/β/α sandwiched conformation, that makes up the core DELLA subdomain. This subdomain is also implicated in DELLA interacting protein (DIP) interactions (Li et al. 2016), as well as interactions with GID1 and SLY1/GID2 as part of the GA-mediated DELLA degradation pathway in rice (Hirano et al. 2010; Bai et al. 2012). Studying the *Rht-A1b* suppressor mutants will therefore provide insights into the effect of single amino acid substitutions and potentially identify amino acids important for RHT-A1 function and interactions with downstream signalling components (Chandler and Harding 2013). In the case of *Rht-A1b.15* and *Rht-A1b.23*, which occur outside of the conserved motifs, these may be mutations that affect amino acids also involved in protein interactions.

Of the 32 *Rht-A1b* suppressor mutations, two occurred in the same codon. The *Rht-A1b.11* allele has a guanine to adenine transition in the 809th nucleotide, resulting in a R270H substitution, whilst in *Rht-A1b.12* a cytosine to thymine transition in the 808th nucleotide results in the R270C substitution. Following backcrossing, these

mutants will provide an opportunity to compare the effects of different amino acid substitutions of the same residue, providing a deeper understanding of the role this residue plays in RHT-A1 function.

4.4.3 Repeated Identification of *Rht-A1b* Intragenic Mutations

Just under a third of the intragenic *Rht-A1b* mutations were identified in multiple pools and occasionally occurred in both suppressor screens (Table 4.6).

Table 4.6: Identification of Intragenic Rht-A1b Mutations in Different Pools and Suppressor Screens

Allele	Intragenic Mutation		Pool Each Mutation Was Identified In	
	Nucleotide	Amino Acid	Suppressor Screen One	Suppressor Screen Two
Rht-A1b.4	C1479T	T493I	F4 and F5	8, 9 and 14
Rht-A1b.6	G1812A	W604*	GH5 and F2	8 and 10
Rht-A1b.7	G1845A	W615*	F4	14 and 20
Rht-A1b.9	G800A	G267D		14 and 20
Rht-A1b.14	G830A	G277D		9, 17 and 18
Rht-A1b.19	G1162A	W387*		8 and 18
Rht-A1b.20	C1201T	Q401*		11 and 14
Rht-A1b.28	G1491A	S497F		8 and 14
Rht-A1b.29	C1580T	S527F		10, 11 and 17
Rht-A1b.31	G1668A	W556*		14 and 20

Table describing the intragenic *Rht-A1b* mutations (*Rht-A1b.x)* identified in multiple pools and suppressor screens. The nucleotide substitution and resulting amino acid substitution are shown. The pools each mutation was identified in e.g. 'F4' in Suppressor Screen One or '8' in Suppressor Screen Two, is shown.

As each pool represents a different M1 population, this suggests that the mutations were the result of independent mutagenesis events. There may be a predilection towards these mutations because of the mutagenesis process used. EMS is not an entirely random process: following analysis of ~18,000 rice EMS mutants with

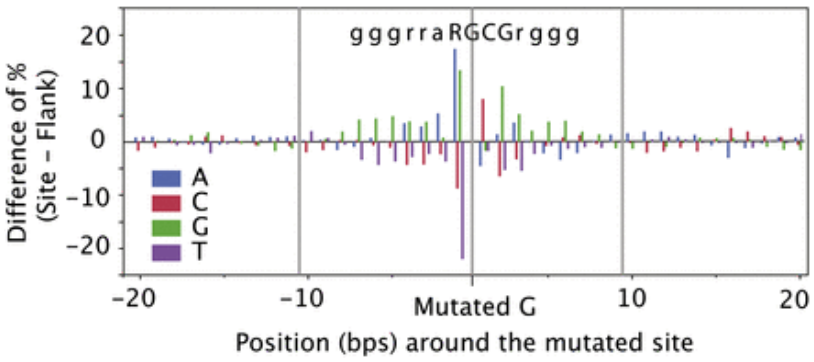

Figure 4.8: Analysis of the Nucleotide Frequencies around EMS Mutations in the Rice Samples. 'R' refers to G or A bases. Taken from Henry, Nagalakshmi et al. 2014.

exome capture and next-generation sequencing, researchers observed that there is a strong bias towards GGC (glycine) and AGC (serine) triplets as targets for EMS mutagenesis (Henry et al. 2014) (Figure 4.8).

This could potentially explain the repeated identification of *Rht-A1b.9* (G267D)*, Rht--A1b.14* (G277D)*, Rht -A1b.28* (S497F) and *Rht-A1b.29* (S527F) mutations (Table 4.6). Henry, Nagalakshmi et al. also observed a positive EMS bias where the 5-6 bp either side of the mutation contained a high proportion of G bases. This principle is consistent with the repeatedly identified *Rht-A1b* mutations (Figure 4.9).

Rht-A1b.4	A	C	T	C	C	A	C	C	A	T	G	T	T
Rht-A1b.6	C	G	G	G	T	G	G	C	A	C	A	C	G
Rht-A1b.7	G	C	A	T	G	G	C	G	C	C	T	G	G
Rht-A1b.9	A	G	G	G	C	G	G	C	G	C	G	A	T
Rht-A1b.14	A	C	T	T	C	G	G	C	G	A	G	G	C
Rht-A1b.19	G	G	G	C	T	G	G	A	A	G	C	T	C
Rht-A1b.20	G	A	C	T	T	C	C	A	G	T	A	C	C
Rht-A1b.28	T	C	G	A	T	T	C	C	C	T	C	G	A
Rht-A1b.29	T	C	A	T	G	T	C	C	G	A	G	G	T
Rht-A1b.31	G	C	A	G	T	G	G	C	G	G	A	A	C

Figure 4.9: Proportion of guanine (G) bases flanking 5-6bp either side of the Rht-A1b intragenic mutations. 'G' bases are highlighted in blue. The bases mutagenised by EMS are highlighted in yellow.

Thus *Rht-A1b.6, Rht-A1b.7, Rht- A1b.9,Rht- A1b.14, Rht-A1b.19, Rht-A1b.29* and *Rht-A1b.31* may occur more than once due to the high proportion of 'G' bases (3 or more flanking 5' or 3' of the mutation) causing a positive bias for mutagenesis. Only two mutations do not involve a serine or glycine substitution or have a high proportion of flanking 'G' bases, *Rht-A1b.4* (T493I) and *Rht-A1b.28* (Q401*). These more unusual mutations may have been identified due to the nature of the forward genetic screen. There are expected to be a limited number of regions in the conserved motifs of the GRAS domain where amino acid substitutions will affect RHT-1 function. *Rht-A1b.4* and *Rht-A1b.28* may reflect such mutations and were therefore be identified during the screen. Additional mutations resulting in amino acid substitutions in the GRAS domain that did not affect RHT-1 function will not have been identified (Chandler and Harding 2013; Derkx et al. 2017).

4.4.4 A Comparison of *Rht-A1b* and *Rht-B1c* Suppressor Mutations

The three *Rht-1* homoeologues have highly conserved functional C-terminal GRAS domains (Peng et al. 1997) (Figure 4.2), so that that equivalent mutations could be identified in the *Rht-A1b* suppressor screens and *Rht-B1c* suppressor screen (Table 4.7).

Table 4.7: Mutations affecting the same residues in the Rht-A1b and Rht-B1c screens

Rht-A1b Intragenic Mutants					*Rht-B1c Intragenic Mutants **		
Allele	Nucleotide Substitution	Amino Acid Substitution	No. Individuals (No. Pools)		Allele	Nucleotide Substitution	Amino Acid Substitution
			2016	2017			
A1b.2	C836T	A279V	1		B1c.7	C2865T	A310V
A1b.4	C1479T	T493I	4 (3)	3 (3)	B1c.16	C3507T	T524I
A1b.6	G1812A	W604*	2 (2)	1	B1c.33	G3841A	W635*
A1b.7	G1845A	W615*	1	2 (2)	B1c.20	G3874A	W646*
A1b.9	G800A	G267D	3 (2)		B1c.4	G2829A	G298D
A1b.10	C803T	A268V	1		B1c.5	G2831A	A299T
A1b.14	C821T	A274V	2 (1)		B1c.6	G2849A	A305T
A1b.20	G1162A	W387*	8 (2)		B1c.13	G3190A	W418*
A1b.28	G1491A	S497F	2 (2)		B1c.17	C3519T	S528F
A1b.31	G1668A	W556*	2 (2)		B1c.19	G3697A	W587*

**Rht-B1c* contains 2kb retrotransposon insertion that is partially removed resulting in a 90-bp in-frame transcription insertion. This is reflected in nucleotide and amino acid numbering. *Rht-B1c* mutations identified in Chandler and Harding 2013 and Derkx, Harding et al. 2017.

Eight of the thirty-two intragenic *Rht-A1b* mutants have an equivalent mutation identified in the *Rht-B1c* suppressor screen: *Rht-A1b.2, A1b.4, A1b.6, A1b.7, A1b.10, A1b.20, A1b.28* and *A1b.31.* Once these lines have been backcrossed, their phenotypes can be compared to the *Rht-B1c* mutants to assess whether the mutations have similar effects (Chandler and Harding 2013; Derkx et al. 2017). Furthermore, *A1b.10* and *A1b.14* cause amino acid substitutions in the same locations as in *B1c.5* and *B1c.6*, respectively. These substitutions were alanine to valine in the *Rht-A1b* screen and alanine to threonine in the *Rht-B1c* screen. As they were generated in separate mutagenesis events using different mutagens this suggests that these codons may be particularly prone to mutagenesis, or that these amino acids are important for conferring RHT-1 repressive activity (Pearce et al. 2011).

4.5 *Rht-A1b* Suppressor Alleles for Backcrossing and Further Study

Of the 32 intragenic *Rht-A1b* mutants identified in the two suppressor screens, 18 mutants will be used for further study (Table 4.8 and Figure 4.10).

Table 4.8: Rht-A1b Intragenic Mutants for Further Study

Allele	Intragenic Mutation	
	Nucleotide	Amino Acid
Rht-A1b.2	C836T	A279V
Rht-A1b.3	G1047A	W349*
Rht-A1b.4	C1479T	T493I
Rht-A1b.5	C1591T	L513F
Rht-A1b.6	G1812A	W604*
Rht-A1b.7	G1845A	W615*
Rht-A1b.9	G800A	G267D
Rht-A1b.11	G809A	R270H
Rht-A1b.12	C808T	R270C
Rht-A1b.13	C821T	A274V
Rht-A1b.14	G830A	G277D
Rht-A1b.21	G1222A	A408T
Rht-A1b.24	G1408A	E470K
Rht-A1b.25	C1460T	S487F
Rht-A1b.26	C1475T	S492F
Rht-A1b.27	G1487A	D496N
Rht-A1b.28	G1491A	S497F
Rht-A1b.29	C1580T	S527F

Table describing intragenic *Rht-A1b* mutations (*Rht-A1b.x).* A * denotes a nonsense amino acid substitution.

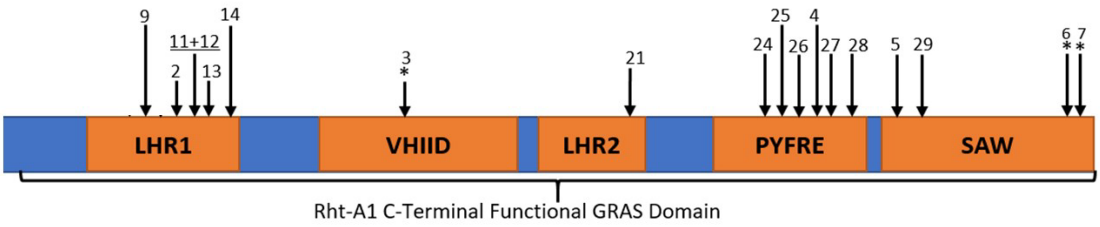

Figure 4.10: Locations of Mutations in the RHT-A1 C-Terminal GRAS Domain, Identified in Suppressor Screens. Orange boxes represent the conserved motifs; LHR1, VHIID, LHR2, PYFRE and SAW. Arrows depict the approximate mutation site. Numbers correspond to allele number. * = nonsense mutation, plain arrow = missense mutation.

The primary aim of the suppressor screen was to identify partial loss-of-function mutants that produced a semi-dwarf phenotype which would allow their potential use as new dwarfing alleles in wheat breeding programs. Therefore, all missense mutations (excluding *Rht-A1b.15* and *Rht-A1b.23)* will be used for further study, as amino acid substitutions in the C-terminal GRAS domain are most likely to cause a

partial reduction in the repressive activity of *Rht-A1b* (Chandler and Harding 2013; Derkx et al. 2017). Although they were identified in the field, *Rht-A1b.15* and *Rht-A1b.23,* were not identified in the M3 generation, potentially due to a harvesting error, and therefore it was not possible to assess them further.

To establish the different phenotypic effects of missense and truncated mutants, *Rht-A1b.3, Rht-A1b.6* and *Rht-A1b.7* were also included in the study. *Rht-A1b.6* and *Rht-A1b.7*, which occur in the SAW motif, were selected as they were identified in multiple pools in suppressor screens one and two. An equivalent mutation for each was also identified in the *Rht-B1c* screen (*Rht-B1c.33* and *Rht-B1c.20* respectively). Despite occurring towards the end of the protein, these *Rht-B1c* mutations resulted in a tall, loss of function phenotype; 98% and 96% the height of *Rht-B1a*. In addition, a study in rice identified a stop codon mutation, *Slr1.4*, resulting in the protein lacking the last 6 amino acids. This also resulted in a tall, slender phenotype (Ikeda et al. 2001), suggesting that *Rht-A1b.6* and *Rht-A1b.7* will also produce complete loss of function phenotypes.

During this process the silent mutant *Rht-A1b.1* was removed from the project. The mutant produced a tall phenotype in the M3 generation but following the first round of backcrossing produced a dwarf *Rht-A1b* phenotype with reduced fertility due to deformed ears. Therefore, it was decided that there was likely to be a background mutation causing the phenotype. Genetic linkage analysis could be used to assess whether the M3 *Rht-A1b.1* phenotype was due to an unlinked mutation. To establish whether this was the case, *Rht-A1b.1* could be crossed to WT Cadenza (*Rht-1*) as well as *Rht-A1b.2* as a positive control. In the F_2 generation the adult phenotype would be assessed, and a 3:1 (*Rht-A1b.2*: Cadenza) height distribution expected for the positive control. A reduced ratio, with intermediate plant heights would be consistent with *Rht-A1b.1* containing an unlinked mutation (Chandler and Harding 2013)

EMS-mutagenesis is not targeted to a single gene (Henikoff, Till, and Comai 2004), therefore additional allelic mutations will have been induced elsewhere in the hexaploid genome. To remove these background mutations and ensure phenotypic measurements are the result of the identified mutations, *Rht-A1b* intragenic

mutants described in Table 4.8 have been backcrossed to Cadenza twice to remove approximately 75% of the background mutations (Derkx et al. 2017). From the BC_2F_2 generation, homozygous mutants and null segregates have been identified.

From this generation homozygous mutants and null segregates have been identified and bulked up to allow a detailed phenotypic characterisation (described in Chapter 5).

Chapter 5: Characterisation of *Rht-A1b* Suppressor Mutants

5.1 Introduction

Chapter 4 discussed the identification of multiple intragenic *Rht-A1b* mutants from suppressor screens of M2 populations of EMS mutagenised *Rht-A1b* (Cadenza var.). In this chapter, 18 of these mutants will be used for further study (described in Section 4.5).

The *Rht-A1b* mutation, a premature stop codon in the N-terminal 'DELLA' motif, results in a short semi-dwarf phenotype in the Cadenza background, which is potentially too short to be beneficial for commercial breeding in some elite wheat varieties (Flintham et al. 1997) (Chapter 4). The current hypothesis for this phenotype suggests that as the *Rht-A1b* mutation is followed by multiple AUG codons, a prematurely aborted N-terminal peptide and a N-terminally truncated protein are produced (Figure 1.16). The N-terminally truncated protein is likely to remain functional, as the functional C-terminal GRAS domain is not disrupted, however the lack of a complete DELLA domain means that the protein is likely to remain resistant to GA-induced degradation. This is expected to lead to constitutive repression of GA signalling, resulting in a dwarf phenotype (Peng et al. 1999).

To assess the effect that the suppressor mutants have on the *Rht-A1b* phenotype, the lines were backcrossed twice to Cadenza (var.) and bulked to the BC_2F_3 generation, to remove approximately 75% of background mutations introduced by the EMS-mutagenesis (Henikoff, Till, and Comai 2004; Derkx et al. 2017). A timeline of this process is shown in Figure 5.

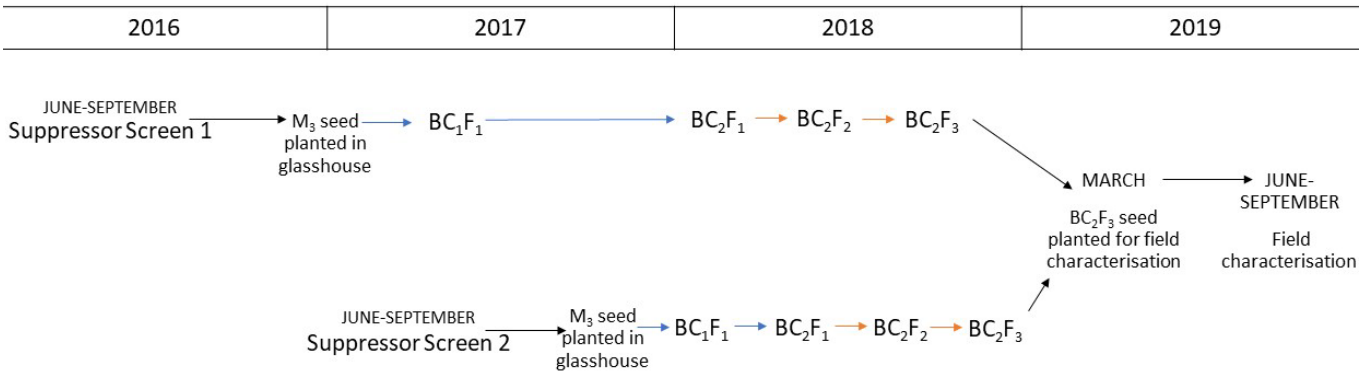

Figure 5: Timeline of Wheat Generations Between Suppressor Screens and Field and Glasshouse Characterisation (BC_2F_3). Backcrossing generations (blue arrow) to WT Cadenza are shown with BCx, and each generation of offspring after self-fertilisation (orange arrow) is shown with Fx.

To establish whether amino acid substitutions resulted in a partial loss-of-function phenotype, the backcrossed lines were assessed in the glasshouse and in the field. As amino acid substitutions in the C-terminal GRAS domain are most likely to cause a partial-loss-of-function in the repressive activity of *Rht-A1b* (Chandler and Harding 2013; Derkx et al. 2017), these lines will be assessed to determine whether they produce a semi-dwarf phenotype that may be beneficial for wheat breeding programs. In this chapter, a semi-dwarf phenotype will be defined as an intermediate phenotype between *Rht-1* and *Rht-A1b*.

Rht-A1b suppressors containing nonsense mutations (*Rht-A1b.3, Rht-A1b.6* and *Rht-A1b.7*) were also phenotyped in the glasshouse to determine whether they resulted in a loss-of-function phenotype (i.e. reverted the phenotype to a tall, due to the remaining presence of *Rht-B1a* and *Rht-D1a*). A loss of function phenotype in the nonsense mutants: *Rht-A1b.3, Rht-A1b.6* and *Rht-A1b.7*, would demonstrate that the presence of the C-terminal coding region is required for the penetrance of the *Rht-A1b* GA-insensitive dwarf phenotype. This would align with the current hypothesis that the semi-dwarf phenotype of *Rht-A1b, Rht-B1b* and *Rht-D1b* is due to translation reinitiation. The outcomes of these characterisation studies are discussed in this chapter.

5.2 Glasshouse Characterisation of *Rht-A1b* Suppressor mutants

The purpose of the suppressor screen was to identify intragenic *Rht-A1b* mutants (Chapter 5) with a partial loss of function phenotype that produced an allelic series with a diverse range of heights between those of *Rht-A1b* and wild type Cadenza. To quantify the effect the *Rht-A1b* intragenic mutations have on plant phenotype, suppressor lines where grown alongside *Rht-A1b, Rht-D1b* and WT Cadenza (*Rht-1)* controls. Additionally, six null segregants (NS) of the *Rht-A1b* suppressor mutants were grown up to help account for effect of background mutations that had not been removed by backcrossing. Five individuals per line were grown up to maturity under standard conditions (section 2.1) in a randomised block design. Phenotypic measurements were taken during plant development and at maturity.

5.2.1 Heading date

As discussed in Section 3.2.1, the *Rht-A1b* mutation results in a later heading date than *Rht-1.* This is potentially due to increased GA insensitivity reducing the rate of peduncle elongation and floral transition (Keyes 1987; Keyes, Paolillo, and Sorrells 1989), resulting in slower ear emergence. As heading date is correlated to final yield under some environmental conditions (Jung and Muller 2009) To assess whether the *Rht-A1b* intragenic mutations result in partial loss of function (i.e. faster heading date) for each plant. Heading date was measured as the number of days between germination and emergence of the first ear on the primary shoot. Residual plots for this data were assessed in GenStat, which confirmed that the data was Normal and did not require transformation. A General Analysis of Variance (ANOVA) was conducted, the output of which is described in Table 5.1 and Figure 5.1

Table 5.1: ANOVA Output for Heading Date for Rht-A1b Intragenic Mutants and Controls

Line	Average	SD	P-Value	SED	5% LSD
Rht-1	53.8	± 0.8			
Rht-A1b	**60.6**	± 0.5			
Rht-D1b	**59.8**	± 2.3			
Rht-A1b.2	**57**	± 1			
Rht-A1b.3	54.8	± 1.3			
Rht-A1b.4	54	± 0.7			
Rht-A1b.5	**60**	± 1.2			
Rht-A1b.6	**57.4**	± 2.5			
Rht-A1b.7	**57.6**	± 2.2			
Rht-A1b.9	55.4	± 0.5			
Rht-A1b.11	**58.6**	± 1.3			
Rht-A1b.12	**59**	± 1.4			
Rht-A1b.13	**61**	± 0.7			
Rht-A1b.14	**61.2**	± 2.9	<0.001	1.1	2.2
Rht-A1b.21	**58**	± 3.1			
Rht-A1b.24	**57.8**	± 1.3			
Rht-A1b.25	55	± 2			
Rht-A1b.26	55.2	± 1.1			
Rht-A1b.27	**57.6**	± 2.5			
Rht-A1b.28	55.2	± 1.3			
Rht-A1b.29	55.89	± 1.9			
NS Rht-A1b.4	55.6	± 2.7			
NS Rht-A1b.5	55.8	± 1.4			
NS Rht-A1b.9	55	± 0.8			
NS Rht-A1b.11	**58.6**	± 2.3			
NS Rht-A1b.12	54.8	± 1.7			
NS Rht-A1b.14	56	± 1.2			

The mean value is shown with its standard deviation (SD), along with the standard error of differences (SED) and 5% least significant difference of means (LSD 5%). Means shown in bold are significantly different from *Rht-1,* underlined means are significantly different from *Rht-A1b.* NS = null segregant of an *Rht-A1b.X* mutation.

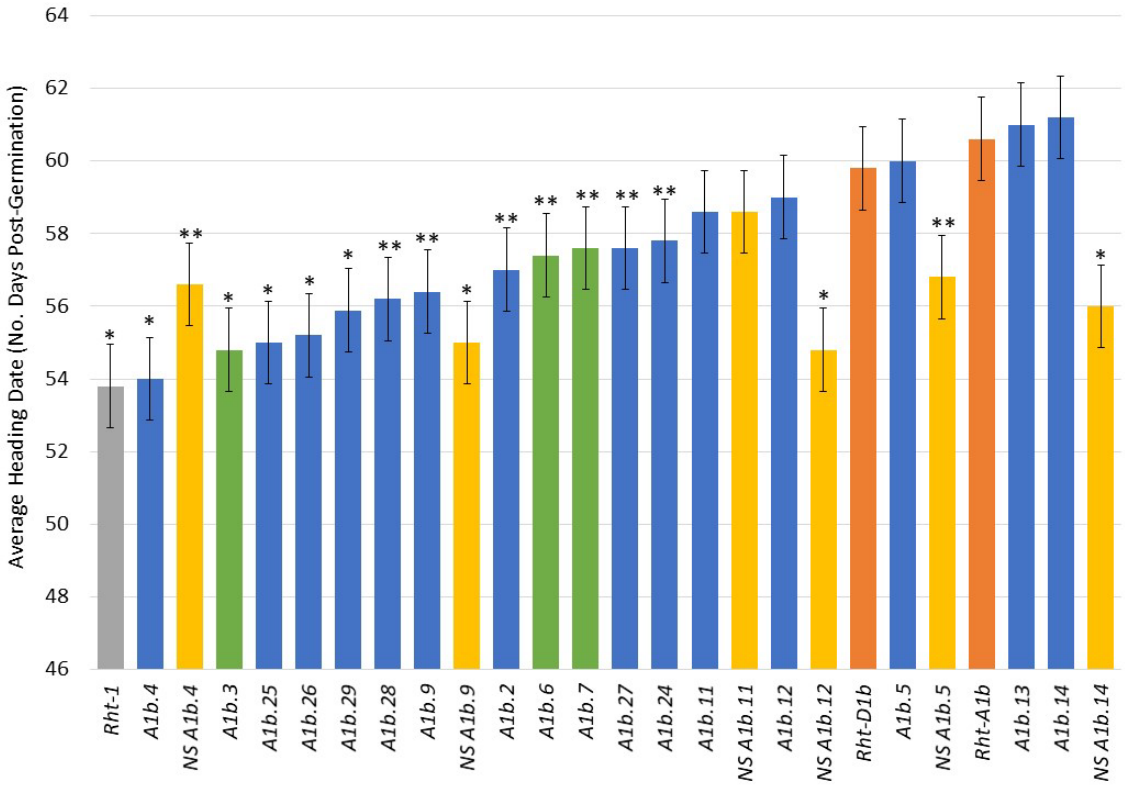

Figure 5.1: Average Heading Date in Rht-A1b Intragenic Mutants and Controls. Shown as number of days post-germination. Grey = *Rht-1,* orange = *Rht-A1b* and *Rht-D1b*, green = *Rht-A1b* intragenic nonsense mutant, blue = *Rht-A1b* intragenic missense mutants, yellow = null segregants (NS) of *Rht-A1b* intragenic missense mutants. Lines are ordered fastest to slowest, with exception to the null segregants, which are to the right of their mutant counterpart. ANOVA P-value = <0.001. Error bars = standard error of means (1.144). * = mean significantly different from *Rht-A1b,* ** = mean significantly different from *Rht-A1b* and *Rht-1*.

The ANOVA confirmed a highly significant interaction between genotype and the time taken for heading date ($p<0.001$). The 5% least significant difference of means (5% LSD) (2.3) was used to assess which genotypes produced significantly different heading dates from each other.

There was no significant difference between the heading dates of *Rht-A1b* and *Rht-D1b* (59.8 and 60.6 days respectively which was 6 and 7.3 days later than *Rht-1*. The majority of the *Rht-A1b* suppressor mutants produced heading date times significantly faster than *Rht-A1b* (marked with a * or ** in Figure 5.1). Six of these; *Rht-A1b.28/9/2/6/7/27* produced an intermediate heading date (55.2-57.8 days),

significantly faster than *Rht-A1b* and slower than *Rht-1.* Four of these; *Rht-A1b.4/3/24/25/26/29*, had even faster heading dates (54-55.9 days) that where not significantly different from *Rht-1.* Five *Rht-A1b* suppressor mutants; *Rht-A1b.11/12/5/13/14* where not significantly different than *Rht-A1b.*

Heading date varied in the null segregants. *NS Rht-A1b.9/12/14* were not significantly different than *Rht-1. NS Rht-A1b.4/5* were significantly intermediate to *Rht-1* and *Rht-A1b*, whilst *NS Rht-A1b.11* was not significantly different from *Rht-A1b.* Two lines, *Ns Rht-A1b.9/11* where not significantly different from their mutant counterpart. This suggests that background mutations are having some effect on heading date as these lines were predicted to produce a WT flowering phenotype identical to Cadenza (*Rht-1*), as these lines have *Rht-A1a* instead of an *Rht-A1b* allele.

5.2.2 Plant Height

The most obvious effect of *Rht-1* dwarf and semi-dwarf alleles is a reduction in plant height, caused by reduced cell elongation (Keyes 1987; Keyes, Paolillo, and Sorrells 1989). To establish whether the suppressor mutants produced taller height phenotypes than *Rht-A1b* as was seen in the *Rht-B1c* suppressor screen (Chandler and Harding 2013; Derkx et al. 2017), total shoot length measurements were taken for the three tallest shoots per plant (Section 2.3.1). Residual plots for this data were assessed in GenStat, which confirmed that the data was Normal and did not require transformation. A General Analysis of Variance (ANOVA) was conducted on each data set, the output of which is described in Table 5.2 and Figure 5.2 .

Table 5.2: ANOVA Output for Total Shoot Length (mm) in Rht-A1b Intragenic Mutants and Controls

Line	Total Shoot Length (mm)	SD (±)	% Height from *Rht-1*	P-Value	SED	5% LSD
Rht-1	824.3	58.4	NA	<0.001	27.7	54.6
Rht-A1b	530.8	54.9	64.4			
Rht-D1b	645.7	41.3	78.3			
Rht-A1b.2	860.2	30.2	104.4			
Rht-A1b.3	**895.1**	24.2	108.6			
Rht-A1b.4	830.2	44.4	100.7			
Rht-A1b.5	**731.4**	61.9	88.7			
Rht-A1b.6	**950.7**	33.8	115.3			
Rht-A1b.7	**935.5**	46.6	113.6			
Rht-A1b.9	**703**	74.3	85.3			
Rht-A1b.11	771.3	81.6	93.6			
Rht-A1b.12	**735.6**	40	89.2			
Rht-A1b.13	**703.2**	75.7	85.3			
Rht-A1b.14	**738.4**	55.8	89.6			
Rht-A1b.21	829	49.1	100.6			
Rht-A1b.24	838.2	123,5	101.7			
Rht-A1b.25	**945.1**	34.3	114.7			
Rht-A1b.26	877.2	225.9	105.4			
Rht-A1b.27	858	45.3	104.1			
Rht-A1b.28	781.2	31.4	94.8			
Rht-A1b.29	**752.4**	122	91.3			
NS Rht-A1b.11	**884.8**	46.1	107.3			
NS Rht-A1b.12	**881.7**	53.4	107.0			
NS Rht-A1b.14	832.7	37.1	101.0			
NS Rht-A1b.4	810.7	36.4	98.4			
NS Rht-A1b.5	812.8	25.5	98.6			
NS Rht-A1b.9	828	97.6	100.4			

The mean value is shown with its standard deviation (SD), along with the standard error of differences (SED) and 5% least significant difference of means (LSD 5%). Means shown in bold are significantly different from *Rht-1,* underlined means are significantly different from *Rht-A1b.* NS = null segregant of an *Rht-A1b.X* mutation.

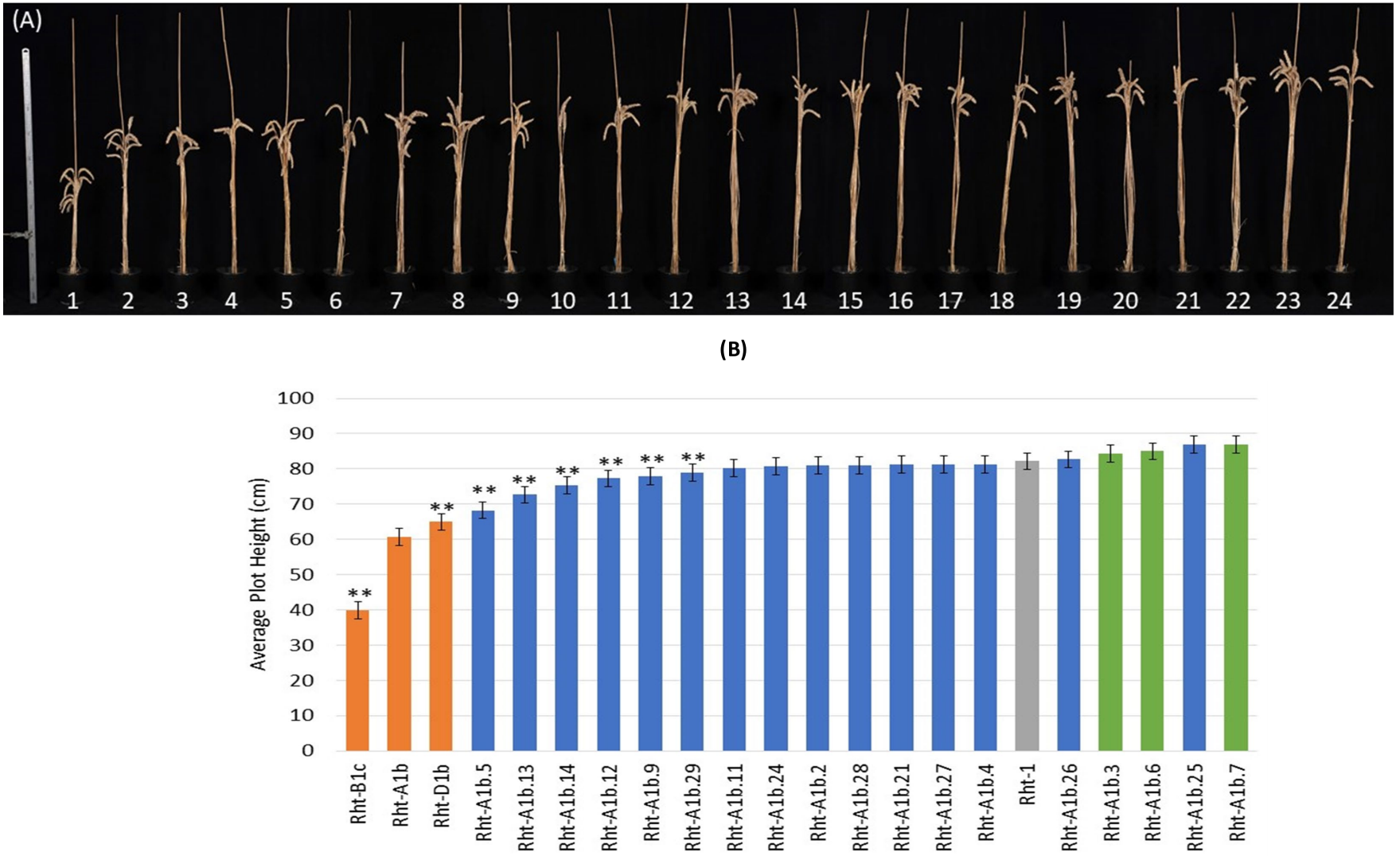

Figure 5.2: Height Characterisation of *Rht-A1b* Suppressors and Controls (A) Photograph of mature *Rht-A1b* intragenic missense mutants with *Rht-A1b, Rht-D1b* and *Rht-1* controls. 1= *Rht-A1b,* 2= *Rht-A1b.9,* 3= *Rht-D1b,* 4= *Rht-A1b.5,* 5= *Rht-A1b.13,* 6= *Rht-A1b.12,* 7= *Rht-A1b.29,* 8= *Rht-A1b.11,* 9= *Rht-A1b.14,* 10= *Rht-A1b.21,* 11= *Rht-A1b.28,* 12= *NS T493I,* 13= *NS G267D,* 14= *Rht-A1b.4,* 15= *ND Rht-A1b.14,* 16= *Rht-A1b.26,* 17= *Rht-A1b.24,* 18= *Rht-A1b.27,* 19= *NS Rht-A1b.12,* 20= *Rht-A1b.2,* 21= *NS Rht-A1b.11,* 22= *Rht-1,* 23= *Rht-A1b.25,* 24= *NS Rht-A1b.5.* **B) ANOVA output comparing total shoot length for each line.** NS = null segregants of *Rht-A1b* intragenic mutants. p<0.001, error bars = standard error of means (SED) (27.73) ** = measurement significantly different than *Rht-A1b* and *Rht-1* using 5% LSD 54.48. The average length of the different shoot segments: ear, peduncle, internode 2 (I2), internode 3 (I3) and internode 4 (I4), for each line are shown. All lines are in Cadenza (var.)

The ANOVA confirmed that there was a significant interaction between shoot length and genotype (P<0.001). The least significant difference of means (54.58) was used to determine which genotypes produced significantly different shoot heights. As seen in Chapter 3, *Rht-A1b, Rht-D1b* and *Rht-1* all produced significantly different shoot lengths, with *Rht-A1b* the shortest and *Rht-1* the tallest. All suppressor mutants and their null segregants produced shoots that were significantly longer than *Rht-A1b*. Some mutants: *Rht-A1b.13, -9, -14, 12* and *-5* produced desirable intermediate shoot lengths, longer than *Rht-A1b* and shorter than *Rht-1*. The shoots of these mutants were 85.3%, 85.3%, 89.6%, 89.2% and 88.7% the length of *Rht-1* respectively, compared to *Rht-A1b* which is 64.4% the length of *Rht-1* (Table 5.2). Four mutants produced shoots significantly longer than *Rht-1, Rht-A1b.3/7/25/6*, which were 108.6-115.3% the height of *Rht-1.* Three of these mutants *Rht-A1b.3/6/7* were the nonsense mutants, this height phenotype therefore confirms that intragenic nonsense mutations can result in a loss of function phenotype in *Rht-A1b.*

As predicted, all remaining mutants produced shoots that were not significantly different than *Rht-1* as they contained *Rht-A1a* (WT) instead of an *Rht-A1b* allele. All null segregants produced significantly longer shoots than their mutant counterparts with the except for *NS Rht-A1b.9.* This suggests that additional background mutations may also be affecting stem elongation in the *Rht-A1b.9 / NS Rht-A1b.9* lines.

To determine the genotypic effect on the length of different internode segments additional ANOVAs were conducted, described in Table 5.3 and Figure 5.3 .

Table 5.3 : ANOVA Output and for Individual Shoot Components in Rht-A1b Intragenic Mutants and Controls

	Internode 5	Internode 4		Internode 3		Internode 2		Peduncle		Ear	
	Mean (mm) ± SD	Mean (mm) ± SD	%	Mean (mm) ± SD	%	Mean (mm) ± SD	%	Mean (mm) ± SD	%	Mean (mm) ± SD	%
Rht-1	21 ± 11.5	77.9 ± 23.4	NA	120.1 ± 19.9	NA	174.1 ± 21.3	NA	348.6 ± 29.4	NA	104.9 ± 16	NA
Rht-A1b	0 ± 0	25 ± 22.7	32.1	49.8 ± 12.4	41.5	109.4 ± 15.7	62.8	260.6 ± 30.1	74.8	104.8 ± 9.9	99.9
Rht-D1b	0 ± 0	27.5 ± 8.5	35.3	77.8 ± 12.1	64.8	135.8 ± 10.3	78	299.8 ± 20.3	85	109.4 ± 5.6	104.3
Rht-A1b.2	22.5 ± 12	61± 25.4	78.3	117.7 ± 9.3	98	178.4 ± 12.7	102.5	**383.6 ± 35.5**	110	**115.8 ± 8.5**	110.4
Rht-A1b.3	0	73.8 ±21.3	94.7	128.1	105.7	**190.8 ± 26.5**	109.6	**385.7 ±32.1**	110.9	**115.7 ±6.4**	110.3
Rht-A1b.4	0 ± 0	59.3 ± 25.6	75.2	125.4 ± 15.1	104.4	187 ± 13.1	107.4	348.9 ± 35.3	100.1	109.6 ± 5.7	104.5
Rht-A1b.5	27 ± 4.9	42.6 ± 23.9	54.8	**94.1 ± 13.4**	78.4	**157.4 ± 17.9**	90.4	327.7 ± 34.1	94	107.3 ± 11.1	102.3
Rht-A1b.6	29.7 ±	**92.9 ±17.4**	119.2	**135.2 ± 19.9**	113.4	**199.2 ± 18.2**	114.4	**394.8 ± 35.4**	113.3	**117.7 ± 9.8**	112.2
Rht-A1b.7	29 ±	**97.6 ± 18.3**	125.2	**145.4 ± 22.3**	121.1	**191.9 ±19.4**	110.2	**372.7 ±33.2**	105.9	**112 ± 9.2**	105.8
Rht-A1b.9	0 ± 0	23.2 ± 7.6	29.8	**85.9 ± 22.9**	71.5	158.9 ± 28.1	91.3	337.8 ± 35.9	95.9	104.8 ± 12.4	99.9
Rht-A1b.11	15 ± 0	49.1 ± 23.7	63.1	**100 ± 18.9**	83.3	**155.9 ± 22.6**	89.5	352.7 ± 35.5	101.2	**115.3 ± 8.9**	110.9
Rht-A1b.12	14 ± 0	31.3 ± 20.3	40.3	**94.9 ± 9.6**	79	**155.7 ± 11.1**	89.4	345.2 ± 35.6	99	109.8 ± 5.9	104.7
Rht-A1b.13	0 ± 0	39.8 ± 23.4	51.2	**93.4 ± 21.1**	77.8	**148.9 ± 21.8**	85.5	**310.1 ± 41.4**	89	**115.3 ± 13.1**	109.9
Rht-A1b.14	0 ± 0	39.1 ± 17.2	50.2	**95.8 ± 14.9**	80.6	169.8 ± 9.6	97.5	328.6 ± 24.1	94.3	110.7 ± 4.8	105.5
Rht-A1b.21	24.5 ± 2.1	72.2 ± 17.1	92.8	115.4 ± 23.2	95.1	**194.3 ± 23.3**	111.6	339.4 ± 25.4	97.4	109.5 ± 5.4	104.4
Rht-A1b.24	35 ± 0	65.1 ± 27.9	84.9	121 ± 22.2	100.7	165.9 ± 28.9	95.9	372.3 ± 60.1	105.8	108 ± 7.9	103
Rht-A1b.25	35 ± 0	70.9 ± 31.2	91	132.9 ± 11.4	110.7	**195.4 ± 9.7**	112.2	**423.2 ± 48**	121.4	**119.7 ± 9.7**	114.1
Rht-A1b.26	28 ± 5.6	64 ± 23.1	82.1	124.7 ± 10.3	103.8	187.5 ± 11.1	107.7	**383.8 ± 33.6**	110.1	112.4 ± 4.9	107.1
Rht-A1b.27	27.6 ± 5.4	75.2 ± 31.1	95.6	129.6 ± 18.4	107.9	188 ± 12.4	108	345.3 ± 53.1	99.1	112.9 ± 12.5	107.6
Rht-A1b.28	0 ± 0	63.1 ± 24.2	81	115.4 ± 19.1	95.1	168.3 ± 11.5	95.7	334.4 ± 25.6	95.9	100 ± 12.1	95.3
Rht-A1b.29	0 ± 0	63.4 ± 29.6	81.4	**105.1 ±22.9**	87.5	174.4 ± 15.6	100.2	359.8 ± 40.4	103.2	**117.9 ± 12.5**	112.4
NS Rht-A1b.11	0 ± 0	79.8 ± 25.3	102.5	130.9 ± 15.6	109	181.4 ± 21.7	104.2	**383.5 ± 28.3**	110	109.2 ± 7.8	104.1
NS Rht-A1b.12	0 ± 0	63.5 ± 20.3	81.5	120.9 ± 15.6	100.7	**200.2 ± 13.2**	115	**388.4 ± 27.5**	111.4	108.8 ± 8	103.7
NS Rht-A1b.14	0 ± 0	49 ± 20.7	62.9	111 ± 13.4	92.4	173.6 ± 9.1	99.7	**394.6 ± 32.1**	113.2	108.7 ± 8.3	103.6
NS Rht-A1b.4	0 ± 0	62.6 ± 21.6	80.4	123.8 ± 17.6	103.1	185.1 ± 9.3	105.3	352.3 ± 30.5	101.1	92.1 ± 8.1	87.8
NS Rht-A1b.5	0 ± 0	55.8 ± 18.2	72.9	118.6 ± 9	98.8	168.3 ± 8.1	95.7	369.1 ± 24.7	105.9	100.1 ± 7.9	95.4
NS Rht-A1b.9	26 ± 1.4	55.2 ± 30.8	70.9	113.7 ± 30.6	94.7	**191.5 ± 24.1**	110	350.7 ± 48.8	100.6	112.6 ± 10.6	107.3
P-Value	0.9	<0.001		<0.001		<0.001		<0.001		<0.001	
SED	NA	17.4		7.9		7.7		15.9		4.4	
5% LSD	NA	34.3		15.6		15.2		33.2		8.7	

The mean value is shown with its standard deviation (SD), along with the standard error of differences (SED) and 5% least significant difference of means (LSD 5%). Means shown in bold are significantly different from *Rht-1,* underlined means are significantly different from *Rht-A1b.* NS = null segregant of an *Rht-A1b.X* mutation. % = % length compared to *Rht-1*

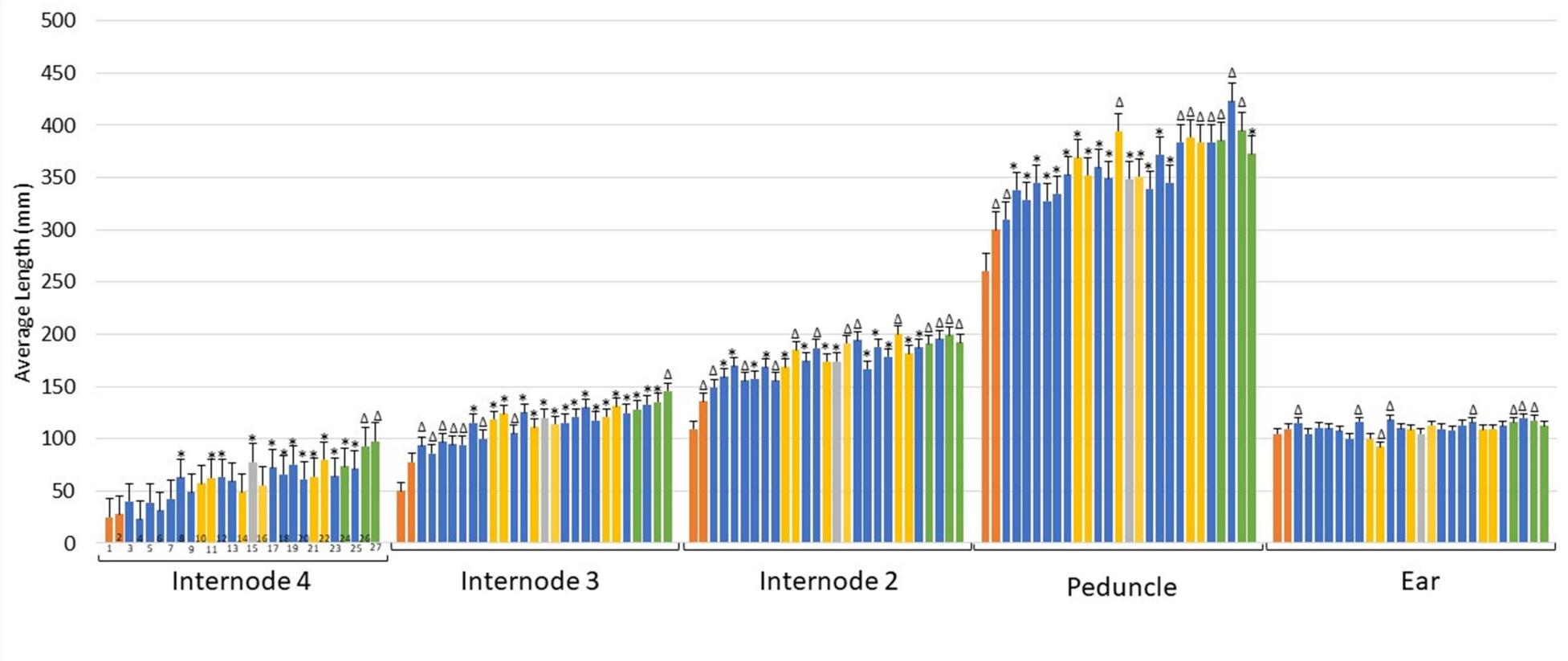

Figure 5.3 : ANOVA outputs for different shoot segment lengths for in Rht-A1b Intragenic Mutants and Controls. Grey = *Rht-1,* orange = *Rht-A1b*, blue = *Rht-A1b* intragenic nonsense mutants, blue = *Rht-A1b* intragenic missense mutants, yellow = null segregants of *Rht-A1b* intragenic mutants Left to Right: *Rht-A1b, Rht-D1b, Rht-A1b.13, Rht-A1b.9, Rht-A1b.14, Rht-A1b.12, Rht-A1b.5, Rht-A1b.28, Rht-A1b.11, NS Rht-A1b. 5, Rht-A1b.4, Rht-A1b.29, Rht-A1b.4, Rht-A1b, NS Rht-A1b.14, Rht-1, NS Rht-A1b.9, Rht-A1b.21, Rht-A1b.24, Rht-A1b.27, Rht-A1b.2, NS Rht-A1b.12, NS Rht-A1b.11, Rht-A1b.26, Rht-A1b.3, Rht-A1b.25, Rht-A1b.6* and *Rht-A1b.7.* **Internode 4** = P<0.001, error bar = standard error of differences (SED) 17.4, 5% least significant difference (5% LSD) 34.3. **Internode 3** = P<0.001, error bar = SED 7.9, 5% LSD 15.5. **Internode 2** = P<0.001, error bar = SED 7.7, 5% LSD 15.2. **Peduncle** = P<0.001, error bar = SED 15.9, 5% LSD 33.2. **Ear** = P<0.001, error bar = SED 4.4, 5% LSD 8.7. * denotes a mean significantly different from *Rht-A1b.* Δ denotes a mean significantly different from *Rht-A1b* and *Rht-1.* Significant differences were calculated with the 5% LSD value.

The ANOVAs confirmed that there was no significant difference between internode 5 lengths across the genotypes (P=0.9), whilst there was a significant interaction between segment length and genotype for internode 4/3/2, peduncle and ear (P<0.001). The non-significant result for internode 5, appears to be because only 8 of the 24 lines that were characterised produced a fifth stem internode. An additional ANOVA was run on just these 8 lines, which returned a p-value of 0.087. This most likely because only 1-7 out of the 15 shoots measured per line had a fifth internode. Overall this suggests that the occurrence of the fifth internode was not influenced by the genotype and that differences in height were due to different elongation of the 4 uppermost shoots.

The internode segments showed a similar trend as was previously observed for the *Rht-1* mutants in Section 3.2.2 four uppermost internodes where approximately proportional to final plant height (Figure 5.3). Ear length appeared to be independent of plant height (Figure 5.3), with no significant difference (LSD 4.4) between *Rht-A1b, Rht-D1b* and *Rht-1* and most of the suppressor mutants. Eight suppressor mutants produced ear lengths that were significantly longer than *Rht-A1b* and *Rht-1 (Rht-A1b.2/11/13/24/29/3/6/7*). These were 109.9-114.1% the length of *Rht-1* ears.

5.2.3 Flag Leaf Dimensions

GA insensitivity in the *Rht-1* dwarf and semi-dwarf mutants (e.g. *Rht-B1c* or *Rht-D1b*) causes reduced leaf size (Tonkinson et al. 1995), due to reduced cell wall extensibility and elongation (Tonkinson et al. 1995; Keyes, Paolillo, and Sorrells 1989). In the *Rht-B1c* suppressor mutants, taller plants were shown to have shorter, narrower leaves, with the opposite being the case for shorter plants. The consequence of this was that shorter plants tended to have a larger leaf areas (Derkx et al. 2017). To determine whether intragenic mutations in *Rht-A1b* influence flag leaf size, measurements of width and length were recorded for three flag leaves per plant. Leaf length and width measurements were taken and used to calculate an approximate leaf area (Section 2.3.4). Residual plots for this data were assessed in GenStat, which confirmed that the data was Normal and did not require

transformation. A General Analysis of Variance (ANOVA) was conducted on each data set, the output of which is described in Table 5.4 and Figure 5.4 .

Table 5.4 : ANOVA Outputs For Flag Leaf Dimensions (mm) in Rht-A1b Suppressor mutants and Controls

Line	Length (mm)		Width (mm)		Area (mm^2)	
	Average	SD	Average	SD	Average	SD
Rht-1	250	±69.4	17.4	±5.7	3686	±1654
Rht-A1b	**333.3**	±88.2	18.9	±1.7	**5272**	±1504
Rht-D1b	**327.6**	±89.3	17.7	±2.7	**4917**	±1501
Rht-A1b.2	263.8	±35.5	17.9	±1.5	**5684**	±881
Rht-A1b.3	**364.1**	±75.5	18.2	±2.3	**5077**	±1599
Rht-A1b.4	**300.6**	±65.4	**14.8**	±2.8	3763	±1291
Rht-A1b.5	253.5	±60.9	**15.1**	±2.9	3447	±1287
Rht-A1b.6	**335.7**	±55.9	18.8	±1.8	**5292**	±1124
Rht-A1b.7	**375.4**	±48	17.3	±2.1	**5464**	±1174
Rht-A1b.9	230.3	±75.3	**15.4**	±2.7	3247	±1558
Rht-A1b.11	**391.9**	±52.1	19.1	±1.5	**6238**	±968
Rht-A1b.12	263.8	±92.4	**15.3**	±2.2	3714	±1735
Rht-A1b.13	**364.1**	±37.8	17.1	±1.9	**5250**	±1090
Rht-A1b.14	**349.4**	±42.4	18.27	±2.1	**5341**	±983
Rht-A1b.21	254.8	±63.6	17.93	±2	3833	±1141
Rht-A1b.24	**380.1**	±42.7	**19.2**	±1.4	**6102**	±874
Rht-A1b.25	**378.6**	±59.1	18.67	±1.6	**5917**	±1136
Rht-A1b.26	**369.5**	±42.2	**15.3**	±2.7	**5074**	±1224
Rht-A1b.27	**345.5**	±84.9	**15.1**	±3.1	4472	±1818
Rht-A1b.28	221.8	±75.5	**15.1**	±21	3054	±1436
Rht-A1b.29	279.4	±85.2	**15.5**	±2.4	3673	±1432
NS Rht-1b.11	**337.7**	±35.1	18.2	±1.7	**5146**	±817
NS Rht-1b.12	282.6	±69.4	19.07	±1.2	4473	±1048
NS Rht-1b.14	**334.5**	±48.7	17.67	±2.3	**4969**	±1151
NS Rht-A1b.4	**349.9**	±81.7	**14.9**	±2.9	4351	±1400
NS Rht-A1b.5	**340.8**	±113	18.07	±2.3	**5287**	±2048
NS Rht-A1b.9	247.3	±79.4	**15.6**	±1.8	3394	±1015
P-Value	<0.001		<0.001		<0.001	
SED	24.7		0.9		485	
5% LSD	48.5		1.8		953	

The mean value is shown with its standard deviation (SD), along with the standard error of differences (SED) and 5% least significant difference of means (LSD 5%). Means shown in bold are significantly different from *Rht-1,* underlined means are significantly different from *Rht-A1b.* NS = null segregant of an *Rht-A1b.X* mutation.

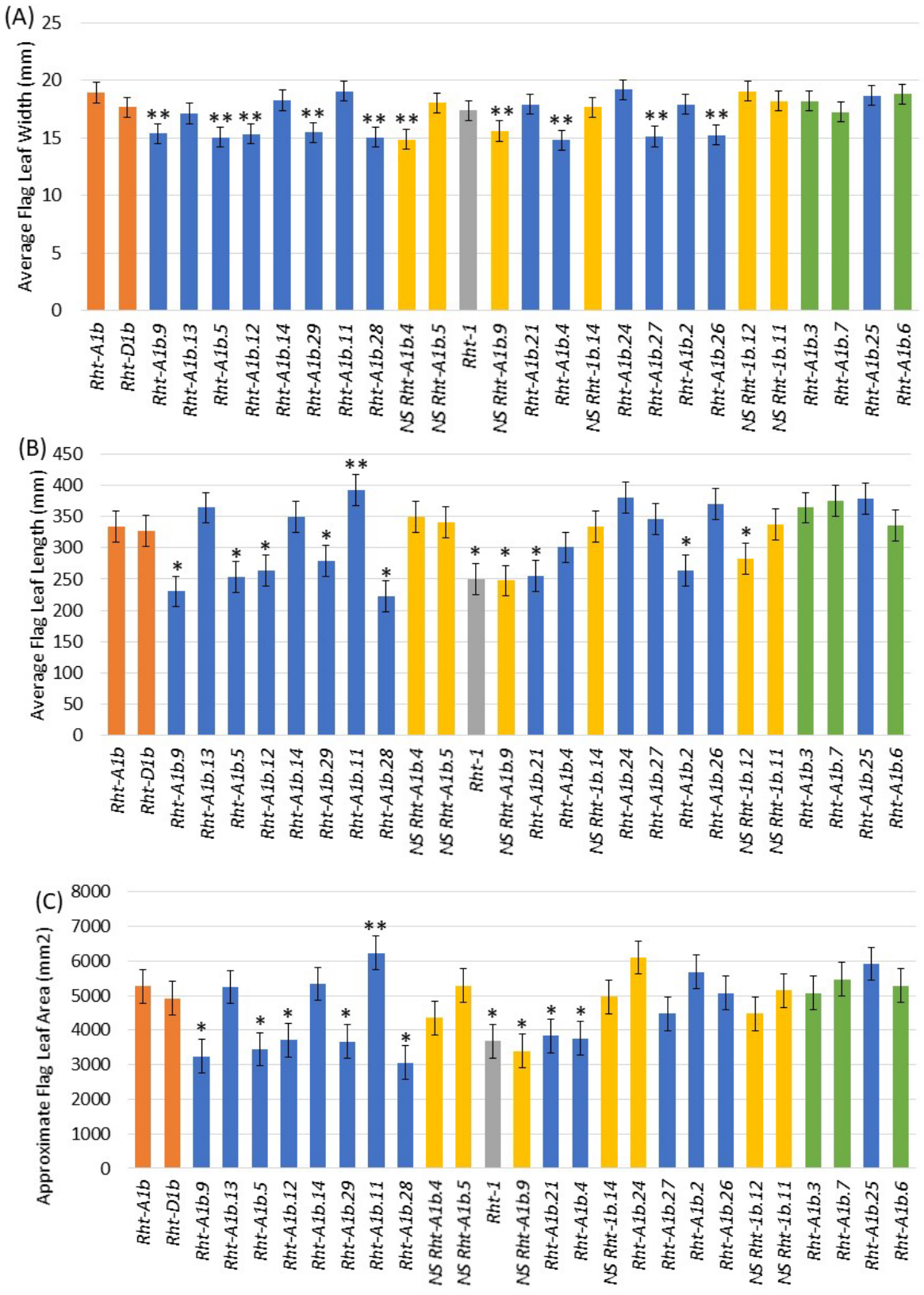

Figure 5.4 : Average Flag Leaf Dimensions (mm) in Rht-A1b Intragenic Mutants and Controls. Grey = *Rht-1,* orange = *Rht-A1b*, blue = *Rht-A1b* intragenic nonsense mutants, blue = *Rht-A1b* intragenic missense mutants, yellow = null segregants of *Rht-A1b* intragenic mutants. Lines are arranged in height order (smallest to largest). * = measurement significantly different that *Rht-A1b.* ** = measurement significantly different from *Rht-A1b* and *Rht-1*. **(A) Average Flag Leaf Width (mm).** ANOVA P-value = <0.001. Error bars = standard error of means (0.9). **(B) Average Flag Leaf Length (mm)** ANOVA P-value = <0.001. Error bars = standard error of means (24.7). **(C) Average Flag Leaf Area (mm^2).** ANOVA P-value = <0.001. Error bars = standard error of means (495).

The ANOVAs confirmed that there was a significant interaction between genotype and flag leaf: width, length and area (P<0.001) (Table 5.4).

The 5% LSD (1.8) was used to establish which genotypes were significantly different. This established that there was no significant difference between *Rht-A1b* (18.9mm)*, Rht-D1b* (17.7mm) and *Rht-1* (17.4mm)*.* Seven missense mutants (*Rht-A1b.13/14/11/21/24/2/25)* and the three nonsense mutants (*Rht-A1b.3/6/7*) were not significantly different from *Rht-A1b*. The remaining missense mutants (*Rht-A1b.9/5/12/29/28/4 27/26)* were all significantly narrower than *Rht-A1b* and *Rht-1* (14.9-15.3mm). There was variation in the null segregant measurements, two lines *NS Rht-A1b.4/9* produced significantly narrower leaves than *Rht-A1b* and *Rht-1* (14.9-15.6mm), whilst the rest were not significantly different from *Rht-A1b*. Two null segregants; *NS A1b.5* and *NS A1b.12* produced significantly wider leaves (18.07-19.07mm) than their mutant counterparts (15.07-15.3mm). The remaining null segregants were not significantly different from their mutant counterparts.

The 5% LSD (24.7), determined that there was no significant difference between *Rht-A1b* (333.3mm) and *Rht-D1b* (327.6mm) lengths*,* whilst *Rht-1* produced significantly shorter leaves (250mm). Two null segregants (*NS Rht-A1b.9/12)* and seven missense mutants (*Rht-A1b.9/5/12/29/28/21/2*) produced shorter leaves than *Rht-A1b* (221.8-282.6mm). One missense mutant, *Rht-A1b.11* produced significantly larger leaves (392.1mm). There was no significant difference between the flag leaf lengths of the remaining between *Rht-A1b* and the other lines. Three null segregants (*NS Rht-A1b.9/14/*12) were not significantly different than their mutant counterparts and the remaining nulls were significantly longer.

The approximate leaf area (mm^2) data showed a similar trend to the flag length results, suggesting that flag leaf length was the greatest factor in determining flag leaf area (Figure 5.4). Using the 5% LSD (953) *Rht-1* (3686mm^2) was confirmed to have smaller leaves than *Rht-A1b* and *Rht-D1b* (5272 and 4917 mm^2)*,* which were not significantly different from each other. *NS Rht-A1b.9* and seven missense mutants (*Rht-A1b.9/12/14/29/28/21/4*) produced significantly smaller leaves than

Rht-A1b (3054-3833mm^2). *Rht-A1b.11* produced the largest leaves (6238mm^2). There was no significant difference between the remaining lines and *Rht-A1b*. *NS Rht-A1b.11* produced leaves that were significantly smaller (5146mm^2) than *Rht-A1b.11* (6238mm^2), whilst *NS Rht-A1b.5* leaves were significantly larger (5287mm^2) than *Rht-A1b.5* (3447mm^2). The remaining null segregants were not significantly different from their mutant counterparts.

In Figure 5.4 , genotypes were arranged in height order (smallest to tallest, left to right) (Section 5.2.2), to establish whether the flag leaf trends identified in the *Rht-B1c* screen (larger plants produced longer, narrower leaves, whilst shorter plants produced shorter wider leaves) (Derkx et al. 2017) was apparent here. The figures suggest that there isn't a consistent pattern governing flag leaf width, length or area in *Rht-A1b* suppressor mutants. As the null segregants produced varied leaf characteristics this suggests that there may be some background mutations affecting leaf growth.

5.2.4 Shooting

In rice, it has been demonstrated that shooting increases in GA-deficient or GA-signalling mutants such as the gain-of-function DELLA mutant, *slr1-d1* (Liao et al. 2019). Although *Rht-A1b* is a gain-of-function DELLA mutant, it doesn't appear to influence shooting in a Cadenza (var.) background (Section 3.2.3). To determine whether missense mutations alter shooting in a Cadenza background, the number of shoots per plant were counted. Residual plots for this data were assessed in GenStat, which confirmed that the data was Normal and did not require transformation. A General Analysis of Variance (ANOVA) was conducted on each data set, the output of which is described in Table 5.5 and Figure 5.5.

Table 5.5 : ANOVA Output for Shoot no. per Plant in Rht-A1b Intragenic Mutants and Controls

Line	Shoot No.	SD	% Difference from *Rht-1*	P-Value	SED	5% LSD
Rht-1	12.8	4.3	NA			
Rht-A1b	12.0	1.2	94.1			
Rht-D1b	10.8	3.3	84.3			
Rht-A1b.2	11.5	1.3	90.2			
Rht-A1b.3	**9.75**	1.2	76.4			
Rht-A1b.4	**9.8**	1.5	75.5			
Rht-A1b.5	11.5	1.6	90.2			
Rht-A1b.6	**8.7**	1.4	63.0			
Rht-A1b.7	11.25	1.6	76.9			
Rht-A1b.9	12.5	1.7	98.0			
Rht-A1b.11	**9.5**	3.0	74.5			
Rht-A1b.12	10.3	2.1	80.4			
Rht-A1b.13	**8.7**	1.5	68.0			
Rht-A1b.14	**7.0**	2.5	54.9	<0.001	1.4	2.8
Rht-A1b.21	**8.3**	3.3	64.7			
Rht-A1b.24	**7.3**	1.2	57.6			
Rht-A1b.25	11.0	1.4	85.3			
Rht-A1b.26	**7.5**	1.9	58.8			
Rht-A1b.27	**7.5**	2.4	58.8			
Rht-A1b.28	**9.8**	1.9	75.5			
Rht-A1b.29	10.8	0.9	84.3			
NS Rht-A1b.11	10.8	2.2	84.3			
NS Rht-A1b.12	**8.3**	1.9	64.7			
NS Rht-A1b.14	10.8	9.0	84.3			
NS Rht-A1b.4	11.0	2.5	85.3			
NS Rht-A1b.5	**5.0**	2.0	47.1			
NS Rht-A1b.9	**9.0**	2.1	70.6			

The mean value is shown with its standard deviation (SD), along with the standard error of differences (SED) and 5% least significant difference of means (LSD 5%). Means in bold are significantly different from *Rht-1,* underlined means are significantly different from *Rht-A1b.* NS = null segregant of an *Rht-A1b.X* mutation.

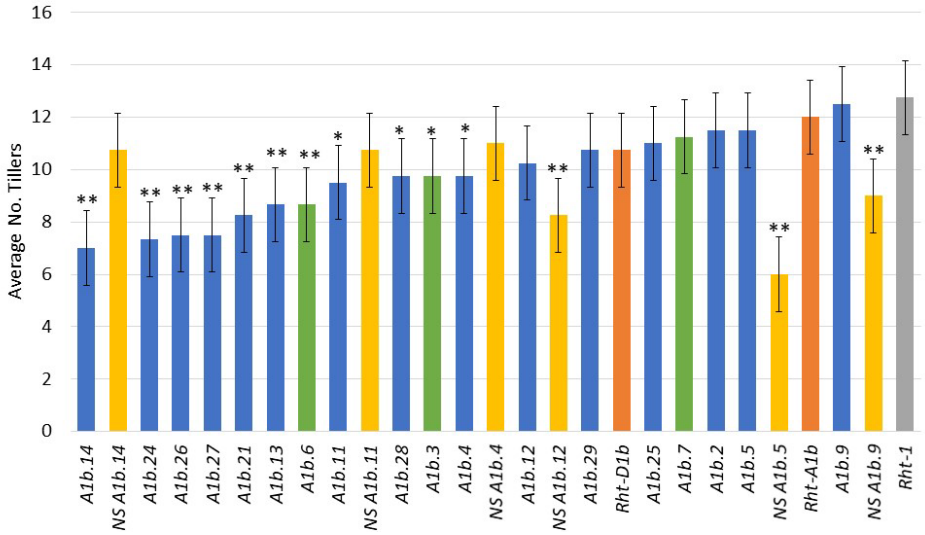

Figure 5.5 : Average No. Shoots Per Plant in Rht-A1b Intragenic Mutants and Controls. Grey = *Rht-1,* orange = *Rht-A1b* and *Rht-D1b*, green= intragenic nonsense mutants, blue = *Rht-A1b* intragenic missense mutants, yellow = null segregants (NS) of *Rht-A1b* intragenic mutants. Lines are ordered from fewest to most shoots, with exception to the null segregants, which are to the right of their mutant counterpart. ANOVA P-value = <0.001. Error bars = standard error of means (1.4). * = mean significantly different from *Rht-A1b,* ** = mean significantly different from *Rht-A1b* and *Rht-1*.

The ANOVA confirmed that there was a significant interaction between genotype and the number of shoots per plant (P<0.001). The 5% least significant difference value (2.8) was used to determine which lines produced significantly different shoot numbers from each other. There was no significant difference between *Rht-A1b, Rht-D1b* and *Rht-1*. Suppressor mutants that were significantly different than *Rht-A1b* had significantly fewer shoots (7-9.8 shoots, compared to 12, lines marked with a * or ** in Figure 5.6). This represented 57.6-75.5% the number of shoots produced by *Rht-1*. *Rht-A1b* produced 94.1% for comparison.

There was no significant difference between the number of shoots in *NS Rht-A1b.11/4/* and their mutant counterparts, whilst *NS Rht-A1b.14* produced significantly more shoots and *NS Rht-A1b.5/9* significantly fewer shoots than their mutant counterparts. This variation in null segregant phenotype suggests that there are background EMS-induced mutations that are affecting shooting.

5.2.5 Spikelet Number

There is evidence that the barley DELLA dwarf *sln1-d* produces fewer spikelets per ear (Serrano-Mislata et al. 2017). Intragenic *sln1-d* mutations in the DELLA C-

terminal GRAS domain, *sln1-d.5* and *sln1-d.6* (Chandler and Harding 2013), have also been shown to uncouple inflorescence growth from plant height, resulting in increased spikelet number per ear compared to *sln1-d* (Serrano-Mislata et al. 2017). Although *Rht-A1b* wasn't found to effect spikelet number compared to WT *Rht-1* (Section 3.2.4), to determine whether the *Rht-A1b* suppressor mutants effect spikelet number, as seen in *sln1-d.5* and *sln1-d.6*, the number of spikelets for three ears per plant were counted (described in Section 2.3.2). To determine the effect genotype has on spikelet number a ANOVA was conducted, described in Table 5.6 and Figure 5.6.

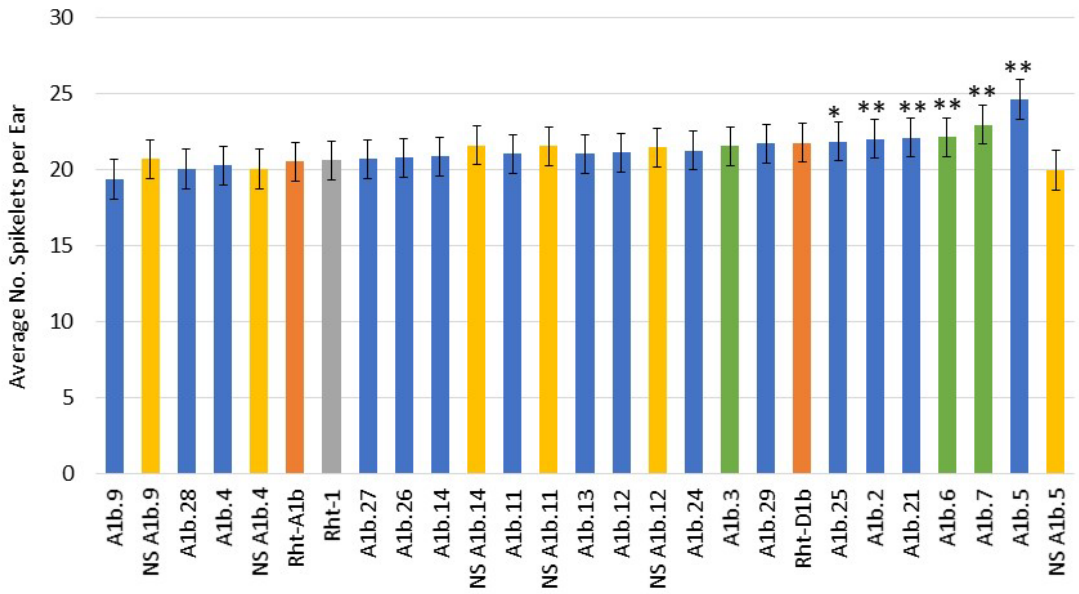

Figure 5.6: Average No. Spikelets Per Ear in Rht-A1b Intragenic Mutants and Controls. Grey = *Rht-1,* orange = *Rht-A1b* and *Rht-D1b*, green= intragenic nonsense mutants, blue = *Rht-A1b* intragenic missense mutants, yellow = null segregants (NS) of *Rht-A1b* intragenic mutants. Lines are ordered smallest to largest, with exception to the null segregants, which are to the right of their mutant counterpart. ANOVA P-value = <0.001. Error bars = standard error of means (0.7). * = mean significantly different from *Rht-A1b,* ** = mean significantly different from *Rht-A1b* and *Rht-1*.

Table 5.6: ANOVA Output for Spikelet No. per Ear in Rht-A1b Intragenic Mutants and Controls

Line	Spikelet No.	SD	% Difference from *Rht-1*	P-Value	SED	5% LSD
Rht-1	20.6	±2.3	NA			
Rht-A1b	20.5	±1.8	99.6			
Rht-D1b	21.8	±1.3	105.7			
Rht-A1b.2	**22.0**	±1.6	105.9			
Rht-A1b.3	**21.5**	2.1	104.4			
Rht-A1b.4	20.3	±0.9	98.4			
Rht-A1b.5	**22.1**	±1.2	107.4			
Rht-A1b.6	**22.1**	1.3	107.7			
Rht-A1b.7	20.5	1.3	99.5			
Rht-A1b.9	19.3	±2.1	93.9			
Rht-A1b.11	21.0	±1.2	102.0			
Rht-A1b.12	21.1	±1.8	102.4			
Rht-A1b.13	21.0	±1.7	102.0			
Rht-A1b.14	20.8	±1.2	101.2	<0.001	0.7	1.3
Rht-A1b.21	**22.1**	±0.9	107.3			
Rht-A1b.24	21.2	±1.6	103.1			
Rht-A1b.25	21.8	±1.5	105.1			
Rht-A1b.26	20.8	±1.4	100.8			
Rht-A1b.27	20.7	±1.6	100.4			
Rht-A1b.28	20.0	±2.7	97.2			
Rht-A1b.29	21.7	±1.6	105.3			
NS Rht-A1b.11	21.5	±1.1	104.5			
NS Rht-A1b.12	21.4	±2.1	104.1			
NS Rht-A1b.14	21.6	±1.4	104.9			
NS Rht-A1b.4	20.0	±1.1	97.2			
NS Rht-A1b.5	19.9	±1.2	95.8			
NS Rht-A1b.9	20.7	±2.9	100.4			

The mean value is shown with its standard deviation (SD), along with the standard error of differences (SED) and 5% least significant difference of means (LSD 5%). Means shown in bold are significantly different from *Rht-1,* underlined means are significantly different from *Rht-A1b.* NS = null segregant of an *Rht-A1b.X* mutation.

The ANOVA confirmed that there was a significant interaction between genotype and the number of spikelets per ear (P<0.001). The 5% least significant difference value (1.3) was used to determine which lines produced significantly different spikelet numbers from each other. Most suppressor mutants, *Rht-1* and *Rht-D1b* were not significantly different from *Rht-A1b*. One mutant *Rht-A1b.25* produced significantly more spikelets than *Rht-A1b,* representing 105.1% of the number of

spikelets produced by *Rht-1.* Five mutants, *Rht-A1b.2/21/6/7/5* produced significantly more spikelets than *Rht-A1b* and *Rht-1*, representing 105.9-107.4 % of the number of spikelets produced by *Rht-1*.

There was no significant difference between the number of spikelets in *NS Rht-A1b.4/14/12* and their mutant counterparts, whilst *NS Rht-A1b.9* produced significantly more spikelets and *NS Rht-A1b.5* significantly fewer spikelets than their mutant counterparts.

5.2.6 Grain Number Per Ear

In Chapter 3, the grain number per ear for *Rht-A1b* was proportional to the severity of GA insensitivity, with *Rht-A1b* producing significantly fewer grains per ear than *Rht-1* or *Rht-D1b* (Section 3.2.5). To establish whether *Rht-A1b* suppressor mutations can alter grain number per ear, the total number of grain per plant was counted and then divided by the number of shoots on that plant. Residual plots for this data were assessed in GenStat, which confirmed that the data was Normal and did not require transformation. A General Analysis of Variance (ANOVA) was conducted on each data set, the output of which is described in Table 5.7 and Figure 5.7.

Table 5.7: ANOVA Output for Grain No. per Ear in Rht-A1b Intragenic Mutants and Controls

Line	Grain No. Per Ear	SD	% Difference from *Rht-1*	P-Value	SED	5% LSD
Rht-1	54.6	13	NA	<0.001	8.1	15.1
Rht-A1b	32.8	9.3	60.1			
Rht-D1b	40.1	9.1	73.4			
Rht-A1b.2	48.9	10.9	89.6			
Rht- A1b.3	**70.2**	22.2	128.6			
Rht-A1b.4	55.9	5.1	102.4			
Rht-A1b.5	48.8	12.1	89.4			
Rht- A1b.6	60.6	8.1	111.0			
Rht- A1b.7	63	9.3	115.4			
Rht-A1b.9	47.7	7.3	87.4			
Rht-A1b.11	47.9	10.3	87.7			
Rht-A1b.12	50.5	12.4	92.5			
Rht-A1b.13	48.9	11.9	89.6			
Rht-A1b.14	**75.2**	28.2	137.7			
Rht-A1b.21	61.5	5.5	112.6			
Rht-A1b.24	54.9	13.3	100.5			
Rht-A1b.25	51.7	22	94.7			
Rht-A1b.26	57.7	5.2	105.7			
Rht-A1b.27	67.9	21.9	124.4			
Rht-A1b.28	49.7	9.1	91.0			
Rht-A1b.29	60.7	7	111.2			
NS Rht-A1b.11	**77.2**	2.4	141.4			
NS Rht-A1b.12	58	14.1	105.2			
NS Rht-A1b.14	61.4	8.8	112.5			
NS Rht-A1b.4	44.9	8.4	82.2			
NS Rht-A1b.5	55.5	8.5	103.5			
NS Rht-A1b.9	57.4	15.1	105.1			

The mean value is shown with its standard deviation (SD), along with the standard error of differences (SED) and 5% least significant difference of means (LSD 5%). Means shown in bold are significantly different from *Rht-1*, underlined means are significantly different from *Rht-A1b*. NS = pull segregant of

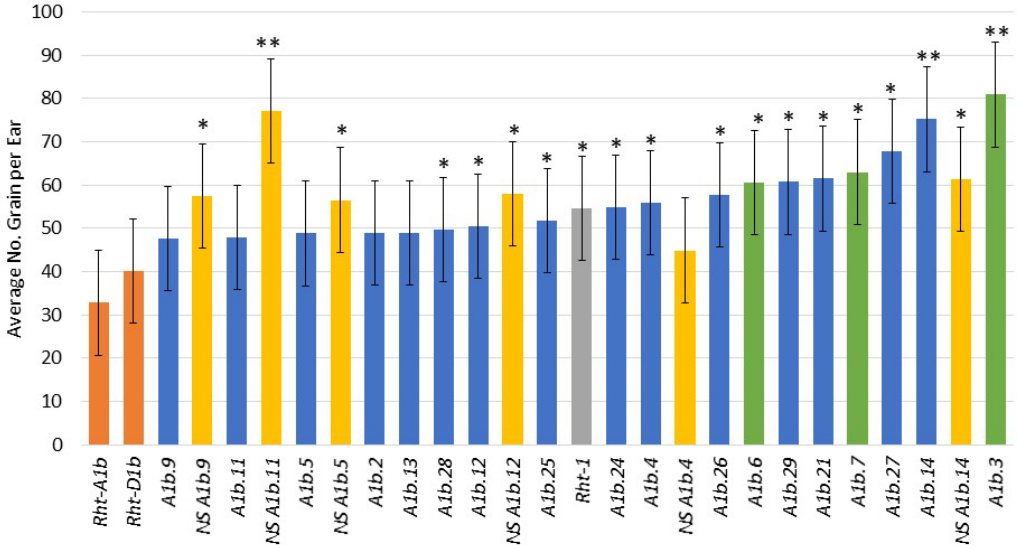

Figure 5.7: Average No. Grain Per Ear in Rht-A1b Intragenic Mutants and Controls. Grey = *Rht-1,* orange = *Rht-A1b* and *Rht-D1b*, green= intragenic nonsense mutants, blue = *Rht-A1b* intragenic missense mutants, yellow = null segregants (NS) of *Rht-A1b* intragenic mutants. Lines are ordered smallest to largest, with exception to the null segregants, which are to the right of their mutant counterpart. ANOVA P-value = <0.001. Error bars = standard error of means (8.1). * = mean significantly different from *Rht-A1b,* ** = mean significantly different from *Rht-A1b* and *Rht-1*.

The ANOVA confirmed that there was a statistically significant interaction between genotype and the number of grain per ear (P=<0.001). The 5% least significant difference value (8.1) was used to determine which lines produced significantly different grain numbers per ear from each other. There was no significant difference between *Rht-A1b* and *Rht-D1b,* whilst *Rht-1* produced significantly more grain per ear than either line. There was a significant increase in grain number (49.7-67.9 grains per ear) in most missense mutants, (marked with a * or ** in Figure 5.7), compared to *Rht-A1b* (32.8 grains per ear). This was the equivalent of 87.7%-124.4% of *Rht-1* grains per ear. Two mutants *Rht-A1b.14/3,* produced significantly more grains per ear than *Rht-A1b* and *Rht-1*. This was the equivalent of 128.6-137.7% of *Rht-1* grains.

There was no significant difference between the number of grains per ear between the null segregants and their mutant counterparts, except for *NS Rht-A1b.11* which produced significantly more grain (77.2 compared to 47.9) than *Rht-A1b.11*. The

variation in the number of grains per ear between the NS lines suggest background mutations may be affecting phenotype, as they lack the *Rht-A1b* alleles and would be expected to produce a phenotype similar to *Rht-1*.

5.2.7 Grain Size

Increased grain number in *Rht-1* dwarfing alleles is often associated with reduced grain size in wheat, potentially due to increased inter-floret competition for assimilates and space (Gooding, Addisu, et al. 2012; Flintham et al. 1997). In Section 3.2.6, *Rht-A1b* was found to produce the smallest grains compared to *Rht-B1c, Rht-D1b* and *Rht-1*, despite producing significantly fewer grains than *Rht-D1b* and *Rht-1*. This is not a desirable crop trait, therefore it was important to determine whether missense mutants produce larger grains, as well as a greater number of grains (Section 5.2.6) which would be desirable for breeding programs. Grain size measurements were conducted on ~200 seeds per genotype, using a Marvin grain analyser (INDOSAW, India). Residual plots for this data were assessed in GenStat, which confirmed that the data was Normal and did not require transformation. A General Analysis of Variance (ANOVA) was conducted on each data set, the output of which is described in Table 5.8 and Figure 5.8.

Table 5.8: ANOVA Output for Grain Size (mm^2) in Rht-A1b Intragenic Mutants and Controls

Line	Grain Size (mm^2)	SD	% Difference from *Rht-1*	P-Value	SED	5% LSD
Rht-1	19.5	2.7	NA			
Rht-A1b	**18.6**	2.7	95.7			
Rht-D1b	**17.9**	2.4	92.0			
Rht-A1b.2	**18.9**	2.6	97.0			
Rht- A1b.3	**20.1**	2.9	103.1			
Rht-A1b.4	**19.0**	3.3	97.7			
Rht-A1b.5	**15.9**	2.7	85.7			
Rht- A1b.6	**19.5**	3	99.8			
Rht- A1b.7	**19.6**	2.7	100.6			
Rht-A1b.9	**18.2**	3.3	93.2			
Rht-A1b.11	**20.1**	2.9	103.0			
Rht-A1b.12	**17.5**	2.4	89.7			
Rht-A1b.13	**20.9**	2.9	107.2			
Rht-A1b.14	**18.7**	2.8	95.0	<0.001	0.2	0.3
Rht-A1b.21	**20.4**	3.2	104.6			
Rht-A1b.24	**20.4**	2.9	104.8			
Rht-A1b.25	**20.3**	2.7	104.0			
Rht-A1b.26	**18.8**	2.7	95.4			
Rht-A1b.27	**19.9**	2.7	102.0			
Rht-A1b.28	**19.0**	2.6	97.3			
Rht-A1b.29	19.5	3	100.3			
NS Rht-A1b.11	**20.0**	2.8	102.8			
NS Rht-A1b.12	19.6	2	100.5			
NS Rht-A1b.14	**18.7**	3	95.8			
NS Rht-A1b.4	**18.8**	3.2	95.3			
NS Rht-A1b.5	**20.1**	2.7	103.3			
NS Rht-A1b.9	**20.3**	3	104.3			

The mean value is shown with its standard deviation (SD), along with the standard error of differences (SED) and 5% least significant difference of means (LSD 5%). Means shown in bold are significantly different from *Rht-1,* underlined means are significantly different from *Rht-A1b.* NS = null segregant of an *Rht-A1b.X* mutation.

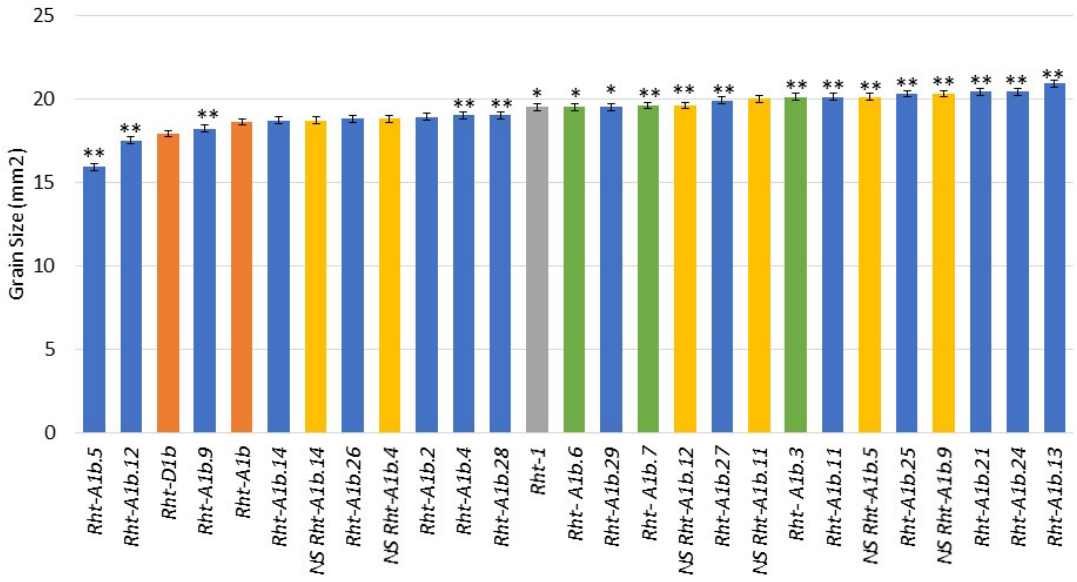

Figure 5.8 : Average Grain Size in Rht-A1b Intragenic Mutants and Controls. Grey = *Rht-1,* orange = *Rht-A1b* and *Rht-D1b*, green= intragenic nonsense mutants, blue = *Rht-A1b* intragenic missense mutants, yellow = null segregants (NS) of *Rht-A1b* intragenic mutants. Lines are ordered smallest to largest, with exception to the null segregants, which are to the right of their mutant counterpart. ANOVA P-value = <0.001. Error bars = standard error of means (0.2). * = mean significantly different from *Rht-A1b,* ** = mean significantly different from *Rht-A1b* and *Rht-1*.

The ANOVA confirmed that there was a statistically significant interaction between genotype and the number of grain per ear (P=<0.001). The 5% least significant difference value (0.3) was used to determine which lines produced significantly different spikelet numbers from each other. Three suppressor mutants *Rht-A1b.5/12/9* (15.9-18.2mm^2) and *Rht-D1b* (17.9mm^2) produced significantly smaller grain than *Rht-A1b* (18.6mm^2) and *Rht-1* (19.5mm^2). There was no significant difference between *Rht-A1b* and *Rht-A1b.14/25.2*. Two mutants, *Rht-A1b.28/4* produced grain that was significantly larger than *Rht-A1b* and smaller than *Rht-1*, equivalent to 97.3% and 97.7% area of *Rht-1* grain. One mutant, *Rht-A1b.29* produced larger grain than *Rht-A1b* (18.6mm^2) that was not significantly different from *Rht-1*. All remaining missense mutants produced grain that was significantly larger (19.9-20.9mm^2) than *Rht-1* and *Rht-A1b*. These grains were 102.8%-107.2% the size of *Rht-1* grain.

The null segregants of missense mutants that produced significantly smaller grain than *Rht-A1b* (*Rht-A1b.5/12/9*) were all significantly larger than their mutant

counterparts. There was no significant difference between the other null segregants and their mutant counterparts.

5.2.8 Hierarchical Clustering Analysis

Hierarchical clustering analysis was performed to compare the relative performance of each mutant line compared to *Rht-1* during the glasshouse characterisation. The methodology of this analysis is explained in Section 2.6.2 and the output shown in Figure 5.8.1.

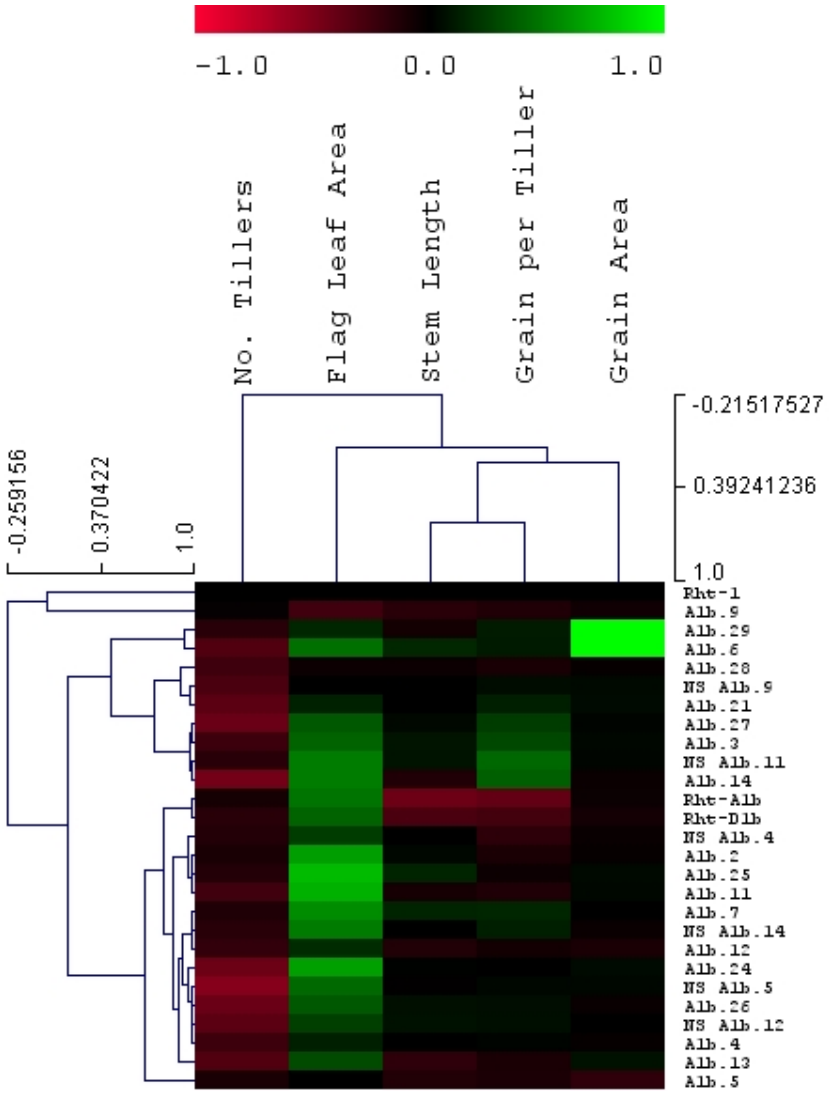

Figure 5.8.1: Hierarchical Cluster Matrix of *Rht-A1b* Intragenic Lines and Control Phenotypes in the Glasshouse. Hierarchical cluster analysis (HCL) of the relative performance of different mutants compared to WT *Rht-1*. Intragenic *Rht-A1b* mutants are named *A1b.*x, null segregates are named *NS A1b.*x. All trait data used in the HCL analysis was obtained during the glasshouse characterisation. Relative performances were analyzed with a Pearson correlation and the mutants were clustered accordingly. A three-point colour scale has been used with a negative performance compared to *Rht-1* (approaching -1) shown in red, a neutral performance (approaching 0) shown in black and a positive performance (approaching 1) shown in green.

Hierarchical clustering shows that the lines cluster into three groups. The first contains *Rht-1* and *Rht-A1b.9,* demonstrating that the *Rht-A1b.9* mutation has a negligible effect of phenotype compared to *Rht-1*. The second group consists of: *A1b.29/6/28/21/27/3/14* and *NS A1b.9/11* and is characterised by the increased number of grains per shoot compared to *Rht-1*. The third group consists of *Rht-A1b, Rht-D1b, NS A1b.4/14/12* and *A1b.2/25/11/7/12/24/26/4/13/5* and is associated with a decline in grains per shoot, except for *A1b.7* and *NS A1b.14* which show an increase in grain yield.

The correlation matrix does not present a clear relationship between phenotypic traits such as shoot number, flag leaf area and stem length with number of grains per shoot or between number of grains per shoot and grain area. Therefore, individual Pearson Correlations were carried out to establish the relationship between these traits. The results are shown in Table 5.8.1 and Figure 5.8.2.

Table 5.8.1: Pearson Correlations for Phenotype / Yield Traits

Trait 1	Trait 2	Correlation	P-value
Shoot number	Grains per shoot	-0.293	0.003
Flag leaf area	Grains per shoot	0.042	0.672
Stem length	Grains per shoot	0.339	0.0001
Grains per shoot	Grain area	0.349	0.074

The Pearson Correlations suggest that during the glasshouse characterisation, there was no correlation between flag leaf area and the no. grains per shoot (P-value = 0.672) or between the no. grains per shoot and grain area (P-value 0.074). However, there is a significant negative (-0.293) correlation between shoot number and the number of grains per shoot, suggesting that fewer shoots are associated with increased grain number. Additionally, there is a significant (p-value =0.0001) positive correlation (0.339) between stem length and no. grains per shoot. As seen in Figure 5.2.8 A and C, plotting these significant results does not suggest a clear optimum height or number of number of shoots for maximal yield. To achieve this result, a larger scale characterisation with more backcrossed lines is likely required.

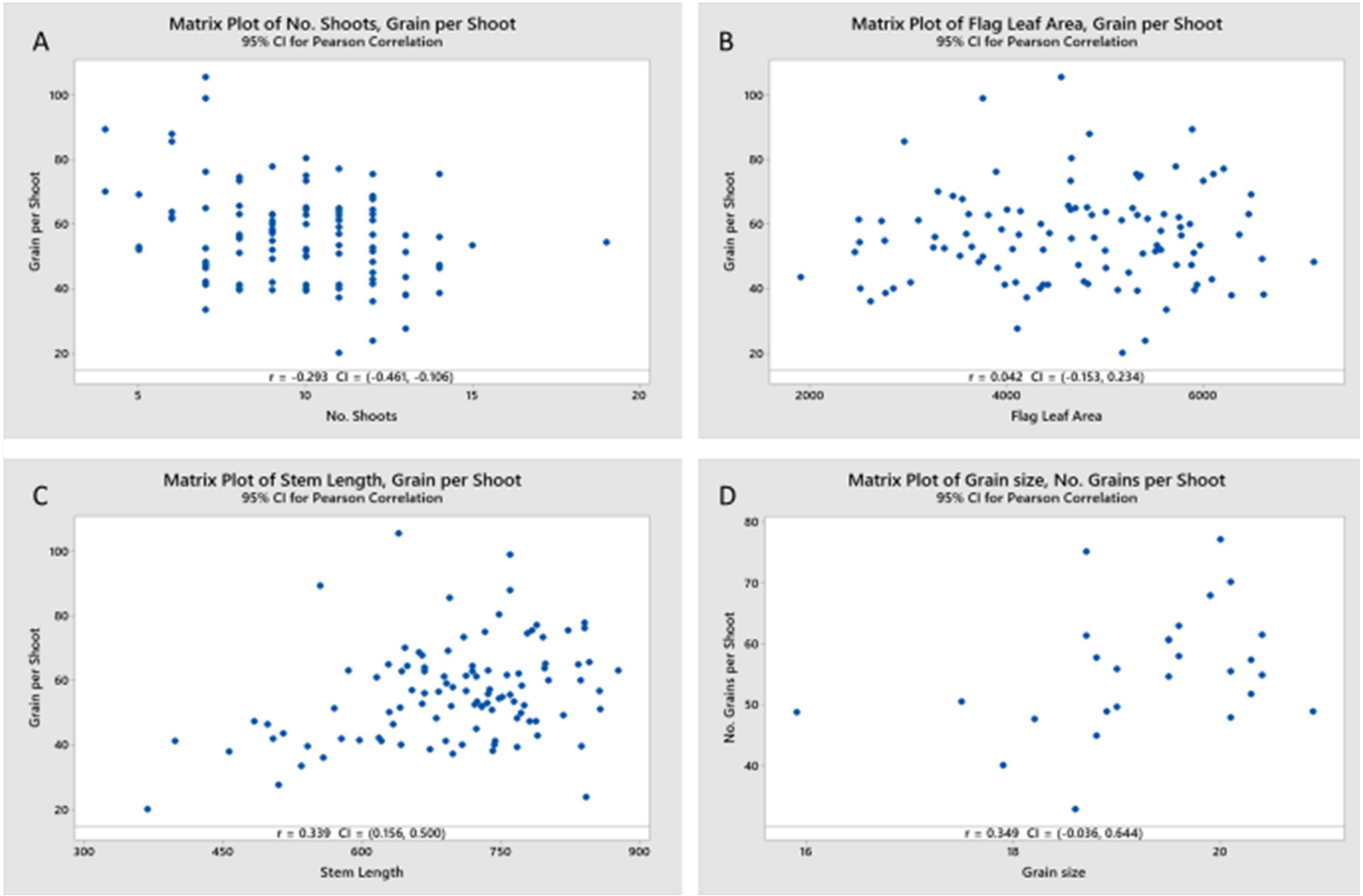

Figure 5.8.2: Pearsons Correlation Analysis Between Different Traits in the *Rht-A1b* Intragenic Mutants and Their Controls. Each Pearson Correlation was carried out at 95% confidence. (A) No. shoots vs grain no. per shoot, p-value 0.003. (B) Flag leaf area vs grain no. per shoot, p-value 0.672. (C) Stem length vs grain no. per shoot, p-value 0.0001. (D) Grain size vs grain no. per shoot, p-value 0.074.

5.3 Field Characterisation of *Rht-A1b* Missense Mutants

As a glasshouse characterisation only looks at the phenotype of plants grown under controlled conditions in pots, a preliminary field characterisation was also conducted. This was to provide information on plant phenotype under field conditions and to establish which alleles are suitable for introducing into commercial lines. BC_2F_4 seed from each of the missense mutants was sown into randomly distributed plots in the field in late March 2019 (Section 2.1.3).

Due to time constraints, there it was not possible to characterise all of the lines. Therefore, average plot height was initially measured (Section 2.3.5) to establish which lines produced a semi-dwarf (significantly intermediate to *Rht-A1b* and *Rht-1*) phenotype. These lines were then further characterised alongside their null segregants and *Rht-A1b, Rht-D1b, Rht-B1c* and *Rht-1* controls. To provide a more detailed account of plant height, 10 shoots per plot were harvested at maturity for measuring (Section 2.3.4) For these 10 shoots, total stem length and individual shoot segments were measured (described in Section 2.3). Flag leaf dimensions were also collected for 10 flag leaves per plot (Section 2.3.5), as well as grain size for 5 ears per plot (Section 2.3.3). These measurements were to provide a rough estimate of crop height in the field and effect on yield traits.

5.3.1 Approximate Plot Height

A General Analysis of Variance (ANOVA) was conducted on the approximate plot height data set, the output of which is described in Table 5.9 and Figure 5.9.

Table 5.9: ANOVA Output; Plot Height for Rht-A1b Intragenic Mutants and Controls in the Field

Line	Average Plot Height (cm)	SD	% Height Compared to *Rht-1*	P-Value	SE	LSD
Rht-B1c	40	1.7	48.6	<0.001	2.4	4.8
Rht-A1b	60.7	2.8	73.8			
Rht-D1b	65	4	79.0			
Rht-A1b.5	68.3	3.8	83.1			
Rht-A1b.13	72.7	5.7	88.4			
Rht-A1b.14	75.3	3.2	92.8			
Rht-A1b.12	77.3	3.1	94.0			
Rht-A1b.9	78	3	94.8			
Rht-A1b.29	79	2.6	95.1			
Rht-A1b.11	80.3	4	97.7			
Rht-A1b.24	80.7	4.5	98.1			
Rht-A1b.2	81	2.6	98.5			
Rht-A1b.28	81	3.7	98.5			
Rht-A1b.21	81.3	1.2	98.9			
Rht-A1b.27	81.3	5.9	98.9			
Rht-A1b.4	81.3	2.3	98.9			
Rht-1	82.2	0.6	NA			
Rht-A1b.26	82.7	2.9	100.5			
Rht-A1b.3	84.3	0.6	102.5			
Rht-A1b.6	85	1.8	103.4			
Rht-A1b.25	87	6	105.8			
Rht-A1b.7	87	4.6	105.8			

The mean value is shown with its standard deviation (SD), along with the standard error of differences (SED) and 5% least significant difference of means (LSD 5%). Green highlighted cells represent missense lines that produced a semi-dwarf phenotype (significantly intermediate to *Rht-A1b* and *Rht-1*).

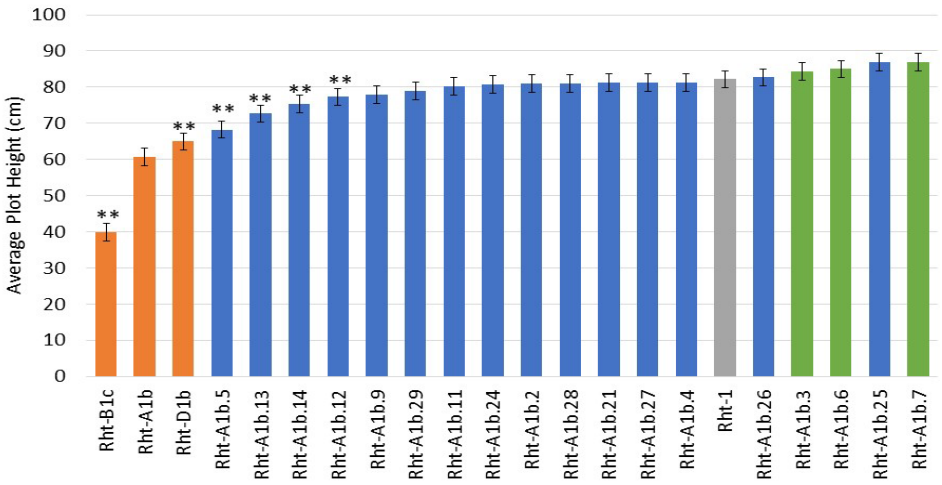

Figure 5.9: Average Plot Height Per Line for Rht-A1b Intragenic Mutants and Controls in the Field. Measurements taken at maturity. Grey = *Rht-1,* orange = *Rht-A1b*, green = *Rht-A1b* intragenic nonsense mutants, blue = *Rht-A1b* intragenic missense mutants. ANOVA P-value = <0.001. Error bars = standard error of means (2.4)., ** = mean significantly different from *Rht-A1b* and *Rht-1*.

The ANOVA confirmed that there was a statistically significant interaction between genotype and the number of grain per ear (P=<0.001). The 5% least significant difference value (4.8) was used to determine which lines produced significantly different heights from each other. *Rht-B1c* plants were 48.6% of *Rht-1* height, followed by *Rht-A1b (*73.8%) and *Rht-D1b* (79%). These height phenotypes were in line with the glasshouse characterisation carried out on the mutants in Section 3.2.2.

Only 4 missense mutants *Rht-A1b.5/13/14/12* produced semi dwarf phenotypes that were significantly taller (68.33-77.33cm) than *Rht-A1b* (60.67cm) and significantly shorter than *Rht-1* (82.24c). These were also identified in the glasshouse characterisation as producing a semi-dwarf phenotype, suggesting that there is some consistency between the phenotypes of plants grown under different conditions. The remaining mutants were not significantly different from *Rht-1* and therefore no further measurements were taken. Although it is important to note that the nonsense mutants *Rht-A1b.3/6/7* were again some of the tallest plants, suggesting that the nonsense mutations do result in a loss-of-function phenotype.

5.3.2 Plant Height

As a reduction in plant height is the most notable effects of *Rht-1* mutants, the total shoot length of each line was measured for 10 shoots per plot. The residual data plots were assessed in GenStat, which confirmed that the data was Normal and did not require transformation. A General Analysis of Variance (ANOVA) was conducted on the data set, the output of which is described in Table 5.10 and Figure 5.10.

Table 5.10: ANOVA Output for Shoot Length (mm) for Rht-A1b Intragenic Mutants and Controls grown in the Field

Line	Total Shoot Length	SD (±)	% of *Rht-1*	P-value	SED	5% LSD
Rht-1	790.5	55.3	NA	<0.001	10.9	21.5
Rht-A1b	**600**	22.5	75.9			
Rht-A1b.12	**761**	35.8	95.3			
Rht-A1b.12NS	781.6	41	98.9			
Rht-A1b.13	**717.5**	58	90.8			
Rht-A1b.13NS	**822.8**	41	104.1			
Rht-A1b.14	**745.7**	34.5	94.3			
Rht-A1b.14NS	**769.6**	34.9	97.4			
Rht-A1b.5	678.8	37.6	85.9			
Rht-A1b.5NS	**868.5**	49.6	109.9			
Rht-B1c	**405.7**	23.7	51.3			
Rht-D1b	**640.3**	35.1	81.0			

The mean value is shown with its standard deviation (SD), along with the standard error of differences (SED) and 5% least significant difference of means (LSD 5%). Means shown in bold are significantly different from *Rht-1,* underlined means are significantly different from *Rht-A1b.* NS = null segregant of an *Rht-A1b.X* mutation.

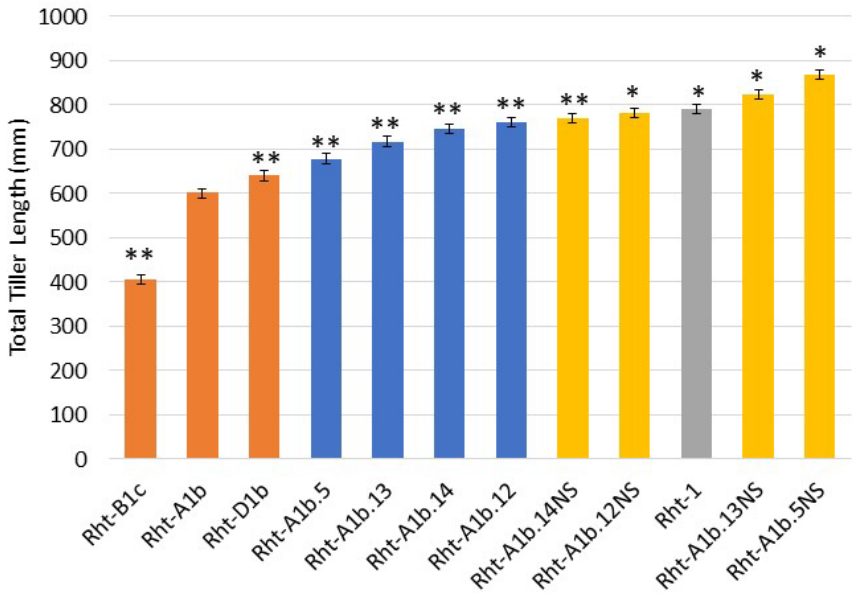

Figure 5.10: Average Shoot Length for Rht-A1b Intragenic Mutants and Controls in the Field. Grey = *Rht-1,* orange = *Rht-A1b* and *Rht-D1b*, blue = *Rht-A1b* intragenic mutants, yellow = null segregants (NS) of *Rht-A1b* intragenic mutants. Lines are ordered smallest to largest, with exception to the null segregants, which are to the right of their mutant counterpart. ANOVA P-value = <0.001. Error bars = standard error of means (10.9). * = mean significantly different from *Rht-A1b,* ** = mean significantly different from *Rht-A1b* and *Rht-1*.

The ANOVA confirmed that there was a statistically significant interaction between genotype and shoot length (cm) (P=<0.001). The 5% least significant difference value (21.5) was used to determine which lines produced significantly different sized shoots. *Rht-B1c* was confirmed to produce the smallest shoots 51.3% of the length of *Rht-1*, followed by *Rht-A1b* (75.9%) and *Rht-D1b* (81%), which were all significantly different from each other. The four missense mutants *Rht-A1b.5/13/14/12* all produced intermediate shoot lengths (85.9%-95.3%), significantly longer than *Rht-A1b* and *Rht-D1b* and shorter than *Rht-1.*

As predicted, the null segregants produced the tallest shoots, alongside *Rht-1,* as these lines lack the *Rht-A1b* mutation (Figure 5.10).

Three of the null segregants produced shoots that were not significantly difference from *Rht-1* (*NS Rht-A1b.12/13/5).* The remaining segregant, *NS Rht-A1b.14*, produced shoots that were significantly shorter (97.4%) than *Rht-1*. Except for *NS Rht-A1b.12,* all the null segregants also produced significantly longer shoots than their mutant counterparts. This suggests that background mutations may be affecting *NS Rht-A1b.12/14* as they weren't entirely uniform with the other null lines or *Rht-1*.

To determine the genotypic effect on the length of different internode segments on total length additional ANOVAs were conducted, described in Table 5.11 and Figure 5.11.

Table 5.11: ANOVA Output for Shoot Length (mm) for Rht-A1b Intragenic Mutants and Controls in the Field

	Internode 4		Internode 3		Internode 2		Peduncle		Ear	
Line	ANOVA	%	ANOVA	%	ANOVA	%	ANOVA	%	ANOVA	%
Rht-1	50.9 ± 31.5	NA	121.7 ± 13.6	NA	191.6 ± 12.3	NA	335 ± 25.6	NA	95.9 ± 10.3	NA
Rht-A1b	**27 ± 19.5**	53.0	**94.6 ± 25.1**	77.8	**140.3 ± 13.3**	73.3	**255.2 ± 20**	75.5	94.2 ± 9.8	98.2
NS Rht-A1b.12	57.5 ± 23.4	113.0	127.8 ± 15.3	105.1	**182.1 ± 15.5**	95.0	**303.5 ± 32.2**	90.6	92.4 ± 5.7	95.4
Rht-A1b.12	51.7 ± 25.6	101.6	119.1 ± 22.7	97.9	185.6 ± 13.7	97.4	342.8 ± 31.8	102.3	**90.8 ± 5.1**	94.7
NS Rht-A1b.13	51.9 ± 28.8	102.0	**105.9 ± 18.2**	87.9	**162.4 ± 19.1**	84.8	**300.4 ± 30.8**	89.7	98.9 ± 9.9	103.1
Rht-A1b.13	**64.6 ± 40.1**	125.9	125.4 ± 14.3	103.9	190.9 ± 15.8	99.7	343 ± 27	102.4	**101.5 ± 9.5**	105.8
Rht-A1b.14	48.4 ± 17.9	95.1	114.8 ± 17.6	94.4	183.8 ± 14.8	95.9	**315 ± 23.3**	94.0	**91.4 ± 8.1**	95.3
NS Rht-A1b.14	41.7 ± 23.6	81.9	117.2 ± 15.9	95.4	193.5 ± 12.8	101.0	339.3 ± 22.7	101.3	**85.6 ± 5.9**	90.3
Rht-A1b.5	44.6 ± 24	87.6	**109.2 ± 15.4**	89.8	**157.7 ± 18.4**	82.3	**284.7 ± 31.3**	85.0	**85.9 ± 8.2**	90.6
NS Rht-A1b.5	**67.5 ± 24.9**	132.6	**133.7 ± 15**	109.9	**204.8 ± 25.4**	105.9	**370.7 ± 43.1**	110.7	97.5 ± 12	101.7
Rht-B1c	**20.4 ± 12.7**	40.1	**40.6 ± 17.2**	33.4	**88.4 ± 11.4**	45.2	**177.6± 13.9**	53.0	**105.3 ± 5.3**	110.8
Rht-D1b	**34.7 ± 22.9**	68.2	**95.6 ± 21.5**	78.6	**160.9 ± 15.9**	84.0	**270.6 ± 30.8**	80.8	**90.3 ± 11.2**	94.2
P-value	<0.001		<0.001		<0.001		<0.001		<0.001	
SED	5.9		4.7		4.2		7.4		2.3	
5% LSD	13.6		9.3		8.3		14.6		4.5	

The mean value is shown with its standard deviation (SD), along with the standard error of differences (SED) and 5% least significant difference of means (LSD 5%). Means shown in bold are significantly different from *Rht-1,* underlined means are significantly different from *Rht-A1b.* NS = null segregant of an *Rht-A1b.X* mutation.

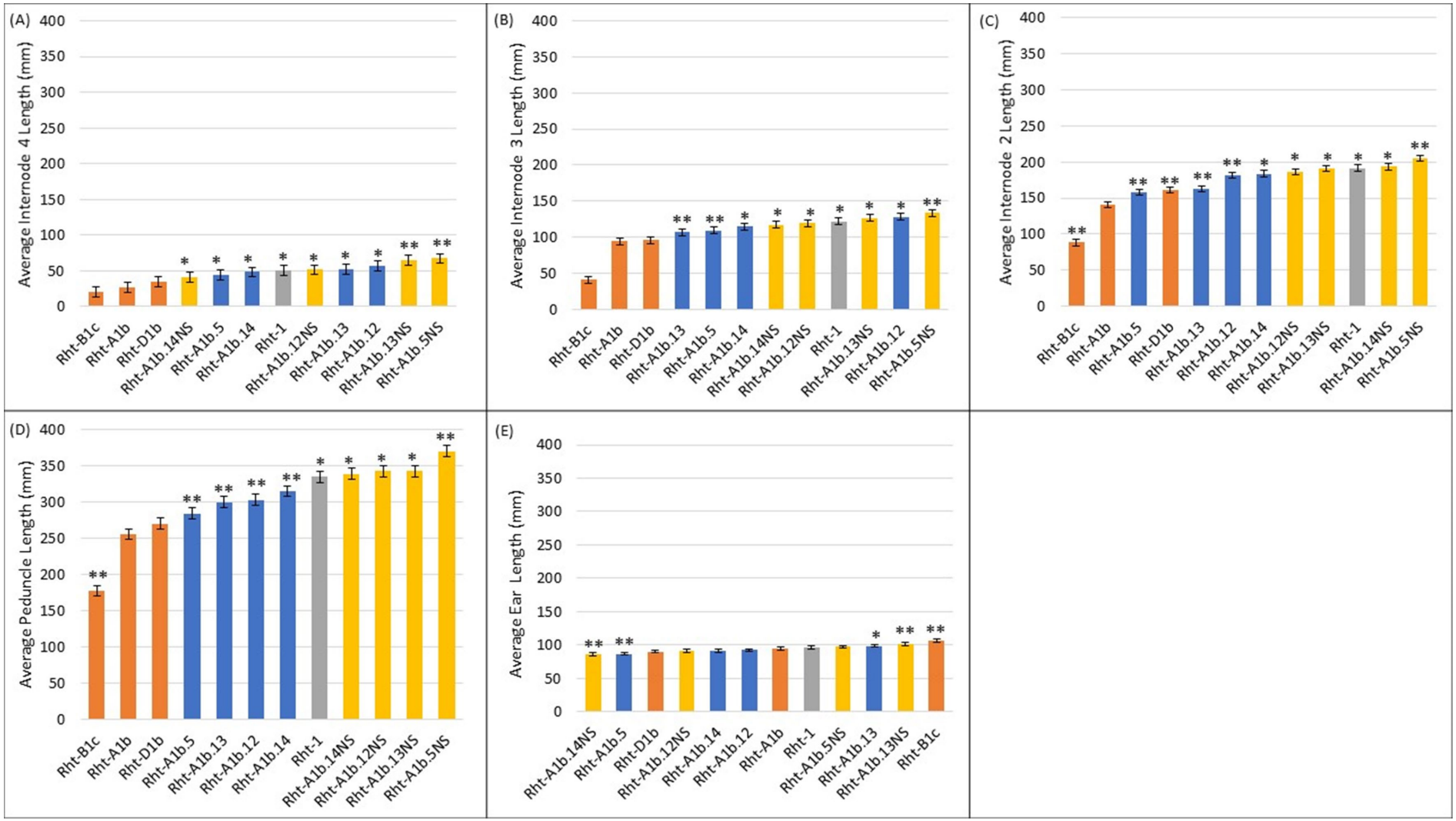

Figure 5.11: Average Shoot Segment Lengths for Rht-A1b Intragenic Mutants and Controls in the Field. Grey = *Rht-1,* orange = *Rht-A1b* and *Rht-D1b*, blue = *Rht-A1b* intragenic mutants, yellow = null segregants (NS) of *Rht-A1b* intragenic mutants. **(A) Average Internode 4 Lengths (mm).** P-value = <0.001, error bars = standard error of means (SED) 5.9, 5% least significant difference (LSD) 13.5. **(B) Average Internode 3 Lengths (mm).** P-value = <0.001, error bars = SED 4.7, LSD = 9.3. **(C) Average Internode 2 Lengths (mm).** P-value = <0.001, error bars = SED 4.2, LSD = 8.3. **(D) Average Peduncle Lengths (mm).** P-value = <0.001, error bars = SED 7.4, LSD = 14.5. **(E) Average Ear Length (mm).** P-value = <0.001, error bars = SED 2.3, LSD = 4.5. * = mean significantly different from *Rht-A1b,* ** = mean significantly different from *Rht-A1b* and *Rht-1*. Significance calculated with the LSD values.

The ANOVAs confirmed that there was a statistically significant interaction between genotype and the different shoot segment lengths (P=<0.001).

The 5% least significant difference value (13.6) was used to determine which lines produced significantly different internode 4 lengths. In the controls *Rht-A1b, B1c* and *D1b* were all significantly shorter than *Rht-1*. *Rht-B1c* (40.1% length of *Rht-1*) was significantly shorter than *Rht-D1b* (68.2%) but neither control line was significantly different from *Rht-A1b* (53%).

RhtA1b.5/14/13/12 were all significantly longer (87.6-113% length of *Rht-1*) than *Rht-A1b* (53%) but not significantly different from *Rht-1*. There was no significant difference between the *NS Rht-A1b.12/13/14* and their mutant counterparts, whilst *NS Rht-A1b.5* produced significantly longer internode 4 than *Rht-A1b.5*.

The 5% least significant difference value (9.3) was used to determine which lines produced significantly different internode 3 lengths. *Rht-B1c* was significantly the shortest (33.4% the length of *Rht-1*), whilst *Rht-A1b* and *Rht-D1b* produced significantly longer lengths (77.8% and 78.6% respectively), that were not significantly different from one another. *Rht-A1b.13* and *Rht-A1b.5* produced intermediate lengths (87.6% and 94.4% respectively), that were significantly longer than *Rht-A1b* and shorter than *Rht-1* although only *Rht-A1b.13* is significantly different than its null segregant. *Rht-A1b.14* and *Rht-A1b.12* produced internodes (95.4 and 105.1% respectively) significantly longer than *Rht-A1b* but not significantly different than *Rht-1*. These were also not significantly different from their null segregants.

The 5% least significant difference value (8.3) was used to determine which lines produced significantly different internode 2 lengths. *Rht-B1c* produced significantly the shortest internodes (45.2% length of *Rht-1*), followed by *Rht-A1b* (73.3%) and then *Rht-A1b.5* (82.3%). There was no significant difference between *Rht-A1b.5* and *Rht-D1b* (84%) and *Rht-A1b.13* (84.8%) which were all significantly shorter than *Rht-1* and longer than *Rht-A1b*. *Rht-A1b.12* (95%) also produced an intermediate phenotype, whilst *Rht-A1b.14* (95.9%) was not significantly different from *Rht-1.*

Except for *Rht-A1b.12* all the missense mutants were significantly different from their null segregants.

The 5% least significant difference value (14.6) was used to determine which lines produced significantly different peduncle lengths. *Rht-B1c* produced the shortest peduncles (53%) followed by *Rht-A1b* (75.5%) and *Rht-D1b* (80.8%) which were not significantly different from each other. The *Rht-A1b.5/13/12/14* all produced significantly intermediate peduncles (85-94%) that were significantly smaller than their null segregant counterparts (101.3%-110.7%).

The 5% least significant difference value (4.5) was used to determine which lines produced significantly different ear lengths. *Rht-B1c* the shortest mutant produced significantly the longest ears (110.8% length of *Rht-1*), followed by *Rht-A1b.13* (103.1%) and *NS Rht-A1b.13* (105.8%), which were not significantly different from each other. *NS Rht-A1b.14* (90.3%) and *Rht-A1b.5* (90.6%) produced the shortest ears whilst there was no significant difference between the other ear measurements.

These results are in line with previous studies of suppressor mutants in *Rht-B1c* and barley *sln1,* which identified that differences in height were due to the accumulative effect of changes in internode lengths, not through changes in internode number (Derkx et al. 2017; Chandler and Harding 2013).

5.3.2 Flag Leaf Characteristics

To examine the effect of the intragenic mutations on flag leaf characteristics in the field, 10 flag leaves per plot were measured. Leaf length and width measurements were taken and used to calculate an approximate leaf area (Section 2.3.4). Residual plots for this data were assessed in GenStat, which confirmed that the data was Normal and did not require transformation. ANOVAs were conducted on the raw data, the outputs of which are described in Table 5.12 and Figure 5.12.

Table 5.12: ANOVA Output for Flag Leaf Measurements (mm) for Rht-A1b Suppressor mutants and Controls in the Field.

Line	Width (mm)		Length (mm)		Area (mm^2)	
	Average	SD (±)	Average	SD (±)	Average	SD (±)
Rht-1	17.6	2.4	219.2	32.8	3265	865
Rht-B1c	**20.6**	1.9	236.9	31.1	**4069**	605
Rht-A1b	16.4	2.3	214.2	39.7	2960	844
Rht-D1b	16.5	3	210.4	42.7	2950	899
Rht-A1b.5	17.1	2.4	230.9	54.7	3331	956
Rht-A1b.12	**16.9**	2.2	220.4	41.1	3142	852
Rht-A1b.13	17.5	2.1	236.6	35.3	3483	805
Rht-A1b.14	17.3	2.7	221.8	33.4	3238	821
NS Rht-A1b.5	**18.4**	2.1	238.4	42.9	**3703**	974
NS Rht-A1b.12	17.9	2.4	210.2	31.8	3182	770
NS Rht-A1b.13	**18.8**	1.7	**238.7**	33.3	**3758**	753
NS Rht-A1b.14	16.8	2.1	223.8	30.9	3169	694
P-Value	<0.001		0.006		<0.001	
SED	0.6		9.8		213	
5% LSD	1.2		19.3		420	

The mean value is shown with its standard deviation (SD), along with the standard error of differences (SED) and 5% least significant difference of means (LSD 5%). Means shown in bold are significantly different from *Rht-1,* underlined means are significantly different from *Rht-A1b.* NS = null segregant of an *Rht-A1b.X* mutation.

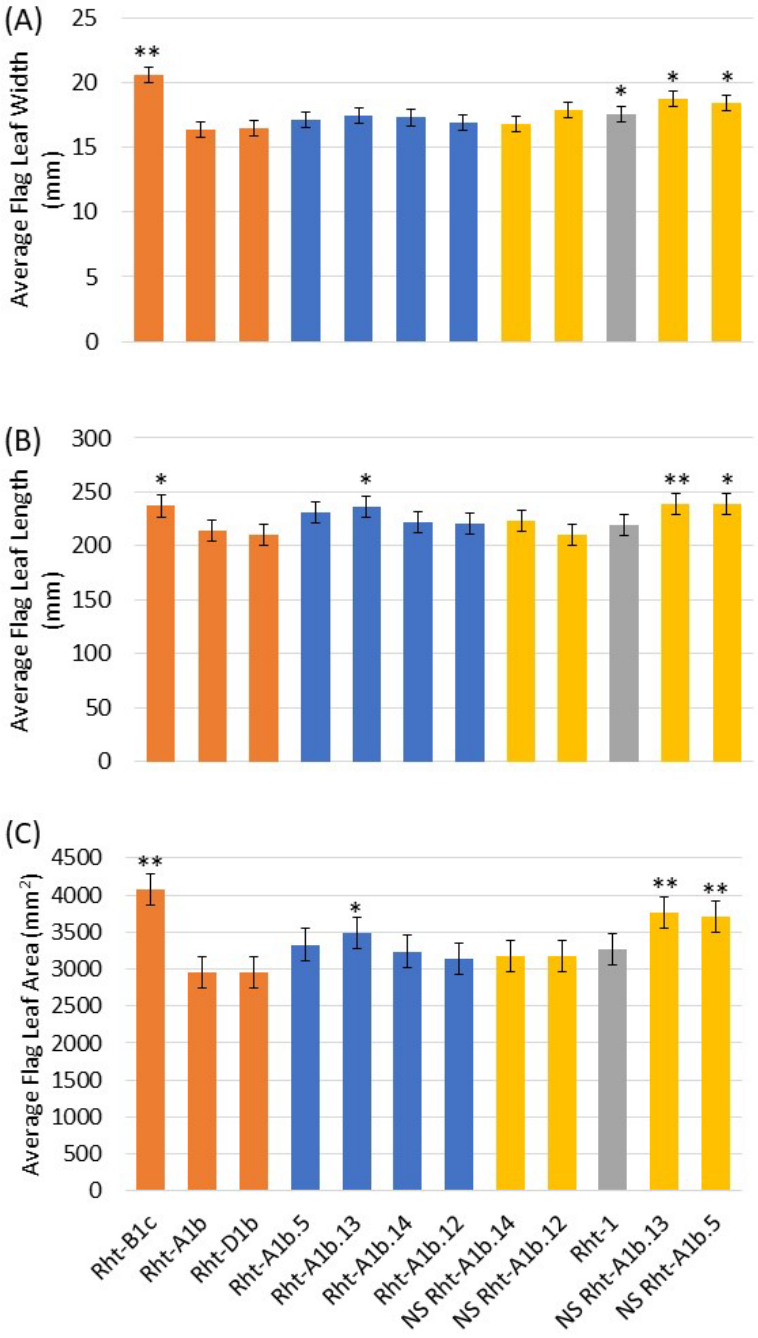

Figure 5.13: Average Flag Leaf Dimensions (mm) in Rht-A1b Intragenic Mutants and Controls. Grey = *Rht-1,* orange = *Rht-A1b*, blue = *Rht-A1b* intragenic mutants, yellow = null segregants of *Rht-A1b* intragenic mutants. Lines are arranged in height order (smallest to largest). * = measurement significantly different that *Rht-A1b.* ** = measurement significantly different from *Rht-A1b* and *Rht-1*. **(A) Average Flag Leaf Width (mm).** ANOVA P-value = <0.001. Error bars = standard error of means (0.6). **(B) Average Flag Leaf Length (mm)** ANOVA P-value = 0.006. Error bars = standard error of means (19.3). **(C) Average Flag Leaf Area (mm^2).** ANOVA P-value = <0.001. Error bars = standard error of means (420).

The ANOVAs confirmed there was a significant interaction between genotype and flag leaf characteristics (P= <0.001 or 0.006). In Figure 5.13, the lines were placed in height order (smallest to tallest, left to right), to establish whether a similar interaction between height and flag leaf dimensions as in the *Rht-B1c* suppressor screen. In this suppressor screen, taller plants produced longer, narrower leaves whilst shorter plants produced shorter, wider leaves which ultimately had a larger leaf area (Derkx et al. 2017).

Although this trend is seen in the *Rht-B1c* leaves, which produced significantly wider leaves with a larger leaf area than the other lines (Figure 5.13A and C), this trend is not observed in the other Cadenza lines, which mostly produced leaves that were not significantly different from one another. The only exception to this is the null segregants *NS Rht-A1b.13/5* which produced significantly wider and longer leaves than *Rht-A1b,* resulting in larger leaf areas (3758 and 3169mm^2, compared to 2960mm^2).

5.3.3 Grain Size

Due to time constraints compounded by a delay in harvesting and lack of available time to process collected samples, no harvest index or grain number measurements can be included in this thesis. However preliminary grain size data was taken by harvesting and threshing 5 ears per plot for each genotype and measuring grain area for ~150 seeds per plot (Section 2.3.3). Residual plots for this data were assessed in GenStat, which confirmed that the data was Normal and did not require transformation. A General Analysis of Variance (ANOVA) was conducted, the output of which is described in Table 5.13 and Figure 5.14.

Table 5.13: ANOVA Output for Grain Size (mm²) for Rht-A1b Intragenic Mutants and Controls Grown in the Field

Line	Area (mm²)	SD	% of *Rht-1*	P-Value	SED	LSD
Rht-1	21.9	2.8	NA	<0.001	0.2	0.4
Rht-A1b	18.8	3.4	85.8			
Rht-A1b.12	19.7	3.2	89.7			
NS Rht-A1b.12	20.0	3.5	91.3			
Rht-A1b.13	20.0	3.2	91.3			
NS Rht-A1b.13	20.5	3.2	93.8			
Rht-A1b.14	19.8	3.4	90.4			
NS Rht-A1b.14	20.2	3.1	92.0			
Rht-A1b.5	18.3	3.2	83.7			
NS Rht-A1b.5	21.4	2	97.7			
Rht-B1c	18.0	2.1	82.0			
Rht-D1b	20.2	3.3	92.1			

The mean value is shown with its standard deviation (SD), along with the standard error of differences (SED) and 5% least significant difference of means (LSD 5%). Means shown in bold are significantly different from *Rht-1,* underlined means are significantly different from *Rht-A1b.* NS = null segregant of an *Rht-A1b.X* mutation.

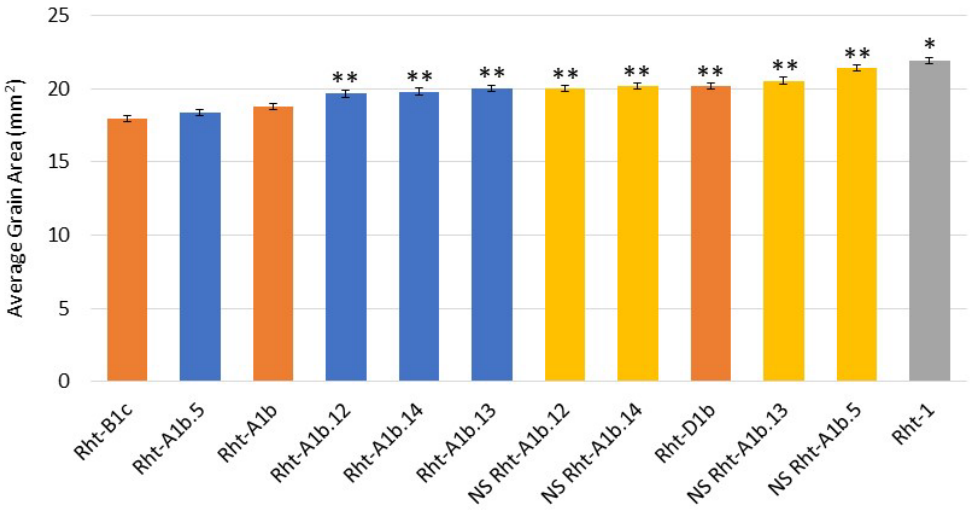

Figure 5.14: Average Grain Area (mm²) for Rht-A1b Intragenic Mutants and Controls in the Field. Grey = *Rht-1,* orange = *Rht-A1b* and *Rht-D1b*, blue = *Rht-A1b* intragenic missense mutants, yellow = null segregants (NS) of *Rht-A1b* intragenic mutants. Lines are ordered smallest to largest, with exception to the null segregants, which are to the right of their mutant counterpart. ANOVA P-value = <0.001. Error bars = standard error of means (0.2). * = mean significantly different from *Rht-A1b,* ** = mean significantly different from *Rht-A1b* and *Rht-1*.

The ANOVA confirmed that there was a statistically significant interaction between genotype and the different grain sizes (P=<0.001). The 5% least significant difference value (0.4) was used to establish which lines produced significantly different grain sizes. *Rht-B1c* (82% of *Rht-1*) and *Rht-A1b.5* (*83.7%*) produced significantly smaller grains than *Rht-A1b* (85.8%). *Rht-D1b* (92.1%) and *Rht-A1b.12/14/13* (89.7-91.3%) produced intermediate grain sizes to *Rht-A1b* and *Rht-1*. The null segregants all produced significantly larger grain than their mutant counterparts.

This suggests that three of the suppressor mutants, *Rht-A1b.12/14/13* significantly improve grain size, in comparison to *Rht-A1b* and that this improvement is unlikely to be the result if background mutations.

5.5 Discussion

This chapter discussed preliminary characterisations of BC_2F_3 intragenic missense and nonsense *Rht-A1b* mutants in the glasshouse and in the field.

The intragenic mutations were expected to result in partial (missense) or total (nonsense) loss of function phenotypes, that rescued height compared to *Rht-A1b* as these lines were initially identified in a screen that looked for increased plant height (Chandler and Harding 2013; Derkx et al. 2017). This was largely reflected in the phenotyping. For example, like *Rht-1*, suppressor mutants produced earlier heading dates than *Rht-A1b* (Section 5.2.1) and more spikelets per ear (Section 5.2.5). However, the most obvious phenotypic effect in the suppressor mutants was increased plant height (Section 5.2.2), all suppressor mutants produced shoots significantly longer than *Rht-A1b.* Most of these mutants were not significantly different from *Rht-1.* Some missense mutants (*Rht-A1b.5/9/12/13/14/29)* produced shoots that there 'semi-dwarf', significantly shorter than *Rht-1* and taller than *Rht-A1b*, whilst one missense (*Rht-A1b.6*) and all the nonsense mutations *(Rht-A1b.3/6/7*) produced an 'overgrowth' phenotype significantly taller than *Rht-1*. These phenotypes appear to be the cumulative effect of elongation of the uppermost 4 internodes, which were proportional to final shoot length. These results compliment the findings of the *Rht-A1b* characterisation in Chapter 3, which

determined that the reduced stature of *Rht-A1b* is most likely due to the GA insensitivity reducing cell wall extensibility and elongation (Keyes, Paolillo, and Sorrells 1989), resulting in shorter stem cells and reduced internode elongation. Intragenic loss of function mutations interrupt the functional GRAS domain of *Rht-A1b* theoretically increasing GA sensitivity and enabling increased cell elongation, producing taller shoots (Chandler and Harding 2013). However, to confirm that this is the case, it will be necessary to conduct GA-dose response assays to compare suppressor mutants and *Rht-A1b* (Chandler and Robertson 1999).

A study characterising intragenic *Rht-B1c* mutants noted a pattern in flag leaf characteristics, taller plants were found to produce longer, narrower leaves whilst more dwarfed plants produced shorter, wider leaves with an increased approximate area (Derkx et al. 2017). This trend was observed in the *Rht-B1c* plants grown in the field but was not observed in the other lines when grown in the glasshouse or the field (Sections 5.2.3 and 5.3.2). This may be due to varietal differences, as the *Rht-B1c* suppressor characterisations occurred in a Maringá background (Derkx et al. 2017) and this characterisation occurred in a Cadenza background, as the phenotypic effects of *Rht-1* alleles varies in different wheat varieties (Flintham et al. 1997). *Rht-B1c* produces a severe dwarf phenotype in most varieties, whilst the effects of more intermediate alleles can be nuanced in different varieties (Flintham et al. 1997). This could explain why there was no significant difference between *Rht-A1b* (BC_6F_3)*, Rht-D1b* (NIL) and *Rht-1* (WT Cadenza) leaf phenotypes. Therefore, there may be noticeable effect on flag leaf dimensions in *Rht-B1c* and *Rht-B1c* suppressors, but these may not be noticeable from *Rht-A1b, Rht-D1b* and *Rht-A1b* suppressors. Further, Cadenza flag leaf measurements appear to be highly variable, as demonstrated in the high standard deviations for these results. Therefore, a pattern may not be possible to produce in this variety without an extensive number of measurements taken. Additionally, the variation in the null segregants flag leaf characterisation suggests that background mutations may be affecting the phenotypes of the suppressor lines, which could partially explain why a trend isn't seen. Additional backcrossing and further characterisation will be required to assess whether this is the case (Derkx et al. 2017)

The primary aim of this characterisation was to identify suppressor mutants with a semi-dwarf phenotype that might have the potential to improve crop yields. Due to this and time constraints, only 4 suppressor mutants (*Rht-A1b.5/12/13/14*) where characterised in the field (discussed in Section 5.5.1). However, the grain measurements (number per ear and size) collected during the glasshouse characterisation suggest that even the taller intragenic *Rht-A1b* mutants may have the potential to improve crop yields (Figure 5.15).

Line	Plant Height (GH)	Plant Height (F)	Grain per Ear (GH)	Grain size (mm^2) (GH)	Grain size (mm^2) (F)
Rht-A1b.5				**	
Rht-A1b.12			*	**	**
Rht-A1b.13				**	**
Rht-A1b.14			**		**
Rht-A1b.9				**	-
Rht-A1b.29			*	*	-
Rht-A1b.2					-
Rht-A1b.4			*	**	-
Rht-A1b.11				**	-
Rht-A1b.21			*	**	-
Rht-A1b.24			*	**	-
Rht-A1b.26			*		-
Rht-A1b.27			*	**	-
Rht-A1b.28			*	**	-
Rht-A1b.25			*	**	-

Colour Key		
	Semi-dwarf	Significantly more grains per ear or larger grains
	Tall	
	Overgrowth	Significantly smaller grains per ear

Figure 5.15: Overview of *Rht-A1b* Missense Mutant Height and Grain Characteristics. A description of the colour code is provided in the key above. * = significantly more/less than *Rht-A1b, ** =* significantly more/less than *Rht-1* and *Rht-A1b*.

Only two of the intragenic lines (*Rht-A1.9* and *Rht-A1b.2*) appear to not improve grain size or grain number per ear, with the remaining lines producing a positive result compared *to Rht-A1b in* at least one of these characteristics. This suggests

that the intragenic lines should not be screened solely on their dwarfing potential, but also on their yield potential. (Fischer and Quail 1990). Improvements to yield in these lines could be due to reduced pleiotropic effects. For example, reduced grain size in the semi-dwarfs *Rht-D1b* and *Rht-B1b* is primarily associated with increased inter-floret competition but may also be due to reduced GA content and signalling in the seed. This is associated with reduced endosperm development, resulting in smaller, lighter seeds (Kondhare et al. 2014). By disrupting the *Rht-A1b* GRAS domain, the suppressor mutants may allow for increased GA signalling and improved endosperm development (Kondhare et al. 2014).

However, these characterisation experiments do suggest that the *Rht-A1b* intragenic lines may require further backcrossing. EMS-mutagenesis is not targeted to a single gene (Henikoff, Till, and Comai 2004), therefore multiple allelelic mutations were introduced into the hexaploid genome during the mutagenesis process. Although the lines were backcrossed twice to remove ~75% of these background mutations (Derkx et al. 2017), there was significant variation in the phenotypes of the null segregants in all the phenotypic measurements taken. This suggests that additional rounds of backcrossing should be undertaken to remove mutations that may be affecting phenotype.

5.5.1 *Rht-A1b* Derived Alleles – Potential Dwarfing Alleles for Wheat Breeding?

Out of the 18 *Rht-A1b* suppressor mutants characterised in this chapter, 6 produced a semi-dwarf phenotype, significantly intermediate to *Rht-A1b* and *Rht-1* (WT Cadenza) (Table 5.14 and Figure 5.16).

Table 5.14: Intragenic Rht-A1b Mutations resulting in an Intermediate of Function Phenotype.

Rht-A1b Intragenic Mutants				*Rht-B1c Intragenic Mutants **			
Allele	Nucleotide Substitution	Amino Acid Substitution	% Height compared to *Rht-A1b*	Allele	Nucleotide Substitution	Amino Acid Substitution	% Height Compared to *Rht-B1c*
A1b.5	C1591T	L513F	138				
A1b.9	G800A	G267D	132	*B1c.4*	G2829A	G298D	156
A1b.12	C808T	R270C	139				
A1b.13	C821T	A274V	132	*B1c.6*	G2849A	A305T	156
A1b.14	C821T	G277D	139				
A1b.29	C1580T	S527F	141				

The nucleotide substitutions and predicted amino acid substitution are shown, * denotes a nonsense mutation. Plant height as a percentage of WT (*Rht*-1) height is shown, with lines characterised in the glasshouse (GH). If an *Rht-A1b* allele was also identified in the in the *Rht-B1c* suppressor screen, then this equivalent mutation is shown. *Rht-B1c* alleles were phenotyped in the glasshouse (Derkx et. al 2017).

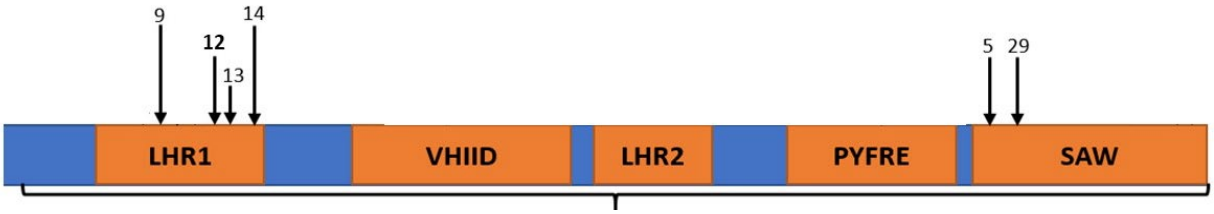

Figure 5.16: Locations of Missense Mutations in the RHT-A1 C-Terminal GRAS Domain, that cause semi-dwarfism. Orange boxes represent the conserved motifs; LHR1, VHIID, LHR2, PYFRE and SAW. Arrows depict the approximate mutation site. Numbers correspond to *Rht-A1b.X* allele name (defined in Table 5.14)

Alleles resulting in an intermediate plant phenotype were caused by amino acid substitutions in the LHR1 and SAW conserved motifs of the DELLA GRAS domain. It is interesting that 4 out of the 6 mutations occurred in the LHR1 domain, as two other missense mutations in this area caused a tall phenotype (discussed in Section 5.5.1). The LHR1 motif has been implicated as vital for DELLA function, as it forms part of the 5 α-helices of the DELLA protein 'cap', which is involved in direct DELLA-DIP interactions, disruption to these cap could therefore reduce DELLA binding potential and ability to repress GA-signalling, resulting in a taller phenotype (Li et

al. 2016; Derkx et al. 2017). These missense mutations perhaps represent less disruptive amino acid substitutions in this motif, affecting amino acids that are not directly involved in DELLA binding to DIPs(Derkx et al. 2017). Evidence for this lies with *Rht-A1b.9* and *Rht-A1b.14. Rht-A1b.9* (132% height restored compared to *Rht-A1b*) is identical to the *Rht-B1c.4* mutation, which resulted in even greater height restoration (156% restoration compared to *Rht-B1c)*. While *Rht-A1b.14* and *Rht-B1c.6* represent different substitutions of the same amino acid (A274V and A305T respectively), that resulted in a height restoration of 139% and 156% compared to their appropriate dwarf. That the *Rht-B1c* mutations resulted in greater height restoration, suggests that not all missense mutations in the LHR1 domain result in a tall phenotype, with different amino acid substitutions have different effects on plant height (Derkx et al. 2017; Chandler and Harding 2013).

Of the 6 intermediate mutations identified, 4 (*Rht-A1b.12/13/14/*29) had grain related characteristics that could potentially identify them as useful to wheat breeding. These lines either produced significantly more grains per ear or larger grains (mm^2) than *Rht-A1b,* signalling an improvement in yield potential (Flintham and Gale 1982; Miralles et al. 1998). In particular, *Rht-A1b.13* appears to be the most promising allele. However, their usefulness in wheat breeding still needs to be thoroughly assessed in the field by testing the allelles in a background in which *Rht-1* alleles will be beneficial.

5.5.2 Mutations in the C-terminal GRAS Domain Disrupt *Rht-A1b* Function

Studying the effect that intragenic *Rht-A1b* mutations have on plant phenotypes has the potential to help develop our understanding of DELLA structure-function and how individual amino acids are potentially involved in mediating interactions with DELLA partner proteins (Van de Velde, Chandler, et al. 2017; Van de Velde, Ruelens, et al. 2017). The nonsense and missense mutations that resulted in a height

phenotype not significantly different, or significantly taller than Cadenza (*Rht-1*) are described in Figure 5.17 and Table 5.17.

Table 5.15: Intragenic Rht-A1b Mutations resulting in a Loss of Function Phenotype.

Rht-A1b Intragenic Mutants				*Rht-B1c Intragenic Mutants* *			
Allele	Nucleotide Substitution	Amino Acid Substitution	% Height compared to *Rht-A1b*	Allele	Nucleotide Substitution	Amino Acid Substitution	% Height Compared to *Rht-B1c*
A1b.2	C836T	A279V	162 (T)	*B1c.7*	C2865T	A310V	211 (T)
A1b.3	G1047A	W349*	169 (Ov)				
A1b.4	C1479T	T493I	156 (T)	*B1c.16*	C3507T	T524I	211 (T)
A1b.6	G1812A	W604*	179 (Ov)	*B1c.33*	G3841A	W635*	227 (T)
A1b.7	G1845A	W615*	176 (OV)	*B1c.20*	G3874A	W646*	223 (T)
A1b.11	G809A	R270H	145 (T)				
A1b.21	G1222A	A408T	156 (T)				
A1b.24	G1408A	E470K	158 (T)				
A1b.25	C1460T	S487F	178 (Ov)				
A1b.26	C1475T	S492F	165 (Ov)				
A1b.27	G1487A	D496N	162 (T)				
A1b.28	G1491A	S497F	147 (T)	*B1c.17*	C3519T	S528F	176 (SD)

The nucleotide substitutions and predicted amino acid substation are shown, * denotes a nonsense mutation. Plant height as a percentage of WT (*Rht*-1) height is shown, with lines characterised in the glasshouse (GH). (SD) = semi-dwarf phenotype, (T) = tall phenotype not significantly different from *Rht-1*, (Ov) = overgrowth phenotype significantly taller than *Rht-1*. If an *Rht-A1b* allele was also identified in the in the *Rht-B1c* suppressor screen, then this equivalent mutation is shown. *Rht-B1c* alleles were phenotyped in the glasshouse (Derkx et. al 2017).

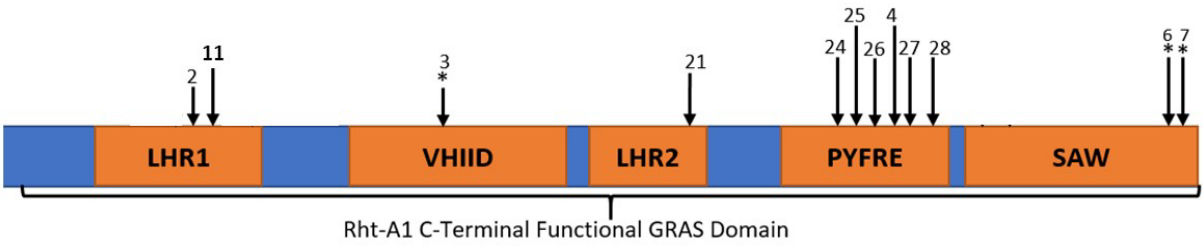

Figure 5.17: Locations of Mutations in the RHT-A1 C-Terminal GRAS Domain, that cause a Tall Phenotype. Orange boxes represent the conserved motifs; LHR1, VHIID, LHR2, PYFRE and SAW. Arrows depict the approximate mutation site. Numbers correspond to allele number. * = nonsense mutation, plain arrow = missense mutation. Numbers correspond to *Rht-A1b.X* allele name (defined in Table 5.15)

Missense mutations resulting in a tall phenotype (not significantly different than *Rht-1*) or an overgrowth phenotype (significantly taller than *Rht-1*) occurred in 4/5 of the conserved DELLA GRAS Domain motifs: LHR1, LHR2, PYFRE and SAW (Figure 5.17). Characterisation of these motifs suggests that they are involved in direct physical interactions between DELLA and DIPs (Li et al. 2016). This characterisation involves the reporting of crystal structure of rice *Scarecrow-like 7,* which shares 35% amino acid identity with the wheat DELLA protein, RHT-1. The shared amino acids are spread evenly through Scarecrow-like 7, which suggests that the main structural features are conserved in RHT-1 (Derkx et al. 2017). Missense mutations resulting in an overgrowth phenotype occur predominantly in the LHR1 and PYFRE motifs, which are part of the 5 α-helices of the protein 'cap' structure, suggesting that this region is integral to RHT-1 function (Li et al. 2016). A high proportion of overgrowth mutations occurring in the LHR1 and PYFRE motifs was also reported in the *Rht-B1c* suppressor screen, suggesting that this is not just a phenomenon of the *Rht-A1b* screen (Derkx et al. 2017). Additionally, a missense mutant identified in the PYFRE motif of *Rht-B1b* also resulted in a tall phenotype (Mo, Pearce, and Dubcovsky 2018).

When grown in similar conditions in the glasshouse, equivalent intragenic mutations in *Rht-B1c* resulted in a greater height restoration. The missense mutants *Rht-A1b.2* (162%), *Rht-A1b.4* (156%) and *Rht-A1b.28* (147%) compared to *Rht-B1c.7* (211%), *Rht-B1c.16* (211%) and *Rht-B1c.17* (176%) respectively. This suggests that the suppressor mutations don't only produce an overgrowth phenotype in *Rht-A1b* but also more severe height restoration in *Rht-B1c* (Flintham et al. 1997; Derkx et al. 2017).

The presence of a nonsense mutation in the VHIID domain or in the SAW domain both resulted in overgrowth phenotypes (Table 5.15). These mutations are predicted to result in C-terminally truncated RHT-A1B proteins that lack the full GRAS functional domain. This inhibits the ability of RHT-A1B to supress GA signalling, resulting in a tall or overgrowth phenotype (Chandler and Harding 2013). Two of the nonsense mutations *Rht-A1b.6* and *7* had an equivalent mutation identified in the *Rht-B1c* screen (*Rht-B1c.33* and 20 respectively), which produced

similar phenotypes. What is interesting about these mutations is that they occur very close to the end of the SAW motif, suggesting that even the loss of the last 5 or 14 amino acids can result in a loss of protein function (Derkx et al. 2017).

5.5.3 Future Experiments

Detailed Field Characterisation of Lines: Following additional rounds of backcrossing, a more extensive characterisation of the intragenic alleles should be conducted in the field. While the glasshouse provided the means to assess the lines within the timeframe of the PhD project, field characterisation would provide a more accurate assessment of their potential for breeding. Characterisation measurements should include:

- **Crop Height**: To assess the dwarfing potential of the *Rht-A1b* suppressor mutants. Measured by harvesting 100 shoots from a plot and measuring their full length and then the lengths of their components (internodes, peduncle and ear).
- **Harvest index**: the grain yield of a wheat crop, expressed as a decimal fraction of the aboveground biomass. This provides an indicator of the ratio of grain and vegetative tissue produced. Higher harvest indexes are desirable in breeding as they demonstrate that a larger amount of the crops biomass is grain (Hay 1995).
- **Hagberg Falling Number (HFN)**: a measure of α-amylase amount and activity in the grain. Measured as the time take for a weighted object to fall through a hot water/flour mixture (Perten 1964). A high HFN is desirable as this represents low α-amylase activity, which is required for breadmaking (Lunn et al. 2001).
-

GA Dose Response Assays: Using the optimised protocol discussed in Chapter 4, GA response assays could be used to confirm that the change in phenotype associated with the suppressor mutants is due to increased GA sensitivity / reduced GA repressive activity (Chandler and Robertson 1999). Early GA response assays in wheat were used to identify GA insensitive alleles (Radley 1970). If tall missense

mutants were found to have a greater response exogenous GA than intermediate mutants, these assays could potentially be used to predict the mature phenotype of suppressor mutants, without having to grow them to maturity (Chandler and Harding 2013).

RNAseq – RNAseq could be used to assess transcription between different suppressor mutants (Wang, Gerstein, and Snyder 2009). This may identify differential expression between mutant lines that could shed light on DELLA structure-function. I.e. which conserved motifs are involved in different DELLA-DIP interactions (Hou et al. 2010; An et al. 2012; Gallego-Bartolome et al. 2012; Hong et al. 2012)

Chapter 6: Characterisation of *Rht-1* Knock-out Lines

6.1 Introduction

As discussed in the previous chapters, DELLA gain-of-function dwarfing alleles in cereals are often caused by mutations that impact the N-terminal region of the protein. These mutations block DELLA binding to the GID1-GA receptor, preventing the formation of the GA-GID1-DELLA complex that is required for targeted degradation of DELLA (Nelson and Steber 2016). In the absence of GA-targeted degradation, DELLA proteins persist in plant tissues, causing constitutive repression of GA signalling (Dill, Jung, and Sun 2001; Murase et al. 2008), the most obvious phenotypic traits associated with these *Rht-1* mutants is a dwarf of semi-dwarf stature and increased grain yield through improved photosynthate partitioning (Hedden 2003; Peng et al. 1997).

The opposite effect is found in DELLA loss-of-function mutants in cereals (Chandler and Robertson 1999; Ikeda et al. 2001). These mutants produce a constitutive GA signalling phenotype, also described as 'slender', with mature plants producing tall slender shoots that are unable to support themselves (Foster 1977). Slender mutants display rapid growth, as if saturated with GA, even in GA deficient backgrounds (Chandler and Robertson 1999; Ikeda et al. 2001) or following treatment with GA biosynthesis inhibitors (Croker et al. 1990). Additionally, although they produce ears that are up to twice the length of WT ears, barley ears are sterile and do not produce pollen (Foster 1977).

In rice, the first DELLA *slender* mutant to be identified and characterised was *slr1-1*. This was the result of a single base pair deletion in the nuclear localization signal domain, which produced a frameshift mutation that abolished protein production (Ikeda et al. 2001). Subsequent studies have demonstrated that the introduction of missense and nonsense mutations into the SLR1 C-terminal GRAS domain also produce a slender phenotype in transgenic lines (Figure: 6.1) (Hirano et al. 2012).

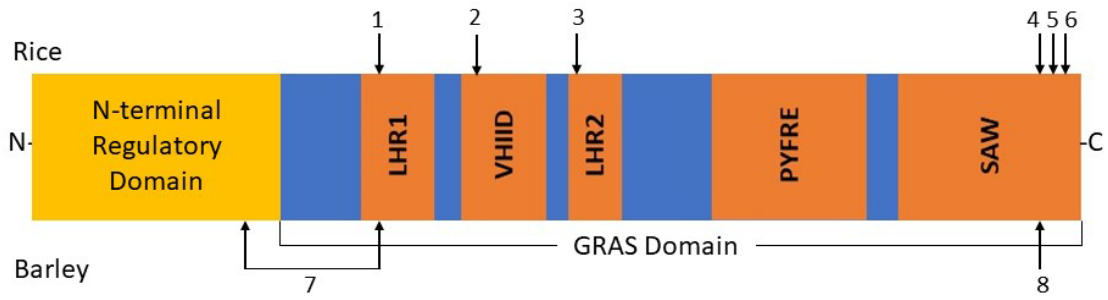

Figure 6.1: Schematic Diagram of DELLA. Conserved motifs of the GRAS domain are shown in orange. The approximate locations of loss-of-function mutations are shown. Rice mutants: 1 = *slr1-6* (V281D), 2 = 420 (DLE420AAA), 3= 321 (PLY321AA), 4 = *slr1-3* (W609*), 5 = *slr1-7* (T617P) and 6= *slr1-4* (W620*). Barley mutants: 7 = *sln1b* (frameshift mutation in codon 93 (ACC to A-C) resulting in W252*), 8 = *sln1c* (W602*).

The severity of the slender phenotype varies according to the mutation and position. Nonsense mutations (*slr1-3* and *slr1*-4) produced the most severe slender phenotypes, whilst missense mutations in the LHR1 (*slr1*-6) and SAW (*slr1*-7) motifs also caused more severe phenotypes compared to mutations in VHIID (420) and LHRII (321) (Hirano et al. 2012). The Similarly, in barley nonsense mutations result in a slender phenotype (Figure 6.3.01). *Sln1b* is caused by a single base deletion in codon 98 (ACC to A-C), resulting in a frameshift and a subsequent nonsense mutation at position 252 (W252*) that is expected to result in a prematurely truncated protein lacking all of the functional GRAS domain. The barley *sln1c* mutant also contains another DELLA nonsense mutant (W602*), which affects the extreme 3' end of the coding sequence (Chandler et al. 2002). At present, it has not yet been established whether loss-of-function mutations in the wheat *RHT-1* genes result in a slender phenotype.

The three *Rht-1* genes have similar expression profiles in the elongating stem (Figure 1.14), but it has also not been determined whether there is functional redundancy or homoeologue specificity in the three homoeologues as is seen in the five *Arabidopsis* DELLA paralogues (Gallego-Bartolome et al. 2010; Tyler et al. 2004). Homoeologue specificity has previously been identified in the GA biosynthesis gene, *TaGA1ox-B1,* which encodes a GA 1-oxidase and is only present in the B-genome. TaGA1ox-B1 is expressed only in developing grains (Pearce et al. 2015) and believed

to responsible for the high levels of 1β-hydroxylated GAs in developing grains (Gaskin et al. 1980).

Generating and stacking knock out lines for each homoeologous *Rht-1* gene will allow us to establish whether a slender phenotype can be generated in wheat and examine whether there is homoeologue specificity. Additionally, a reverse genetics-based approach generating and characterising knock outs of the *RHT-1* genes, will enable us to confirm whether *RHT-A1*, *RHT-B1* and *RHT-D1* are the key DELLA genes controlling GA-responsive growth in wheat. A recent phylogenetic study has demonstrated that cereals contain DELLA-related (DGLLA) proteins that do not exist in *Arabidopsis* (Van de Velde, Ruelens, et al. 2017). These related genes encode predicted proteins characterised by slightly different conserved motifs: DGLLA and LERLE instead of DELLA and LEQLE. Overexpression of the rice DGLLA, SLRL1, results in severe GA-insensitivity and dwarfism, suggesting that it has similar GA suppressive activity to the DELLA SLR1 (Itoh et al. 2005). Furthermore, SLRL1 is not degraded in the presence of GA and its expression is reduced in *gid1* mutants that accumulate SLR1. This suggests that SLRL1 may function as a backup GA repressor, when SLR1 levels decline (Fukao and Bailey-Serres 2008).

Prior to the start of this project a Cadenza population containing the WT *RHT-1* alleles (*Rht-A1a, Rht-B1a* and *Rht-D1a*) was mutagenised using ethyl methanesulfonate (EMS). An M2 population, consisting of 2200 individuals was screened to identify novel *Rht-1* mutations using a TILLING based approach (Chen et al. 2014). Three nonsense mutations; W615*, W616* and W559* in *Rht-A1, Rht-B1* and *Rht-D1* respectively, were identified (Figure 6.2).

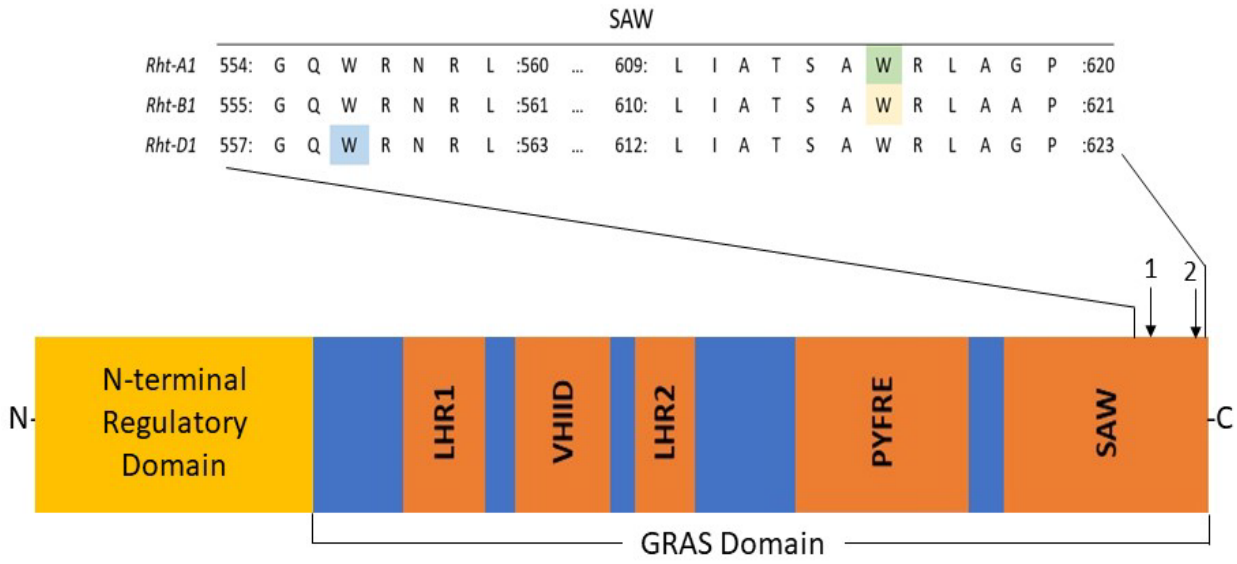

Figure 6.2: Schematic Diagram of RHT, Showing the Locations of Nonsense Mutations. Conserved motifs of the GRAS domain are shown in orange. The approximate locations of the nonsense mutations in the SAW motif are shown with arrows. 1 = W559* in *Rht-D1, 2* = W615* and W616* in *Rht-A1* and *Rht-B1* respectively.

The *Rht-1* nonsense mutations that were identified are located in the SAW motif coding domain, the same as *slr1-3 (*W609*), slr1-4* (W620*) and *sln1c* (W602*) in rice and barley (Figure 6.1) (Chandler et al. 2002; Ikeda et al. 2001). Based on their position in the coding sequence, they are predicted to cause a loss-of-function phenotype. To establish whether loss of function mutations affect the wheat phenotype a triple mutant, made from stacking the three genes, was produced by Dr Stephen Thomas.

Two rounds of backcrossing to Cadenza was performed to remove ~75% of background mutations, introduced into the genome during the EMS mutagenesis (Derkx et al. 2017). Lines were then crossed together to generate BC_2F_2 single or double mutant lines. As the triple mutant was male sterile, this was generated by identifying BC_2F_2 double mutants that were heterozygous for the third mutations and then identifying the triple mutants in BC_2F_3 segregating lines. All material that was characterised was at the BC_2F_3 Generation.

To assess whether there are phenotypic characteristics associated with each homoeologue, 5 individuals per line, plus five wild type Cadenza (var.) controls were grown up under standard conditions in the glasshouse (Section 2.1) in a randomised

block design. Phenotypic measurements were then taken during plant development and at maturity. This chapter will discuss the outcomes of this characterisation experiment.

6.2 Results

6.2.1 Heading date

Loss of function DELLA mutants are characterised by their rapid growth rate (Foster 1977), resulting in earlier ear emergence (Lanahan and Ho 1988). To examine whether this trait is found in the triple knock out line and to establish if there is any homoeologue specificity in its control, the number of days between germination and first heading date was recorded. Residual plots for this data were assessed in GenStat, which confirmed that the data was Normal and did not require transformation. A General Analysis of Variance (ANOVA) was conducted, the output of which is described in Table 6.1 and Figure 6.3.

Table 6.1: ANOVA Output for Heading date in Rht knock out and Control Lines

Line	Heading date (days)	SD (±)	Days Difference from *Rht-1*	P-Value	SED	LSD
WT Cadenza (Rht-1)	82.4	1.5	NA			
AABBDD	83.4	0.9	1			
aaBBDD	84.4	0.9	2			
AAbbDD	81	0.9	-1.4			
AABBdd	83.4	1.3	1	<.001	1.2	2.3
AAbbdd	**79.4**	2.6	-3			
aaBBdd	84	2.9	1.6			
aabbDD	83.6	0.5	1.2			
aabbdd	**78.2**	3.1	-4.2			

The mean value is shown with its standard deviation (SD), along with the standard error of differences (SED) and 5% least significant difference of means (LSD 5%). Means shown in bold are significantly different from *Rht-1,* underlined means are significantly different from the null segregant (AABBDD).

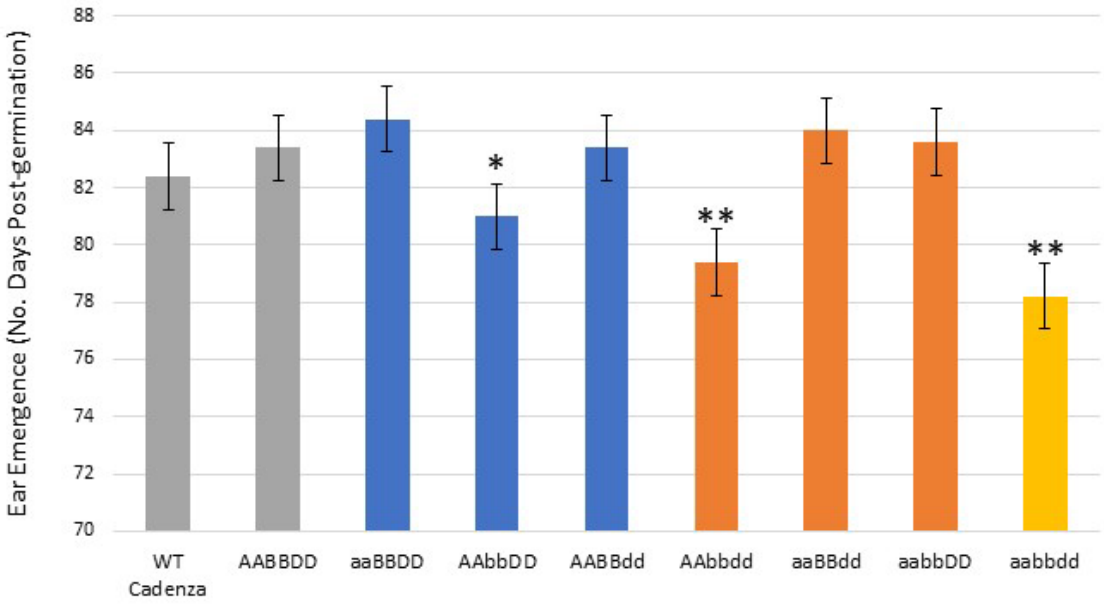

Figure 6.3: Average Time for First Heading date in *Rht-1* Knock Out Lines and WT Cadenza Control. Shown as number of days post-germination. Grey = no loss of function mutations, blue = single loss of function mutant, orange = double loss of function mutant and yellow = triple loss of function mutant. Capital letters (AA, BB and DD) denote wild-type homeologues, lower case letters denote loss of function mutations; aa = W615*, bb = W616* and dd = W559*, in *Rht-A1, Rht-B1* and *Rht-D1* respectively. All lines are in the Cadenza (var.). ANOVA P-Value = <0.001. Error Bars = standard error of differences of means (1.2). * denotes a result significantly different from AABBDD. ** denotes a result significantly different from WT Cadenza and AABBDD.

The ANOVA confirmed a highly significant interaction between genotype and the time taken for first heading date ($p<0.001$). The least significant difference of means (2.3) was used to assess which genotypes produced significantly different heading dates from each other. There was no significant difference between WT Cadenza and the null segregant control (AABBDD). The single mutant AAbbDD, demonstrated a significantly faster heading date (2.4 days) than the null segregant (AABBDD) line but was not significantly different from the WT Cadenza control (1.4 days). The double mutant AAbbdd and the triple mutant aabbdd produced the fastest ear emergence times (3 and 4.2 days earlier than WT Cadenza) but were not significantly different from each other.

6.2.2 Flag Leaf Characteristics

Loss-of-function DELLA mutants produce significantly longer, narrower leaves than their WT counterparts (Foster 1977). To establish whether the triple knock out mutant produces this phenotype and examine whether there is a specific homoeologue controlling this characteristic flag leaf dimensions (leaf length and width measurements) were taken for three shoots per plant, approximately one week after heading. Residual plots for this data were assessed in GenStat, which confirmed that the data was Normal and did not require transformation. A General Analysis of Variance (ANOVA) was conducted, the output of which is described in Table 6.2 and Figure 6.4.

Table 6.2: ANOVA Output for Flag Leaf Dimensions (mm) in Rht-1 knock out and Control Lines

Line	Leaf Width (mm)	% Difference from *Rht-1*	Leaf Length (mm)	% Difference from *Rht-1*
WT Cadenza (Rht-1)	18.7 ± 1.9	NA	356.4 ± 38.4	NA
AABBDD	18.2 ± 1.8	97.5	342.9 ± 78.6	96.2
aaBBDD	17.7 ± 1.5	94.6	365.3 ± 46.6	102.5
AAbbDD	17.4 ± 1.7	93.2	351 ± 60.7	98.5
AABBdd	17.2 ± 2.1	91.4	354.2 ± 71.3	99.4
AAbbdd	**15.1 ± 3.2**	81.0	345.4 ± 67.3	96.9
aaBBdd	**15.5 ± 2.9**	82.9	321.3 ± 61.3	90.2
aabbDD	**19.2 ± 1.5**	102.8	352.1 ± 30.4	98.8
aabbdd	**12.4 ± 2.7**	66.4	**405.9 ± 51.7**	113.9
P-Value	<0.001		0.026	
SED	0.8		21.2	
LSD	1.6		42	

The mean value is shown with its standard deviation (SD), along with the standard error of differences (SED) and 5% least significant difference of means (LSD 5%). Means shown in bold are significantly different from *Rht-1,* underlined means are significantly different from the null segregant (AABBDD).

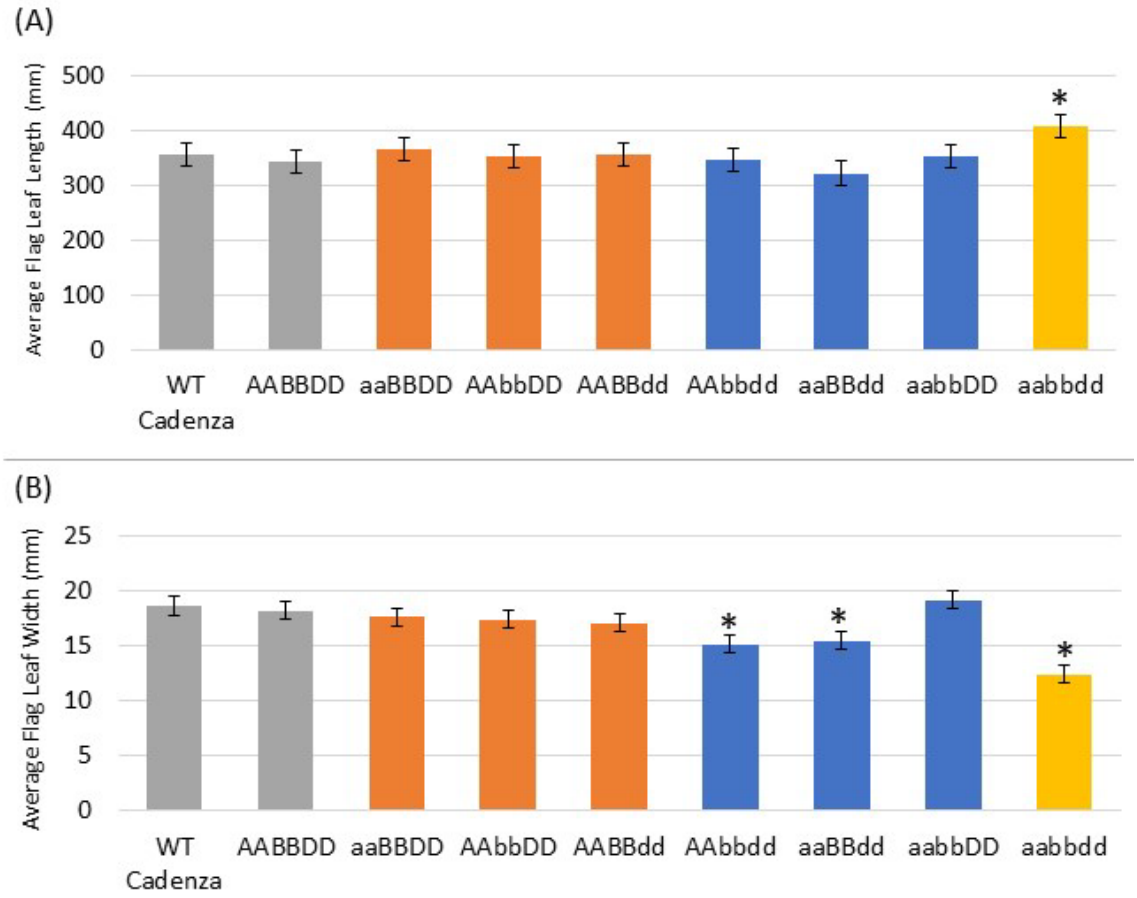

Figure 6.4: Average Flag Leaf Dimensions (mm) in *Rht-1* Knock Out Lines and WT Cadenza Control. Grey = no *RHT-1* mutations, blue = single loss of function mutant, orange = double loss of function mutant and yellow = triple loss of function mutant. Capital letters (AA, BB and DD) denote wild-type homeologues, lower case letters denote loss of function mutations; aa = W615*, bb = W616* and dd = W559*, in *Rht-A1, Rht-B1* and *Rht-D1* respectively. All lines are in the Cadenza (var.). * denotes a result significantly different from AABBDD, ** denotes a result significantly different from AAbbdd and aaBBdd. **(A) Average Flag Leaf Length (mm).** ANOVA P-value = 0.026. Error Bars = standard error of differences of means (SED) (21.24 on 126d.f.). **(B) Average Flag Leaf Width (mm).** ANOVA P-value = <0.001. Error Bars = standard error of differences of means (SED) (0.82 on 126d.f.).

The ANOVA assessing flag leaf length (Figure 6.3B) confirmed a highly significant interaction between genotype and flag leaf length (0.026). The least significant difference of means (42) determined that the triple mutant (aabbdd) produced significantly longer flag leaves (113% the length of WT Cadenza) than the other genotypes, which were not significantly different from one another.

The ANOVA assessing flag leaf width (Figure 6.3C) confirmed a highly significant interaction between genotype and flag leaf length ($p<0.001$). The least significant

difference of means (1.6) determined that the triple mutant and double mutants; AAbbdd and aaBBdd produced significantly narrower flag leaves than the other genotypes (66.4%, 81% and 82.9% respectively).

6.2.3 Plant Height

Changes in plant height are the most obvious effects of DELLA gain-of-function (dwarf phenotype) or loss-of-function mutations (slender phenotype). The slender rice and barley mutants are characterised by their GA overdose phenotype: over-elongated shoots that are unable to support themselves (Ikeda et al. 2001; Chandler et al. 2002; Foster 1977). In barley this has been shown to be due to hyper-elongated internodes and ears (Lanahan and Ho 1988). To assess the effect that knocking out the three *RHT-1* homoeologues has on wheat height, ear and internode measurements were taken for the three tallest shoots per plant. Residual plots for this data were assessed in GenStat, which confirmed that the data was Normal and did not require transformation. A General Analysis of Variance (ANOVA) was conducted on each data set, the output of which is described in Table 6.3 and Figure 6.5

Table 6.3: ANOVA Output for Shoot Length (mm) in Rht-1 knock out and Control Lines

Line	Shoot Length (mm)	SD (±)	% Difference from *Rht-1*	P-Value	SED	LSD
WT Cadenza (Rht-1)	941.1	34.3	NA	<0.001	23.7	47.1
AABBDD	**815.3**	35.4	86.6			
aaBBDD	**893.8**	35.2	95.0			
AAbbDD	**810.9**	37.4	86.2			
AABBdd	**785.7**	49.5	83.5			
AAbbdd	**822.5**	38.5	87.4			
aaBBdd	**767.8**	126	81.6			
aabbDD	**863.1**	38.2	91.7			
aabbdd	**1195.4**	54.4	127.0			

The mean value is shown with its standard deviation (SD), along with the standard error of differences (SED) and 5% least significant difference of means (LSD 5%). Means shown in

bold are significantly different from *Rht-1,* underlined means are significantly different from the null segregant (AABBDD).

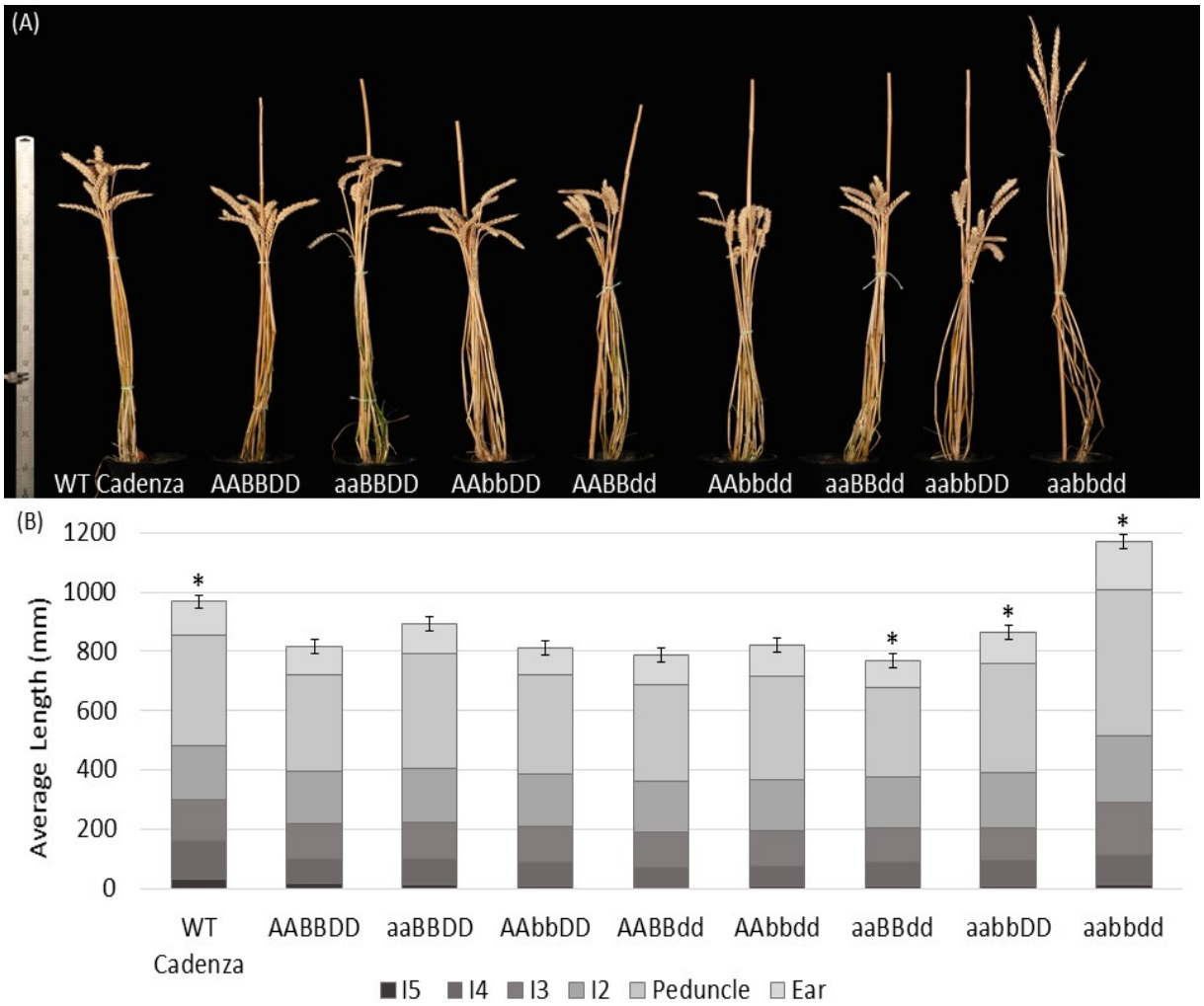

Figure 6.5: (A) Photograph of mature *Rht-1* Knock Out (KNOCK OUT) Lines and a WT Cadenza Control. Capital letters (AA, BB and DD) denote wild-type homeologues, lower case letters denote loss of function mutations; aa = W615*, bb = W616* and dd = W559*, in *Rht-A1, Rht-B1* and *Rht-D1* respectively. All lines are in the Cadenza (var.). Meter ruler is shown on the left for scale. **(B) ANOVA output comparing total plant height for each line.** p<0.001, error bars = standard error of means (SED) (26.70 on 96d.f.). The average length of the different shoot segments; ear, peduncle, internode 2 (I2), internode 3 (I3), internode 4 (I4) and internode 5 (I5), for each line are shown. A result significantly different from AABBDD is denoted with an *.

A ANOVA confirmed that there was a significant interaction between genotype and total shoot length (p<0.001), as shown in Figure 6.5A. The least significant difference of means (47.1) confirmed that WT Cadenza produced shoots

significantly longer than the null segregant (AABBDD) (86.6% the length of WT Cadenza*)*, although this may be due to Cadenza growing longer than anticipated in this characterisation (usually 80-85cm, Section 4.4.3 and 5.2.2). There was no significant difference between the null segregant and the double mutant AAbbdd. The double mutant aaBBdd produced the shortest shoots (81.6%) whilst the double mutant aabbDD produced shoots that were significantly longer than the null segregant (91.7%). The triple mutant (aabbdd) produced the longest shoots overall, 127% the length of WT Cadenza.

To determine the effect genotype has on the length of different internode segments additional ANOVAs were conducted (Table 6.4 and Figure 6.6).

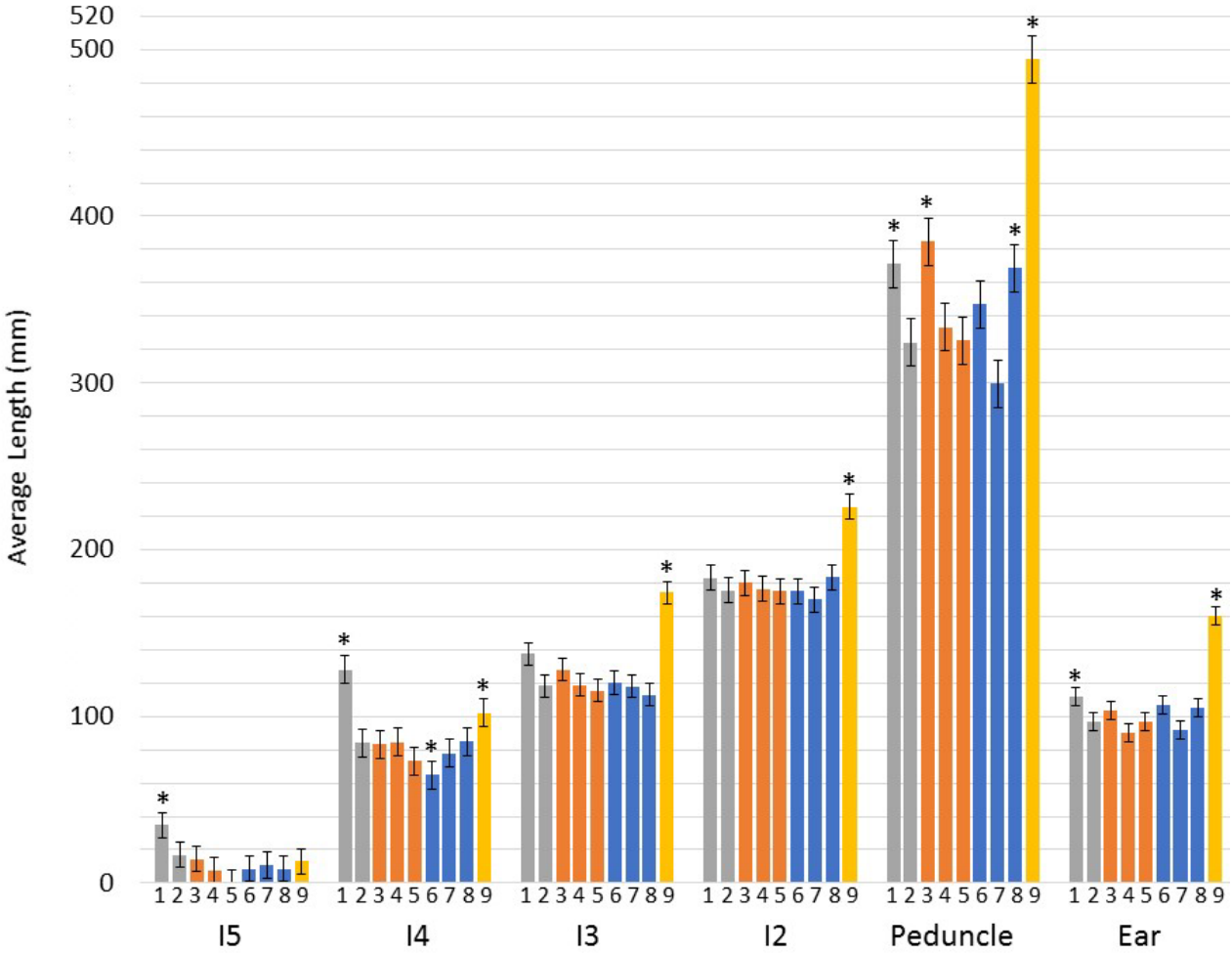

Figure 6.6: ANOVA output comparing shoot segments for *RHT-1* knocknock outut lines and controls. 1 = Cadenza, 2 = AABBDD, 3 = aaBBDD, 4 = AAbbDD, 5 = AABBdd, 6 = AAbbdd, 7 = aaBBdd, 8 = aabbDD and 9 = aabbdd. Capital letters (AA, BB and DD) denote wild-type homeologues, lower case letters denote loss of function mutations; aa = W615*, bb = W616* and dd = W559*, in *Rht-A1, Rht-B1* and *Rht-D1* respectively. All lines are in the Cadenza (var.). **Internode 5** (I5) p=0.003, error bars = standard error of means (SED) (7.57 on 96d.f). **Internode 4** (I4) p<0.001, error bars = SED (8.35 on 96d.f). **Internode 3** (I3) p<0.001, error bars = SED (6.77 on 96d.f). **Internode 2** (I2) p<0.001, error bars = SED (7.57 on 96d.f). **Peduncle** p<0.001, error bars = SED (14.19 on 96d.f). **Ear** p<0.001, error bars = SED (5.43 on 96d.f). A

Table 6.4: ANOVA Outputs for Shoot Segments (mm) in RHT-1 knock-out and Control Lines

Line	Internode 5	% Difference from *Rht-1*	Internode 4	% Difference from *Rht-1*	Internode 3	% Difference from *Rht-1*	Internode 2	% Difference from *Rht-1*	Peduncle	% Difference from *Rht-1*	Ear	% Difference from *Rht-1*
WT Cadenza (Rht-1)	34.8 ± 18.3	NA	102.1 ± 17.4	NA	137.5 ± 7.9	NA	182.9 ± 10.5	NA	371.5 ± 32.5	NA	112.2 ± 4.9	NA
AABBDD	**16.7 ± 20.4**	48.0	**83.9 ± 19.5**	82.2	**118.3 ± 6.9**	86.0	175.4 ± 10.1	95.9	**324 ± 27.1**	87.2	97 ± 11.5	86.5
aaBBDD	**14.2 ± 5.8**	40.8	**83.2 ± 19.9**	81.5	127.8 ± 8.5	92.9	180.2 ± 10.5	98.5	384.6 ± 34.6	103.5	103.7 ± 5.9	92.4
AAbbDD	**7.7 ± 5.2**	22.1	**84.6 ± 13.5**	82.9	**118.7 ± 8.8**	86.3	176.5 ± 13.9	96.5	**333.4 ± 29.9**	89.7	**90 ± 27**	80.2
AABBdd	**0**	0.0	**73.2 ± 17.6**	71.7	**115.3 ± 30.3**	83.9	175.2 ± 27.4	95.8	**325.3 ± 32.7**	87.6	96.6 ± 5.5	86.1
AAbbdd	**8.5 ± 9.8**	24.4	**65 ± 18.4**	63.7	**120.1 ± 9.3**	87.3	175.1 ± 20.6	95.7	**347 ± 33.9**	93.4	106.8 ± 8.8	95.2
aaBBdd	**10.8 ± 8.5**	31.0	**77.7 ± 22**	76.1	**117.8 ± 16.4**	85.7	170.2 ± 27.8	93.1	**299.7 ± 53.1**	80.7	**91.4 ± 16.4**	81.5
aabbDD	**8.6 ± 5.8**	24.7	**84.7 ± 23.2**	83.0	**113 ± 28.3**	82.2	183.3 ± 12.7	100.2	368.7 ± 29.3	99.2	104.8 ± 7.6	93.4
aabbdd	**13.1 ± 38.8**	37.6	**21.9**	125.3	**174.1 ± 13.4**	126.6	**225.7 ± 21**	123.4	**494.2 ± 34.8**	133.0	**160.4 ± 21.2**	143.0
P-Value	0.003		<0.001		<0.001		<0.001		<0.001		<0.001	
SED	7.6		8.4		6.8		7.6		14.2		5.4	
LSD	15		16.6		13.4		15		28.2		10.8	

The mean value is shown with its standard deviation (SD), along with the standard error of differences (SED) and 5% least significant difference of means (LSD 5%). Means shown in bold are significantly different from *Rht-1,* underlined means are significantly different from the null segregant (AABBDD).

The ANOVAs confirmed that there was a significant interaction between genotype and the internode and ear length ($p<0.001$ or $p=0.003$) (Table 6.4).

The 5% least significant difference of means (LSD) was used to confirm which genotypes produced significantly longer or shorter segment lengths. These confirmed that the two tallest genotypes WT Cadenza (*Rht-1*) and the triple knock out generally produced the longest internode and ear lengths. The GA-overdose phenotype of the triple knock out, was due to the accumulative effect of its internode 4, 3, 2, peduncle and ear elongation, which were 125.3%, 126.6%, 123.4%, 133% and 143% the length of *Rht-1* respectively. The double mutant aabbDD produced shoots longer than the null segregant (AABBDD) because of significantly increased internode 2, peduncle and ear elongation (100.2%, 99.2% and 93.4% the length of *Rht-1,* compared to 95.9%, 87.2% and 86.5% with AABBDD). The double mutant aaBBdd produced significantly shorter shoots than AABBDD (Table 6.3) due to the accumulative effect of reduced elongation in all the shoot segments, although none of these individual measurements were significantly different from AABBDD (Table 6.4).

6.2.4 Shoots

The slender barley mutant exhibits basal internode elongation alongside shooting, resulting in aerial branching (Foster 1977). The shooting characteristics of slender rice have not been reported (Ikeda et al. 2001). However, SLR1 gain of function mutants (*slr1-d1*) have been found to produce a greater number of shoots by stabilising the shoot regulator MONOCULM 1 (MOC1) against GA mediated degradation. Loss of function mutants may therefore result in increased MOC1 degradation and lower shoot number. To assess whether loss-of-function *RHT-1* mutations affect wheat shooting, the number of shoots per plant were counted for each plant. Residual plots for this data were assessed in GenStat, which confirmed that the data was Normal and did not require transformation. A General Analysis of Variance (ANOVA) was conducted on each data set, the output of which is described in Table 6.5 and Figure 6.7.

Table 6.5: ANOVA Output for Shoot Number in RHT-1 Knock out and Control Lines

Line	Shoot Number	SD (±)	% Difference from *Rht-1*	P-Value	SED	LSD
WT Cadenza (Rht-1)	10	1.8	NA	<0.001	1	2.1
AABBDD	10.8	1.5	107.5			
aaBBDD	11.3	1.5	112.5			
AAbbDD	**12.3**	1.5	122.5			
AABBdd	11	0.8	110.0			
AAbbdd	10.8	2.2	107.5			
aaBBdd	10.7	2.5	106.7			
aabbDD	8	1.4	80.0			
aabbdd	**4.8**	0.5	47.5			

The mean value is shown with its standard deviation (SD), along with the standard error of differences (SED) and 5% least significant difference of means (LSD 5%). Means shown in bold are significantly different from *Rht-1,* underlined means are significantly different from the null segregant (AABBDD).

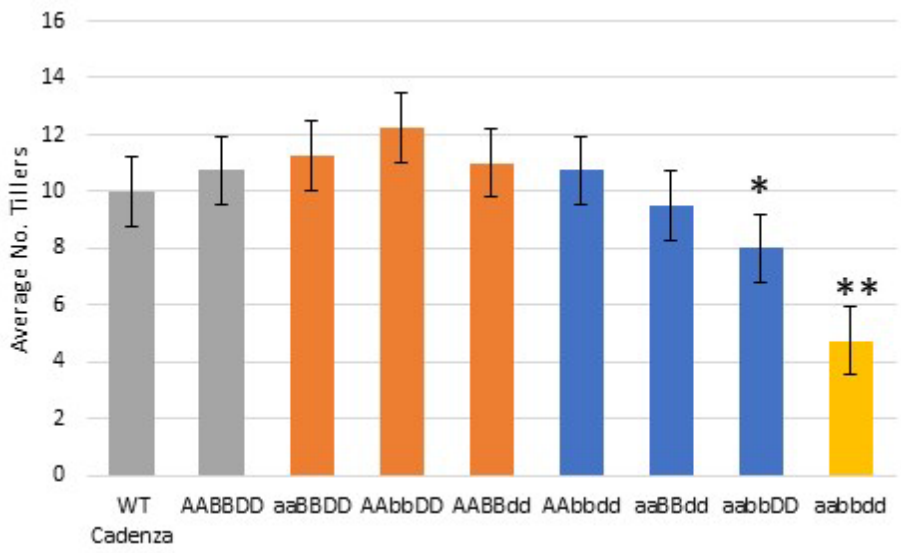

Figure 6.7: Average Shoot Number per Plant in *Rht-1* Knock Out Lines and WT Cadenza Control. Grey = no loss of function mutations, blue = single loss of function mutant, orange = double loss of function mutant and yellow = triple loss of function mutant. Capital letters (AA, BB and DD) denote wild-type homeologues, lower case letters denote loss of function mutations; aa = W615*, bb = W616* and dd = W559*, in *Rht-A1, Rht-B1* and *Rht-D1* respectively. All lines are in the Cadenza (var.). ANOVA P-Value = <0.001. Error Bars = standard error of differences of means (1). * denotes a result significantly different from AABBDD. ** denotes a result significantly different from WT Cadenza and AABBDD.

The ANOVA confirmed that there was a significant interaction between genotype and the number of shoots per plant. The 5% LSD (2.1) was used to assess which genotypes were significantly different from one another. This identified that the double mutant aabbDD and the triple mutant aabbdd produced significantly fewer shoots than the other phenotypes (80% and 47.5% the number of shoots compared to WT Cadenza). The single mutant AAbbDD also produced significantly more shoots per plant than WT Cadenza (122.5%) but was not significantly different from the null segregant .

6.2.5 Spikelet Number

There is no recorded association between spikelet number and DELLA loss of function mutations (Ikeda et al. 2001; Chandler et al. 2002). However as previously discussed (Section 4.2.4) barley gain-of-function DELLA mutants have been shown to produce significantly fewer spikelets per ear due to reduced spikelet initiation (Serrano-Mislata et al. 2017), therefore in is conceivable that loss-of-function mutations may result in increased spikelet number. To establish whether this is the case, the number of spikelets were counted on three ears per plant. Residual plots for this data were assessed in GenStat, which confirmed that the data was Normal and did not require transformation. A General Analysis of Variance (ANOVA) was conducted on each data set, the output of which is described in Table 6.6 and Figure 6.8

Table 6.6: ANOVA Output for Spikelet Number per Ear in RHT-1 Knock out and Control Lines

Line	Spikelet No.	SD (±)	% Difference from *Rht-1*	P-Value	SED	LSD
WT Cadenza (Rht-1)	21.5	0.9	NA	<0.001	0.6	1.2
AABBDD	**20.1**	1.2	93.5			
aaBBDD	20.2	0.8	94.0			
AAbbDD	**19.8**	1.7	92.1			
AABBdd	**19**	1.3	88.4			
AAbbdd	**19.4**	1.6	90.2			
aaBBdd	**17.8**	2.9	82.8			
aabbDD	20.4	1.4	94.9			
aabbdd	**17.7**	1.7	82.3			

The mean value is shown with its standard deviation (SD), along with the standard error of differences (SED) and 5% least significant difference of means (LSD 5%). Means shown in bold are significantly different from *Rht-1,* underlined means are significantly different from the null segregant (AABBDD)

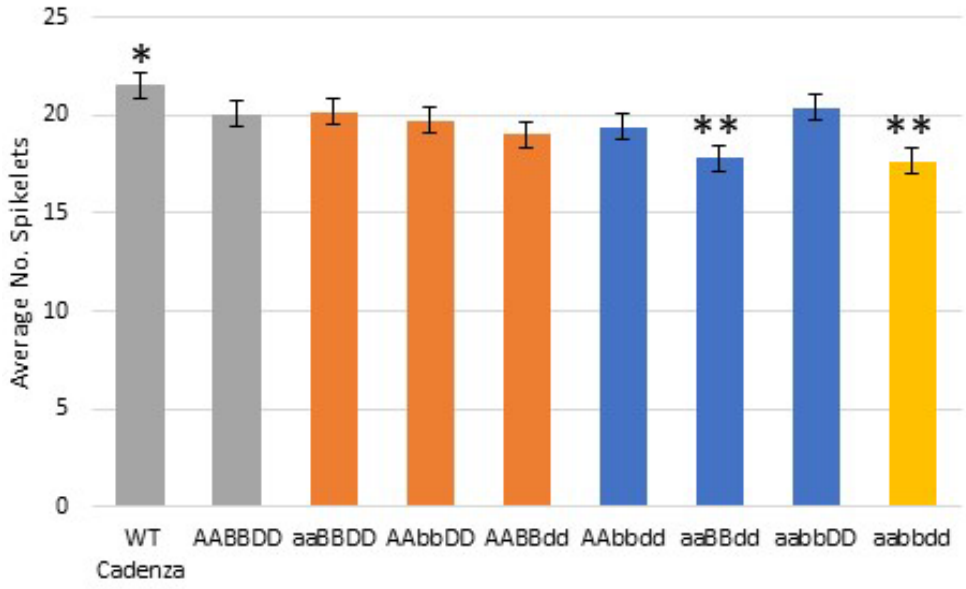

Figure 6.8: Average No. Spikelets per Ear in *Rht-1* Knock Out Lines and WT Cadenza Control. Grey = no loss of function mutations, blue = single loss of function mutant, orange = double loss of function mutant and yellow = triple loss of function mutant. Capital letters (AA, BB and DD) denote wild-type homeologues, lower case letters denote loss of function mutations; aa = W615*, bb = W616* and dd = W559*, in *Rht-A1, Rht-B1* and *Rht-D1* respectively. All lines are in the Cadenza (var.). ANOVA P-Value = <0.001. Error Bars = standard error of differences of means (0.6). * denotes a result significantly different from AABBDD. ** denotes a result significantly different from WT Cadenza and AABBDD.

The ANOVA confirmed that there was a significant interaction between genotype and the number of spikelets per ear (P<0.001). The 5% LSD (1.2) was used to confirm which genotypes produced a significantly different number of spikelets per ear. This demonstrated that WT Cadenza produced the most spikelets per ear (21.5) in comparison to all other genotypes. The double mutant aaBBdd and the triple mutant aabbdd also produced the fewest number of spikelets per ear (17.8 and 17.7, 82.8% and 82.3% the number of spikelets per ear of WT Cadenza). There was no significant difference between the other genotypes.

6.2.6 Grain Number Per Ear

DELLA loss-of-function mutations are associated male sterility (Foster 1977; Lanahan and Ho 1988) due to disrupted pollen production (Croker et al. 1990). To assess whether this phenotype is present in the triple knock out and if there is homoeologue specific control, the total number of grains per plant were counted and then divided by the number of shoots for that plant (Section 2.3.3). Residual plots for this data were assessed in GenStat, which confirmed that the data was Normal and did not require transformation. A General Analysis of Variance (ANOVA) was conducted on each data set, the output of which is described in Table 6.7 and Figure 6.9.

Table 6.7: ANOVA Output for No. Grain per Ear in Rht-1 knock out and Control Lines

Line	Grain No. Per Ear	SD (±)	% Difference from *Rht-1*	ANOVA including aabbdd			ANOVA excluding aabbdd
				P-Value	SED	LSD	P-Value
WT Cadenza (*Rht-1*)	51.5	3.3		<0.001	5.1	10.5	0.075
AABBDD	44.2	6.5	85.8				
aaBBDD	44.8	5.5	87.0				
AAbbDD	44.1	10.5	85.6				
AABBdd	42.7	10.8	82.9				
AAbbdd	46.9	4.5	91.1				
aaBBdd	44.7	27.2	86.8				
aabbDD	57.1	10.8	110.9				
aabbdd	**0**	0	0.0				

The mean value is shown with its standard deviation (SD), along with the standard error of differences (SED) and 5% least significant difference of means (LSD 5%). Means shown in bold are significantly different from *Rht-1,* underlined means are significantly different from the null segregant (AABBDD).

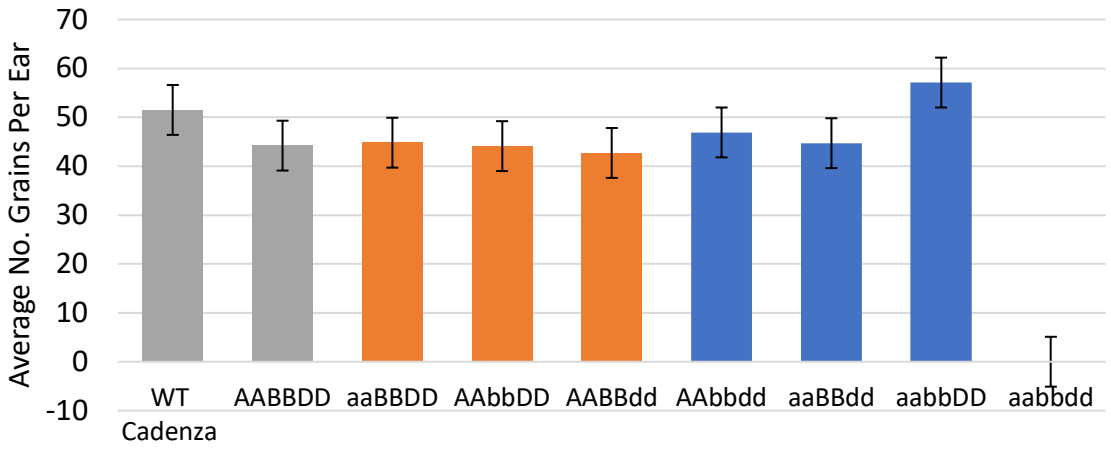

Figure 6.9: Average No. Grains per Ear in *Rht-1* Knock Out Lines and WT Cadenza Control. Grey = no loss of function mutations, blue = single loss of function mutant, orange = double loss of function mutant and yellow = triple loss of function mutant. Capital letters (AA, BB and DD) denote wild-type homeologues, lower case letters denote loss of function mutations; aa = W615*, bb = W616* and dd = W559*, in *Rht-A1, Rht-B1* and *Rht-D1* respectively. All lines are in the Cadenza (var.). ANOVA P-Value = <0.001. Error Bars = standard error of differences of means (0.6). * denotes a result significantly different from AABBDD. ** denotes a result significantly different from WT Cadenza and AABBDD.

Initially, the ANOVA was conducted using all the available data. This identified that there was a significant interaction between genotype and the number of grains per ear ($p<0.001$). The 5% LSD (10.5) was then used to assess which genotypes produced significantly different results. This identified that only the triple mutant produced a significant result as these plants produced no grain. The ANOVA was repeated excluding the aabbdd data and the returned p-value was non-significant (0.075). This confirmed that grain number is only affected in the triple mutant, there is no significant effect on grain number in the other genotypes.

6.2.7 Grain Size (mm^2)

To assess the effect of loss of function mutations on grain size, a Marvin grain analyser (INDOSAW, India) was used to measure the area (mm^2) of 120-150 randomly selected grain from each plant that produced grain (therefore aabbdd was excluded from this analysis) (Section 2.3.3). Residual plots for this data were assessed in GenStat, which confirmed that the data was Normal and did not require transformation. An Unbalanced Analysis of Variance (ANOVA) was conducted on the data set, the output of which is described in Table 6.8 and Figure 6.10.

Table 6.8: ANOVA Output for Grain Size (mm^2) in Rht-1 knock out and Control Lines

Line	Grain Size (mm^2)	SD (±)	% Difference from *Rht-1*	P-Value	SED	LSD
WT Cadenza (Rht-1)	21.3	3.1	NA			
AABBDD	**20.**	2.4	94.2			
aaBBDD	**20.1**	2.6	94.7			
AAbbDD	**20.1**	2.8	94.7	<0.001	0.2	0.3
AABBdd	**20.9**	2.9	98.5			
AAbbdd	**19.6**	2.9	92.0			
aaBBdd	21.2	3	99.7			
aabbDD	**20**	2.5	94.1			

The mean value is shown with its standard deviation (SD), along with the standard error of differences (SED) and 5% least significant difference of means (LSD 5%). Means shown in bold are significantly different from *Rht-1,* underlined means are significantly different from the null segregant (AABBDD).

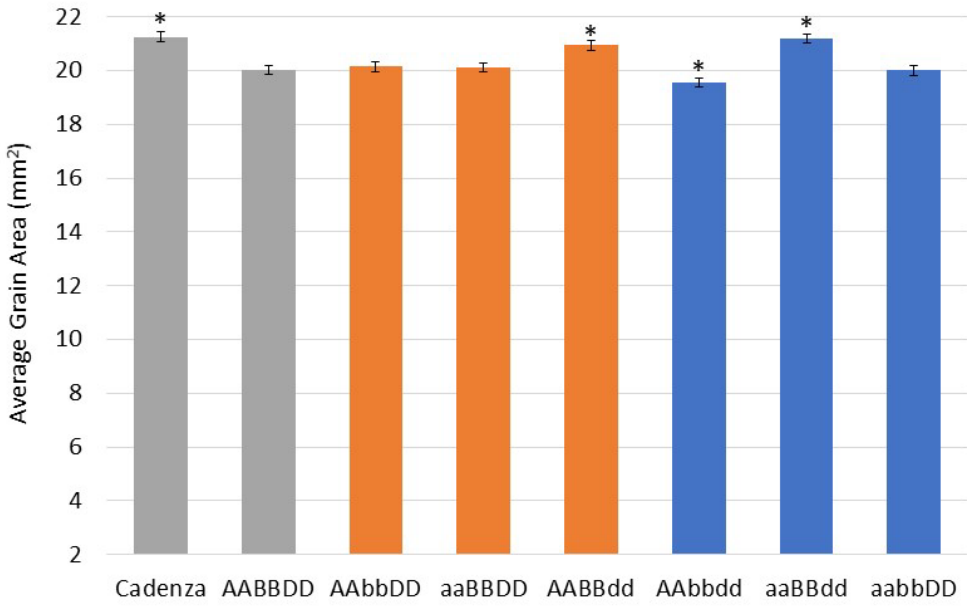

Figure 6.10: Grain Area (mm^2) for *Rht* KNOCK OUTs and Cadenza (*Rht-1)* controls. Grey = no mutations, blue = single loss of function mutant, orange = double loss of function mutant. Capital letters (AA, BB and DD) denote wild-type homeologues, lower case letters denote loss of function mutations; aa = W615*, bb = W616* and dd = W559*, in *Rht-A1, Rht-B1* and *Rht-D1* respectively. The triple mutant (aabbdd) was not included in this analysis as it didn't set grain. All mutations are backcrossed into Cadenza (var). * denotes a measurement significantly different from AABBDD. Error bar = standard error of means 0.2.

The ANOVA confirmed that there was a significant interaction between grain area and genotype ($P<0.001$). The least significant difference of means (LSD) 0.3 was used to determine which genotypes produced significantly different grain sizes from each other. WT Cadenza produced significantly larger grains than AABBDD (94.2% the size of WT Cadenza). There was no significant difference between AABBDD and AAbbDD, aaBBDD and aabbDD. The single mutant AAbbdd produced the smallest grains (92%), whilst AABBdd and aaBBdd produced larger grains than AABBDD (98.5% and 99.7% the size of WT Cadenza respectively).

6.3 Discussion

6.3.1 The *Rht-1* Triple Mutant Displays a Slender Phenotype

The *Rht-1* triple knock out mutant produced a consistent slender DELLA loss-of-function phenotype, consistent with what has been observed in rice (*slr1*) and barley (*sln1*) (Foster 1977; Ikeda et al. 2001). The most obvious similarity was the production of over-extended internodes (Section 6.2.3), which may contribute to the earlier heading date than the other knock out lines and controls (Section 6.2.1). More detailed characterisation will be required to establish whether the triple also displays changes to floral transition, by recording when different developmental stages were met (e.g. four-leaf stage, five-leaf stage, seven-leaf stage, booting and anthesis) (Derkx et al. 2017)

The triple also failed to set any grain due to absence of pollen production, as seen in slender barley mutants (Foster 1977; Lanahan and Ho 1988), as repression of GA signalling disrupts pollen production at the bicellular and tricellular stages (Tang et al. 2010) (Section 1.4.7), preventing the production of viable pollen. In addition, the flag leaf characteristics of the triple mutant (Section 6.2.2) are consistent with *Rht-B1c* loss of function mutants, which produced longer, narrower leaves in the taller plants (Derkx et al. 2017).

To confirm that the triple knock out mutant also displays GA insensitive growth, additional studies examining its growth in the absence of GA must be conducted. Slender barley seedlings have been shown to produce the same overgrowth phenotype following treatment with the GA biosynthesis inhibitor paclobutrazol

(PAC)(Croker et al. 1990). PAC dose curves were conducted to establish the effect of GA biosynthesis inhibition had on the slender phenotype. In WT seedlings, treatment with 1µM PAC caused a significant decrease in leaf sheath length, whilst slender phenotypes did not respond to PAC until the highest dose 100µM (Croker et al. 1990), at which point the PAC treatment may have had additional inhibitory effects of sterol biosynthesis (Burden, Clark, and Holloway 1987), so the effect may not have been due solely to a severe reduction in endogenous GA levels.

If the triple mutant responded to PAC (through a reduction in plant height), this would indicate that it retains some GA sensitivity. This could indicate that the triple mutant is not a complete knock out. Although the knock out mutations were similar to those identified in rice and barley (Figures 6.1 and 6.2) (Chandler et al. 2002; Ikeda et al. 2001), all three *Rht-1* mutations were located towards the end of the coding region for the 'SAW' motif. This means that a large section of the proteins would be produced and may potentially have some level of function. To check that this is not the case an additional triple knock out line has been generated, using different knock out mutations. Instead of stacking the predicted mutations W615*, W616* and W559*, this second line has stacked W604*, Q472* and Q421*, which would be expected to result in greater disruption of RHT-1 protein function. The phenotypic characterisation of these alleles was not possible during the course of this project because the stacking of mutations was incomplete.

If the second triple KNOCK OUT demonstrated a response to PAC, this would suggest that there are additional DELLA genes in wheat. As discussed in the chapter introduction, DGLLA genes have recently been identified in wheat (Van de Velde, Ruelens, et al. 2017). These are sister proteins to DELLA, that also appear to confer GA insensitivity and dwarfism (Itoh et al. 2005), potentially acting as a backup regulator for when DELLA levels decline (Fukao and Bailey-Serres 2008). If the triple DELLA knock outs in wheat did not produce a GA insensitive phenotype, this would suggest that GA signalling regulation is more complex than previously thought, with both DELLA and DGLLA proteins involved in GA signalling regulation (Van de Velde, Ruelens, et al. 2017).

6.9.2 Homoeologue Specificity in *Rht-1*

Phenotypic characterisation of *RHT-1* knockout lines in Cadenza (var.) suggests that there is limited homoeologue specificity between *Rht-A1/B1/D1,* which aligns with the three homoeologues being expressed similarly throughout the plant (Pearce et al. 2011). The triple knock-out mutant produced a classic GA overgrowth phenotype similar to other DELLA loss-of-function mutants: *slr1-1* in rice and *sln1* in barley (Foster 1977; Ikeda et al. 2001). The increased height and longer narrow leaves are associated with increased GA sensitivity (Lanahan and Ho 1988) due to the removal of DELLA repression by disruption to the functional C-terminal GRAS domain (Peng et al. 1997). The inability to set grain is also associated with DELLA loss of function mutants, due to aborted pollen production (Foster 1977; Plackett et al. 2014).

There appears to be a cumulative effect of the bb and dd knock outs, with AAbbDD and AAbbdd ears emerging on average 3 and 5 days earlier than other lines. There was no significant difference between the average ear emergence times of AAbbdd and the triple knock out aabbdd. This suggests *Rht-D1* and *Rht-B1* may have larger roles in inhibiting GA signalling of peduncle elongation for ear emergence than *Rht-A1* (Gardner, Hess, and Trione 1985), a trait that has been seen in the gain of function mutant *Rht-B1c* which produces a severe dwarf phenotype (Wu et al. 2011).

The double knock out also affected flag leaf width, with aabbDD averaging 19.2mm and AAbbdd and aaBBdd 15.1 and 15.4mm respectively. These measurements were significantly wider (aabbDD) and narrower (AAbbdd and aaBBdd) than AABBDD (18.2mm) which contained no *RHT-1* mutations. There was no significant difference between the flag leaf lengths of the double knock outs. This suggests that *Rht-A1* and *Rht-B1* may play more dominant roles in inhibiting epidermal cell expansion than *Rht-D1* which would explain the narrower leaves in the AAbbdd and aaBBdd mutants (Keyes, Paolillo, and Sorrells 1989).

DELLA proteins also predominantly control plant height by reducing cell wall extensibility and elongation (Keyes, Paolillo, and Sorrells 1989; Tonkinson et al. 1995). However only the final plant height of aaBBdd (720.8mm) was significantly

shorter than AABBDD (768.3), with aabbDD (816.1mm) producing shoots significantly longer than AABBDD and AAbbdd having no significant difference (775.5mm). These differences in height were primarily due to the variation in peduncle length, which has been shown in previous studies to be highly associated with dwarfism in *Rht* alleles (Chen et al. 2013).

There is some homoeologue specificity associated with grain yield. The double mutant aabbDD produced significantly more grain per ear than AABBDD (section 6.2.6). This result may be associated with the significantly reduced number of shoots in the aabbDD mature plants (8) compared to AABBDD (10.8), as reduced shoot number limits competition for assimilates between shoots, enabling a great grain number per ear (Xie, Mayes, and Sparkes 2016). Additionally, grain size is affected. AAbbdd (19.6mm^2) produced significantly smaller grain than AABBDD (20mm^2), whilst aaBBdd (21.2mm^2) produced significantly larger grain. These changes may be due to differences in endosperm production, which is regulated by GA (Kondhare et al. 2014).

The differences in phenotypic characteristics between the double knock out mutants where significant depending on the trait, suggesting that there is homoeologue specificity determining phenotypic traits. The C-terminal nonsense mutations stacked in these knock out lines were the same, or similar to intragenic nonsense mutations identified in the semi-dwarf *Rht-A1b* (Chapter X) and severe dwarf *Rht-B1c* (Chandler and Harding 2013) that restored plant height. Furthermore, the triple mutant displayed a classic DELLA loss of function phenotype. Therefore, it is unlikely that the limited differences between the lines was due to the stacking of only partial loss-of-function alleles. To confirm that there is homoeologue specificity, it would be beneficial to repeat the characterisation with the second allelic series of *Rht-1* KNOCK OUTs Additionally, using microscopy to assess cell dimensions in different knock out tissues would be beneficial to confirm that differences in stem and flag leaf lengths are due to differences in cell wall extensibility and elongation (Keyes, Paolillo, and Sorrells 1989; Tonkinson et al. 1995).

Chapter 7: General Discussion

7.1 Project Summary

This project has met the objectives outlined in the introduction.

Objective 1: Characterise the novel Rht-1 mutant Rht-A1b.

This project has confirmed that *Rht-A1b* is the first characterised GA insensitive *Rht-A1* mutants, producing an intermediate mature phenotype compared to the severe dwarf *Rht-B1c* and the semi-dwarf *Rht-D1b*. This intermediate phenotype is not reflected during seedling elongation, which more closely aligns with *Rht-D1b*, suggesting that GA insensitivity may more strongly affect *Rht-A1b* later in plant development. As seen in previous studies into *Rht-1* mutants (Lenton, Hedden, and Gale 1987), *Rht-A1b, D1b* and *B1c* seedlings were found to accumulate bioactive GA_1. However, this study also demonstrated that GA_4 accumulated in *Rht-1* dwarf lines which has not previously been reported. It still needs to be established whether accumulation of bioactive GAs is due to upregulation of biosynthesis genes.

Objective 2: Identify and characterise Rht-A1b suppressor mutants.

Rht-A1b suppressors where identified during both field screens and characterised in the BC_2F_3 generation. These suppressor mutants were found to produce phenotypes representing a partial to total loss of *Rht-A1b* function, providing additional evidence that the RHT C-terminal GRAS domain regulates DELLA function.

Of the 32 intragenic mutants identified 10 mutants produced phenotypes associated with increased grain yield and/or grain size compared to *Rht-A1b* and *Rht-1* (Figure 7.1)

Line	Amino Acid Substitution	DELLA Domain Location of Mutation	Plant Height (GH)	Plant Height (F)	Grain per Ear (GH)	Grain size (mm^2) (GH)	Grain size (mm^2) (F)
Rht-A1b.12	R270C	LHR1			*	**	**
Rht-A1b.13	A274V	LHR1				**	**
Rht-A1b.14	G277D	LHR1			**		**
Rht-A1b.29	S527F	SAW			*	*	-
Rht-A1b.4	T493I	PYFRE			*	**	-
Rht-A1b.21	A408T	LHR2			*	**	-
Rht-A1b.24	E470K	PYFRE			*	**	-
Rht-A1b.27	D496N	PYFRE			*	**	-
Rht-A1b.28	S497F	PYFRE			*	**	-
Rht-A1b.25	S487F	PYFRE			*	**	-

Colour Key	Semi-dwarf	Significantly more grains per ear or larger grains
	Tall	
	Overgrowth	Significantly smaller grains per ear

Figure 7.1: Overview of *Rht-A1b* Missense Mutant Height and Grain Characteristics. A description of the colour code is provided in the key above. * = significantly more/less than *Rht-A1b, ** =* significantly more/less than *Rht-1* and *Rht-A1b*.

These mutants produced a range of height phenotypes (semi-dwarf, tall and overgrowth) suggesting that the original hypothesis that a semi-dwarf phenotype would be the most beneficial was incorrect. These mutants also arose from 4 out of the 5 conserved DELLA GRAS motifs. Further study of these suppressors will therefore provide insights into DELLA structure-function, potentially identifying semi-dwarfing alleles with fewer pleiotropic effects, which will be beneficial for commercial wheat breeding.

Objective 3: Is there homoeologue specificity in Rht-1?

Characterisation of double knock outs of *Rht-A1/B1/D1* suggests that there is homoeologue specificity in *Rht-1,* particularly relating to heading date, flag leaf width, stem length, grain number per ear and grain size. Although a larger scale characterisation using more plants and additional knock out lines with different mutations will be required to confirm this.

Characterisation of the triple knock out mutant, confirmed the production of a classic 'slender' total loss of function phenotype. This suggests that DELLA is the lead negative regulator of GA responses in wheat and that the recently discovered DGLLA protein may have a redundant role.

7.2 A Gene to Field Method

Wheat is one of the most important crops on the planet, grown across more land than any other crop and accounting for 1/5 of global human calorie consumption (OECD/FAO 2012). Since the 1960s, semi-dwarf wheat varieties have dominated the commercial market and are a key factor in the trebling of wheat yields over the last forty years (Khush 2001).Their lodging resistance allows for increased fertiliser usage, whilst improved photosynthate partitioning in the ear enables increased grain number (Hedden 2003). Today, the alleles that cause this semi-dwarf phenotype, *Rht-D1b* and *Rht-B1b,* are present in approximately 70% of all modern wheat varieties (Hedden 2003). However, wheat yields are now showing signs of plateauing (Slafer 2001; Mayer et al. 2014), despite needing to increase annually by ~2% to keep up with predicted population growth (Ray et al. 2013; OECD/FAO 2012). Concurrent to this, some climate change models predict agricultural regions will become warmer and drier (Mayer et al. 2014), conditions that have been shown to erode the yield benefits of *Rht-B1b* and *Rht-D1b* (Hoogendoorn and Gale 1988). A potential solution towards this problem could be the development of novel wheat dwarfing alleles, informed by improved understanding of the underlying molecular mechanisms of the *Rht-1* alleles.

This project discusses a method for producing and identifying a novel series of *Rht-1* dwarfing alleles, which will be used to provide insights into RHT-1 structure-function. Further study is required to establish whether these intragenic mutations uncouple negative pleiotropic effects from the beneficial semi-dwarf traits (Derkx et al. 2017), potentially generating a 'toolkit' of alleles that could be used to help adapt wheat cultivars to different environments (Pearce et al. 2011; Chandler and Harding 2013) (Chapter 4 and 5).

Generating *Rht-A1b* intragenic mutants through mutagenesis and suppressor screens is a multi-year approach requiring multiple generations for seed bulking and backcrossing before allele characterisation and additional generations to introgress the mutation into elite cultivars for further analysis (Chandler and Harding 2013; Derkx et al. 2017). Recent developments in the gene editing technique, base editing, provides the means to rapidly introduce specific single nucleotide changes into the wheat genome (Williams 2019). In a base editing technique adapted to plants, Cas9 proteins lacking nuclease activity are fused to a tRNA adenosine deaminase, enabling A•T to G•C nucleotide conversions. When delivered into immature wheat embryos via particle bombardment, up to 59.1% of the regenerated plants displayed the specific conversion in the target *TaDEP1 and TaGW2* genes (Li et al. 2018). This technology could therefore be used to introduce novel *Rht-1* alleles directly into elite cultivars, without the requirement for backcrossing (Li et al. 2018). However, plants that have undergone gene editing are classified as GMOs under a European Court of Justice ruling (Case C-528/16) (Gelinsky and Hilbeck 2018) and are therefore subject to stringent growth regulations and are not presently available for consumption (DEFRA 2019). Therefore, gene edited plants can only be used for research purposes. For example, testing the efficacy of novel *Rht-1* alleles in different elite cultivar backgrounds, as the yield potential of *Rht-1* alleles has been demonstrated to vary depending on the background it is placed in (Flintham et al. 1997). This methodology could provide the means to test whether alleles deserve the time investment of introgression.

On the other hand, GM laws in the UK may soon be subject to change. During his first speech as Prime Minister, Boris Johnson said he wanted the UK to have 'a bioscience sector liberated from anti genetic modification rules… we will be the seedbed for the most exciting and most dynamic business investments on the planet.' Suggesting that post-Brexit the UK may look to revise its GM laws. It remains to be seen whether this is will come into fruition in the future, as public opinion on GMOs ranges mostly from skeptical to negative (Hudson, Caplanova, and Novak 2015).

Nonetheless, if achieved a law change would dramatically alter the potential for wheat breeding in the UK (Li et al. 2018). A fully annotated reference genome for bread wheat was published this year, providing a resource that will undoubtedly accelerate our understanding of wheat genetics (Appels et al. 2018). As our understanding of RHT-1 structure-function and the genetic basis of its interactors expands, the opportunity to design novel dwarfing alleles directly in elite cultivars arises (Williams 2019).

7.3 Loss-of-Function *Rht-A1b* and *Rht-1* Mutants Provide Evidence for the Translation Re-Initiation Hypothesis

The reinitiation hypothesis is the current explanation for the gain-of-function semi-dwarf phenotype of *Rht-A1b, Rht-B1b* and *Rht-D1b* (Peng et al. 1999). The premature stop codons in the DELLA domain are followed by multiple AUG codons, potentially resulting in the production of a prematurely aborted N-terminal peptide and a N-terminally truncated protein (Figure 1.16). The N-terminally truncated protein predicted to be fully functional, as the functional C-terminal GRAS domain is not disrupted. However, the partial DELLA domain means that the protein cannot be recognised for GA induced degradation so accumulates, resulting in constitutive repression of GA signalling (Peng et al. 1999). By contrast, mutant DELLA genes with nonsense mutations in the C-terminal GRAS domain produce slender, loss of function phenotypes as these due to disrupted protein function (Peng et al. 1997; Ikeda et al. 2001; Chandler et al. 2002)

The translation reinitiation hypothesis suggests nonsense mutations produce tall phenotypes through loss of RHT-1 / RHT-A1B protein function (Peng et al. 1999; Pearce et al. 2011; Mo, Pearce, and Dubcovsky 2018) and that missense mutations should predominantly result in a partial loss-of-function phenotype between the mutagenised (*Rht-A1b*) line and the WT line (Cadenza), as was the case in the *Rht-B1c* suppressor screen (Chandler and Harding 2013; Derkx et al. 2017; Peng et al. 1999). As height reduction is the most notable effect of *Rht-1* dwarfing alleles on plant phenotype (Lenton, Hedden, and Gale 1987; Lenton and Appleford 1991; Pinthus et al. 1989), this is characteristic was primarily used to determine the effect of intragenic mutations (Chandler and Harding 2013; Derkx et al. 2017). The triple

Rht-1 knock out (KO) produced a classic, loss of function, slender phenotype (Chapter 6) (Foster 1977; Ikeda et al. 2001). Whilst all intragenic *Rht-A1b* mutants produced a phenotype that was significantly taller than the non-mutagenised *Rht-A1b* controls (Chapter 5). These results align with the translation reinitiation hypothesis, as mutations in the GRAS domain of the truncated protein would be expected to disrupt protein function, resulting in reduced repression of GA signalling and a taller phenotype (Peng et al. 1999; Chandler and Harding 2013).

The expression of the an equivalent N-terminally truncated GAI protein in transgenic *Arabidopsis* has been demonstrated to produce a protein resistant to GA degradation that induces a GA-insensitive dwarf phenotype (Willige et al. 2007). However direct evidence for the existence of these proteins *in planta* in wheat remains elusive. Previous studies in this lab group, involving polyclonal antibodies raised against RHT-D1, were unable to identify a GA-responsive immunoreactive protein in any wheat tissues. This included tissue *GA2ox* overexpression transgenic lines which deactivates bioactive GA, theoretically increasing RHT-D1 levels by reducing targeted degradation (Pearce 2009). This work was conducted ~10 years ago, during which time there have been improvements to digital imagers for western blots potentially increasing the sensitivity required to identify these proteins (Ghosh, Gilda, and Gomes 2014). Additionally, wheat GA biosynthesis KO mutants are currently being stacked from the TILLING lines, which may produce more stable RHT-1 proteins (Dr Andy Phillips, personal comms). Exploring these resources, and potentially gene editing *Rht-B1b* and *Rht-D1b* mutations into GA biosynthesis KOs (Li et al. 2018) could provide the means to demonstrate and characterise endogenous RHT-1, RHT-B1B or RHT-D1B proteins.

7.4 Nonsense DELLA Mutations – Why are these Semi-Dwarfing Alleles Found Only in Wheat?

To date, semi-dwarf nonsense mutations in the N-terminal DELLA domain have only been identified in wheat. In maize and *Arabidopsis* N-terminal DELLA mutations resulting in a GA insensitive dwarf phenotype are associated with in-frame deletions (Peng et al. 1999)(Figure 7.2).

Figure 7.2: Deletions and Non-Sense DELLA Mutations Resulting in a Dwarf/Semidwarf Phenotype. N-terminal segments of predicted proteins encoded by mutant alleles *gai, D8-1, D8-2023, D8-Mpl, Rht-B1b* and *Rht*-D1b are compared with those of their respective wild-type alleles (GAI, d8, Rht-B1a and Rht-D1a). For each locus, the wild-type sequence is shown above and below the mutant sequence(s). Differences between wild-type and mutant sequences (deletions and substitutions) are highlighted in white, the position of translational stop codons is represented by an asterisk, and the previously identified highly conserved regions DELLA and TVHYNP. Adapted from (Peng et al. 1999).

Dwarf phenotypes arise in *gai, D8-1* and *D8-2023* mutants which have 17, 4 and 12 amino acids deleted respectively. *D8-Mpl* has a 330-bp deletion that extends from 5' untranslated sequence and through the normal start ATG codon to V84. This allele has been demonstrated to produce a protein product, assumed to be a N-terminally truncated protein following translation re-initiation at the next ATG codon, M106 (Peng et al. 1999). Meanwhile a dwarf phenotype in barley *Sln1-d,* arises from a G to A nucleotide substitution (GGG to GAG) in the 46th amino acid

residue, causing a Gly to Glu change in the DELLA motif region (^{39}DELLAALG^{46} > ^{39}DELLAALE^{46}) (Chandler et al. 2002).

The absence of DELLA N-terminal nonsense mutations or N-terminal DELLA mutations that result in a semi-dwarf phenotype in other plant species such as rice (where large mutant collections have been generated and screened) (Itoh et al. 2002) may be a consequence of the ploidy level. For example, it is conceivable that these mutations only manifest a phenotype in polyploid plant species such as wheat. Preliminary studies into *Rht-1* KOs suggest that the three homoeologous *Rht-1* genes are functionally redundant (Chapter 6). Therefore, the WT alleles *Rht-A1a/B1a/D1a* may buffer or compensate for the presence of gain of function mutations (e.g. *Rht-D1b* and *Rht-B1b*), preventing total constitutive GA signalling repression and producing a semi-dwarf phenotype.

The *Rht-1* KOs will provide a valuable resource to test whether this is the case. Introducing a single gain-of-function mutation (e.g. *Rht-D1b* or *Rht-A1b*) into a background where the other two *Rht-1* genes are knocked out (in this example *Rht-B1* and *Rht-D1*), to establish whether the presence of the *Rht-B1a* and *Rht-D1a* are required for the *Rht-D1b* semi-dwarf phenotype. Understanding this could provide insights into the roles of the three *RHT-1* genes in wheat.

Appendix: Supplementary Data

Supplementary Table 1: Components of the GA Biosynthesis Pathway

Function	**Gene Name**	**RefSeqv1.1**
Gibberellin Biosynthesis	*CPS-A1*	TraesCS7A02G552600
	CPS-A2	TraesCS7A02G552700
	CPS-B	TraesCS7B02G476400
	CPS-D1	TraesCS7D02G538600
	CPS-D2	TraesCS7D02G539200

Function	**Gene Name**	**RefSeqv1.1**
Gibberellin Inactivation	*GA2ox1-A*	TraesCS1A02G106200
	GA2ox1-B	TraesCS1B02G123500
	GA2ox1-D	TraesCS1D02G108800
	GA2ox2-A	TraesCS7A02G450000
	GA2ox2-B	TraesCS7B02G349700

	KS-A	TraesCS2A02G425400
	KS-B	TraesCS2B02G445700
	KS-D	TraesCS2D02G423300
	KO-A	TraesCS7A02G362300
	KO-B	TraesCS7B02G265800
	KO-D	TraesCS7D02G360700
	KAO-A	TraesCS4A02G460100
	KAO-B	TraesCS7A02G029600
	KAO-D	TraesCS7D02G026000
	GA20ox1-A	TraesCS4A02G319100
	GA20ox1-B	TraesCS5B02G560300
	GA20ox1-D	TraesCS5D02G566200
	GA20ox2-A	TraesCS3A02G406200
	GA20ox2-B	TraesCS3B02G439900
	GA20ox2-D	TraesCS3D02G401400
	GA20ox3-A	TraesCS3A02G399800
	GA20ox3-B	TraesCS3B02G432800
	GA20ox3-D1	TraesCS3D02G393900
	GA20ox3-D2	TraesCS3D02G394000
	GA20ox4-A	TraesCS1A02G263600
	GA20ox4-B	TraesCS1B02G274200
	GA20ox4-D	TraesCS1D02G263700
	GA13ox-A	TraesCS2A02G103900
	GA13ox-B	TraesCS2B02G121000
	GA13ox-D	TraesCS2D02G103600
	GA1ox1-B	TraesCS2B02G570800
	GA3ox2-A	TraesCS3A02G122600
	GA3ox2-B	TraesCS3B02G141800
	GA3ox2-D	TraesCS3D02G124500
	GA3ox3-A	TraesCS2A02G540400
	GA3ox3-B	TraesCS2B02G570900
	GA3ox3-D	TraesCS2D02G542100
	GA2ox2-D	TraesCS7D02G439200
	GA2ox3-A	TraesCS3A02G294000
	GA2ox3-B	TraesCS3B02G328700
	GA2ox3-D	TraesCS3D02G293800
	GA2ox4-A	TraesCS1A02G334400
	GA2ox4-B	TraesCS1B02G347600
	GA2ox4-D	TraesCS1D02G336900
	GA2ox6-A1	TraesCS2A02G379000
	GA2ox6-A2	TraesCS4A02G033200
	GA2ox6-A3	TraesCS5A02G543100
	GA2ox6-B1	TraesCS2B02G396000
	GA2ox6-B2	TraesCS4B02G272100
	GA2ox6-B3	TraesCS4B02G376200
	GA2ox6-B4	TraesCS4B02G376100
	GA2ox6-D1	TraesCS2D02G375300
	GA2ox6-D2	TraesCS4D02G271300
	GA2ox7-A	TraesCS3A02G133400
	GA2ox7-B	TraesCS3B02G166100
	GA2ox7-D	TraesCS3D02G149600
	GA2ox8-A	TraesCS1A02G392500
	GA2ox8-B	TraesCS1B02G420800
	GA2ox8-D	TraesCS1D02G400700
	GA2ox9-A	TraesCS6A02G221900
	GA2ox9-B	TraesCS6B02G259200
	GA2ox9-D	TraesCS6D02G213100
	GA2ox10-A	TraesCS1A02G126400
	GA2ox10-B	TraesCS1B02G145600
	GA2ox10-D	TraesCS1D02G127000
Gibberellin Receptors	*GID1-A*	TraesCS1A02G255100
	GID1-B	TraesCS1B02G265900
	GID1-D	TraesCS1D02G254500
	GID2-A1	TraesCS3A02G056000
	GID2-A2	TraesCS3A02G055700
	GID2-A3	TraesCS3A02G511800
	GID2-B1	TraesCS3B02G068800
	GID2-B2	TraesCS3B02G068100
	GID2-D1	TraesCS3D02G056100
GA Signalling Repression	*Rht1-A*	TraesCS4A02G271000
	Rht1-B	TraesCS4B02G043100
	Rht1-D	TraesCS4D02G040400

Table describing the function, gene name, genome (A,B,D) and RefSeqv1.1 reference for GA biosynthesis and signalling genes in wheat.

References

Aach, H., H. Bode, D. G. Robinson, and J. E. Graebe. 1997. 'ent-kaurene synthase is located in proplastids of meristematic shoot tissues', *Planta*, 202: 211-19.

Achard, P., J. P. Renou, R. Berthome, N. P. Harberd, and P. Genschik. 2008. 'Plant DELLAs restrain growth and promote survival of adversity by reducing the levels of reactive oxygen species', *Current Biology*, 18: 656-60.

Alabadi, D., J. Gallego-Bartolome, L. Orlando, L. Garcia-Carcel, V. Rubio, C. Martinez, M. Frigerio, J. M. Iglesias-Pedraz, A. Espinosa, X. W. Deng, and M. A. Blazquez. 2008.

'Gibberellins modulate light signaling pathways to prevent Arabidopsis seedling de-etiolation in darkness', *Plant Journal*, 53: 324-35.

Alghabari, F., M. Lukac, H. E. Jones, and M. J. Gooding. 2014. 'Effect of Rht Alleles on the Tolerance of Wheat Grain Set to High Temperature and Drought Stress During Booting and Anthesis', *Journal of Agronomy and Crop Science*, 200: 36-45.

Amram, Avishay, Aviya Fadida-Myers, Guy Golan, Kemal Nashef, Roi Ben-David, and Zvi Peleg. 2015. 'Effect of GA-sensitivity on wheat early vigor and yield components under deep sowing', *Frontiers in Plant Science*, 6.

An, F., X. Zhang, Z. Zhu, Y. Ji, W. He, Z. Jiang, M. Li, and H. Guo. 2012. 'Coordinated regulation of apical hook development by gibberellins and ethylene in etiolated Arabidopsis seedlings', *Cell Research*, 22: 915-27.

Anders, Simon, and Wolfgang Huber. 2010. 'Differential expression analysis for sequence count data', *Genome Biology*, 11.

Appels, R., K. Eversole, C. Feuillet, B. Keller, J. Rogers, N. Stein, C. J. Pozniak, F. Choulet, A. Distelfeld, J. Poland, G. Ronen, A. G. Sharpe, C. Pozniak, O. Barad, K. Baruch, G. Keeble-Gagnere, M. Mascher, G. Ben-Zvi, A. A. Josselin, A. Himmelbach, F. Balfourier, J. Gutierrez-Gonzalez, M. Hayden, C. Koh, G. Muehlbauer, R. K. Pasam, E. Paux, P. Rigault, J. Tibbits, V. Tiwari, M. Spannagl, D. Lang, H. Gundlach, G. Haberer, K. F. X. Mayer, D. Ormanbekova, V. Prade, H. Simkova, T. Wicker, D. Swarbreck, H. Rimbert, M. Felder, N. Guilhot, G. Kaithakottil, J. Keilwagen, P. Leroy, T. Lux, S. Twardziok, L. Venturini, A. Juhasz, M. Abrouk, I. Fischer, C. Uauy, P. Borrill, R. H. Ramirez-Gonzalez, D. Arnaud, S. Chalabi, B. Chalhoub, A. Cory, R. Datla, M. W. Davey, J. Jacobs, S. J. Robinson, B. Steuernagel, F. van Ex, B. B. H. Wulff, M. Benhamed, A. Bendahmane, L. Concia, D. Latrasse, M. Alaux, J. Bartos, A. Bellec, H. Berges, J. Dolezel, Z. Frenkel, B. Gill, A. Korol, T. Letellier, O. A. Olsen, K. Singh, M. Valarik, E. van der Vossen, S. Vautrin, S. Weining, T. Fahima, V. Glikson, D. Raats, J. Cihalikova, H. Toegelova, J. Vrana, P. Sourdille, B. Darrier, D. Barabaschi, L. Cattivelli, P. Hernandez, S. Galvez, H. Budak, J. D. G. Jones, K. Witek, G. T. Yu, I. Small, J. Melonek, R. N. Zhou, T. Belova, K. Kanyuka, R. King, K. Nilsen, S. Walkowiak, R. Cuthbert, R. Knox, K. Wiebe, D. Q. Xiang, A. Rohde, T. Golds, J. Cizkova, B. A. Akpinar, S. Biyiklioglu, L. L. Gao, A. N'Daiye, M. Kubalakova, J. Safar, F. Alfama, A. F. Adam-Blondon, R. Flores, C. Guerche, M. Loaec, H. Quesneville, J. Condie, J. Ens, R. Maclachlan, Y. F. Tan, A. Alberti, J. M. Aury, V. Barbe, A. Couloux, C. Cruaud, K. Labadie, S. Mangenot, P. Wincker, G. Kaur, M. C. Luo, S. Sehgal, P. Chhuneja, O. P. Gupta, S. Jindal, P. Kaur, P. Malik, P. Sharma, B. Yadav, N. K. Singh, J. Khurana, C. Chaudhary, P. Khurana, V. Kumar, A. Mahato, S. Mathur, A. Sevanthi, N. Sharma, R. S. Tomar, K. Holusova, O. Plihal, M. D. Clark, D. Heavens, G. Kettleborough, J. Wright, B. Balcarkova, Y. Q. Hu, E. Salina, N. Ravin, K. Skryabin, A. Beletsky, V. Kadnikov, A. Mardanov, M. Nesterov, A. Rakitin, E. Sergeeva, H. Handa, H. Kanamori, S. Katagiri, F. Kobayashi, S. Nasuda, T. Tanaka, J. Z. Wu, F. Cattonaro, M. Jiumeng, K. Kugler, M. Pfeifer, S. Sandve, X. Xun, B. J. Zhan, J. Batley, P. E. Bayer, D. Edwards, S. Hayashi, Z. Tulpova, P. Visendi, W. N. Song, L. C. Cui, X. H. Du, K. W. Feng, X. J. Nie, W. Tong, L. Wang, and R. Iglesias-Fernandez. 2018. 'Shifting the limits in wheat research and breeding using a fully annotated reference genome', *Science*, 361: 661-+.

Appleford, N. E. J., D. J. Evans, J. R. Lenton, P. Gaskin, S. J. Croker, K. M. Devos, A. L. Phillips, and P. Hedden. 2006. 'Function and transcript analysis of gibberellin-biosynthetic enzymes in wheat', *Planta*, 223: 568-82.

Appleford, N. E. J., and J. R. Lenton. 1991. 'Gibberellins and leaf expansion in near-isogenic wheat lines containing RHT1 and RHT3 dwarfing alleles', *Planta*, 183: 229-36.

Arana, M. V., N. Marin-de la Rosa, J. N. Maloof, M. A. Blazquez, and D. Alabadi. 2011. 'Circadian oscillation of gibberellin signaling in Arabidopsis', *Proceedings of the National Academy of Sciences of the United States of America*, 108: 9292-97.

Asano, K., K. Hirano, M. Ueguchi-Tanaka, R. B. Angeles-Shim, T. Komura, H. Satoh, H. Kitano, M. Matsuoka, and M. Ashikari. 2009. 'Isolation and characterization of dominant dwarf mutants, Slr1-d, in rice', *Molecular Genetics and Genomics*, 281: 223-31.

Aya, Koichiro, Miyako Ueguchi-Tanaka, Maki Kondo, Kazuki Hamada, Kentaro Yano, Mikio Nishimura, and Makoto Matsuoka. 2009. 'Gibberellin Modulates Anther Development in Rice via the Transcriptional Regulation of GAMYB', *Plant Cell*, 21: 1453-72.

Bai, M. Y., J. X. Shang, E. Oh, M. Fan, Y. Bai, R. Zentella, T. P. Sun, and Z. Y. Wang. 2012. 'Brassinosteroid, gibberellin and phytochrome impinge on a common transcription module in Arabidopsis', *Nature Cell Biology*, 14: 810-U78.

Balyan, H. S., and O. Singh. 1994. 'PLEIOTROPIC EFFECTS OF GA-INSENSITIVE RHT GENES ON GRAIN-YIELD AND ITS COMPONENT CHARACTERS IN WHEAT', *Cereal Research Communications*, 22: 195-200.

Bazhenov, M. S., M. G. Divashuk, Y. Amagai, N. Watanabe, and G. I. Karlov. 2015. 'Isolation of the dwarfing Rht-B1p (Rht17) gene from wheat and the development of an allele-specific PCR marker', *Molecular Breeding*, 35.

Bennett, M. D., and I. J. Leitch. 1995. 'Nuclear DNA amounts in angiosperms', *Annals of Botany*, 76: 113-76.

Boerner, A., A. J. Worland, J. Plaschke, Erika Schumann, and C. N. Law. 1993. 'Pleiotropic effects of genes for reduced height (Rht) and day-length insensitivity (Pdd) on yield and its components for wheat grown in Middle Europe', *Plant Breeding*, 111: 204-16.

Boeven, Philipp H. G., C. Friedrich H. Longin, Willmar L. Leiser, Sonja Kollers, Erhard Ebmeyer, and Tobias Wuerschum. 2016. 'Genetic architecture of male floral traits required for hybrid wheat breeding', *Theoretical and Applied Genetics*, 129: 2343-57.

Borlaug, N. 1981. 'Breeding methods employed and the contributions of Norin 10 derivatives to the development of the high yielding broadly adapted Mexican wheat varieties.', *The International Maize and Wheat Improvement Center (CIMMYT) El Batan, Mexico*.

Borlaug, N. . 1968. 'The Impact of Wheat Breeding on World Food Supply', *The Third International Wheat Genetics Symposium*, 1: 1-36.

Börner, A. , CO. Lehmann, D. Mettin, J. Plaschke, Rd Schlegel, G. Melz, and V. Thiele. 1991. 'GA-insensitivity of "Ai-bian 1a"/Pleiotropic effects of isogenic *Rht*-lines', *Annual wheat newsletter*, 37: 59-60.

Börner, A., and D. Mettin. 1988. 'The genetic control of gibberellic acid insensitivity of the wheat variety Ai-Bain', *I.E. Miller & R.M.D. Koebner (Eds). Proc. 7th Int. Wheat Genet. Symp., Cambridge, England, Bath Press, Bath, Avon*: 489-92.

Börner, A., J. Plaschke, V. Korzun, and A. J. Worland. 1996. 'The relationships between the dwarfing genes of wheat and rye', *Euphytica*, 89: 69-75.

Börner, A., M. Roder, and V. Korzun. 1997. 'Comparative molecular mapping of GA insensitive Rht loci on chromosomes 4B and 4D of common wheat (Triticum aestivum L.)', *Theoretical and Applied Genetics*, 95: 1133-37.

Borojevic, K. 2005. 'The transfer and history of "reduced height genes" (Rht) in wheat from Japan to Europe', *Journal of Heredity*, 96: 455-59.

Borrell, A. K., L. D. Incoll, and M. J. Dalling. 1991. 'The influence of RHT1 and RHT2 alleles on the growth of wheat stems and ears', *Annals of Botany*, 67: 103-10.

Braun, Eva-Maria, Natalia Tsvetkova, Bjoern Rotter, Doerthe Siekmann, Konrad Schwefel, Nicolas Krezdorn, Joerg Plieske, Peter Winter, Gilbert Melz, Anatoly V. Voylokov,

and Bernd Hackauf. 2019. 'Gene Expression Profiling and Fine Mapping Identifies a Gibberellin 2-Oxidase Gene Co-segregating With the Dominant Dwarfing Gene Ddw1 in Rye (Secale cereale L.)', *Frontiers in Plant Science*, 10.

Brian, P. W., and H. G. Hemming. 1955. 'The effect of gibberellic acid on shoot growth of pea seedlings', *Physiologia Plantarum*, 8: 669-81.

Brian, P.W. 1957. 'The effects of some microbial metabolic products on plant growth', *Symposia of the Society of Experimental Biology*, 11: 166-82.

Burden, R. S., T. Clark, and P. J. Holloway. 1987. 'Effects of sterol biosynthesis-inhibiting fungicides and plant growth regulators on the sterol composition of barley plants', *Pesticide Biochemistry and Physiology*, 27: 289-300.

Bush, M. G., and L. T. Evans. 1988. 'Growth and development in tall and dwarf isogenic lines of spring wheat', *Field Crops Research*, 18: 243-70.

Chamberlain, N., T.H. Collins, and E.E. McDermott. 1982. 'The influence of α-amylase on loaf properties in the UK', *Progress in Cereal Chemistry and Technology, Proceedings of the VIIth World Cereal and Bread Congress*: 841-45.

Chandler, P. M., and C. A. Harding. 2013. ''Overgrowth' mutants in barley and wheat: new alleles and phenotypes of the 'Green Revolution' Della gene', *Journal of Experimental Botany*, 64: 1603-13.

Chandler, P. M., A. Marion-Poll, M. Ellis, and F. Gubler. 2002. 'Mutants at the Slender1 locus of barley cv Himalaya. molecular and physiological characterization', *Plant Physiology*, 129: 181-90.

Chandler, PM , and M Robertson. 1999. 'Gibberellin dose-response curves and the characterization of dwarf mutants of barley', *Plant Physiology*, 120: 623-32.

Chen, L., L. G. Hao, M. A. J. Parry, A. L. Phillips, and Y. G. Hu. 2014. 'Progress in TILLING as a tool for functional genomics and improvement of crops', *Journal of Integrative Plant Biology*, 56: 425-43.

Chen, L., L. Z. Huang, D. H. Min, A. Phillips, S. Q. Wang, P. J. Madgwick, M. A. J. Parry, and Y. G. Hu. 2012. 'Development and Characterization of a New TILLING Population of Common Bread Wheat (Triticum aestivum L.)', *Plos One*, 7.

Chen, L., A. L. Phillips, A. G. Condon, M. A. J. Parry, and Y. G. Hu. 2013. 'GA-Responsive Dwarfing Gene Rht12 Affects the Developmental and Agronomic Traits in Common Bread Wheat', *Plos One*, 8.

Chiang, H. H., I. Hwang, and H. M. Goodman. 1995. 'Isolation of the Arabidopsis GA4 Locus', *Plant Cell*, 7: 195-201.

Cho, CH., HO. Kyu, and SH. Lee. 1993. 'Origin, dissemination and utilization of semi dwarf genes in Korea', *Miller TE. Koebner RMD (eds) Proceedings of 7th International Wheat Genetic Symposium, Bath Press, Bath*: 223-31.

Coolbaugh, R. C. 1985. 'Sites of gibberellin biosynthesis in pea-seedlings', *Plant Physiology*, 78: 655-57.

Costa, Carlota, Ana Gimenez-Capitan, Niki Karachaliou, and Rafael Rosell. 2013. 'Comprehensive molecular screening: from the RT-PCR to the RNA-seq', *Translational lung cancer research*, 2: 87-91.

Cowling, R. J., and N. P. Harberd. 1999. 'Gibberellins control Arabidopsis hypocotyl growth via regulation of cellular elongation', *Journal of Experimental Botany*, 50: 1351-57.

Croker, S. J., P. Hedden, J. R. Lenton, and J. L. Stoddart. 1990. 'Comparison of gibberellins in normal and slender barley seedlings', *Plant Physiology*, 94: 194-200.

Dai, C., and H. W. Xue. 2010. 'Rice early flowering1, a CKI, phosphorylates DELLA protein SLR1 to negatively regulate gibberellin signalling', *Embo Journal*, 29: 1916-27.

Dai, M. Q., Y. Zhao, Q. F. Ma, Y. Hu, P. F. Hedden, Q. Zhang, and D. X. Zhou. 2007. 'The rice YABBY1 gene is involved in the feedback regulation of gibberellin metabolism', *Plant Physiology*, 144: 121-33.

Dalrymple, D. G. 1986. 'Development and spread of high-yielding wheat varieties in developing countries', *Development and spread of high-yielding wheat varieties in developing countries.*: xi + 99pp.-xi + 99pp.

Dalziel, J., and D. K. Lawrence. 1984. 'Biochemical and biological effects of kaurene oxidase inhibitors, such as paclobutrazol', *Monograph, British Plant Growth Regulator Group*: 43-57.

Daviere, J. M., and P. Achard. 2013. 'Gibberellin signaling in plants', *Development*, 140: 1147-51.

Davies, PJ. 1995. 'Plant Hormones: Physiology, Biochemistry and Molecular Biology.', *Kluwer Academic Publishers*.

de Lucas, M., J. M. Daviere, M. Rodriguez-Falcon, M. Pontin, J. M. Iglesias-Pedraz, S. Lorrain, C. Fankhauser, M. A. Blazquez, E. Titarenko, and S. Prat. 2008. 'A molecular framework for light and gibberellin control of cell elongation', *Nature*, 451: 480-U11.

DEFRA. 2019. 'Genetically Modified Organism: Applications and Decisions', DEFRA, Accessed September 2019. https://www.gov.uk/government/collections/genetically-modified-organisms-applications-and-consents.

Derkx, Adinda P., Carol A. Harding, Asemeh Miraghazadeh, and Peter M. Chandler. 2017. 'Overgrowth (Della) mutants of wheat: development, growth and yield of intragenic suppressors of the Rht-B1c dwarfing gene', *Functional plant biology*, 44: 525-37.

Dev, G., S. Saggar, R. Singh, and B. S. Sidhu. 1980. 'Root distribution patterns of some wheat varieties in arid brown soil under rainfed condition', *Journal of Nuclear Agriculture and Biology*, 9: 89-90.

Dill, A., H. S. Jung, and T. P. Sun. 2001. 'The DELLA motif is essential for gibberellin-induced degradation of RGA', *Proceedings of the National Academy of Sciences of the United States of America*, 98: 14162-67.

Dill, A., and T. P. Sun. 2001. 'Synergistic derepression of gibberellin signaling by removing RGA and GAI function in Arabidopsis thaliana', *Genetics*, 159: 777-85.

Dill, A., S. G. Thomas, J. H. Hu, C. M. Steber, and T. P. Sun. 2004. 'The Arabidopsis F-box protein SLEEPY1 targets gibberellin signaling repressors for gibberellin-induced degradation', *Plant Cell*, 16: 1392-405.

Divashuk, M. G., L. A. Bespalova, A. V. Vasilyev, I. A. Fesenko, O. Y. Puzyrnaya, and G. I. Karlov. 2013. 'Reduced height genes and their importance in winter wheat cultivars grown in southern Russia', *Euphytica*, 190: 137-44.

Dong, C. M., J. Dalton-Morgan, K. Vincent, and P. Sharp. 2009. 'A Modified TILLING Method for Wheat Breeding', *Plant Genome*, 2: 39-47.

Dubcovsky, J., and J. Dvorak. 2007. 'Genome plasticity a key factor in the success of polyploid wheat under domestication', *Science*, 316: 1862-66.

Duwayri, M. 1984. 'Comparison of wheat cultivars grown in the field under different levels of moisture', *Cereal Research Communications*, 12: 27-34.

Edwards, R. A., A. S. Ross, D. J. Mares, F. W. Ellison, and J. D. Tomlinson. 1989. 'Enzymes from rain-damaged and laboratoty gernminated wheat .1. Effects on product quality', *Journal of Cereal Science*, 10: 157-67.

Ehrlich, P. 1968. 'The Population Bomb'.

Ellis, M. H., G. J. Rebetzke, P. Chandler, D. Bonnett, W. Spielmeyer, and R. A. Richards. 2004. 'The effect of different height reducing genes on the early growth of wheat', *Functional plant biology*, 31: 583-89.

Fath, A., P. Bethke, J. Lonsdale, R. Meza-Romero, and R. Jones. 2000. 'Programmed cell death in cereal aleurone', *Plant Molecular Biology*, 44: 255-66.

Feldman, M. , A. Bonjean, and WJ. Angus. 2001. 'Origin of cultivated wheat, The world wheat book: a history of wheat breeding ,' *Paris, FranceLavoisier Publishing*: (pg. 3-56).

Feng, N., G. Y. Song, J. T. Guan, K. Chen, M. L. Jia, D. H. Huang, J. J. Wu, L. C. Zhang, X. Y. Kong, S. F. Geng, J. Liu, A. L. Li, and L. Mao. 2017. 'Transcriptome Profiling of Wheat Inflorescence Development from Spikelet Initiation to Floral Patterning Identified Stage-Specific Regulatory Genes', *Plant Physiology*, 174: 1779-94.

Feng, S. H., C. Martinez, G. Gusmaroli, Y. Wang, J. L. Zhou, F. Wang, L. Y. Chen, L. Yu, J. M. Iglesias-Pedraz, S. Kircher, E. Schafer, X. D. Fu, L. M. Fan, and X. W. Deng. 2008. 'Coordinated regulation of Arabidopsis thaliana development by light and gibberellins', *Nature*, 451: 475-U9.

Finkelstein, R., W. Reeves, T. Ariizumi, and C. Steber. 2008. 'Molecular aspects of seed dormancy', *Annual Review of Plant Biology*, 59: 387-415.

Fischer, R. A., and K. J. Quail. 1990. 'The effect of major dwarfing genes on yield potential in spring wheats', *Euphytica*, 46: 51-56.

Fischer, R. A., and Y. M. Stockman. 1986. 'Increased kernel number in Norin-10 derived dwarf wheat - evaluation of the cause', *Australian Journal of Plant Physiology*, 13: 767-84.

Fischer, R. A., and J. T. Wood. 1978. 'Drought resistance in spring wheat cultivars. III. Yield associations with morpho-physiological traits', *Australian Journal of Agricultural Research*, 30: 1001-20.

Fletcher, R. A., G. Hofstra, and J. G. Gao. 1986. 'Comparative fungitoxic and plant-growth regulating properties of triazole derivatives', *Plant and Cell Physiology*, 27: 367-71.

Flintham, J. E., A. Borner, A. J. Worland, and M. D. Gale. 1997. 'Optimizing wheat grain yield: Effects of Rht (gibberellin-insensitive) dwarfing genes', *Journal of Agricultural Science*, 128: 11-25.

Flintham, J. E., and M. D. Gale. 1982. 'THE TOM THUMB DWARFING GENE, RHT3 IN WHEAT .1. REDUCED PREHARVEST DAMAGE TO BREADMAKING QUALITY', *Theoretical and Applied Genetics*, 62: 121-26.

Flintham, JE., and MD. Gale. 1983. 'The Tom Thumb dwarfing gene RHT3 in Wheat .2. Effects on grain quality', *Theoretical and Applied Genetics*, 66: 249-56.

Ford, B. A., E. Foo, R. Sharwood, M. Karafiatova, J. Vrana, C. MacMillan, D. S. Nichols, B. Steuernagel, C. Uauy, J. Dolezel, P. M. Chandler, and W. Spielmeyer. 2018. 'Rht18 Semidwarfism in Wheat Is Due to Increased GA 2-oxidaseA9 Expression and Reduced GA Content', *Plant Physiology*, 177: 168-80.

Foster, C.A. 1977. 'Slender: an accelerated extension growth mutant of barley', *Barley Genetics Newsletter*, 7: 24-27.

Fowler, BD. 2018. 'Growth Stages of Wheat', *Winter Wheat Production Manual*: Chapter 10.

Fujioka, S., H. Yamane, C. R. Spray, P. Gaskin, J. Macmillan, B. O. Phinney, and N. Takahashi. 1988. 'Qualitative and quantitative analyses of gibberellins in vegetative shoots of normal, Dwarf-1, Dwarf-2, Dwarf-3 and Dwarf-5 seedlings of Zea mays', *Plant Physiology*, 88: 1367-72.

Fukao, Takeshi, and Julia Bailey-Serres. 2008. 'Submergence tolerance conferred by Sub1A is mediated by SLR1 and SLRL1 restriction of gibberellin responses in rice', *Proceedings of the National Academy of Sciences of the United States of America*, 105: 16814-19.

Fukazawa, J., M. Mori, S. Watanabe, C. Miyamoto, T. Ito, and Y. Takahashi. 2017. 'DELLA-GAF1 Complex Is a Main Component in Gibberellin Feedback Regulation of GA20 Oxidase 2', *Plant Physiology*, 175: 1395-406.

Fukazawa, J., M. Nakata, T. Ito, S. Yamaguchi, and Y. Takahashi. 2010. 'The transcription factor RSG regulates negative feedback of NtGA20ox1 encoding GA 20-oxidase', *Plant Journal*, 62: 1035-45.

Fukazawa, J., H. Teramura, S. Murakoshi, K. Nasuno, N. Nishida, T. Ito, M. Yoshida, Y. Kamiya, S. Yamaguchi, and Y. Takahashi. 2014. 'DELLAs Function as Coactivators of

GAI-ASSOCIATED FACTOR1 in Regulation of Gibberellin Homeostasis and Signaling in Arabidopsis', *Plant Cell*, 26: 2920-38.
Futterer, J., and T. Hohn. 1996. 'Translation in plants - Rules and exceptions', *Plant Molecular Biology*, 32: 159-89.
Gale, M. , and G. Marshall. 1975. 'Nature and genetic-control of gibberellin insensitivity in dwarf wheat grain', *Heredity*, 35: 55-&.
Gale, M. D., C. N. Law, G. A. Marshall, and A. J. Worland. 1975. 'The genetic control of gibberellic acid insensitivity and coleoptile length in a "dwarf" wheat', *Heredity*, 34: 393-99.
Gale, M. D., and G. A. Marshall. 1973. 'INSENSITIVITY TO GIBBERELLIN IN DWARF WHEATS', *Annals of Botany*, 37: 729-35.
Gale, M. D., and S. Youssefian. 1985. 'Dwarfing genes in wheat ', *Progress in Plant Breeding*, 1 1-35.
Gale, M.D. , and GA Marshall. 1976. 'The chromosomal location of Gai1 and Rht1 genes for gibberellin insensitivity and semidwarfism, in a derivate of Norin 10 wheat.', *Heredity*, 37: 283-89.
Gale, MD., C. Law, and A. J. Worland. 1975. 'The chromosomal location of a major dwarfing gene from Norin 10 in new British semi-dwarf wheats', *Heredity*, 35: 417-21.
Galinat, W.C. 1959. 'The phytomer in relation to floral homologies in the American Maydae', *Botanical Museum Leaflets, Harvard Museum*, 19: 1-32.
Gallego-Bartolome, J., D. Alabadi, and M. A. Blazquez. 2011. 'DELLA-Induced Early Transcriptional Changes during Etiolated Development in Arabidopsis thaliana', *Plos One*, 6.
Gallego-Bartolome, J., E. G. Minguet, F. Grau-Enguix, M. Abbas, A. Locascio, S. G. Thomas, D. Alabadi, and M. A. Blazquez. 2012. 'Molecular mechanism for the interaction between gibberellin and brassinosteroid signaling pathways in Arabidopsis', *Proceedings of the National Academy of Sciences of the United States of America*, 109: 13446-51.
Gallego-Bartolome, J., E. G. Minguet, J. A. Marin, S. Prat, M. A. Blazquez, and D. Alabadi. 2010. 'Transcriptional Diversification and Functional Conservation between DELLA Proteins in Arabidopsis', *Molecular Biology and Evolution*, 27: 1247-56.
Gardner, J. S., W. M. Hess, and E. J. Trione. 1985. 'Development of the young wheat spike - a SEM study of Chinese Spring Wheat', *American Journal of Botany*, 72: 548-59.
Gaskin, P., P. S. Kirkwood, J. R. Lenton, J. Macmillan, and M. E. Radley. 1980. 'IDENTIFICATION OF GIBBERELLINS IN DEVELOPING WHEAT-GRAIN', *Agricultural and Biological Chemistry*, 44: 1589-93.
Gelinsky, E., and A. Hilbeck. 2018. 'European Court of Justice ruling regarding new genetic engineering methods scientifically justified: a commentary on the biased reporting about the recent ruling', *Environmental Sciences Europe*, 30.
Ghosh, R., J. E. Gilda, and A. V. Gomes. 2014. 'The necessity of and strategies for improving confidence in the accuracy of western blots', *Expert Review of Proteomics*, 11: 549-60.
Gibson, U. E. M., C. A. Heid, and P. M. Williams. 1996. 'A novel method for real time quantitative RT PCR', *Genome Research*, 6: 995-1001.
Gol, L., F. Tome, and M. von Korff. 2017. 'Floral transitions in wheat and barley: interactions between photoperiod, abiotic stresses, and nutrient status', *Journal of Experimental Botany*, 68: 1399-410.
Gold, CM., and CM Duffus. 1993. 'The effect of gibberellic acid-insensitive dwarfing genes on pre-maturity α-amylase and sucrose relationship during grain development in wheat.', *In: Walker Simmons MK, Reid JL (eds) Sixth international symposium on pre-harvest sprouting in cereals,*: 171-77.

Gooding, M. J., M. Addisu, R. K. Uppal, J. W. Snape, and H. E. Jones. 2012. 'Effect of wheat dwarfing genes on nitrogen-use efficiency', *Journal of Agricultural Science*, 150: 3-22.

Gooding, M. J., R. K. Uppal, M. Addisu, K. D. Harris, C. Uauy, J. R. Simmonds, and A. J. Murdoch. 2012. 'Reduced height alleles (Rht) and Hagberg falling number of wheat', *Journal of Cereal Science*, 55: 305-11.

Griffiths, Jayne, Kohji Murase, Ivo Rieu, Rodolfo Zentella, Zhong-Lin Zhang, Stephen J. Powers, Fan Gong, Andrew L. Phillips, Peter Hedden, Tai-ping Sun, and Stephen G. Thomas. 2006. 'Genetic characterization and functional analysis of the GID1 gibberellin receptors in Arabidopsis', *Plant Cell*, 18: 3399-414.

Griffiths, Simon, James Simmonds, Michelle Leverington, Yingkun Wang, Lesley Fish, Liz Sayers, Leodie Alibert, Simon Orford, Luzie Wingen, and John Snape. 2012. 'Meta-QTL analysis of the genetic control of crop height in elite European winter wheat germplasm', *Molecular Breeding*, 29: 159-71.

Groot, S. P. C., and C. M. Karssen. 1987. 'Gibberellins regulate seed-germination in tomato by endosperm weakening - a study with gibberellin-deficient mutants', *Planta*, 171: 525-31.

Grover, G., A. Sharma, H. S. Gill, P. Srivastava, and N. S. Bains. 2018. 'Rht8 gene as an alternate dwarfing gene in elite Indian spring wheat cultivars', *Plos One*, 13.

Gubler, F., R. Kalla, J. K. Roberts, and J. V. Jacobsen. 1995. 'Gibberellin-regulated expression of a MYB gene in barley aleurone cells - evidence for MYB transactivation of a HIGH-PL ALPHA-AMYLASE GENE PROMOTER', *Plant Cell*, 7: 1879-91.

Hashimoto, T. 1959. "Increase in percentage of gibberellin-induced dark germination of tobacco seeds by N-compounds." In, 430-31. Bot. Mag. Tokyo,.

Hay, R. K. M. 1995. 'Harvest index - a review of its use in plant breeding and crop phyisology', *Annals of Applied Biology*, 126: 197-216.

He, X. Y., P. K. Singh, S. Dreisigacker, S. Singh, M. Lillemo, and E. Duveiller. 2016. 'Dwarfing Genes Rht-B1b and Rht-D1b Are Associated with Both Type I FHB Susceptibility and Low Anther Extrusion in Two Bread Wheat Populations', *Plos One*, 11.

Hedden, P., and S. J. Croker. 1992. 'Regulation of gibberellin biosynthesis in maize seedlings', *Progress in Plant Growth Regulation*, 13: 534-44.

Hedden, P., and Y. Kamiya. 1997. 'Gibberellin biosynthesis: Enzymes, genes and their regulation', *Annual Review of Plant Physiology and Plant Molecular Biology*, 48: 431-60.

Hedden, P., and A. L. Phillips. 2000. 'Gibberellin metabolism: new insights revealed by the genes', *Trends in Plant Science*, 5: 523-30.

Hedden, P., and S. G. Thomas. 2012. 'Gibberellin biosynthesis and its regulation', *Biochemical Journal*, 444: 11-25.

Hedden, Peter. 2003. 'The Genes of the Green Revolution ', *Trends in Genetics*, 19: 5-9.

Helliwell, C. A., P. M. Chandler, A. Poole, E. S. Dennis, and W. J. Peacock. 2001. 'The CYP88A cytochrome P450, ent-kaurenoic acid oxidase, catalyzes three steps of the gibberellin biosynthesis pathway', *Proceedings of the National Academy of Sciences of the United States of America*, 98: 2065-70.

Helliwell, C. A., C. C. Sheldon, M. R. Olive, A. R. Walker, J. A. D. Zeevaart, W. J. Peacock, and E. S. Dennis. 1998. 'Cloning of the Arabidopsis ent-kaurene oxidase gene GA3', *Proceedings of the National Academy of Sciences of the United States of America*, 95: 9019-24.

Helliwell, C. A., J. A. Sullivan, R. M. Mould, J. C. Gray, W. J. Peacock, and E. S. Dennis. 2001. 'A plastid envelope location of Arabidopsis ent-kaurene oxidase links the plastid and endoplasmic reticulum steps of the gibberellin biosynthesis pathway', *Plant Journal*, 28: 201-08.

Henikoff, S., and L. Comai. 2003. 'Single-nucleotide mutations for plant functional genomics', *Annual Review of Plant Biology*, 54: 375-401.
Henikoff, S., B. J. Till, and L. Comai. 2004. 'TILLING. Traditional mutagenesis meets functional genomics', *Plant Physiology*, 135: 630-36.
Henry, Isabelle M., Ugrappa Nagalakshmi, Meric C. Lieberman, Kathie J. Ngo, Ksenia V. Krasileva, Hans Vasquez-Gross, Alina Akhunova, Eduard Akhunov, Jorge Dubcovsky, Thomas H. Tai, and Luca Comai. 2014. 'Efficient Genome-Wide Detection and Cataloging of EMS-Induced Mutations Using Exome Capture and Next-Generation Sequencing', *Plant Cell*, 26: 1382-97.
Heun, M., R. SchaferPregl, D. Klawan, R. Castagna, M. Accerbi, B. Borghi, and F. Salamini. 1997. 'Site of einkorn wheat domestication identified by DNA fingerprinting', *Science*, 278: 1312-14.
Hirano, K., E. Kouketu, H. Katoh, K. Aya, M. Ueguchi-Tanaka, and M. Matsuoka. 2012. 'The suppressive function of the rice DELLA protein SLR1 is dependent on its transcriptional activation activity', *Plant Journal*, 71: 443-53.
Hirano, Ko, Kenji Asano, Hiroyuki Tsuji, Mayuko Kawamura, Hitoshi Mori, Hidemi Kitano, Miyako Ueguchi-Tanaka, and Makoto Matsuoka. 2010. 'Characterization of the Molecular Mechanism Underlying Gibberellin Perception Complex Formation in Rice', *Plant Cell*, 22: 2680-96.
Holzapfel, J., H. H. Voss, T. Miedaner, V. Korzun, J. Haberle, G. Schweizer, V. Mohler, G. Zimmermann, and L. Hartl. 2008. 'Inheritance of resistance to Fusarium head blight in three European winter wheat populations', *Theoretical and Applied Genetics*, 117: 1119-28.
Hong, G. J., X. Y. Xue, Y. B. Mao, L. J. Wang, and X. Y. Chen. 2012. 'Arabidopsis MYC2 Interacts with DELLA Proteins in Regulating Sesquiterpene Synthase Gene Expression', *Plant Cell*, 24: 2635-48.
Hoogendoorn, J., and M. D. Gale. 1988. 'The effects of dwarfing genes on heat tolerance in CIMMYT germplasm', *Cereal breeding related to integrated cereal production. Proceedings of the conference of the Cereal Section of EUCARPIA, Wageningen, Netherlands, 24-26 February 1988*: 61-66.
Hoogendoorn, J., J. M. Rickson, and M. D. Gale. 1990. 'Differences in leaf and stem anatomy related to plant height of tall dwarf wheat (Triticum aestivum L)', *Journal of Plant Physiology*, 136: 72-77.
Hooley, R. 1994. 'Gibberellins - perception, transduction and responses', *Plant Molecular Biology*, 26: 1529-55.
Hou, X. L., L. Y. C. Lee, K. F. Xia, Y. Y. Yen, and H. Yu. 2010. 'DELLAs Modulate Jasmonate Signaling via Competitive Binding to JAZs', *Developmental Cell*, 19: 884-94.
Huang, J., D. Tang, Y. Shen, B. X. Qin, L. L. Hong, A. Q. You, M. Li, X. Wang, H. X. Yu, M. H. Gu, and Z. K. Cheng. 2010. 'Activation of gibberellin 2-oxidase 6 decreases active gibberellin levels and creates a dominant semi-dwarf phenotype in rice (Oryza sativa L.)', *Journal of Genetics and Genomics*, 37: 23-36.
Huang, Y. Y., W. L. Yang, Z. Pei, X. L. Guo, D. C. Liu, J. Z. Sun, and A. M. Zhang. 2012. 'The genes for gibberellin biosynthesis in wheat', *Functional & Integrative Genomics*, 12: 199-206.
Hudson, J., A. Caplanova, and M. Novak. 2015. 'Public attitudes to GM foods. The balancing of risks and gains', *Appetite*, 92: 303-13.
Humphries, EC., and AW Wheeler. 1963. 'The Physiology of Leaf Growth', *Annual Review of Plant Physiology*, Vol. 14:385-410.
Huq, E., and P. H. Quail. 2002. 'PIF4, a phytochrome-interacting bHLH factor, functions as a negative regulator of phytochrome B signaling in Arabidopsis', *Embo Journal*, 21: 2441-50.

Ikeda, A., M. Ueguchi-Tanaka, Y. Sonoda, H. Kitano, M. Koshioka, Y. Futsuhara, M. Matsuoka, and J. Yamaguchi. 2001. 'slender rice, a constitutive gibberellin response mutant, is caused by a null mutation of the SLR1 gene, an ortholog of the height-regulating gene GAI/RGA/RHT/D8', *Plant Cell*, 13: 999-1010.

Ito, S., D. Yamagami, and T. Asami. 2018. 'Effects of gibberellin and strigolactone on rice tiller bud growth', *Journal of Pesticide Science*, 43: 220-23.

Itoh, H., A. Shimada, M. Ueguchi-Tanaka, N. Kamiya, Y. Hasegawa, M. Ashikari, and M. Matsuoka. 2005. 'Overexpression of a GRAS protein lacking the DELLA domain confers altered gibberellin responses in rice', *Plant Journal*, 44: 669-79.

Itoh, H., T. Tatsumi, T. Sakamoto, K. Otomo, T. Toyomasu, H. Kitano, M. Ashikari, S. Ichihara, and M. Matsuoka. 2004. 'A rice semi-dwarf gene, Tan-Ginbozu (D35), encodes the gibberellin biosynthesis enzyme, ent-kaurene oxidase', *Plant Molecular Biology*, 54: 533-47.

Itoh, H., M. Ueguchi-Tanaka, Y. Sato, M. Ashikari, and M. Matsuoka. 2002. 'The gibberellin signaling pathway is regulated by the appearance and disappearance of SLENDER RICE1 in nuclei', *Plant Cell*, 14: 57-70.

Jacobsen, John V., Frank Gubler, and Peter M. Chandler. 1995. 'Gibberellin action in germinated cereal grains', *Plant hormones: Physiology, biochemistry and molecular biology, 2nd edition*: 246-71.

Jasinski, S., A. Tattersall, P. Piazza, A. Hay, J. F. Martinez-Garcia, G. Schmitz, K. Theres, S. McCormick, and M. Tsiantis. 2008. 'PROCERA encodes a DELLA protein that mediates control of dissected leaf form in tomato', *Plant Journal*, 56: 603-12.

Jung, C., and A. E. Muller. 2009. 'Flowering time control and applications in plant breeding', *Trends in Plant Science*, 14: 563-73.

Kami, C., S. Lorrain, P. Hornitschek, and C. Fankhauser. 2010. 'Light Regulated Plant Growth and Development', *Plant Development*, 91: 29-66.

Kaneko, M., H. Itoh, Y. Inukai, T. Sakamoto, M. Ueguchi-Tanaka, M. Ashikari, and M. Matsuoka. 2003. 'Where do gibberellin biosynthesis and gibberellin signaling occur in rice plants?', *Plant Journal*, 35: 104-15.

Karssen, C. M., S. Zagorski, J. Kepczynski, and S. P. C. Groot. 1989. 'KEY ROLE FOR ENDOGENOUS GIBBERELLINS IN THE CONTROL OF SEED-GERMINATION', *Annals of Botany*, 63: 71-80.

Kearse, Matthew, Richard Moir, Amy Wilson, Steven Stones-Havas, Matthew Cheung, Shane Sturrock, Simon Buxton, Alex Cooper, Sidney Markowitz, Chris Duran, Tobias Thierer, Bruce Ashton, Peter Meintjes, and Alexei Drummond. 2012. 'Geneious Basic: An integrated and extendable desktop software platform for the organization and analysis of sequence data', *Bioinformatics*, 28: 1647-49.

Kebrom, Tesfamichael H., Peter M. Chandler, Steve M. Swain, Rod W. King, Richard A. Richards, and Wolfgang Spielmeyer. 2012. 'Inhibition of Tiller Bud Outgrowth in the tin Mutant of Wheat Is Associated with Precocious Internode Development', *Plant Physiology*, 160: 308-18.

Kertesz, Z., J. E. Flintham, and M. D. Gale. 1991. 'Effects of RHT dwarfing genes on wheat grain yield and its components under Eastern-European conditions', *Cereal Research Communications*, 19: 297-304.

Keyes, G. J. 1987. 'Genetic Control of Sensitivity to Gibberellic Acid in Wheat: Some Developmental Consequences '.

Keyes, G. J., D. J. Paolillo, and M. E. Sorrells. 1989. 'THE EFFECTS OF DWARFING GENES RHT1 AND RHT2 ON CELLULAR DIMENSIONS AND RATE OF LEAF ELONGATION IN WHEAT', *Annals of Botany*, 64: 683-90.

Khakwani, A. A., M. D. Dennett, M. Munir, and M. Abid. 2012. 'GROWTH AND YIELD RESPONSE OF WHEAT VARIETIES TO WATER STRESS AT BOOTING AND ANTHESIS STAGES OF DEVELOPMENT', *Pakistan Journal of Botany*, 44: 879-86.

Khush, G. S. 2001. 'Green revolution: the way forward', *Nature Reviews Genetics*, 2: 815-22.
Kim, Daehwan, Ben Langmead, and Steven L. Salzberg. 2015. 'HISAT: a fast spliced aligner with low memory requirements', *Nature Methods*, 12: 357-U121.
Kim, J. Y., H. K. Yi, G. Choi, B. Shin, P. S. Song, and G. S. Choi. 2003. 'Functional characterization of phytochrome interacting factor 3 in phytochrorne-mediated light signal transduction', *Plant Cell*, 15: 2399-407.
Kirby, E. J. M., and M. Appleyard. 1981. 'Cereal Development Guide 2nd Edition', Arable Unit, National Agricultural Centre, Stoneleigh, Warwickshire, UK.
Kirby, E. J. M., M. Appleyard, and G. Fellowes. 1985. 'Leaf Emergence and Tillering in Barley and Wheat', *Agronomie*, 5: 193-200.
Kondhare, K. R., P. Hedden, P. S. Kettlewell, A. D. Farrell, and J. M. Monaghan. 2014. 'Use of the hormone-biosynthesis inhibitors fluridone and paclobutrazol to determine the effects of altered abscisic acid and gibberellin levels on pre-maturity alpha-amylase formation in wheat grains', *Journal of Cereal Science*, 60: 210-16.
Koning, Ross E. 1994. 'Seeds and Seed Germination', *Plant Physiology Information Website*, http://plantphys.info/plants_human/seedgerm.shtml. (7-4-2019).
Koornneef, M., A. Elgersma, C.J. Hanhart, and et al. 1985. 'A gibberellin-insensitive mutant of Arabidopsis thaliana', *Physiologia Plantarum*, 65: 33-39.
Koornneef, M., and J. H. Vanderveen. 1980. 'INDUCTION AND ANALYSIS OF GIBBERELLIN SENSITIVE MUTANTS IN ARABIDOPSIS-THALIANA (L) HEYNH', *Theoretical and Applied Genetics*, 58: 257-63.
Kozaki, A., and J. Colasanti. 2005. 'The maize flowering time regulator, ID1, is a zinc finger protein with novel DNA binding properties', *Plant and Cell Physiology*, 46: S29-S29.
Kurosawa, E 1926. 'Experimental studies on the nature of the substance secreted by the "bakanae" fungus', *Nat Hist soc Formosa*, 16: 213 - 27.
Lanahan, M. B., and T. H. D. Ho. 1988. 'Slender barley - a constitutive gibberellin response mutant', *Planta*, 175: 107-14.
Lange, T. 1997. 'Cloning gibberellin dioxygenase genes from pumpkin endosperm by heterologous expression off enzyme activities in Escherichia coli', *Proceedings of the National Academy of Sciences of the United States of America*, 94: 6553-58.
Law, C. N., J. W. Snape, and A. J. Worland. 1978. 'GENETIC RELATIONSHIP BETWEEN HEIGHT AND YIELD IN WHEAT', *Heredity*, 40: 133-51.
Lecain, D. R., J. A. Morgan, and G. Zerbi. 1989. 'Leaf anatomy and gas-exhange in nearly isogenic senidwarf and tall winter-wheat', *Crop Science*, 29: 1246-51.
Lee, D. J., and J. A. D. Zeevaart. 2007. 'Regulation of gibberellin 20-oxidase1 expression in spinach by photoperiod', *Planta*, 226: 35-44.
Lee, Li Yen Candy. , Xingliang. Hou, Lei. Fang, Shuguo Fan, Prakash P. Kumar, and Hao. Yu. 2012. 'STUNTED mediates the control of cell proliferation by GA in Arabidopsis', *Development*, 139: 1568-76.
Leivar, P., E. Monte, Y. Oka, T. Liu, C. Carle, A. Castillon, E. Huq, and P. H. Quail. 2008. 'Multiple Phytochrome-Interacting bHLH Transcription Factors Repress Premature Seedling Photomorphogenesis in Darkness', *Current Biology*, 18: 1815-23.
Lenton, J. R., and N. E. J. Appleford. 1991. 'Gibberellin production and action during germination of wheat', *Gibberellins*: 125-35.
Lenton, J. R., P. Hedden, and M. D. Gale. 1987. 'Gibberellin insensitivity in wheat - consequences for development': 145-60.
Lester, D. R., J. J. Ross, J. J. Smith, R. C. Elliott, and J. B. Reid. 1999. 'Gibberellin 2-oxidation and the SLN gene of Pisum sativum', *Plant Journal*, 19: 65-73.
Lewis, D. H. 1973. 'Concepts in Fungal Nutrition and Origin of Biotrophy', *Biological Reviews of the Cambridge Philosophical Society*, 48: 261-78.

Li, A. X., W. L. Yang, X. L. Guo, D. C. Liu, J. Z. Sun, and A. M. Zhang. 2012. 'Isolation of a gibberellin-insensitive dwarfing gene, Rht-B1e, and development of an allele-specific PCR marker', *Molecular Breeding*, 30: 1443-51.

Li, C., Y. Zong, Y. P. Wang, S. Jin, D. B. Zhang, Q. N. Song, R. Zhang, and C. X. Gao. 2018. 'Expanded base editing in rice and wheat using a Cas9-adenosine deaminase fusion', *Genome Biology*, 19.

Li, S. P., Y. H. Zhao, Z. Zhao, X. L. Wu, L. F. Sun, Q. S. Liu, and Y. K. Wu. 2016. 'Crystal Structure of the GRAS Domain of SCARECROW-LIKE7 in Oryza sativa', *Plant Cell*, 28: 1025-34.

Li, Y. Y., J. H. Xiao, J. J. Wu, J. L. Duan, Y. Liu, X. G. Ye, X. Zhang, X. P. Guo, Y. Q. Gu, L. C. Zhang, J. Z. Jia, and X. Y. Kong. 2012. 'A tandem segmental duplication (TSD) in green revolution gene Rht-D1b region underlies plant height variation', *New Phytologist*, 196: 282-91.

Liao, Y., G. K. Smyth, and W. Shi. 2014. 'featureCounts: an efficient general purpose program for assigning sequence reads to genomic features', *Bioinformatics*, 30: 923-30.

Liao, Z. G., H. Yu, J. B. Duan, K. Yuan, C. J. Yu, X. B. Meng, L. Q. Kou, M. J. Chen, Y. H. Jing, G. F. Liu, S. M. Smith, and J. Y. Li. 2019. 'SLR1 inhibits MOC1 degradation to coordinate tiller number and plant height in rice', *Nature Communications*, 10.

Lim, S., J. Park, N. Lee, J. Jeong, S. Toh, A. Watanabe, J. Kim, H. Kang, D. H. Kim, N. Kawakami, and G. Choi. 2013. 'ABA-INSENSITIVE3, ABA-INSENSITIVE5, and DELLAs Interact to Activate the Expression of SOMNUS and Other High-Temperature-Inducible Genes in Imbibed Seeds in Arabidopsis', *Plant Cell*, 25: 4863-78.

Lo, S. F., S. Y. Yang, K. T. Chen, Y. L. Hsing, J. A. D. Zeevaart, L. J. Chen, and S. M. Yu. 2008. 'A Novel Class of Gibberellin 2-Oxidases Control Semidwarfism, Tillering, and Root Development in Rice', *Plant Cell*, 20: 2603-18.

Locascio, A., M. A. Blazquez, and D. Alabadi. 2013. 'Dynamic Regulation of Cortical Microtubule Organization through Prefoldin-DELLA Interaction', *Current Biology*, 23: 804-09.

Lunn, G.D. , B.J. Major, P.S. Kettlewell, and R.K. Scott. 2001. 'Mechanisms leading to excess α-amylase activity in wheat (Triticum aestivum L.) grain in the U.K', *Cereal Science*, 33: 313-29.

MacMillan, J. 1997. 'Biosynthesis of the gibberellin plant hormones', *Natural Product Reports*, 14: 221-43.

Magome, H., T. Nomura, A. Hanada, N. Takeda-Kamiya, T. Ohnishi, Y. Shinma, T. Katsumata, H. Kawaide, Y. Kamiya, and S. Yamaguchi. 2013. 'CYP714B1 and CYP714B2 encode gibberellin 13-oxidases that reduce gibberellin activity in rice', *Proceedings of the National Academy of Sciences of the United States of America*, 110: 1947-52.

Marcussen, Thomas, Simen R. Sandve, Lise Heier, Manuel Spannagl, Matthias Pfeifer, Kjetill S. Jakobsen, Brande B. H. Wulff, Burkhard Steuernagel, Klaus F. X. Mayer, Odd-Arne Olsen, and Sequencing Int Wheat Genome. 2014. 'Ancient hybridizations among the ancestral genomes of bread wheat', *Science*, 345.

Mares, D., and K. Mrva. 2008. 'Late-maturity alpha-amylase: Low falling number in wheat in the absence of preharvest sprouting', *Journal of Cereal Science*, 47: 6-17.

Martin, D. N., W. M. Proebsting, and P. Hedden. 1999. 'The SLENDER gene of pea encodes a gibberellin 2-oxidase', *Plant Physiology*, 121: 775-81.

Matsui, T., K. Omasa, and T. Horie. 1999. 'Mechanism of anther dehiscence in rice (Oryza sativa L.)', *Annals of Botany*, 84: 501-06.

Matsushita, A., T. Furumoto, S. Ishida, and Y. Takahashi. 2007. 'AGF1, an AT-hook protein, is necessary for the negative feedback of AtGA3ox1 encoding GA 3-oxidase', *Plant Physiology*, 143: 1152-62.

Mayer, K. F. X., J. Rogers, J. Dolezel, and C. Pozniak. 2014. 'A chromosome-based draft sequence of the hexaploid bread wheat (Triticum aestivum) genome', *Science*, 345: 11.
McCormick, S. 1993. 'Male gametophyte development', *Plant Cell*, 5: 1265-75.
McFadden, E. S., and E. R. Sears. 1946. 'THE ORIGIN OF TRITICUM SPELTA AND ITS FREE-THRESHING HEXAPLOID RELATIVES', *Journal of Heredity*, 37: 81-89.
McGinnis, K. M., S. G. Thomas, J. D. Soule, L. C. Strader, J. M. Zale, T. P. Sun, and C. M. Steber. 2003. 'The Arabidopsis SLEEPY1 gene encodes a putative F-box subunit of an SCF E3 ubiquitin ligase', *Plant Cell*, 15: 1120-30.
McVitte, JA., MD. Gale, D. Marshall, and B. Westcotte. 1978. 'The intrachromosomal mapping of the Norin 10 and Tom Thumb dwarfing genes', *Heredity*, 40: 67-70.
Middleton, Alistair M., Susana Ubeda-Tomas, Jayne Griffiths, Tara Holman, Peter Hedden, Stephen G. Thomas, Andrew L. Phillips, Michael J. Holdsworth, Malcolm J. Bennett, John R. King, and Markus R. Owen. 2012. 'Mathematical modeling elucidates the role of transcriptional feedback in gibberellin signaling', *Proceedings of the National Academy of Sciences of the United States of America*, 109: 7571-76.
Miralles, D. J., D. F. Calderini, K. P. Pomar, and A. D'Ambrogio. 1998. 'Dwarfing genes and cell dimensions in different organs of wheat', *Journal of Experimental Botany*, 49: 1119-27.
Miralles, D. J., R. A. Richards, and G. A. Slafer. 2000. 'Duration of the stem elongation period influences the number of fertile florets in wheat and barley', *Australian Journal of Plant Physiology*, 27: 931-40.
Miralles, D. J., and G. A. Slafer. 1995. 'INDIVIDUAL GRAIN WEIGHT RESPONSES TO GENETIC REDUCTION IN CULM LENGTH IN WHEAT AS AFFECTED BY SOURCE-SINK MANIPULATIONS', *Field Crops Research*, 43: 55-66.
———. 1997. 'Radiation interception and radiation use efficiency of near-isogenic wheat lines with different height', *Euphytica*, 97: 201-08.
Mo, Y., S. Pearce, and J. Dubcovsky. 2018. 'Phenotypic and transcriptomic characterization of a wheat tall mutant carrying an induced mutation in the C-terminal PFYRE motif of RHT-B1b', *Bmc Plant Biology*, 18.
Mrva, K., and D. J. Mares. 1996. 'Expression of late maturity alpha-amylase in wheat containing gibberellic acid insensitivity genes', *Euphytica*, 88: 69-76.
Muangprom, A., S. G. Thomas, T. P. Sun, and T. C. Osborn. 2005. 'A novel dwarfing mutation in a green revolution gene from Brassica rapa', *Plant Physiology*, 137: 931-38.
Murase, K., Y. Hirano, T. P. Sun, and T. Hakoshima. 2008. 'Gibberellin-induced DELLA recognition by the gibberellin receptor GID1', *Nature*, 456: 459-U15.
Nakamura, H., M. Hakata, K. Amano, A. Miyao, N. Toki, M. Kajikawa, J. Pang, N. Higashi, S. Ando, S. Toki, M. Fujita, A. Enju, M. Seki, M. Nakazawa, T. Ichikawa, K. Shinozaki, M. Matsui, Y. Nagamura, H. Hirochika, and H. Ichikawa. 2007. 'A genome-wide gain-of-function analysis of rice genes using the FOX-hunting system', *Plant Molecular Biology*, 65: 357-71.
Navarro, Lionel, Rajendra Bari, Patrick Achard, Purificacion Lison, Adnane Nemri, Nicholas P. Harberd, and Jonathan D. G. Jones. 2008. 'DELLAs control plant immune responses by modulating the balance and salicylic acid signaling', *Current Biology*, 18: 650-55.
Nelson, Sven K. , and Camille M. Steber. 2016. 'Gibberellin Hormon Signal Perception: Down-Regulating Dell Repressors of Plant Growth and Development', *Annual Plant Reviews*, 49: 152-88.
Nizam Uddin, M., and D. R. Marshall. 1989. 'Effects of dwarfing genes on yield and yield components under irragated and rainfed conditions in wheat Triticum aestivum L', *Euphytica*, 42: 127-34.
OECD/FAO. 2012. 'OECD-FAO Agricultural Outlook 2012–2021', *OECD Publishing and FAO*, Available: http://dx.doi.org/10.1787/agr_outlook-2012-en.

Ogawa, M., T. Kusano, M. Katsumi, and H. Sano. 2000. 'Rice gibberellin-insensitive gene homolog, OsGAI encodes a nuclear-localized protein capable of gene activation at transcriptional level', *Gene*, 245: 21-29.

Page, E. R., M. Tollenaar, E. A. Lee, L. Lukens, and C. J. Swanton. 2010. 'Shade avoidance: an integral component of crop-weed competition', *Weed Research*, 50: 281-88.

Parish, R. W., and S. F. Li. 2010. 'Death of a tapetum: A programme of developmental altruism', *Plant Science*, 178: 73-89.

Park, J., K. T. Nguyen, E. Park, J. S. Jeon, and G. Choi. 2013. 'DELLA Proteins and Their Interacting RING Finger Proteins Repress Gibberellin Responses by Binding to the Promoters of a Subset of Gibberellin-Responsive Genes in Arabidopsis', *Plant Cell*, 25: 927-43.

Park, J., D. H. Oh, M. Dassanayake, K. T. Nguyen, J. Ogas, G. Choi, and T. P. Sun. 2017. 'Gibberellin Signaling Requires Chromatin Remodeler PICKLE to Promote Vegetative Growth and Phase Transitions', *Plant Physiology*, 173: 1463-74.

Pearce, S. 2009. 'Understanding the roles of green revolution genes in wheat', *University of Nottingham and Rothamsted Research*.

Pearce, S., A. K. Huttly, I. M. Prosser, Y. D. Li, S. P. Vaughan, B. Gallova, A. Patil, J. A. Coghill, J. Dubcovsky, P. Hedden, and A. L. Phillips. 2015. 'Heterologous expression and transcript analysis of gibberellin biosynthetic genes of grasses reveals novel functionality in the GA3ox family', *Bmc Plant Biology*, 15.

Pearce, Stephen, Robert Saville, Simon P. Vaughan, Peter M. Chandler, Edward P. Wilhelm, Caroline A. Sparks, Nadia Al-Kaff, Andrey Korolev, Margaret I. Boulton, Andrew L. Phillips, Peter Hedden, Paul Nicholson, and Stephen G. Thomas. 2011. 'Molecular Characterization of Rht-1 Dwarfing Genes in Hexaploid Wheat', *Plant Physiology*, 157: 1820-31.

Pearce, Stephen, Leonardo S. Vanzetti, and Jorge Dubcovsky. 2013. 'Exogenous Gibberellins Induce Wheat Spike Development under Short Days Only in the Presence of VERNALIZATION1', *Plant Physiology*, 163: 1433-45.

Peng, J. R., P. Carol, D. E. Richards, K. E. King, R. J. Cowling, G. P. Murphy, and N. P. Harberd. 1997. 'The Arabidopsis GAI gene defines a signaling pathway that negatively regulates gibberellin responses', *Genes & Development*, 11: 3194-205.

Peng, J. R., D. E. Richards, N. M. Hartley, G. P. Murphy, K. M. Devos, J. E. Flintham, J. Beales, L. J. Fish, A. J. Worland, F. Pelica, D. Sudhakar, P. Christou, J. W. Snape, M. D. Gale, and N. P. Harberd. 1999. ''Green revolution' genes encode mutant gibberellin response modulators', *Nature*, 400: 256-61.

Perten, H. 1964. 'Application of falling number method for evaluation alpha-amylase activity', *Cereal Chemistry*, 41: 127-&.

Phillips, Andrew L 2016. 'Genetic control of gibberellin metabolism and signalling in crop improvement', *Annual Plant Reviews*, 49.

Phinney, B. O. 1956. 'Growth response of single-gene dwarf mutants in maize to gibberellin acid', *Proceedings of the National Academy of Sciences of the United States of America*, 42: 185-89.

Pinthus, M. J., M. D. Gale, N. E. J. Appleford, and J. R. Lenton. 1989. 'Effect of temperature on gibberellin (GA) responsiveness and on engodgenous GA1 content of tall and dwarf wheat genotypes', *Plant Physiology*, 90: 854-59.

Plackett, A. R. G., A. C. Ferguson, S. J. Powers, A. Wanchoo-Kohli, A. L. Phillips, Z. A. Wilson, P. Hedden, and S. G. Thomas. 2014. 'DELLA activity is required for successful pollen development in the Columbia ecotype of Arabidopsis', *New Phytologist*, 201: 825-36.

Plackett, A. R. G., S. G. Thomas, Z. A. Wilson, and P. Hedden. 2011. 'Gibberellin control of stamen development: a fertile field', *Trends in Plant Science*, 16: 568-78.

Population Council. 2013. 'Productivity Growth in Global Agriculture', *Population and Development Review*, 39: 361-65.
Power, J. F., and J. Alessi. 1978. 'Tiller Development and Yield of Standard and Semi-Dwarf Spring Wheat Varieties As Affected by Nitrogen-Fertilizer', *Journal of Agricultural Science*, 90: 97-108.
Pysh, L. D., J. W. Wysocka-Diller, C. Camilleri, D. Bouchez, and P. N. Benfey. 1999. 'The GRAS gene family in Arabidopsis: sequence characterization and basic expression analysis of the SCARECROW-LIKE genes', *Plant Journal*, 18: 111-19.
Qi, T. C., H. Huang, D. W. Wu, J. B. Yan, Y. J. Qi, S. S. Song, and D. X. Xie. 2014. 'Arabidopsis DELLA and JAZ Proteins Bind the WD-Repeat/bHLH/MYB Complex to Modulate Gibberellin and Jasmonate Signaling Synergy', *Plant Cell*, 26: 1118-33.
R Core Team. 2019. 'R: A Language and Environment for Statistical Computing', *R Foundation for Statistical Computing, Vienna, Austria*.
Radley, M. 1970. 'COMPARISON OF ENDOGENOUS GIBBERELLINS AND RESPONSE TO APPLIED GIBBERELLIN OF SOME DWARF AND TALL WHEAT CULTIVARS', *Planta*, 92: 292-&.
Ray, D. K., N. D. Mueller, P. C. West, and J. A. Foley. 2013. 'Yield Trends Are Insufficient to Double Global Crop Production by 2050', *Plos One*, 8.
Razumov, VI., RS Lmarj, and T. Ke-Wei. 1960. 'The effect of gibberellic acid on development of winter cereals.', *Bot Z*, 45: 1732-38.
Rebetzke, G. J., R. A. Richards, V. M. Fischer, and B. J. Mickelson. 1999. 'Breeding long coleoptile, reduced height wheats', *Euphytica*, 106: 159-68.
Reitz, L. P., and S. C. Salmon. 1968. 'Origin history and use of Norin 10 wheat', *Crop Science*, 8: 686-&.
Robertson, M., S. M. Swain, P. M. Chandler, and N. E. Olszewski. 1998. 'Identification of a negative regulator of gibberellin action, HvSPY, in barley', *Plant Cell*, 10: 995-1007.
Sakamoto, T., K. Miura, H. Itoh, T. Tatsumi, M. Ueguchi-Tanaka, K. Ishiyama, M. Kobayashi, G. K. Agrawal, S. Takeda, K. Abe, A. Miyao, H. Hirochika, H. Kitano, M. Ashikari, and M. Matsuoka. 2004. 'An overview of gibberellin metabolism enzyme genes and their related mutants in rice', *Plant Physiology*, 134: 1642-53.
Sakamoto, T., Y. Morinaka, K. Ishiyama, M. Kobayashi, H. Itoh, T. Kayano, S. Iwahori, M. Matsuoka, and H. Tanaka. 2003. 'Genetic manipulation of gibberellin metabolism in transgenic rice', *Nature Biotechnology*, 21: 909-13.
Salamini, F., H. Ozkan, A. Brandolini, R. Schafer-Pregl, and W. Martin. 2002. 'Genetics and geography of wild cereal domestication in the Near East', *Nature Reviews Genetics*, 3: 429-41.
Sasaki, A., H. Itoh, K. Gomi, M. Ueguchi-Tanaka, K. Ishiyama, M. Kobayashi, D. H. Jeong, G. An, H. Kitano, M. Ashikari, and M. Matsuoka. 2003. 'Accumulation of phosphorylated repressor for gibberellin signaling in an F-box mutant', *Science*, 299: 1896-98.
Saville, R. J., N. Gosman, C. J. Burt, J. Makepeace, A. Steed, M. Corbitt, E. Chandler, J. K. M. Brown, M. I. Boulton, and P. Nicholson. 2012. 'The 'Green Revolution' dwarfing genes play a role in disease resistance in Triticum aestivum and Hordeum vulgare', *Journal of Experimental Botany*, 63: 1271-83.
Schomburg, F. M., C. M. Bizzell, D. J. Lee, J. A. D. Zeevaart, and R. M. Amasino. 2003. 'Overexpression of a novel class of gibberellin 2-oxidases decreases gibberellin levels and creates dwarf plants', *Plant Cell*, 15: 151-63.
Serrano-Mislata, Antonio, Stefano Bencivenga, Max Bush, Katharina Schiessl, Scott Boden, and Robert Sablowski. 2017. 'DELLA genes restrict inflorescence meristem function independently of plant height', *Nature Plants*, 3: 749-54.

Sestili, F., E. Botticella, Z. Bedo, A. Phillips, and D. Lafiandra. 2010. 'Production of novel allelic variation for genes involved in starch biosynthesis through mutagenesis', *Molecular Breeding*, 25: 145-54.

Shen, Q., J. Cui, X. Q. Fu, T. X. Yan, and K. X. Tang. 2015. 'Cloning and characterization of DELLA genes in Artemisia annua', *Genetics and Molecular Research*, 14: 10037-49.

Shewry, P.R. 2009. 'Wheat', *J. Exp. Bot.*, 60.

Silverstone, A. L., C. W. Chang, E. Krol, and T. P. Sun. 1997. 'Developmental regulation of the gibberellin biosynthetic gene GA1 in Arabidopsis thaliana', *Plant Journal*, 12: 9-19.

Silverstone, A. L., C. N. Ciampaglio, and T. P. Sun. 1998. 'The Arabidopsis RGA gene encodes a transcriptional regulator repressing the gibberellin signal transduction pathway', *Plant Cell*, 10: 155-69.

Silverstone, A. L., H. S. Jung, A. Dill, H. Kawaide, Y. Kamiya, and T. P. Sun. 2001. 'Repressing a repressor: Gibberellin-induced rapid reduction of the RGA protein in Arabidopsis', *Plant Cell*, 13: 1555-65.

Šimura, Jan, Ioanna Antoniadi, Jitka Siroka, Danuse Tarkowska, Miroslav Strnad, Karin Ljung, and Ondrej Novak. 2018. 'Plant Hormonomics: Multiple Phytohormone Profiling by Targeted Metabolomics', *Plant Physiology*, 177: 476-89.

Slade, A. J., S. I. Fuerstenberg, D. Loeffler, M. N. Steine, and D. Facciotti. 2005. 'A reverse genetic, nontransgenic approach to wheat crop improvement by TILLING', *Nature Biotechnology*, 23: 75-81.

Slafer, GA. 2001. 'Photoperiod sensitivity during stem elongation as an avenue to raise potential yield in wheat', *Euphytica*, 119: 191-97.

Sojka, R. E., L. H. Stolzy, and R. A. Fischer. 1981. 'Seasonal drought response of selected wheat cultivars', *Agronomy Journal*, 73: 838-45.

Spielmeyer, W., M. Ellis, M. Robertson, S. Ali, J. R. Lenton, and P. M. Chandler. 2004. 'Isolation of gibberellin and metabolic pathway genes from barley and comparative mapping in barley, wheat and rice', *Theoretical and Applied Genetics*, 109: 847-55.

Spray, C. R., M. Kobayashi, Y. Suzuki, B. O. Phinney, P. Gaskin, and J. MacMillan. 1996. 'The dwarf-1 (d1) mutant of Zea mays blocks three steps in the gibberellin-biosynthetic pathway', *Proceedings of the National Academy of Sciences of the United States of America*, 93: 10515-18.

Stern, W. R., and E. J. M. Kirby. 1979. 'PRIMORDIUM INITIATION AT THE SHOOT APEX IN 4 CONTRASTING VARIETIES OF SPRING WHEAT IN RESPONSE TO SOWING DATE', *Journal of Agricultural Science*, 93: 203-15.

Stoddart, J. L., and E. J. Lloyd. 1986. 'Modification by Gibberellin of The Temperature Relationship in Mutant and Normal Genotypes of Several Cereals', *Planta*, 167: 364-68.

Sukai, M., T. Sakamoto, T. Saito, M. Matsuoka, T. Kayano, H. Tanaka, and M. Kobayashi. 2002. 'A novel gibberellin 2-oxidase regulates the level of endogenous gibberellin in rice', *Plant and Cell Physiology*, 43: S144-S44.

Sun, Linhe, Wenlong Yang, Yafei Li, Qiangqiang Shan, Xiaobin Ye, Dongzhi Wang, Kang Yu, Weiwen Lu, Peiyong Xin, Zhong Pei, Xiaoli Guo, Dongcheng Liu, Jiazhu Sun, Kehui Zhan, Jinfang Chu, and Aimin Zhang. 2019. 'A wheat dominant dwarfing line with Rht12, which reduces stem cell length and affects gibberellic acid synthesis, is a 5AL terminal deletion line', *Plant Journal*, 97: 887-900.

Sun, T. P. 2010. 'Gibberellin-GID1-DELLA: A Pivotal Regulatory Module for Plant Growth and Development', *Plant Physiology*, 154: 567-70.

Sun, T. P., H. M. Goodman, and F. M. Ausubel. 1992. 'CLONING THE ARABIDOPSIS GA1 LOCUS BY GENOMIC SUBTRACTION', *Plant Cell*, 4: 119-28.

Sun, TP. 2011. 'The Molecular Mechanism and Evolution of the GA-GID1-DELLA Signaling Module in Plants', *Current Biology*, 21: R338-R45.

Sun, X. L., W. T. Jones, and E. H. A. Rikkerink. 2012. 'GRAS proteins: the versatile roles of intrinsically disordered proteins in plant signalling', *Biochemical Journal*, 442: 1-12.
Swain, S. M., and N. E. Olszewski. 1996. 'Genetic analysis of gibberellin signal transduction', *Plant Physiology*, 112: 11-17.
Talerico, M., and S. M. Berget. 1990. 'Effect of 5' splice site mutations on splicing of the preceding intron', *Molecular and Cellular Biology*, 10: 6299-305.
Talon, M., M. Koornneef, and J. A. D. Zeevaart. 1990. 'Accumulation of C19-gibberellins in the gibberellin insensitive dwarf mutant GAI of Arabidopsis thaliana (L) heynh', *Planta*, 182: 501-05.
Tamaki, S., S. Matsuo, H. L. Wong, S. Yokoi, and K. Shimamoto. 2007. 'Hd3a protein is a mobile flowering signal in rice', *Science*, 316: 1033-36.
Tan, M. K., J. Koval, and A. Ghalayini. 2013. 'Novel Genetic Variants of GA-Insensitive Rht-1 Genes in Hexaploid Wheat and Their Potential Agronomic Value', *Plos One*, 8.
———. 2014. 'Novel Genetic Variants of GA-Insensitive Rht-1 Genes in Hexaploid Wheat and Their Potential Agronomic Value (vol 8, e69690, 2013)', *Plos One*, 9.
Tang, Xiang, Zhi-Yong Zhang, Wen-Juan Zhang, Xing-Ming Zhao, Xuan Li, Dong Zhang, Qiao-Quan Liu, and Wei-Hua Tang. 2010. 'Global Gene Profiling of Laser-Captured Pollen Mother Cells Indicates Molecular Pathways and Gene Subfamilies Involved in Rice Meiosis', *Plant Physiology*, 154: 1855-70.
Teplyakova, Serafima, Marina Lebedeva, Nadezhda Ivanova, Valentina Horeva, Nina Voytsutskaya, Olga Kovaleva, and Elena Potokina. 2017. 'Impact of the 7-bp deletion in HvGA20ox2 gene on agronomic important traits in barley (Hordeum vulgare L.)', *Bmc Plant Biology*, 17.
Thomas, S. G., A. L. Phillips, and P. Hedden. 1999. 'Molecular cloning and functional expression of gibberellin 2-oxidases, multifunctional enzymes involved in gibberellin deactivation', *Proceedings of the National Academy of Sciences of the United States of America*, 96: 4698-703.
Till, B. J., J. Cooper, T. H. Tai, P. Colowit, E. A. Greene, S. Henikoff, and L. Comai. 2007. 'Discovery of chemically induced mutations in rice by TILLING', *Bmc Plant Biology*, 7.
Till, B. J., T. Zerr, L. Comai, and S. Henikoff. 2006. 'A protocol for TILLING and Ecotilling in plants and animals', *Nature Protocols*, 1: 2465-77.
Till, Bradley J., Luca Comai, and Steven Henikoff. 2008. 'Tilling and ecotilling for crop improvement', *Springer Series on Biofilms*, 2: 333-49.
Toledo-Ortiz, G., E. Huq, and P. H. Quail. 2003. 'The Arabidopsis basic/helix-loop-helix transcription factor family', *Plant Cell*, 15: 1749-70.
Tonkinson, C. , R. Lyndon, G. Arnold, and J. Lenton. 1997. 'The effects of temperature and the Rht3 dwarfing gene on growth, cell extension, and gibberellin content and responsiveness in the wheat leaf', *Journal of Experimental Botany*, 48: 963-70.
Tonkinson, C. L., R. F. Lyndon, G. M. Arnold, and J. R. Lenton. 1995. 'Effect of the R*ht3* dwarfing gene on dynamics of cell extenstion in wheat leaves and its modification by gibberellic-acid and paclobutrazol', *Journal of Experimental Botany*, 46: 1085-92.
Toyomasu, T., T. Kagahara, Y. Hirose, M. Usui, S. Abe, K. Okada, J. Koga, W. Mitsuhashi, and H. Yamane. 2009. 'Cloning and Characterization of cDNAs Encoding ent-Copalyl Diphosphate Synthases in Wheat: Insight into the Evolution of Rice Phytoalexin Biosynthetic Genes', *Bioscience Biotechnology and Biochemistry*, 73: 772-75.
Tyler, L., S. G. Thomas, J. H. Hu, A. Dill, J. M. Alonso, J. R. Ecker, and T. P. Sun. 2004. 'DELLA proteins and gibberellin-regulated seed germination and floral development in Arabidopsis', *Plant Physiology*, 135: 1008-19.
Uauy, Cristobal, Francine Paraiso, Pasqualina Colasuonno, Robert K. Tran, Helen Tsai, Steve Berardi, Luca Comai, and Jorge Dubcovsky. 2009. 'A modified TILLING approach to detect induced mutations in tetraploid and hexaploid wheat', *Bmc Plant Biology*, 9.

Ueguchi-Tanaka, M., M. Ashikari, M. Nakajima, H. Itoh, E. Katoh, M. Kobayashi, T. Y. Chow, Y. I. C. Hsing, H. Kitano, I. Yamaguchi, and M. Matsuoka. 2005. 'GIBBERELLIN INSENSITIVE DWARF1 encodes a soluble receptor for gibberellin', *Nature*, 437: 693-98.

Van de Velde, K., P. M. Chandler, D. Van der Straeten, and A. Rohde. 2017. 'Differential coupling of gibberellin responses by Rht-B1c suppressor alleles and Rht-B1b in wheat highlights a unique role for the DELLA N-terminus in dormancy', *Journal of Experimental Botany*, 68: 443-55.

Van de Velde, K., P. Ruelens, K. Geuten, A. Rohde, and D. Van der Straeten. 2017. 'Exploiting DELLA Signaling in Cereals', *Trends in Plant Science*, 22: 880-93.

Vergne, P., I. Delvallee, and C. Dumas. 1987. 'Rapid Assessment of microspore and pollen development stage in wheat and maize using DAPI and membrane permeabilization', *Stain Technology*, 62: 299-304.

Vikhe, Parimal, Ravindra Patil, Ajit Chavan, Manoj Oak, and Shubhada Tamhankar. 2017. 'Mapping gibberellin-sensitive dwarfing locus Rht18 in durum wheat and development of SSR and SNP markers for selection in breeding', *Molecular Breeding*, 37.

Villareal, R. L., S. Rajaram, and E. Deltoro. 1992. 'Yield and agronomic traits of Norin-10 dervied spring wheats adapted to northwestern Mexico', *Journal of Agronomy and Crop Science-Zeitschrift Fur Acker Und Pflanzenbau*, 168: 289-97.

Walton, J. R. 2000. 'Feeding the ten billion. Plants and population growth', *Agricultural History Review*, 48: 128-29.

Wang, Z., M. Gerstein, and M. Snyder. 2009. 'RNA-Seq: a revolutionary tool for transcriptomics', *Nature Reviews Genetics*, 10: 57-63.

Webb, S. E., N. E. J. Appleford, P. Gaskin, and J. R. Lenton. 1998. 'Gibberellins in internodes and ears of wheat containing different dwarfing alleles', *Phytochemistry*, 47: 671-77.

Wen, C. K., and C. Chang. 2002. 'Arabidopsis RGL1 encodes a negative regulator of gibberellin responses', *Plant Cell*, 14: 87-100.

Wen, W., Q. Y. Deng, H. Y. Jia, L. Z. Wei, J. B. Wei, H. S. Wan, L. M. Yang, W. J. Cao, and Z. Q. Ma. 2013. 'Sequence variations of the partially dominant DELLA gene Rht-B1c in wheat and their functional impacts', *Journal of Experimental Botany*, 64: 3299-312.

West, M. A. L., and J. J. Harada. 1993. 'AN OVERVIEW Embryogenesis in higher plants', *Plant Cell*, 5: 1361-69.

Weston, D. E., R. C. Elliott, D. R. Lester, C. Rameau, J. B. Reid, I. C. Murfet, and J. J. Ross. 2008. 'The pea DELLA proteins LA and CRY are important regulators of gibberellin synthesis and root growth', *Plant Physiology*, 147: 199-205.

Weyers, J. D. B., N. W. Paterson, R. Abrook, and Z. Y. Peng. 1995. 'Quantitative analysis of the control of physiological phenomena by plant hormones', *Physiologia Plantarum*, 95: 486-94.

Wilhelm, E. P., R. M. Howells, N. Al-Kaff, J. Z. Jia, C. Baker, M. A. Leverington-Waite, S. Griffiths, A. J. Greenland, M. I. Boulton, and W. Powell. 2013. 'Genetic characterization and mapping of the Rht-1 homoeologs and flanking sequences in wheat', *Theoretical and Applied Genetics*, 126: 1321-36.

Wilhelm, Edward P., Margaret I. Boulton, Tobias E. S. Barber, Andy J. Greenland, and Wayne Powell. 2013. 'Genotype analysis of the wheat semidwarf Rht-B1b and Rht-D1b ancestral lineage', *Plant Breeding*, 132: 539-45.

Williams, R. 2019. 'Better Base Editing in Plants A new technique extends the engineering capabilities of crop developers and plant geneticists alike', *Scientist*, 33: 23-23.

Willige, B. C., S. Ghosh, C. Nill, M. Zourelidou, E. M. N. Dohmann, A. Maier, and C. Schwechheimer. 2007. 'The DELLA domain of GA INSENSITIVE mediates the

interaction with the GA INSENSITIVE DWARF1A gibberellin receptor of Arabidopsis', *Plant Cell*, 19: 1209-20.
Wilson, Z. A., and D. B. Zhang. 2009. 'From Arabidopsis to rice: pathways in pollen development', *Journal of Experimental Botany*, 60: 1479-92.
Worland, A. J. 1986. 'GIBBERELLIC-ACID INSENSITIVE DWARFING GENES IN SOUTHERN EUROPEAN WHEATS', *Euphytica*, 35: 857-66.
Worland, A. J., and S. Petrovic. 1988. 'The gibberellic-acid insensitive dwarfing gene from the wheat variety Saitama-27', *Euphytica*, 38: 55-63.
Worland, A. J., and E. J. Sayers. 1995. 'Rht1 (B dw), an alternative allelic variant for breeding semi-dwarf wheat varieties', *Plant Breeding*, 114: 397-400.
Wu, J., X. Y. Kong, J. M. Wan, X. Y. Liu, X. Zhang, X. P. Guo, R. H. Zhou, G. Y. Zhao, R. L. Jing, X. D. Fu, and J. Z. Jia. 2011. 'Dominant and Pleiotropic Effects of a GAI Gene in Wheat Results from a Lack of Interaction between DELLA and GID1', *Plant Physiology*, 157: 2120-30.
Wu, Y. S., K. Zhou, T. Toyomasu, C. Sugawara, M. Oku, S. Abe, M. Usui, W. Mitsuhashi, M. Chono, P. M. Chandler, and R. J. Peters. 2012. 'Functional characterization of wheat copalyl diphosphate synthases sheds light on the early evolution of labdane-related diterpenoid metabolism in the cereals', *Phytochemistry*, 84: 40-46.
Wu, Zhigang, Ding Tang, Kai Liu, Chunbo Miao, Xiaoxuan Zhuo, Yafei Li, Xuelin Tan, Mingfa Sun, Qiong Luo, and Zhukuan Cheng. 2018. 'Characterization of a new semi-dominant dwarf allele of SLR1 and its potential application in hybrid rice breeding', *Journal of Experimental Botany*, 69: 4703-13.
Xie, Q., S. Mayes, and D. L. Sparkes. 2016. 'Optimizing tiller production and survival for grain yield improvement in a bread wheat x spelt mapping population', *Annals of Botany*, 117: 51-66.
Yamaguchi, S., T. Saito, H. Abe, H. Yamane, N. Murofushi, and Y. Kamiya. 1996. 'Molecular cloning and characterization of a cDNA encoding the gibberellin biosynthetic enzyme ent-kaurene synthase B from pumpkin (Cucurbita maxima L)', *Plant Journal*, 10: 203-13.
Yamaguchi, S., T. P. Sun, H. Kawaide, and Y. Kamiya. 1998. 'The GA2 locus of Arabidopsis thaliana encodes ent-kaurene synthase of gibberellin biosynthesis', *Plant Physiology*, 116: 1271-78.
Yang, D. L., J. Yao, C. S. Mei, X. H. Tong, L. J. Zeng, Q. Li, L. T. Xiao, T. P. Sun, J. G. Li, X. W. Deng, C. M. Lee, M. F. Thomashow, Y. N. Yang, Z. H. He, and S. Y. He. 2012. 'Plant hormone jasmonate prioritizes defense over growth by interfering with gibberellin signaling cascade', *Proceedings of the National Academy of Sciences of the United States of America*, 109: E1192-E200.
Yoshida, H., K. Hirano, T. Sato, N. Mitsuda, M. Nomoto, K. Maeo, E. Koketsu, R. Mitani, M. Kawamura, S. Ishiguro, Y. Tada, M. Ohme-Takagi, M. Matsuoka, and M. Ueguchi-Tanaka. 2014. 'DELLA protein functions as a transcriptional activator through the DNA binding of the INDETERMINATE DOMAIN family proteins', *Proceedings of the National Academy of Sciences of the United States of America*, 111: 7861-66.
Youssefian, S., E. J. M. Kirby, and M. D. Gale. 1992a. 'PLEIOTROPIC EFFECTS OF THE GA-INSENSITIVE RHT DWARFING GENES IN WHEAT .1. EFFECTS ON DEVELOPMENT OF THE EAR, STEM AND LEAVES', *Field Crops Research*, 28: 179-90.
———. 1992b. 'PLEIOTROPIC EFFECTS OF THE GA-INSENSITIVE RHT DWARFING GENES IN WHEAT .2. EFFECTS ON LEAF, STEM, EAR AND FLORET GROWTH', *Field Crops Research*, 28: 191-210.
Zentella, R., Z. L. Zhang, M. Park, S. G. Thomas, A. Endo, K. Murase, C. M. Fleet, Y. Jikumaru, E. Nambara, Y. Kamiya, and T. P. Sun. 2007. 'Global analysis of DELLA direct targets in early gibberellin signaling in Arabidopsis', *Plant Cell*, 19: 3037-57.

Zhang, D. B., and L. Yang. 2014. 'Specification of tapetum and microsporocyte cells within the anther', *Current Opinion in Plant Biology*, 17: 49-55.
Zhang, D., Y. J. Jing, Z. M. Jiang, and R. C. Lin. 2014. 'The Chromatin-Remodeling Factor PICKLE Integrates Brassinosteroid and Gibberellin Signaling during Skotomorphogenic Growth in Arabidopsis', *Plant Cell*, 26: 2472-85.
Zhang, Z. L., M. Ogawa, C. M. Fleet, R. Zentella, J. H. Hu, J. O. Heo, J. Lim, Y. Kamiya, S. Yamaguchi, and T. P. Sun. 2011. 'SCARECROW-LIKE 3 promotes gibberellin signaling by antagonizing master growth repressor DELLA in Arabidopsis', *Proceedings of the National Academy of Sciences of the United States of America*, 108: 2160-65.